

A DERMAL SLUDGE FOR TARGETED GENETIC AUTO-INFLAMMATORY SKIN DISORDERS

SIMPHIWE MAVUSO

A dissertation submitted to the Faculty of Health Sciences, University of the Witwatersrand, in fulfilment of the requirements for the degree of Master of Pharmacy.



Supervisor:

Professor Viness Pillay, Department of Pharmacy and Pharmacology, University of the Witwatersrand, Johannesburg, South Africa

Co-Supervisors:

Associate Professor Yahya Essop Choonara, Department of Pharmacy and Pharmacology, University of the Witwatersrand, Johannesburg, South Africa

Associate Professor Lisa Clare du Toit, Department of Pharmacy and Pharmacology, University of the Witwatersrand, Johannesburg, South Africa

Mr Pradeep Kumar Department of Pharmacy and Pharmacology, University of the Witwatersrand, Johannesburg, South Africa

2016

DECLARATION

I, Simphiwe Mavuso, declare that this dissertation is my own work. It is being submitted for the degree of Master of Pharmacy in the Faculty of Health Sciences at the University of the Witwatersrand, Johannesburg, South Africa. It has not been submitted before for any degree or examination at this or any other University.

Signature

On the 2nd of December 2016 at Wits Medical School.

ANIMAL ETHICS DECLARATION

I, Simphiwe Mavuso, hereby confirm that the study entitled “*In vivo* transdermal delivery of a copper complex ([Copper(glycylglycine)(Prednisolone)]) in the rat model employing a composite polymeric delivery system” was approved by the Animal Ethics Committee of the University of Witwatersrand with Ethics Clearance Number 2015/08/32B (Certificate in Appendix A and AESC M&Es in Appendix B and C).

DEDICATION

This dissertation is dedicated to my grandma Galinah Mamba who can't even write nor spell her name but believes so much in the richness of learning. Grandma thank you for your endearing love and support, without you my parents wouldn't be who they are.

RESEARCH PRESENTATIONS

1. Simphiwe Mavuso, Thashree Marimuthu, Pradeep Kumar, Lisa C. Du Toit, Yahya E. Choonaraand Viness Pillay. A novel bioactive Cu(II) complex with prednisolone succinate and glycylglycine: Synthesis, characterisation and biological evaluations. (**Poster Presentation**). Academic Pharmaceutical Society, Cederwood, Sandton, 14-15 September 2015 (Abstract in Appendix D).
2. Simphiwe Mavuso, Thashree Marimuthu, Pradeep Kumar, Lisa C. Du Toit, Yahya E. Choonaraand Viness Pillay. *In vitro* evaluation of novel redox/pH dual stimuli-responsive nanoliposomes loaded with Copper-liganded bioactive complex. (**Poster Presentation**). Academic Pharmaceutical Society, Cederwood, Sandton, 14-15 September 2015 (Abstract in Appendix E).

PUBLICATIONS

1. A review of polymeric colloidal nanogels in transdermal drug delivery. Simphiwe Mavuso, Viness Pillay, Yahya E. Choonara, Lisa C. du Toit, Pradeep Kumar, Thashree Marimuthu. *Current Pharmaceutical Design* (2015). 21(20), 2801-13 (Abstract in Appendix F).
2. Dual pH/redox responsive nanoliposomes for the delivery of a Copper-liganded bioactive complex in inflammation. Simphiwe Mavuso, Thashree Marimuthu, Yahya E. Choonara, Pradeep Kumar, Lisa C. du Toit, Pierre Kondiah and Viness Pillay (2016). *International Journal of pharmaceutics*. 25;509(1-2):348-59(Abstract in Appendix G).

RESEARCH FUNDING

1. Funded by Professor Viness Pillay's NRF Research Chair Grant, to complete a Master of Pharmacy degree in the department of Pharmacy and Pharmacology, University of the Witwatersrand, Johannesburg.

ABSTRACT

Genetic auto-inflammatory inflammatory skin disorders (GAISDs) are a group of inherited disorders which are characterized by seemingly unprovoked recurrent episodes of fever and severe localised inflammation. GAISDs are associated with abnormal activation of the innate immune system, leading to clinical inflammation and high levels of acute-phase reactants. The most common disorder is Familial Mediterranean Fever (FMF), followed by Tumor Necrosis Factor Receptor-Associated Periodic Syndrome (TRAPS). TRAPS episodes generally last longer than FMF and FMF patients tend to respond well with colchicine while TRAPS management seems to be challenging. Hence this work is directed towards improving TRAPS diseases management. A definitive treatment for TRAPS has yet to be identified, and current corticosteroid treatment is mainly limited by the long-term side-effects due to high systemic drug exposure, and the poor availability of drugs at the site of action.

A number of measures were taken in order to overcome the limitations of corticosteroids. Herein a novel stimuli responsive nanocolloidal gel system was developed. A nanoliposomal gel was the stimuli responsive gel system of choice due to its advantages of skin penetration enhancement in transdermal drug delivery system. In this research, a phospholipid based system with Eudragit® E100 (EuE100) chemically modified into EuE100-cystamine derivative for dual pH/redox responsive delivery of [Copper-glycylglycine-prednisolone succinate] ([Cu(glygly)(PS)]) was developed. The rationale of using [Cu(glygly)(PS)] complex instead of the pure PS corticosteroid was supported by comparing the biological activities of these two compounds. Results indicated a high inflammatory/oxidant inhibitory activity of [Cu(glygly)(PS)] in comparison to the free PS drug. The [Cu(glygly)(PS)] complex exhibited a significant free radical-scavenging activity ($60.1 \pm 1.2\%$) and lipoxygenase (LOX-5) inhibitory activity ($36.6 \pm 1.3\%$) in comparison to PS which gave activity of $4.4 \pm 1.4\%$ and inhibition of $6.1 \pm 2.6\%$ respectively. The [Cu(glygly)(PS)] loaded NLs showed a low level of [Cu(glygly)(PS)] release of $22.9 \pm 5.4\%$ in 6h at pH 7.4, in comparison to a significant accelerated release at pH 5 in a reducing environment of $75.9 \pm 3.7\%$ in 6h. Thereafter optimized [Cu(glygly)(PS)]-loaded NLs were dispersed in hydroxypropyl methylcellulose (HPMC)/Polyvinyl alcohol (PVA) gel resulting in a [Cu(glygly)(PS)]-loaded nanoliposomal gel termed as dermal sludge. A dermal sludge is defined as a viscous gel suspended with solid particles ([Cu(glygly)(PS)]-loaded nanoliposomes). The sludge was characterized using *ex vivo* permeation, *in vitro* release, cytotoxicity and *in vivo* studies, and compared to the conventional PS formulations. The results indicated that the novel dual redox/pH responsive nanoliposomal dermal sludge holds great potential for targeted bioactive delivery in TRAPS through the transdermal route, hence improving the therapeutic outcome.

ACKNOWLEDGMENTS

Foremost I would like to thank the almighty God with whom all was possible, His guidance and unconditional love made me come to this far.

Then I would like to thank my family, Mom and Dad, I can't thank you enough for loving and believing in me throughout, without your support and prayers I wouldn't be me. I hope I will continue making you proud. My grandmothers Mrs G Mamba and H Shongwe-Mavuso, thank you for your encouraging words, support and prayers, I thank God for keeping you. To my siblings especially Dumi and Ndumi, knowing that you were always looking up to me gave me so much courage and I thank God for you. To my Mamba uncles, aunts and cousins, thank you for showing me what the word family really mean, I am grateful to have you in my life.

I would like to thank my supervisor Prof. Viness Pillay firstly for granting me the opportunity to be part of Wits Advanced drug delivery platforms, what I have learned for the past two years is beyond this Masters. Thank you for you for pushing our boundaries, supporting and encouraging us.

To Prof. Yahya E. Choonara thank you for all the advice, your critics and views on my research, my project wouldn't have been a success without you.

I would like to thank Dr T Marimuthu for being the kind of supervisor she was, I will never forget her favorite phrase every time something went wrong "It's not the end of the world, after all it is research", she would say. I know I was not an easy student to deal with at times, thank you for not giving up on me throughout my study.

To Prof. L.C. du Toit and Mr Pradeep Kumar, I am grateful for being there for me every time I needed your assistance. I wouldn't have made it without your inputs, thank you.

To the head of department Prof. Danckwerts and the rest of the pharmacy and pharmacology department staff, thank you making my stay in the department worth a while.

To the technical staff Mr Ramarumo, Bafana, Kleeinboi and Phumzile thank you for all the support.

I would also like to thank all my friends who have been my extended family for the past few years thank you for being with me throughout the bad and good moments in my life, especially for pulling up with all my different personalities, I love you all.

To the animal unit staff and Prof Kennedy thank you for the support, advice and assistance throughout my *ex vivo* and *in vivo* studies.

To the chemistry department especially Dr Johnson thank you for your assistance with NMR.

To the post-doctorates thank you for your contribution into my project, special thanks to Dr Divya Bijukmar who assisted me with my *in vitro* cytotoxicity studies.

To the National Research Foundation and the University of the Witwatersrand thank you for the financial assistant.

God was, is and will forever be in complete control

TABLE OF CONTENTS

DECLARATION	i
ANIMAL ETHICS DECLARATION	ii
DEDICATION.....	iii
RESEARCH PRESENTATIONS	iv
PUBLICATIONS.....	v
RESEARCH FUNDING	vi
ABSTRACT.....	vii
ACKNOWLEDGMENTS.....	viii
TABLE OF CONTENTS	x
LIST OF ABBREVIATIONS AND SYMBOLS	xx
LIST OF FIGURES	xxi
LIST OF TABLES.....	xxvi
LIST OF EQUATIONS	xxvii

CHAPTER 1

BACKGROUND ON GENETIC AUTO-INFLAMMATORY SKIN DISORDERS – THE POTENTIAL BENEFITS OF THE NOVEL TARGETED DERMAL SLUDGE

1.1.Introduction.....	2
1.2.Rationale and Motivation for the Study.....	6
1.3.The Dermal sludge for Targeted Drug Delivery in TRAPS: Concept and Outline.....	8
1.4.Potential Benefits of this Study.....	9
1.5.Aim and Objectives.....	10
1.6.Overview of this Dissertation.....	11

CHAPTER 2

A REVIEW OF POLYMERIC COLLOIDAL NANOGELS IN TRANSDERMAL DRUG DELIVERY

2.1. Introduction.....	13
2.2. Limitations of Conventional Transdermal Drug Delivery Systems.....	15
2.3. Fabrication Techniques of Polymeric Nanogel Networks in DPCNs	16
2.3.1. Physical self-assembly of interactive polymers.....	17
2.3.2. Monomer polymerization in a homogeneous or heterogeneous microscale or nanoscale environment.....	18
2.3.3. Chemical cross-linking of preformed polymers	18
2.3.4. Template-assisted nanofabrication of nanogels particles (imprint photolithographic techniques)	19
2.4. Polymeric Colloidal Nanogel Properties	19
2.4.1. Swelling and de-swelling properties	19
2.4.2. Biocompatibility and biodegradability.....	20
2.4.3. Morphology	21
2.4.4. The drug loading capacity	21
2.4.5. Sustained and controlled drug release	22
2.4.6. Site specific targeting	23
2.4.7. Penetration enhancing property	24

2.4.8. Miscellaneous nanogel properties	24
2.4.8.1. <i>Superior colloidal stability</i>	24
2.4.8.2. <i>No immunological responses stimulated</i>	25
2.4.8.3. <i>Can be used as a carrier for both hydrophobic and hydrophilic drugs</i>	25
2.4.8.4. <i>Solubility</i>	25
2.5. Therapeutic Significance of Polymeric Nanogels in Transdermal Drug Delivery Systems ..	25
2.6. Recent Advances in Polymeric Colloidal Nanogels	29
2.6.1. Stimuli responsive polymeric colloidal nanogels / Targeted polymeric colloidal nanogels	29
2.6.2. Multiple (dual) stimuli responsive polymeric colloidal nanogels	33
2.6.3. Nanogels as carriers for liposomes / liposomal nanogels	34
2.6.4. Enzymatically crosslinked nanogels	36
2.7. Concluding Remarks	36

CHAPTER 3

A NOVEL BIOACTIVE COPPER COMPLEX WITH PREDNISOLONE SUCCINATE AND GLYCYLGLYCINE: SYNTHESIS, CHARACTERIZATION AND BIOLOGICAL EVALUATION FOR TRAPS MANAGEMENT

3.1. Introduction	38
3.2. Materials and Methods	39
3.2.1. Materials	39
3.2.2. Synthesis of the [Copper(glycylglycine)(prednisolone succinate)] complex	40
3.2.3. Chemical structural analysis of the [Copper(glycylglycine)(prednisolone succinate)] complex	40
3.2.4. Analysis of the chemical shifts of the [Copper(glycylglycine)(prednisolone succinate)] complex	40
3.2.5. Analysis of the UV–visible absorption spectrometry of the [Copper(glycylglycine)(prednisolone succinate)] complex	41
3.2.6. Identification of the molecular fragmentations of the [Copper(glycylglycine)(prednisolone succinate)] complex	41
3.2.7. Evaluation of the degree of structural order of the the [Copper(glycylglycine)(prednisolone succinate)] complex	41

3.2.8. Determination of thermal properties of the [Copper(glycylglycine)(prednisolone succinate)] complex	41
3.2.9. Determination of thermal properties of the [Copper(glycylglycine)(prednisolone succinate)] complex	42
3.2.10. Evaluation of the antioxidant/ antiinflammatory activities of the Copper(glycylglycine)(prednisolone succinate)] complex	42
3.2.10.1. DPPH free radical scavenging assay.....	42
3.2.10.2. 5-lipoxygenase inhibition assay.....	42
3.2.11. <i>In vitro</i> permeation studies	43
3.2.12. <i>In vitro</i> cytotoxicity analysis	44
3.3. Results and Discussions	45
3.3.1. Characterisation and evaluation of the formulations	45
3.3.2. Chemical structural evaluation of the the [Copper(glycylglycine)(prednisolone succinate)] complex.....	47
3.3.3. Evaluation of the chemical shifts of the [Copper(glycylglycine)(prednisolone succinate)] complex.....	49
3.3.4. Evaluation of the UV–visible absorption spectrometry of the [Copper(glycylglycine)(prednisolone succinate)] complex	51
3.3.5. Identification of the molecular fragmentations of the [Copper(glycylglycine)(prednisolone succinate)] complex.....	52
3.3.6. Evaluation of the degree of structural order of the [Copper(glycylglycine)(prednisolone succinate)] complex.....	52
3.3.7. Evaluation of thermal properties of the [Copper(glycylglycine)(prednisolone succinate)] complex.....	53
3.3.8. Evaluation of thermal properties of the [Copper(glycylglycine)(prednisolone succinate)] complex.....	54
3.3.9. Antioxidant/anti-inflammatory activities of the [Copper(glycylglycine)(prednisolone succinate)] complex.....	55
3.3.10. <i>Ex vivo</i> permeation studies.....	57
3.3.11. Cytotoxic potential of the [Copper(glycylglycine)(prednisolone succinate)] complex.....	59
3.4. Concluding Remarks.....	60

CHAPTER 4

IN VITRO EVALUATION OF NOVEL REDOX/PH DUAL STIMULI-RESPONSIVE NANOLIPOSOMES LOADED WITH COPPER-LIGANDED BIOACTIVE COMPLEX

4.1. Introduction	61
4.2. Materials and Methods	64
4.2.1. Materials	64
4.2.2. Formulation of dual pH/redox responsive [Cu(glygly)PS]-loaded nanoliposomes	64
4.2.2.1. <i>Synthesis of the [Cu(glygly)(PS)] complex</i>	64
4.2.2.3. <i>Coupling of the Eudragit® E100</i>	64
4.2.2.2. <i>Determination of thiol groups</i>	65
4.2.2.3. <i>Preparation of the nanoliposomes</i>	65
4.2.3. Chemical structural analysis of EuE100, EuE100-Cyst, [Cu(glygly)(PS)]-loaded and unloaded NLs using Fourier transform infrared spectroscopy.....	66
4.2.4. Analysis of the chemical shifts of EuE100 and EuE100-cyst using Nuclear magnetic resonance spectroscopy	66
4.2.5. X-ray diffraction Analysis of EuE100 and EuE100-cyst.....	66
4.2.6. Determination of the thermal properties of EuE100 and EuE100-cyst	66
4.2.6.1. <i>Differential scanning calorimeter analysis</i>	66
4.2.6.2. <i>Thermogravimetric analysis</i>	66
4.2.7. Determination of particle size and zeta potential of [Cu(glygly)(PS)]-loaded intelligent nanoliposomes.....	67
4.2.8. Transmission electron microscopy of the [Cu(glygly)(PS)]-loaded intelligent nanoliposomes.....	67
4.2.9. Investigation of redox/pH Sensitivity of the [Cu(glygly)(PS)]- loaded intelligent nanoliposomes.....	67
4.2.10. Determination of entrapment efficiency of [Cu(glygly)(PS)]-loaded intelligent NLs.....	68

4.2.11. <i>In vitro</i> drug release from the NLs	68
4.2.12. <i>In vitro</i> cytotoxicity studies.....	68
4.2.13. Statistical analysis	68
4.3. Results and Discussion	69
4.3.1. Synthesis and Characterisation of EuE100-Cyst	69
4.3.2. Chemical structural evaluation using Fourier transform infrared (FTIR) spectroscopy	70
4.3.3. Evaluation of the magnetic properties using Nuclear magnetic resonance spectroscopy	72
4.3.4. Evaluation of the thermal properties of EuE100 and EuE100-Cyst using differential scanning calorimeter analysis	74
4.3.5. Evaluation of the thermal properties using thermogravimetric analysis (TGA)	75
4.3.6. Assessment of the degree of structural order using X-ray Diffraction	76
4.3.7. Determination of particle size in functionalised nanoliposomes	77
4.3.8. Transmission electron microscopy of the [Cu(gly)(PS)]-loaded intelligent nanoliposomes	78
4.3.9. Investigation of redox/pH sensitivity of nanoliposomes.....	79
4.3.10. Entrapment efficiency and <i>in vitro</i> [Cu(glygly)PS] release studies	80
4.3.11. Evaluation of <i>in vitro</i> cytotoxicity.....	81
4.4. Concluding Remarks.....	82

CHAPTER 5

APPLICATION OF BOX-BEHNKEN DESIGN IN THE FORMULATION AND OPTIMISATION OF DUAL RESPONSIVE [COPPER-GLYCYLGLYCINE-PREDNISOLONE SUCCINATE] LOADED NANOLIPOSOMAL SLUDGE FOR TRANSDERMAL DRUG DELIVERY

5.1. Introduction	83
5.2. Materials and Methods	84
5.2.1. Materials	84
5.2.2. Preparation of dual pH/redox [Cu(glygly)(PS)]-loaded nanoliposomes	85

5.2.2.1. Optimisation using a Box–Behnken design	85
5.2.2.2. Formulation of the [Cu(glygly)(PS)]-loaded nanoliposomes.....	86
5.2.3. Dermal sludge preparation	86
5.2.4. Preparation of Conventional prednisolone Gel	87
5.2.5. Determination of entrapment efficiency and drug loading of the nanoliposomes.....	87
5.2.6. Chemical structural analysis of [Cu(glygly)(PS)] complex, optimised [Cu(glygly)(PS)]-loaded and unloaded NLs using Fourier transform infrared (FTIR) spectroscopy	87
5.2.7. Determination of the thermal properties of the [Cu(glygly)(PS)] complex, optimised [Cu(glygly)(PS)]-loaded and unloaded NLs	88
5.2.7.1. Differential scanning calorimeter analysis.....	88
5.2.7.2. Thermogravimetric analysis.....	88
5.2.8. Determination of the size and zeta potential of the nanoliposomes	88
5.2.9. Analysis of the surface and structure morphology of the optimised dual pH/redox responsive nanoliposomes.....	88
5.2.9.1. Scanning electron microscopy.....	88
5.2.9.2. Transmission electron microscopy	89
5.2.10. Analysis of the rheological behaviour of the nanoliposomal sludge	89
5.2.11. Analysis of the textural properties of the optimized nanoliposomal sludge.....	89
5.2.12. <i>In vitro</i> drug release studies of the PS, [Cu(glygly)(PS)]-loaded NLs and [Cu(glygly)(PS)]-loaded nanoliposomal sludge.....	90
5.2.13. <i>Ex vivo</i> permeation studies of the [Cu(glygly)(PS)]-loaded nanoliposomal sludge compared to conventional formulations.....	91
5.2.13.1. Determination of complex and drug retention in the Skin.....	91
5.3. Results and Discussions	91
5.3.1.1. The results of optimization using the Box–Behnken design.....	91
5.3.1.2. Statistical validity of the optimized formulation.....	94
5.3.1.3. Dermal sludge formulation.....	95
5.3.2. Structural characterisation of the optimized nanoliposomes and sludge	96

5.3.3. Evaluation of the thermal properties of the optimized nanoliposomes and sludge	97
5.3.4. Particle size and zeta potential of the optimised nanoliposomes	100
5.3.5. The electron micrographs of the optimized [Cu(glygly)(PS)]-Loaded nanoliposomes	101
5.3.6. Rheological evaluation of the optimized nanoliposomal sludge	102
5.3.7. Determination of the texture properties of the optimized nanoliposomal sludge.....	103
5.3.8. Drug release analysis of PS, [Cu(glygly)(PS)]-loaded NLs and [Cu(glygly)(PS)]- loaded nanoliposomal sludge	104
5.3.9. Skin Permeation evaluation.....	107
5.4. Concluding Remarks.....	109

CHAPTER 6

***IN VIVO* EVALUATION OF A [COPPER(GLYCYLGLYCINE)(PREDNISOLONE SUCCINATE)]- LOADED NANOLIPOSOMAL SLUDGE IN SPRAGUE-DAWLEY RATS FOR TRANSDERMAL DRUG DELIVERY**

6.1. Introduction	110
6.2. Materials and Methods	111
6.2.1. Materials	111
6.2.2. Nanoliposomal sludge sterilization and lyophilisation.....	111
6.2.3. Experimental design.....	112
6.2.4. Histological assessment.....	116
6.2.5. Determination of retained complex in skin	117
6.2.6. Prednisolone analysis using Ultra-performance liquid chromatography (UPLC)	117
6.2.6.1. <i>The chromatographic system</i>	117
6.2.6.2. <i>Internal standard</i>	117
6.2.6.3. <i>Calibration curve standards</i>	117
6.2.6.4. <i>Liquid-liquid extraction procedure</i>	118

6.2.6.5. Plasma sample handling and preparation from rats.....	118
6.2.6.6. Method validation	118
6.3. Results and Discussion	119
6.3.1. Validity of the sterility procedure.....	119
6.3.2. Pilot study using five rats from group B	119
6.3.3. <i>In vivo</i> evaluation of the anti-inflammatory/anti-oxidant activity of the [Cu(glyg)(PS)] delivered from the sludge.....	120
6.3.4. <i>In vivo</i> evaluation of the [Cu(glyg)(PS)] complex delivery from the sludge.....	125
6.3.4.1. Validation of the extraction procedure	125
6.3.4.2. Chromatographic separation and validation assay	125
6.3.4.3. Determination of the [Cu(glyg)(PS)] concentrations in the rats blood plasma	126
6.4. Concluding Remarks.....	129

CHAPTER 7

CONCLUSIONS AND RECOMMENDATIONS

7.1. Conclusions	130
7.2. Recommendations	131

8. References	132
9. Appendices	164
Appendix A: Animal Ethics Clearance certificate	165
Appendix B: First animal ethics “Modification and Extension of Experiments” certificate	166
Appendix C: Second animal ethics “Modification and Extension of Experiments” certificate..	167
Appendix D: Abstract for The Academic Pharmaceutical Society, Sandton, September 2015 research conference first poster presentation.....	168

Appendix E: Abstract for The Academic Pharmaceutical Society, Sandton, September 2015 research conference second poster presentation.....169

Appendix F: Abstract for a review paper published from this dissertation.....170

Appendix G: Abstract for a research paper published from this dissertatin.....171

Appendix H: IDEXX laboratory histopathological report172

LIST OF ABBREVIATIONS AND SYMBOLS

[Cu(glygly)PS] - [Copper(glycylglycine)(prednisolone succinate)]

CAPS - Cryopyrin-associated periodic syndrome

CINCA - Chronic infantile neurological cutaneous articular syndrome

DPCNs - drug-loaded polymeric colloidal nanogels

DPPH - 1, 1-diphenyl-2-picrylhydrazyl

DSPE - 1,2-distearoyl-sn-glycero-3-phosphatidyl-ethanolamine

DTNB - 5, 5' dithiobis(nitrobenzoic acid) (Ellman's agent)

EDC - 1-Ethyl-3-(3dimethylaminopropyl) carbodiimide hydrochloride

FCAS - Familial cold autoinflammatory syndrome

FMF - Familial Mediterranean fever

GAISDs - Genetic auto-inflammatory inflammatory skin disorders

HIDS - Hyper immunoglobulin D syndrome with periodic fever

MKD/HIDS - Mevalonate kinase deficiency/hyperimmunoglobulin D syndrome

MTT - 3-(4,5-dimethylthiazol-2-yl)-2,5-diphenyltetrazolium bromide

MWS - Muckle–Wells syndrome

NIPAM - N-isopropylacrylamide

PAPA - Pyogenic arthritis, pyoderma gangrenosum, and acne

PTSPIP1 - Proline-serine-threonine phosphatase interacting protein 1

TRAPS - Tumor necrosis factor receptor-associated periodic syndrome

LIST OF FIGURES

Figure 1.1: Mutated proteins are denoted by stars, and the terms in green circles denote the diseases with which they are associated (Adapted from Ozen and Bilginer, 2014).	3
Figure 1.2: (a) Casting of tumor necrosis factor receptor (TNFR) and atypical signaling in TRAPS. (b) Edematous erythema noticed in cheeks and periorbital area of a TRAPS patient. (c) Multiple serpiginous patches and plaques in lower extremities (Adapted from Kanazawa and Furukawa, 2007).	4
Figure 1.3: (a) Vesicles on the abdomen. (b) Linearly arranged papules on the neck. (c) Diffuse erythema on the nose. (d) Serpiginous rash (Adapted from Yao et al., 2012).	5
Figure 1.4: Hydrocortisone succinate is shown coordinated on the metal (M), M may be Fe, Cu, Co, Mn, or Zn.	7
Figure 1.5: Schematic diagram representing the proposed metal-drug complex loaded nanoliposome, and briefly its mechanism of release. The nanoliposome formulation would detect the inflammatory mediators through the stimuli responsive nanocolloidal gel system chemical groups, and then it would swell, erode, and release the coordinated metal-drug complex.	9
Figure 2.1: Representation of drug penetration pathways through the skin with the two major routes shown on the upper right corner. (Adapted with the permission from Alexander et al. (2012). Copyright (2012) Elsevier).	15
Figure 2.2: Schematic representation of the synthesis of nanogels via the polymer precursor method and the emulsion method respectively. (Adapted with the permission from Chacko et al. (2012). Copyright (2012) Elsevier).	19
Figure 2.3: Representation of a novel surfactant-free route for the preparation of a biocompatible, biodegradable and stimuli responsive nanogel for potential targeted gene delivery. (Adapted with the permission from Urakami et al. (2013). Copyright (2013) American Chemical Society).	24
Figure 2.4: Proposed drug release from a nanogel in response to a stimulus applied. The model shows that the stimulus triggers physical changes in structure of the nanogel, resulting in swelling, erosion and ultimately releases the drug. (Adapted with the permission from Chacko et al. (2012). Copyright (2012) Elsevier).	30
Figure 2.5: Cumulative permeation profiles of a caffeine-loaded nanogel at (a) 2–4 °C, and (b) room temperature (RT). A loaded polyNIPAM nanogel and a saturated caffeine solution was	

used as a control (Adapted with the permission from Samah and Heard (2013). Copyright (2013) Elsevier).....32

Figure 2.6: This nanogel-polyelectrolyte complex is modified with two stimuli responsive functionalities. (Adapted with the permission from Zhuang et al. (2014). Copyright (2014) American Chemical Society).34

Figure 2.7: Route to the preparation of alginate nanogel liposomal templates. Reaction involves treating liposomes encapsulating sodium alginate to a 10 mmol/L CaCl₂ solution at temperatures near the *T_m* of the lipid. The increased transmembrane permeability permits Ca²⁺ to diffuse into the liposomes and ionically cross-link the alginate to form a nanogel. Upon removal of the lipid shell, alginate nanogels are isolated (Adapted with the permission from Hong et al. (2008). Copyright (2008) American Chemical Society).....35

Figure 3.1: The calibration curve of (a) PS at 248nm and (b) [Cu(glygly)PS] complex at 242nm.44

Figure 3.2: Visualization of geometrical preferences of (a)(i) PS and (ii) [Cu(glygly)PS] complex after molecular simulation. Color codes: C (grey), O (red), N (white), H (pink) and Cu (blue) and (b) reaction scheme for the preparation of the [Cu(glygly)PS] complex..46

Figure 3.3: The proposed anti-inflammatory effects caused by [Cu(glygly)(PS)] complex (Adapted with modifications from Lewis, 1984).47

Figure 3.4: The FTIR spectra of a) Glycylglycine, b) PS, c) [Cu(glygly)(PS)].48

Figure 3.5: The FTIR of the complex and drug at lower wavelengths, the red spectrum being the [Cu(glygly)(PS)] complex.....49

Figure 3.6: Comparison of ¹H NMR for (a) PSA and (b) the [Cu(glygly)(PS)] complex in CD₃OD.50

Figure 3.7: Comparison of ¹³C NMR for (a) PSA and (b) the [Cu(glygly)(PS)] complex in CD₃OD51

Figure 3.8: The UV/Visible of complex at (a) 200-300nm and (b) 400-800nm in methanol.51

Figure 3.9: The powder XRD of the (a) PS and (b) [Cu(glygly)(PS)] complex is shown.53

Figure 3.10: The DSC spectrometry of the (a) free PS and (b) [Cu(glygly)(PS)] complex.54

Figure 3.11: TG/DTGA) analysis of the (a) PS, and (b) [Cu(glygly)(PS)] complex.55

Figure 3.12: The percentage lipid peroxidation and antiradical activities of ascorbic acid (1) as the control, and the free PS drug (2), compared to [Cu(glygly)(PS)] complex (3)57

Figure 3.13: The permeability of the drug or/and Cu²⁺ was quantified in terms of cumulative amount permeated per unit time and per unit area and the permeability was plotted against the time.....59

Figure 3.14: The % Cell viability of the PS and complex with MTT assay	60
Figure 4.1: Proposed chemical structure of EuE100-cyst and its ICM degradation through the disulfide link in the presence of a reducing agent (GSH)	63
Figure 4.2: Visualization of geometrical preferences of (a)(i) EuE100 and (ii) EuE100-cyst after molecular simulation. Color codes: C (grey), O (red), N (white), H (pink) and S-S (yellow) and reaction scheme for the preparation of the EuE100-cyst.	69
Figure 4.3: The expected sequential degradation of the NLs in the inflamed tissue: 1. The initial degradation; as the NL passes through the extracellular matrix into the cell it encounters a reduced pH up to pH 5, and it swells. 2. The NL passes through the cell into the ICM (cytosol) where there is increased GSH concentration up to 10mM during inflammation, the NL undergoes full degradation. 3. The complex is finally released to the nucleus of the cell where it exert its improved ant-inflammatory effects.	70
Figure 4.4: The FTIR spectra of EuE100 and its derivatives are shown. (a) EuE100-Cyst. (b) EuE100.....	71
Figure 4.5: FTIR spectroscopic analysis of (a) [Cu(glygly)(PS)]- loaded NLs, (b) unloaded NLs and (c) complex.	72
Figure 4.7: Comparative COSY NMR in MeOD.....	74
Figure 4.8: The DSC graphs, a) EuE100, b) EuE100-cyst.....	75
Figure 4.9: (a) TG/DTA of the EuE100 and (b) TG/DTA of EuE100-cyst.	76
Figure 4.10: The X-ray diffraction of the (a) EuE100-Cyst powder and (b) EuE100.....	77
Figure 4.11: Size distribution of the [Cu(gly)(PS)]-loaded intelligent NLs is shown.	78
Figure 4.12: Surface charge (zeta potential) of the [Cu(gly)(PS)]-loaded intelligent NLs	78
Figure 4.13: The TEM micrographs of [Cu(gly)(PS)]-loaded intelligent nanoliposomes in uranyl acetate (negative stain).....	79
Figure 4.14: The particle size of NLs: (a) at pH 5 with 10mM GSH, (b) at pH 5 without any GSH, (c) at pH 7.4 with 10mM GSH and (d) at pH 7.4 without any GSH.....	80
Figure 4.15: Drug-release profile of [Cu(glygly)(PS)] from pH/redox sensitive NLs at pH 7.4 and 5, with and without 10mM GSH.....	81
Figure 4.16: The % Cell viability of the [Cu(glygly)(PS)]-loaded and unloded NLs with MTT assay.	82
Figure 5.1: The resulted generated using MINITAB® for the optimized formulation, the desirable results are also shown.	94

Figure 5.2: (a) The expected penetration of the nanoliposomal sludge through the skin and (b) thereafter its sequential degradation of the inflamed site occur as described in Chapter 3, Figure 4.3.....95

Figure 5.4: The comparative FTIR spectroscopic analysis of the placebo gel and loaded NLs compared to the nanolipoosomal sludge which is the combination of the two.97

Figure 5.5: DSC analysis of [Cu(glygly)(PS)] complex, (b) unloaded NLs and (c) [Cu(glygly)(PS)]-loaded NLs.....98

Figure 5.6: TG/DTG) analysis of the (a) [Cu(glygly)(PS)], (b) [Cu(glygly)(PS)]-loaded and (b) unloaded NLs.....99

Figure 5.7: The size (a+c) and zeta potential (b+d) distribution of the unloaded (a+b) and loaded (b+d) NLs100

Figure 5.8:a) The TEM analysis of the [Cu(glygly)(PS)]- Loaded NLs in a negative stain (uranyl acetate) and b) SEM evaluation of the cryoprotected freeze dried NLs at 1260X102

Figure 5.9: The rheological analysis of the nanoliposomal sludge103

Figure 5.10: Typical force versus time plot of the nanoliposomal sludge.104

Figure 5.11: (a) The % [Cu(glygly)(PS)] release from the nanolipoosomal sludge treated with GSH (10 mM) in acid (pH 5.0) and normal pH 7.4 at 37 °C. (b) The comparative combined data of all the marketed PS formulations (cream, tablet and syrup), conventional gel and novel [Cu(glygly)(PS)] loaded nanolipsomal sludge formulation. (c) The % PS release from the tablet treated with GSH (10 mM) in acid (pH 5.0) and normal pH 7.4 at 37 °C. (d) The % PS release from the syrup treated with GSH (10 mM) in acid (pH 5.0) and normal pH 7.4 at 37 °C. (e) The PS release from the conventional gel treated with GSH (10 mM) in acid (pH 5.0) and normal pH 7.4 at 37 °C. (f) The [Cu(glygly)(PS)] release from the PVP/HPMC gel treated with GSH (10 mM) in acid (pH 5.0) and normal pH 7.4 at 37 °C. (g) The PS release from the cream treated with GSH (10 mM) in acid (pH 5.0) and normal pH 7.4 at 37 °C. (Data represent mean ±S.D. (n=3)).107

Figure 5.12: Comparative permeation studies throught the pig skin in PBS pH7.4 at 37 °C. ..108

Figure 6.1: The flow diagram showing the steps involved in the pilot of the in vivo studies using sprague–dawley rats.114

Figure 6.2: The flow diagram showing the steps involved in the main in vivo studies using sprague–dawley rats.115

Figure 6.3: The photographic procedure of the *in vivo* studies using rats. Wherein (i) An anesthesia was administered to all rats, (ii) all rats were shaved on their dorsum and shaved area wiped with water, (iii) at 0h different gels were applied on an area of 1.44cm² of the shaved

portion, while group 3 rats were gavaged, (iv) all rats except group 5 rats received an SC injection at 0.5h after gel application, (v) all rats were bandaged to keep the formulations in place, (vi) blood was collected through cardiac puncture, (vii) and rats were euthanized immediately after blood collection and skin was excised.116

Figure 6.4: the agar plate streaked with sludge, after it has been incubated for 24h at 37°C..119

Figure 6.5: The light microscope images of the H&E stained slides showing the pilot study images (a) the subcutaneous region at 2h, (b) the subcuneus region at 4h, (c) the dermis region at 2h, and (d) the dermis region at 4h.120

Figure 6.6: The light microscope images of the H&E stained slides showing some of the main study images (a) the subcutaneous region with no infiltration (grade 0), (b) the subcutaneous region with mild infiltration (grade 1), (c) the subcuneus region with moderate infiltration (grade 2), and (d) the subcuneus region with severe infiltration (grade 3).124

Figure 6.7: The UPLC PS and dexamethasone (internal standard,(a) in the mobile phase and (b) blood serum.....126

Figure 6.8: The plasma levels of PS in Sprague-Dawley rats after the application of the different formulations in all the groups (standard deviations (n=3)).128

Figure 6.9: The AUC of the formulations applied on the different groups of rats at various time intervals with the standard deviations (n=3).128

LIST OF TABLES

Table 2.1: Specialized polymeric nanogel systems in transdermal drug delivery.	27
Table 3.1: Antioxidant/anti-inflammatory activity	57
Table 3.2: The ex vivo studies concentration and flux values (n=3)	58
Table 5.1: The Box–Behnken design independent and dependent variables are shown.....	85
Table 5.2: The BB design formulations.....	86
Table 5.3: Textural analysis parameter settings for determining the nanoliposomal sludge textural properties.	90
Table 5.4: Responses measured for the Box–Behnken design.....	93
Table 5.5: The predicted responses versus the actual responses from the optimized formulation.	95
Table 5.6: Comparative skin conductivity values before and after ex vivo studies.	109
Table 6.1: Grading of the anti-inflammatory effects of the formulations applied on the different groups of rats.	124
Table 6.2: Average and relative standard deviations (RSDs) of PS recoveries from spiked plasma blanks.	125

LIST OF EQUATIONS

Equation3.1: The percentage inhibition of radical scavenging activity.....	41
Equation3.2: The percentage inhibition assay of 5-lipoxygenase.....	42
Equation3.3: The membrane permeation flux	42
Equation3.4: The permeation coefficient.....	42
Equation3.5: The percentage cell viability.....	44
Equation4.1: The percentage entrapment efficiency	67
Equation5.1: The Drug loading capacity	86
Equation6.1: The percentage entrapment efficiency	114
Equation6.2: The Drug loading capacity	115

CHAPTER 1

BACKGROUND ON GENETIC AUTO-INFLAMMATORY SKIN DISORDERS – THE POTENTIAL BENEFITS OF THE NOVEL TARGETED DERMAL SLUDGE

1.1. Introduction

Genetic auto-inflammatory inflammatory skin disorders (GAISDs) are a group of inherited disorders which are characterized by seemingly unprovoked recurrent episodes of fever and severe localised inflammation (McDermott et al., 1999; Kastner and O'Shea, 2001; Meiorin et al., 2013; Vitale et al., 2013). Most GAISDs are monogenic diseases caused by mutated protein-coding genes and these genes are critical for regulating inflammation. These disorders include familial Mediterranean fever (FMF), hyper immunoglobulin D syndrome with periodic fever (HIDS), tumor necrosis factor receptor-associated periodic syndrome (TRAPS), cryopyrin-associated periodic syndrome (CAPS) familial cold autoinflammatory syndrome (FCAS), pyogenic arthritis, pyoderma gangrenosum and acne (PAPA), Muckle–Wells syndrome (MWS), mevalonate kinase deficiency/hyperimmunoglobulin D syndrome (MKD/HIDS), and chronic infantile neurological cutaneous articular syndrome (CINCA) (Kanazawa and Furukawa, 2007; Dainichi et al., 2014; Ozen and Bilginer, 2014).

In general, all these GAISDs follow different specific characteristic patterns each time they occur, a summary of these patterns is shown in Figure 1.1. In case of TRAPS, mutant TNFR1 (misfolded protein) leads to an abnormal inflammatory response through NF κ B activation; in Blau syndrome, mutant NOD2 is activated after stimulation with MDP leading to NF κ B activation; in FMF, mutant pyrin is suggested to be associated with the inflammasome adaptor protein ASC and increase IL-1 β processing; in CAPS, activated NLRP3 oligomerizes and interacts with the adaptor protein ASC and caspase 1 to form macromolecular complexes (inflammasomes) that process IL-1 β into its active form; in PAPA syndrome, proline-serine-threonine phosphatase interacting protein 1 (PTSPIP1) has been implicated through its binding to pyrin; and in MKD/HIDS, a shortage of nonsterol isoprenoid end products results in increased IL-1 β production (Meiorin et al., 2013; Dainichi et al., 2014; Ozen and Bilginer, 2014).

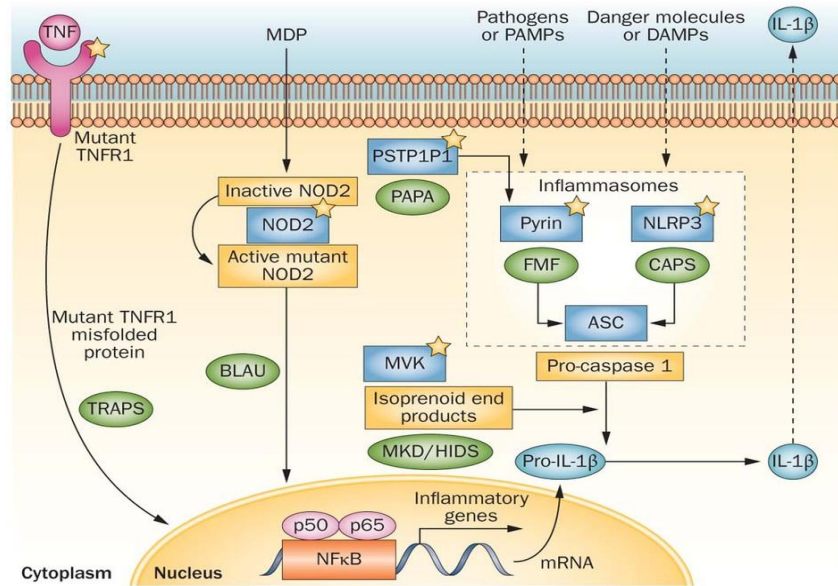


Figure 1.1: Mutated proteins are denoted by stars, and the terms in green circles denote the diseases with which they are associated (Adapted from Ozen and Bilginer, 2014).

These GAIDs are associated with abnormal activation of the innate immune system, leading to clinical inflammation and high levels of acute-phase reactants. The innate system reacts even though there are no notable autoantibodies or antigen-specific T cells (Touitou, 2008; Kastner et al., 2010; Dainichi et al., 2014) and normal inflammation pathway is followed after the abnormal activation of the innate system. The most common periodic fever disease is FMF followed by TRAPS (Jesus et al., 2008; Standing et al., 2013). TRAPS episodes generally last longer than FMF and FMF patients tend to respond well with colchicine while TRAPS treatment is problematic, thus this work is mostly directed towards improving TRAPS disease treatment.

The first description of TRAPS illness dates back to 1982, when a large Irish family came to light with several of its members affected by a hereditary periodic fever syndrome (Aróstegu, 2011). This condition was initially among the Irish-Scottish population, it has been reported in nearly all population groups, including Black Americans, Japanese and persons of Mediterranean ancestry (Kanazawa and Furukawa 2007; Ozen and Bilginer, 2014). TRAPS is an inherited autosomal dominant disorder caused by mutations in the TNF receptor, coded by the TNFRSF1A gene (Meiorin et al., 2013; Standing et al., 2013). In normal conditions, TNF receptor activation by TNF leads to the activation of a protease that favors the shedding of the receptor from the cell surface. This process produces a reduction in TNF cell signaling, and the shed receptor is able to bind a free TNF and limit the inflammatory response. Patients affected by this syndrome have a defect in receptor shedding that results in a continuous TNF signaling,

leading to an inflammatory response (Meiorin et al., 2013). Periods of inflammation are predominantly triggered following unnoticed pro-inflammatory signals. The levels of serum markers of inflammation such as C-reactive protein are always increased during attacks, however autoantibodies remain mostly undetectable (Touitou et al., 2013).

Normally TRAPS begin in the early childhood with prolonged symptomatic episodes lasting 1-3 weeks and symptom free intervals varying within individual patients, these episodes may be triggered by factors such as stress and infections (Meiorin et al., 2013). During symptom free intervals, when the physical state and inflammatory variables are normalized, the patients may retain their normal way of living. Clinically, TRAPS is characterized by recurrent episodes of fever, rash, arthralgia, abdominal pain and conjunctivitis that usually last relatively longer, from 5 to 21 days. The most common TRAPS manifestation is cutaneous, including symptoms such as a centrifugal migratory, erythematous patch overlying the area with urticaria-like plaques and generalized serpiginous patches and plaques occur. Figure 1.2 and 1.3 shows the photographic images reported by Kanazawa and Furukawa (2007) and Yao and co-workers (2012), respectively. These lesions are painful and hot, and when they involve the limbs, they are associated with secondary conditions such as myalgias (Kanazawa and Furukawa, 2007; Yao et al., 2012; Meiorin et al., 2013).

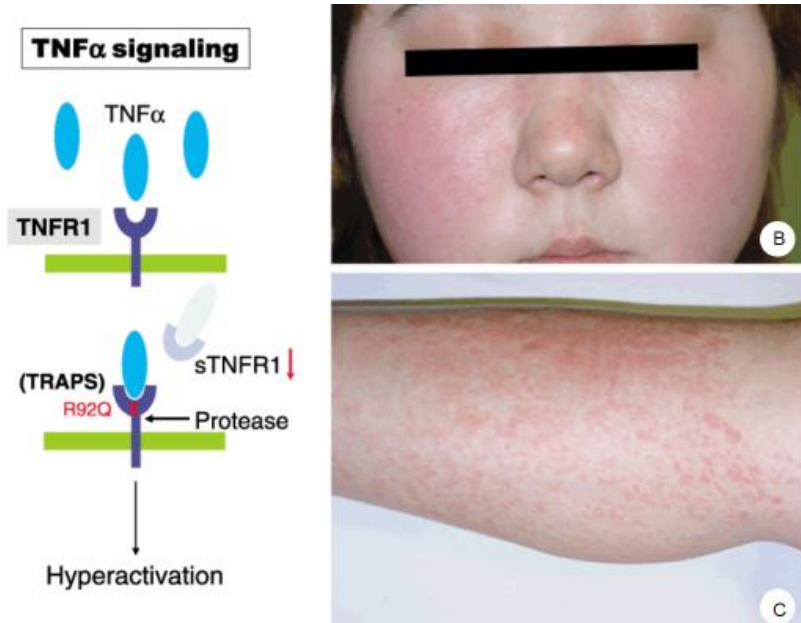


Figure 1.2: (a) Casting of tumor necrosis factor receptor (TNFR) and atypical signaling in TRAPS. (b) Edematous erythema noticed in cheeks and periorbital area of a TRAPS patient. (c) Multiple serpiginous patches and plaques in lower extremities (Adapted from Kanazawa and Furukawa, 2007).



Figure 1.3: (a) Vesicles on the abdomen. (b) Linearly arranged papules on the neck. (c) Diffuse erythema on the nose. (d) Serpiginous rash (Adapted from Yao et al., 2012).

A definitive treatment for TRAPS has yet to be identified (Ozen and Bilginer, 2014). The main treatment for TRAPS has been steroids until 1999 when the big search for alternative treatments began, as steroidal treatment resulted in many side effects including dependency syndrome especially in younger patients (Aróstegu, 2011). Currently TRAPS treatment depends on the severity and frequency of the disease attacks. Patients with moderate disease and less frequent episodes use corticosteroids when necessary during the attacks only, and patients with severe condition and high frequency of attacks require prolonged high doses of steroids, therefore patients become prone to steroid withdrawal symptoms (Ozen and Bilginer, 2014). Non-steroidal anti-inflammatory drugs and TNF- α inhibitors have been reported to relieve symptoms in some cases. Presently used TNF- α inhibitors are not effective in all patients, they involve invasive administration procedures (i.e. subcutaneous treatment twice a week using etanercept) and patient compliance is a major problem (Grateau, 2004; Bulua et al., 2012; Dermz 2013). Therefore corticosteroids remain the main and most effective treatment in this condition, as they are the almost only anti-inflammatory class that inhibits all the major components of inflammation (Greaves, 1976).

Corticosteroids are hormonal based substances, with sturdier anti-inflammatory effects than non-steroidal medicines (Congradyova and Jomova, 2012). In dermatological disorders their clinical significance is associated with their anti-inflammatory, vasoconstrictive, anti-proliferative

and immunosuppressive effects (Senyigit and Ozer, 2012). Besides their major anti-inflammatory benefits, this class of drugs is associated with a variety of serious side effects such as: immune system suppression (prone to infections), bone loss, cataract, mood changes, high blood pressure and bone marrow suppression (Rabe et al 2005; Congradyova and Jomova, 2012). The severity of these side effects depend on the dosage, duration of use, dosing regime and the highest risk factor being prolonged use of the corticosteroids along with individual patient variability (Senyigit and Ozer, 2012).

Over the years, research has focused on approaches to improve the potency of steroids while diminishing adverse effects, such that different types of corticosteroids have been developed. However, “ideal” drug delivery of corticosteroids especially for chronic treatment has not yet been produced. Hence the current research is directed towards improving the delivery of the corticosteroids drugs, thus increasing the safety of these agents in chronic treatment of conditions such as TRAPS (Senyigit and Ozer, 2012). Ideal corticosteroids for TDDS should be able to permeate the stratum corneum (SC) and reach adequate concentrations in the epidermis without reaching high systemic concentrations (Brazzin and Pimpinelli, 2003). Such characteristics can be obtained by optimizing a stimuli responsive nanocolloidal gel system. The aim of this project is to develop a new formulation that would improve the risk/benefit ratio of corticosteroids delivered through the transdermal route. This system would be formulated into a dermal sludge that is more likely to suit the patient’s needs. A dermal sludge being a viscous gel suspended with solid particles (nanocolloidal gel system).

1.2. Rationale and Motivation for the Study

This study relates to a dermally applied sludge for transdermal drug delivery system (TDDS) and this route of drug delivery was chosen due to its unique properties such as avoiding first pass metabolism, and increased patients’ compliance as they more acceptable compared to other forms of drug delivery e.g. injections. This will consist of three synergistic components, resulting in a metal-drug complex loaded into a stimuli responsive nanocolloidal gel system. Firstly the drug will be complexed by coordinating the drug into the centre of the metal and then loaded into the nanocolloidal gel system. The proposed structure for the drug-metal complex is shown Figure 1.4, where one of the corticosteroids, hydrocortisone succinate sodium salt is demonstrated chelated to a metal (ratio of metal to drug is 1:1). This complex alone is expected to improve the anti-inflammatory/ anti-oxidants properties of the parent drug, while the stimuli

responsive nanocolloidal gel systems are expected to release the complex in a controlled manner at the specific sites of inflammation in TRAPS.

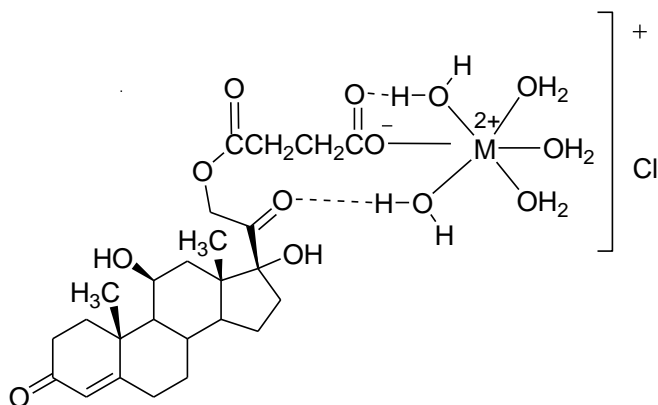


Figure 1.4: Hydrocortisone succinate is shown coordinated on the metal (M), M may be Fe, Cu, Co, Mn, or Zn.

The ultimate goal of this research is to design a metal-drug loaded stimuli responsive nanocolloidal gel system termed a dermal sludge that will dramatically improve the management of TRAPS. The factors contributing to this enhancement may include one or more of the following:

- The synergistic effect of the corticosteroid drug-metal complex and the coordination residue once the complex is degraded in the biological environment.
- The protection from any degradations and sustained release of the complex once it is loaded into the stimuli responsive nanocolloidal gel system.
- Improved skin permeability due to the modification of the hydrophobicity/hydrophilicity of the complex and polymeric system.

The novelty of this study involves the delivery of a corticosteroid drug-metal complex in a stimuli responsive nanocolloidal gel system using an optimized combination of polymer(s) and phospholipids to yield the desired release properties for TRAPS management. This study was motivated by a number of social and scientific factors including:

- The possibility of re-activating an old drug into new a superior bioactive by coordinating the drug with a transition metal hence improving its properties. This may be of an economic advantage over designing new drugs.
- The ability of a transition metal to enhance the anti-inflammatory/anti-oxidant activities of drugs when coordinated to them.

- The possibility of making a convenient easily acceptable TDDS for TRAPS management as it is a lifelong condition.
- The generation of logical data to be published in high-impact peer reviewed/accredited journals for further progression in the science of medicine.

1.3. The Dermal Sludge for Targeted Drug Delivery in TRAPS: Concept and Outline

Several drug delivery systems are currently being investigated to bypass the limitations of conventional dosage forms and enhance the potential of the respective drug. Based on the findings of Lee and co-workers (2010), with a nanotechnology designed drug delivery system, it is possible to tailor drug deposition, disposition, and permeation kinetics through formulation engineering (altered composition, drug loading, droplet size, etc.) thus this design is expected to circumvent most of the limitations associated with current corticosteroid treatment. This new drug delivery system being considered here is expected to have:

- Improved antioxidant/anti-inflammatory properties.
- Improved bio-distribution such that more drug molecules reach the target site.
- Improved local bioavailability of the drug
- Minimal systemic side effects.

A liposomal nanogel was the stimuli responsive nanocolloidal gel system of choice in this study as it has been established that it enhances drug permeation through the skin in TDD system (Pierre and Costa, 2011; Zhao et al., 2013). The superiority of this system would be achieved by combining the advantages of the nanoliposomes and a gel-based matrix. This system is expected to target the oxidative and low pH occurring during TRAPS inflammatory episodes. This would overcome the dose-limiting systemic toxicity of the currently used corticosteroid drugs, while increasing the concentration of the drug at the site of action. With the drug-metal complex loaded into the liposomal nanogel, the pharmaceutical efficacy of the drug will be potentiated and side effects associated with the drug will be reduced as well (Hostynek, Dreher, Maibach, 2011; Congradyova and Jomova, 2012; Feng et al., 2014).

The metal-drug loaded liposomal nanogel is expected to release the complex in a controlled manner as seen in Figure 1.5. During TRAPS disorder, reactive oxygen species (ROS) are formed when oxygen undergoes a partial electron reduction to super oxide anion, and subsequently forms hydrogen peroxide (H_2O_2), and other oxidants (Mahmoud et al., 2012).

Hence the formulated sludge would be triggered by both ROS molecules and low pH which are typical in inflamed tissue, this design would lead to a better targeted drug delivery.

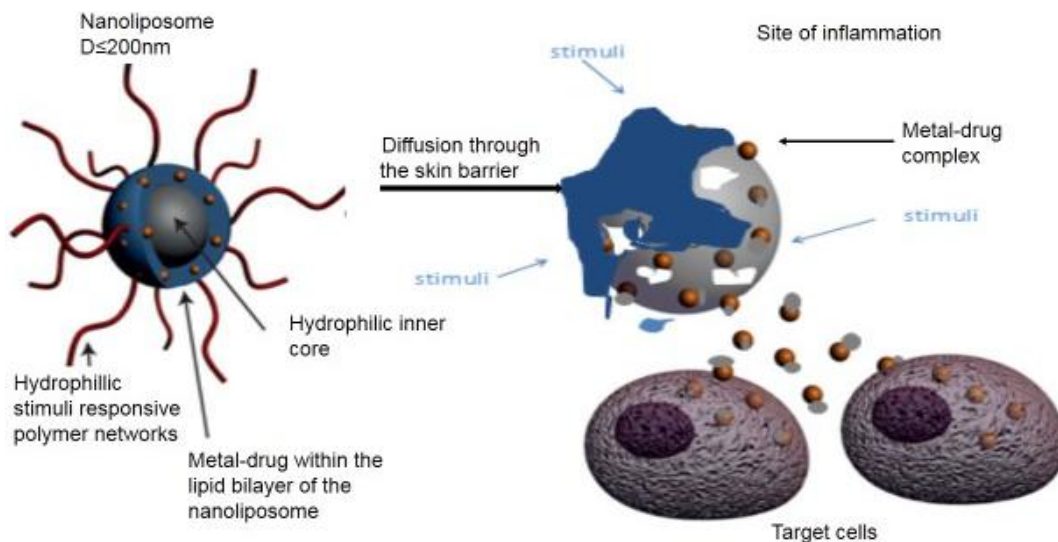


Figure 1.5: Schematic diagram representing the proposed metal-drug complex loaded nanoliposome, and briefly its mechanism of release. The nanoliposome formulation would detect the inflammatory mediators through the stimuli responsive nanocolloidal gel system chemical groups, and then it would swell, erode, and release the coordinated metal-drug complex.

1.4. Potential Benefits of this Study

Although the complexation of metal centers to drugs is not an entirely new area, the application towards and its development in drug delivery systems is relatively new and full of further research opportunities. The reactivation of drugs into novel metal-drug complexes with improved properties may result in complexes that may not only be used for the traditional parent ligand (free drug) function but for treatment of other inflammatory related conditions, for instance Cu(II) complexes of NSAIDs have shown anti-cancer properties through pharmaceutical modification (Roy, Banerjee and Sarkar, 2006). This could be a less costly process of obtaining bioactives for other diseases. Generally the effects of metal coordinations are expected to improve treatment options, therefore creating unique research expansion, diagnostic and therapeutic opportunities.

Loading the metal-drug complex into the stimuli responsive nanocolloidal gel system further enhances the overall therapeutic outcome of the complex by releasing the complex in a controlled manner. As one of the major limitations associated with long-term therapy in conditions such as TRAPS are side effects associated with the anti-inflammatory drugs and with

this design these limitations may be circumvented. The stimuli responsive nanocolloidal gel system could also be applied in the treatment of other inflammatory diseases such as acne, where inflammation is involved. Overall the data obtained from this study could be used to build on information for further development in the science of drug delivery systems.

Possible drug applications of this delivery system include:

- The complex may be used to treat other conditions, as a number of complexes possess other functions such as anti-parasitic, anti-cancer and anti-microbial agent i.e. Gold complexes are used in malaria and as a chemotherapeutic agent against other tropical diseases such as Trypanosomiasis and Leishmaniasis.
- Site-specific sustained release of metal-antibiotic drugs to improve the design of compounds and reduce toxic drug side effects.
- Controlled drug delivery for treatment of other skin inflammatory conditions such as acne.

1.5. Aim and Objectives

The aim of this study was to design and prepare a synergistic metal-drug complex-loaded stimuli responsive nanocolloidal gel system, termed a dermal sludge, which possesses superior permeation, anti-inflammatory and anti-oxidant properties compared to the free ligand (active drug). The objectives for the study are:

1. Preparation of a metal-drug complex and evaluation of its physicochemical (i.e. Fourier transform infrared spectroscopy (FTIR)), and biological (i.e. 1,1-diphenyl-2-picrylhydrazyl (DPPH) free radical scavenging assay) profiles
2. The design and synthesis of the polymer and the initial nanocolloidal preparation, as well as manipulation of the parameters to achieve an optimum control of particle size and surface properties.
3. Loading of the metal-drug complex into the designed nanocolloidal and evaluation of the nanocarrier produced in order to determine the efficiency of preparation methods used in terms of drug encapsulation efficiency, particle size, zeta potential, and morphology.
4. Formulation of the TDDS, termed the nonosludge, using the designed nanocolloidal system
5. Determination of further physicochemical and physicomechanical profiles such as thermal and rheological properties of the dermal sludge.
6. Evaluation of the drug release properties of the dermal sludge *in vitro* and *ex vivo*.
7. *In vivo* animal studies for the preclinical assessment of the dermal sludge.

1.6. Overview of this Dissertation

Chapter one: this chapter introduces and outlines the background to the study. Description of the genetic disorder, its current treatment options and limiting factors is provided. The chapter also discusses how the use of the metal-drug complex loaded stimuli responsive polymeric colloidal nanogel system (stimuli responsive nanocolloidal gel system) (dermal sludge) for transdermal drug delivery systems (TDDS) would enhance the treatment of TRAPS. It outlines the rationale, motivation, aim and objectives of the study and the potential benefits of the study.

Chapter two: this chapter presents a literature review focusing on the application of drug-loaded polymeric colloidal nanogels (DPCNs) in transdermal drug delivery systems (TDDS). It entails the limitations of conventional TDDS, fabrication techniques of DPCNs networks, ideal properties of DPCNs, and therapeutic significance of polymeric nanogels in TDDS. It further details how DPCNs have recently advanced with drug delivery systems in order to manage chronic diseases such as TRAPS.

Chapter three: this chapter a [copper(glyglycine)(prednisolone succinate)] complex for application in transdermal drug delivery was synthesized. The formulated complex was confirmed by X-ray diffraction, Nuclear magnetic resonance (NMR), FTIR and UV-visible absorption spectroscopy. Furthermore the complex was differentiated from parent drug (prednisolone) by Differential scanning calorimetry (DSC), thermogravimetric analysis (TGA), antioxidant activity assay, mass spectrometry and *in vitro* permeation studies. Additionally *in vitro* cytotoxicity studies were undertaken.

Chapter four: this chapter describes the development and characterization of Eudragit® E100-cystamine (EuE100-cyst) and dual pH/redox responsive nanoliposomes. The EuE100-Cyst was conjugated with the phospholipid film to form the a dual pH/redox responsive nanoliposomes and the [copper(glyglycine)(prednisolone succinate)] complex was loaded into the EuE100-Cyst for controlled release. The drug loading into the NLs was confirmed using FTIR and the actual drug entrapment efficacy was measured. The morphology and size of the NLs was confirmed using TEM and Zetasizer analysis, respectively. The pH/redox sensitivity of the NLs was established by the change in particle size using the zeta sizer and drug release studies. Furthermore cytotoxicity studies were performed on both the loaded and non-loaded nanoliposomes.

Chapter five: this chapter describes the formulation and optimisation of the stimuli responsive nanocolloidal gel system (dermal sludge) for transdermal delivery of [copper(glycylglycine)(prednisolone succinate)] complex. A 3-factor, 3-level Box-Behnken design was used to derive a second-order polynomial equation to construct contour plots for prediction of responses. Independent variables studied were the two different lipids ratios, cholesterol ratio and sonication time. The dependent variables studied were the Z-average particle size, polydispersity Index (PDI), zeta potential, entrapment efficiency (% EE) and amount of complex released per hour in the presence of pH(5) and 10mM GSH. Response surface plots were drawn and statistical validity of the polynomials was established to find the compositions of optimized formulations which were evaluated using a Franz-type diffusion cell and drug release studies.

Chapter six: this chapter describes the *in vivo* studies performed which involved dermal application of the sludge for transdermal delivery of the [Copper(glycylglycine)(prednisolone succinate)] complex in Sprague–Dawley rats. At predetermined time points blood samples were taken and the rats were euthanized. On completion of *in vivo* experimentation, the euthanized rats were excised for skin samples to be used for further histopathological examination. In the chapter, detection and quantification of the drug from withdrawn plasma samples, and in tissues were performed using Ultra-performance liquid chromatography (UPLC).

Chapter seven: this chapter presents the concluding remarks and recommendations for further research on transdermal drug delivery system of advanced polymeric nanocolloidal systems with a focus on the recommendations for further work.

CHAPTER 2

A REVIEW OF POLYMERIC COLLOIDAL NANOGELS IN TRANSDERMAL DRUG DELIVERY

2.1. Introduction

Nanogels are colloidal, cross-linked particles with a size that is ideally less than 200 nanometres (nm). Generally, they are made from synthetic or natural polymers, (Vinogradov, 2010; Binions, 2012; Sultana et al., 2013; Zan et al., 2014; Pedrosa et al., 2014) which are chemically or physically crosslinked polymer networks depending on the gel applications (Samah and Heard, 2013; Sultana et al., 2013; Chen et al., 2014). When these colloidal nanogels are loaded with active compounds, they are referred to as Drug-loaded polymeric colloidal nanogels (DPCNs). Much interest has been directed towards the potential use of DPCNs to deliver a variety of drugs to diverse parts of the body system for either controlled or sustained drug delivery systems (Huppertz and de Kruif, 2008; Singka et al., 2010). Additionally, they may change their size (swell and de-swell) in response to environmental incentives such as ionic strength, pH, type of solvent in contact with the gel and surrounding temperature (Murray and Snowden, 1995; Gonçalves et al., 2010; Singka et al., 2010; Samah and Heard, 2013). These environmentally responsive properties depend on the chemical nature of the monomers, polymers and cross-linkers used to synthesize the DPCNs (Zhang and Granick, 2006; Kim et al., 2013). The overall rational design of DPCNs takes into account the efficient synthesis and functionalization of DPCNs, while maintaining good stability and control of nano- particle size. To this end these applications have led to the development of innovative DDS that has been coined as smart drug delivery systems (Yan and Tsujii, 2005; Almeida et al., 2012; Lu et al., 2013; Mura et al., 2013; Meléndez-Ortiz et al., 2014).

Moreover, DPCNs employed for TDDs applications have shown that DPCNs have the ability to reach the smallest capillary vessels, which facilitates penetration through the skin tissues and they remain in the skin longer promoting more drug absorption (Gonçalves et al., 2010). A number of recent studies have indicated that DPCNs are successful in treating skin cancer through the TDDS route, of which this application may be extended to other chronic skin conditions treatment such as genetic auto-inflammatory skin disorders (Mangalathillam et al., 2012; Sabitha et al., 2013; Zhang et al., 2013b). Polymeric nanogels have been successfully

formulated for TDDS using a number of polymers including chitosan, chitin, poly(N-isopropyl acrylamide-co-acrylic) acid (poly(NIPAM-co-AAc)) and poly (lactic-co-glycolic acid) (PLGA) (Mangalathillam et al., 2012; Shah et al., 2012; Sabitha et al., 2013; Samah and Heard, 2013). Despite all these encouraging research reports, there are still some shortcomings that need to be circumvented in order to improve the therapeutic effectiveness of the current DPCNs in TDDS.

TDDS is defined as the non-invasive application of a drug containing formulation to the skin for direct delivery of the drug through the skin into system (Bajaj et al., 2011; Shingade, 2012). This system releases the drug at predetermined rates through the dermis for either systemic or localised tissues underlying the skin (Bajaj et al., 2011). TDDS have attracted much interest as a route of drug administration for both systemic and local effects due to their advantageous properties compared to other conventional dosage forms, such as parenteral and oral. Bio-actives from DPCNs can penetrate deeper into the skin and give better absorption (Shingade, 2012). Additionally, TDDS are non-invasive, generally cost effective, and they can be self-administered and easily accepted by patients (Shingade, 2012). Further they are capable of providing a prolonged therapeutic drug release, releasing for up to a week or longer periods of time (Phatak and Chaudhari, 2012; Shingade, 2012; Chen et al., 2014). Overall these properties lead to improved patient compliance and better therapeutic outcomes. However one of the main drawbacks of TDDS is the low penetration rates of most active drug molecules through the skin.

Most TDDS present with an occlusive effect, they are highly concentrated and drug release is driven by concentration gradient between the skin and patch, diffusing from formulation to the skin (Bajaj et al., 2011). For the drug to pass through the skin it has to bypass the stratum corneum (SC) limitation barrier. SC is the outermost layer of the skin layer and acts as skin barrier resulting into low penetration rates of the drug (Prausnitz and Langer, 2008). The skin's structure and its function as a barrier have been widely reported in the literature (Barry, 1987; Williams, 2003; Bharadwaj and Gwalior, 2012; Zhang et al., 2013b). Human skin encompasses a number of layers with hair shafts and gland ducts penetrating through the layers, the hair follicles and sweat ducts open directly into the skin surface, hence they are appendage for drug delivery through the skin Figure 2.1 (Scheuplein, 1965; Kabanov and Vinogradov, 2009). The main skin layers starting from outside to inside are: the cellular epidermis, stratified avascular, dermis of connective tissue, and fatty subcutaneous layer (hypodermis) (Bissett et al., 1987; Maghraby et al., 2006; Kabanov and Vinogradov, 2009). Despite the skin acting as a barrier, it

is also used as a special delivery pathway that may be used for therapeutic agents and any other molecules applied to the skin. There are two main routes (Figure 2.1) that are used by the colloidal molecules to permeate across the SC the intracellular and intercellular pathways, and the other being the follicular (appendageal) pathway (Scheuplein, 1965; Maghraby et al., 2006; Alexander et al., 2012). The nanometer particulate size of the DPCNs allows them to bypass the skin barrier limitation for drug delivery, hence they may be the potential solution for a low drug penetration rate.

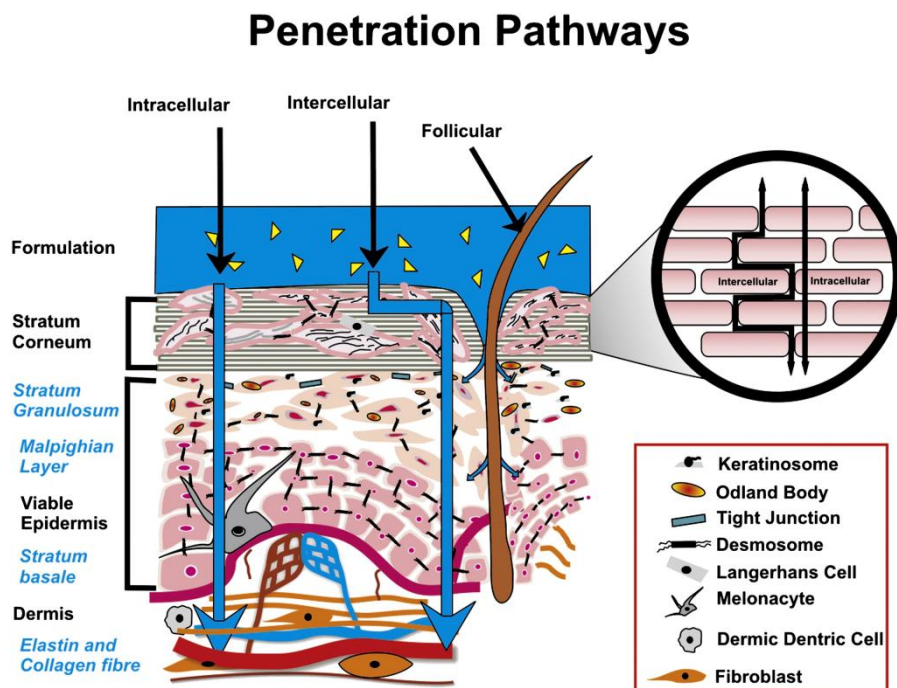


Figure 2.1: Representation of drug penetration pathways through the skin with the two major routes shown on the upper right corner. (Adapted with the permission from Alexander et al. (2012). Copyright (2012) Elsevier).

2.2. Limitations of Conventional Transdermal Drug Delivery Systems

Conventional drug formulations that are currently being used for TDDS include formulations such as creams, gels and ointments, and some new formulations such as sprays, foams, and patches (Lee et al., 2010). These formulations have shown notable limitations leading to sub-therapeutic outcomes mostly due to permeation and specificity issues. Presently most of these transdermal therapies are associated with poor skin permeation, insufficient reach to disease tissue (lack of specificity), low retention at target site, poor intracellular/intercellular penetration and skin irritation potential (pain, itching, burning, hypersensitivity reactions and inflammation) and low therapeutic index (high toxicity) (Donnelly et al., 2012; Isaac and Holvey, 2012; Shingade, 2012). Lack of dosing precision is one of the major limitations associated with gels

and creams, as the systemic bioavailability is dependent on the total dose applied on the skin (Thomas and Finnin, 2004). Even though dose precision is not an issue with patches the flexibility of dosing is restricted (Thomas and Finnin, 2004). These shortcomings may lead to the development of several undesirable therapeutic outcomes such as nonspecific cytotoxicity to critical normal tissues, sub-therapeutic outcomes, development of resistance and other drug associated adverse effects.

Several drug delivery systems are currently being investigated to overcome the limitations of conventional dosage forms and enhance the potential of the respective drug. These new drug delivery systems being considered are expected to have: a) improved properties; b) improved bio-distribution such that more drug molecules reach the target site; c) improved local bioavailability of the drug; and c) minimal or no systemic side effects (Kala and Sundeeep, 2012). Based on the findings of Lee and co-workers (Lee et al., 2010) with a nanotechnology designed drug delivery system it is possible to tailor drug deposition, disposition, and permeation kinetics through formulation engineering (altered composition, drug loading, droplet size, etc.) thus overcoming most of the limitations associated with current transdermal treatment.

According to various findings that have been reported on nanogels it can be concluded that DPCNs deserve a special consideration for use in TDDS because of their favorable physicochemical properties, such as their narrow size distribution capable of penetrating through the skin barrier (Escobar-Chávez, 2012). Nanogels have the tendency to absorb water when placed in an aqueous environment and their affinity to aqueous solutions, superior colloidal stability, inertness in the blood stream and the internal aqueous environment, and suitability for bulky drugs incorporation, renders them ideal candidates for TDDS. Hence the use of more specific, superior DPCNs aids the TDDS by improving the drug permeation through the skin, drug bioavailability and reduces severe side effects i.e. toxicity associated with conventional therapeutic agents.

2.3. Fabrication Techniques of Polymeric Nanogel Networks in DPCNs

Generally there are two basic goals that should be satisfied in the design of a TDDS namely: (i) efficient drug entrapment and loading to the polymeric matrix accompanied by the release of the drugs in a controlled fashion and (ii) ability to release through a local or externally applied trigger by changing the binding affinity between the drug and the polymeric matrix. Therefore, a clear

understanding on the interaction of the nanogel networks is important for the development of an efficient drug delivery system (Tian et al., 2007).

Biodegradable and biocompatible polymeric nanogels used for drug delivery purposes in pharmaceuticals are formulated from a number of natural and synthetic polymers (Nagarwal et al., 2009). Synthetic polymers are mostly preferred because their physical and chemical properties can be easily manipulated compared to the natural polymers which are hard to work with (Sanson and Rieger, 2010). These polymers enhance the aqueous properties of the delivery systems by modifying the viscosity, emulsification, stabilization and gelation of the nanogel (Kadajji and Betageri, 2011). Examples of synthetic polymers that have been used for transdermal formulations are poly (ethylene glycol) (PEG), polyvinyl pyrrolidone (PVP) polyacrylic acid (PAA) and polyacrylamides (PAAm). Examples of natural polymers are xanthan gum, pectins, chitosan derivatives and dextran (Kadajji and Betageri, 2011; Ferreira et al., 2013; Zhang et al., 2013a). A brief discussion on the techniques employed for nanogels preparations using polymers are presented below, considering that there are several methods for the preparation of nanogels, four commonly used techniques will be highlighted (Kabanov and Vinogradov, 2009; Ferreira et al., 2013).

2.3.1. Physical self-assembly of interactive polymers

This method is the most utilized procedure in nanogel production due to its simplicity which involves mixing of the polymer as a carrier and the drug that has to be loaded. The driving and /or limiting forces of the physical interaction of the polymer networks include hydrophobicity, hydrogen bonding, van der Waal forces of interaction and electrostatic interaction within the polymer networks (Akiyoshi et al., 1993; Chacko et al., 2012; Sultana et al., 2013). The number of functional groups in the polymer chemical structure also affect the physical assembly of the nanogel (Binions, 2012). Hydrophilic polymers are the most favoured polymers in this method of nanogel formulation as they produce the most stable crosslinked nanogels due to the strong hydrophilic interactions involved. The degree of crosslinking determines the nanogel properties i.e. the nanoparticle size of the nanogel and the degree of swelling and thus drug release profile and the overall therapeutic outcome. A number of studies on physical self-assembly of polymers in nanogel formulations have been reported and an example is the cholesterol-bearing pullulan (CHP) nanogel which has the potential to form complexes with various proteins, drugs, and DNA (Akiyoshi et al., 1993; Nishikawa et al., 1996; Akiyoshi et al., 1999; Akiyoshi et al., 2000; Kuroda et al., 2002; Chacko et al., 2012).

2.3.2. Monomer polymerization in a homogeneous or heterogeneous microscale or nanoscale environment

This technique describes the polymerization of monomers using preformed polymers in heterogeneous colloidal environments, mostly in water-in-oil inverse microemulsions (Sanson and Rieger, 2010; McAllister et al., 2002). In this method the biomacromolecules and micromolecules of the drug are entangled within the nanogel networks (Khmelnitsky et al., 1992; Mitra et al., 2001). It is a relatively intense method and involves a purification step to remove the unreacted monomer(s) and some of impurities such as the surfactants used for formulation stability (Ryu et al., 2010; Chacko et al., 2012). Figure 2.2. shows a nanogel formulated using this method. This technique provides control over the nanogel composition, size, and swelling behavior by varying the crosslinker and charged monomer concentrations in the polymerization step (McAllister et al., 2002). Yuan et al. (2012) reported the efficiency of the polymerization technique in the production of polyphosphate nanogels using a moisture sensitive cyclic phosphoester monomer and cyclohexane as the microemulsion liquid. The nanogel demonstrated controlled protein adsorption, and offers an emerging route for use as functionalized carriers to the blood circulation.

2.3.3. Chemical cross-linking of preformed polymers

Generally this technique includes core crosslinking or shell crosslinking of the preformed linear polymers to obtain nanogels. The crosslinking mostly occurs through the covalent bond crosslinking method (Cheng and Mahato, 2013). Figure 2.2 shows the preparation of nanogels from polymer precursors and crosslinking. This approach is of particular importance in the preparation of functionalized drug delivery carriers (Cheng and Mahato, 2013). A number of nanogels have been formulated and used in drug- loaded polymer carriers (Cheng et al., 2013). Work by Kabanov and Vinogradov (2009) and Vinogradov et al. (2002) have presented examples of cross-linked, functionalized polymers. It has been demonstrated that chemically crosslinked nanogels can generally provide opportunities to vary the structure and properties of nanogels and due to their covalently crosslinked structures they show no dissociation and destabilisation in aqueous media and in the blood stream (Cheng and Mahato, 2013).

2.3.4. Template-assisted nanofabrication of nanogels particles (imprint photolithographic techniques)

In this method polymer nanogel particulates are fabricated according to their sizes, hence controlling the particle composition, shape, size, and surface properties (Kabanov and Vinogradov, 2009). According to Band and Bronich (2014) this may take place in a two-step process, which is the condensation of block ionomers into spherical self-assembled block ionomer complexes (BIC) and cross-linking reaction of BIC templates by bifunctional agents. Although this is not one of the commonly applied fabrication methods, Maggi et al. (2011) reported that chitosan covalent nanogels were cross-linked with genipin using template chemical cross-linking of chitosan in polyion complex micelle (PIC) nanoreactors. This method yielded chitosan nanogels from solely biocompatible materials avoiding the use of organic solvents, and thus offers an ideal method for synthesis of moisture sensitive polymers.

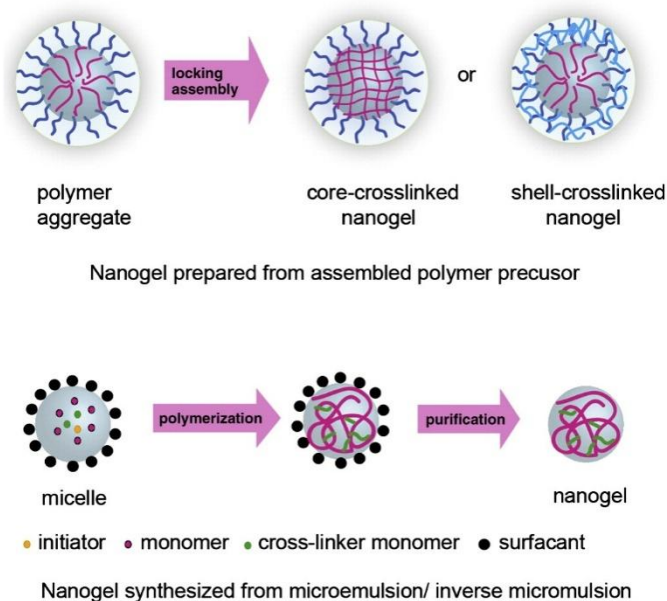


Figure 2.2: Schematic representation of the synthesis of nanogels via the polymer precursor method and the emulsion method respectively. (Adapted with the permission from Chacko et al. (2012). Copyright (2012) Elsevier).

2.4. Polymeric Colloidal Nanogel Properties

2.4.1. Swelling and de-swelling properties

The swelling/de-swelling characteristic of nanogels allows the colloidal particles to take the form of microsponges. Swelling promotes the diffusion of the liquid phase into the DPCNs bulk and de-swelling (shrinking) causes the release of the drug with the flow of liquid into the target site, this is called the “volume transition” of the DPCNs (Alvarez-Lorenzo and Concheiro, 2008;

Maggi et al., 2011; Farag and Mohamed, 2012; Yao et al., 2013; Band and Bronich, 2014). DPCNs are capability of rapidly swelling and de-swelling depending on the surrounding environment (Sultana et al., 2013; Kettel et al., 2014). This allows them to be responsive to the surrounding environment; they may respond to stimuli such as pH, and temperature changes and this ensures a targeted controlled drug delivery from the DPCNs (Oh et al., 2007; du Toit et al., 2014). The swelling property of the DPCNs is controlled by the chemical structures of polymeric precursors used to formulate the gel (polymer networks) and external environments (pH, ionic strength, and temperature) (Kabanov and Vinogradov, 2009; Farag and Mohamed, 2012; Yao et al., 2013). These properties are of vital importance for drug loading and release optimisation, and therefore the drug release profile is dependent on the degree of swelling/de-swelling of the nanogel particles (Kabanov and Vinogradov, 2009; Messenger et al., 2013). Generally, nanogels have displayed improved drug loading capacities compared to other nanosized drug carriers such as micelles due to the increased space for incorporation of bioactives when the particles are swollen (Kabanov and Vinogradov, 2009). Farag and Mohamed (2012) developed nanogels comprising of a binary system of carboxymethyl chitosan (CMCh) and poly- (vinyl alcohol) PVA which reached up to 500% swelling in the presence of acidic pH within two hours. The swelling was dependent on the crosslinking behavior of the polymers and environmental stimuli as the more crosslinker was added the more polar the polymer became and the more acidic the pH was the more swollen the nanoparticulates were, respectively enhancing the drug delivery. Another exemplary study was done by Samah and Heard (2013) where a high loading drug capacity increased with the degree of swelling due to the network behavior of polymers (polyNIPAM)- co-AAc in response to both temperatures and pH, and thus showing an improved transdermal drug delivery.

2.4.2. Biocompatibility and biodegradability

Carriers used for drug/gene delivery (polymers) to the intracellular compartments are required to deposit the drugs/genes inside the cells. These polymers are expected to remain intact in the extracellular environment and disintegrate intracellularly releasing the drugs/genes without any toxicity inside the body and for this purpose the polymers used have to be biocompatible and biodegradable (Behl et al., 2012; Urakami et al., 2013). Polymeric based nanogels are highly biodegradable and biocompatible, due to the high water content. The biodegradability of nanogels allows them to be responsive to stimuli such as pH and oxidants which promotes selective drug delivery carriers (Oh et al., 2007). This property also reduces the DPCNs toxicity (Vinogradov et al., 2002) as they are easily excreted from the body. A variety of polymers have

been studied and proven to be bio-compatible and degradable (Behl et al., 2012; Singh et al., 2013; Medeiros et al., 2010; Pujana et al., 2014; Steinhilber et al., 2013), thus making them excellent candidates for encapsulation into nanogels for biomedical applications (Rancan et al., 2014). In a study reported by Urakami et al. (2013) disulfide-based tetralysine and oligoethylenimine based prepolymers were formulated and the polymer precursors and nanogel particles were determined to be biodegradable, biocompatible, and stimuli-responsive nanocarriers for the delivery of drugs and genes. Figure 2.2 shows the structure of a biodegradable and compatible nanogel. However, to confirm the biodegradability and compatibility of any polymeric nanogel in drug delivery *in vitro* studies are required, which is another platform for research.

2.4.3. Morphology

The particle size and shape composition may be co-designed to enhance the utility of the DPCNs. DPCNs are colloidal, cross-linked particles with smaller particles which degrade into even smaller particles that are easily eliminated through the renal clearance (Hans and Lowman, 2002; Klinger and Landfester, 2012; Sultana et al., 2013). It has been determined that the smaller the size of the nanoparticles the slower is the elimination of the residuals by renal clearance (Kadam et al., 2012; Zhang et al., 2013b). It is vital for particle size to be controlled for sustained drug delivery, as smaller particles (20-200nm) avoid rapid renal clearance (Sultana et al., 2013). This improves the pharmacokinetics of the drug by extending the serum half-life. Considering the fact that DPCNs have significantly more particles in situ compared to other nanocomposites, they have the ability to exhibit an improved porosity. This high degree of porosity allows for efficient encapsulation of therapeutic molecules (Liang and Kiick, 2014).

2.4.4. The drug loading capacity

Nanogels have the potential of incorporating therapeutics of diverse nature using simple techniques (Soni and Yadav, 2014) and the loading capacity of a polymeric nanogel depends on the properties of the polymer used to formulate the gel. DPCNs may be loaded with drugs using controlled self-assembly, physical entrapment and covalent conjugation methods (Oh et al., 2007). The chemical structural relationship (the functional groups present) of the polymer determines the sites available for the binding of the drug to the polymer, hence drug loading capacity. More functional groups increase the capability of drug binding to the polymer. The structure of the nanogel should ensure efficient encapsulation stability such that the encapsulated drug will not leak ahead of time and this will ensure uttermost therapeutic efficacy

with negligible side effects (Nishikawa et al., 1996). Ideally a high loading capacity of drug is desired in drug delivery, and if the loading capacity of the drug on the polymer is high, then less of the nanocarrier is required to deliver the therapeutic treatment (Chacko et al., 2012). Hence it is important to optimize the loading capacity of the nanocarrier(s) used in order to minimize any polymer inherent side effects. The measured loading capacity on its own is not a sufficient indicator for a stable nanocarrier. Moreover encapsulation stability studies are necessary and also it is important that drug loading does not affect the ability of targeted nanogels to interact with the receptors (Nukolova et al., 2011) therefore further studies directed to this specific application may be beneficial.

2.4.5. Sustained and controlled drug release

The ability of nanogels to swell/deswell in an appropriate environment allows them to be likely candidates for the development of controlled/sustained drug delivery systems (Behl et al., 2012). A number of biodegradable, biocompatible and non-toxic polymeric nanoparticle gel-based drug delivery studies have been reported using a variety of polymers. Some mentionable examples include, poly(D,L-lactide) and poly(D,L-lactide-co-glycolide) where they were successfully investigated for releasing the drug from a PDCN in a sustained and controlled manner (Vinogradov et al., 2002; Binions, 2012). The use of nanogels to bring about controlled and or sustained drug delivery release has been extensively studied (Vinogradov et al., 2002; Shah et al., 2012;Khurana et al., 2013a; Khurana et al., 2013b; Samah and Heard, 2013; Singh et al., 2013) and the following advantages were noted: a) improved drug pharmacokinetics, b) lower side effects and c) safe degradation. Based on these reported advantages, renewed interest in TDDS is evident in both pharmaceutical and medical fields like dermatology (Medeiros et al., 2010). According to Singh and co-workers (2013) it is established that the release kinetics of DPCNs follow a diffusion predominant drug delivery mechanism. The gels behaved as homogeneous-planar matrices, coupled with maintenance of structural integrity, and the drug was released in a sustained manner. Although most studies have proved that nanogels can be effective systems for controlled and sustained drug release, these properties are highly dependent on the type of polymers used and their concentrations, and therefore these results allow for further optimisation studies and may be used as a benchmark for new research. Controlled TDD can be successfully attained using various pathways including:

- I. Physical stimuli induced volume phase transition (Sultana et al., 2013)
- II. Diffusion – drug diffuses throughout the network (Sultana et al., 2013)

- III. Erosion – drug molecules erode from the crosslinked nanogel network through the disruption of intermolecular bonds or intramolecular degradation (Maggi et al., 2011, 2013)

Controlled drug release is said to be dependent on the nature of the polymer structure such as the solubility, length, crystallinity and its hydrophobicity. Additionally the rate of polymer degradation is affected by the diffusion of the drug through the nanogel particles, extent of swelling of nanogels in aqueous media and the technique of nanogel fabrication. Controlled degradation is essential for an ideal nanocarrier for sustained release applications (Asadi et al., 2011).

2.4.6. Site specific targeting

Generally, DPCNs display a smaller particulate diameter promoting drug delivery to the target sites in TDDS (Escobar-Chávez, 2012). Furthermore nanogel particles have the ability to penetrate through the transcellular and paracellular pathways into the targeted tissues (Gonçalves et al., 2010) hence there is potential use of these nanoparticles for the design of site specific TDDS. The ability of nanogels to respond to stimuli allows them to turn on/off in response to surrounding signals and release the drug in a controlled manner only to the affected cells. Specific targeted nanogels play a major role in the drug delivery platform: (i) they have the ability to incorporate a variety of drugs including steroidal agents with severe side effects and chemotherapies; (ii) they may coat the surface of the drug and exhibit ligands targeting properties; (iii) they allow for long storage after lyophilization, prolonging the therapeutic activity; (iv) due to the crosslinking property they enhance the retention time of the drug within the nanogel core (Murphy et al., 2011); and (v) they avoid accumulating in non-target tissues thereby lower the therapeutic dosage and minimize harmful side effects (Soni and Yadav, 2014). Additionally nanogels can be effectively functionalized to attain any desired stimuli responsive characteristic such as temperature, pH, ionic and mechanical changes, and these modifications are mostly due to the nanogel large specific surface area (small particle size), colloidal stability and easily tunable size (Brunel et al., 2009; Richtering and Pich, 2012; Pan et al., 2013). Through integration of these specific nanogel functions, targeted drug delivery systems are achieved and they hold a great promise in a number of biomedical applications including dermatological therapeutical treatments.

2.4.7. Penetration enhancing property

The use of DPCNs can also significantly enhance the penetration of the drug through the skin (Phatak and Chaudhari, 2012; Shingade, 2012) without the use of chemical additives. They are effective carriers for transdermal preparations and the improved penetration of the formulated nanogel may be due to the elongated contact between the drug and the skin, more surface area of the nanoparticulates and improved skin hydration due to the gel occlusive property. Hence polymeric nanogels have great potential for use in transdermal drug delivery systems. A new proposed method of improving skin penetration with the use of colloids was reported (Steinhilber et al., 2013; Urakami et al., 2013). Figure 2.3 shows the new method where a nanogel with improved skin penetration effects was formulated without the use of penetration enhancers i.e. surfactant.

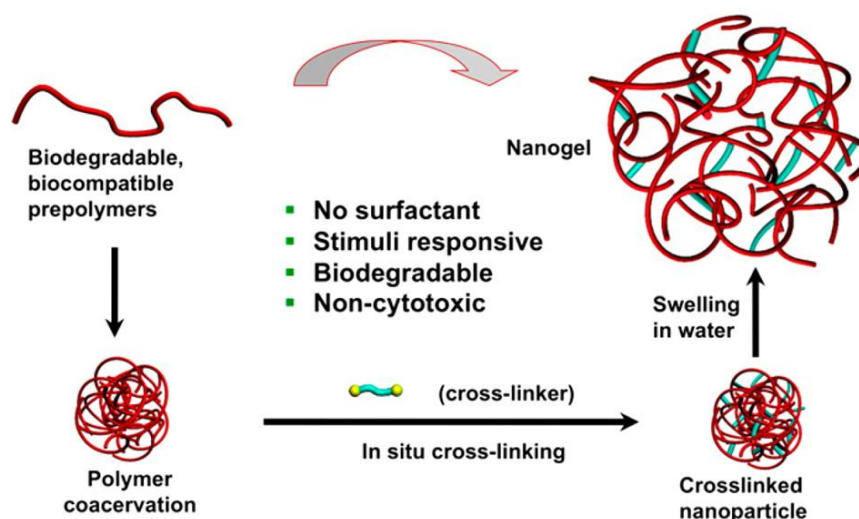


Figure 2.3: Representation of a novel surfactant-free route for the preparation of a biocompatible, biodegradable and stimuli responsive nanogel for potential targeted gene delivery. (Adapted with the permission from Urakami et al. (2013). Copyright (2013) American Chemical Society).

2.4.8. Miscellaneous nanogel properties

2.4.8.1. Superior colloidal stability

With the application of nanogels principles it is possible to produce more stable DPCNs for transdermal administration with or without the use of surfactants (Brunel et al., 2009; Rigogliuso et al., 2012).

2.4.8.2. No immunological responses stimulated

DPCNs do not stimulate any immune response such as skin reaction when applied on the skin and they may also protect the skin from any reaction that may result due to the drug as the drug is coated inside the crosslinked polymeric networks. Although, when desired, nanogels may be used to stimulate immune responses (Nochi et al., 2010; Vinogradov, 2010) and this allows for the use of nanogels for immune response controlling vaccine delivery.

2.4.8.3. Can be used as a carrier for both hydrophobic and hydrophilic drugs

DPCNs may be chemically altered to encapsulate a variety of ligands i.e. both hydrophobic and hydrophilic drug molecules (Soni and Yadav, 2014).

2.4.8.4. Solubility

Nanogels are very soluble in biological fluids, and the core or networks of the gel further enhance the solubility of hydrophobic drugs (Soni and Yadav, 2014).

2.5. Therapeutic significance of polymeric nanogels in transdermal drug delivery systems

Although oral drug therapy is the most customary form of drug delivery, it may not be the best option for all disease treatment and it has a number of undesirable side effects such as erratic absorption. TDD provides an alternative delivery route and may be preferred in the treatment of skin related disorders such as skin inflammatory disorders. Effective application of transdermal drugs relies on the delivery of an efficient drug concentration at the target site (Sahoo et al., 2008). Consequently the development of a TDD is of optimum significance in systemic delivery of drug molecules, to attenuate adverse effects associated with absorption, by pass the first pass metabolism and be easily accepted by patients hence facilitate drug efficacy. Various DPCNs have been reported to be effective nanogels in the field of TDD and their utilization and therapeutic effects were also exploited (Sahoo et al., 2008). For instance a DPCNs delivery system was formulated to deliver methotrexate drug which is one of the problematic drugs to deliver, the drug was efficiently delivered through the skin and *in vivo* studies were also done to prove the effect (Singka et al., 2010).

According to studies done so far it may be established that DPCN formulations may be an effective delivery system for the treatment of skin diseases, as they have the capacity to deliver a sufficient concentration of drug into the deeper tissue to treat the skin symptomology (Egbaria

and Weiner, 1990), however it can also be used for systemic treatment as sufficient drug penetrates through the skin. Generally, the penetration of nanoparticle-mediated drug delivery into the epidermis and dermis without barrier modification is usually less successful, and PDCNs drug delivery systems makes it possible to encapsulate penetration enhancers for molecule permeation through the skin to the target site (Egbaria and Weiner, 1990; Prow et al., 2010), also with relevant functionalization the DPCNs may also be used as penetration enhancers without any additional chemical enhancer (Barry, 1987). They may release drugs in a sustained or stimuli-triggered fashion and the nanoscale particles passively accumulate in specific tissues (e.g., tumors) through the enhanced permeability and retention effect (Shi et al., 2010) and translate into even fewer side effects related to the drug. Due to targeted drug therapy the overall biopharmaceutical (pharmacokinetics and pharmacodynamics) properties are improved, while toxicity, biological recognition of particular stimuli and immunogenicity of the delivery system are also enhanced which ultimately gives better therapeutic outcome (Sahoo et al., 2008; Lee et al., 2010; Shi et al., 2010).

In a study done by Sultana et al. (2013) it was resolved that nanogel-based drug delivery formulations may improve the safety and effectiveness of particular anti-cancer drugs such as doxorubicin, due to their chemical composition. Although these studies have also been evaluated using the *in vivo* animal studies, more studies still have to be conducted before these products enter clinical trials (Oh et al., 2010; Sultana et al., 2013). In this system the silver ions were released in a controlled and sustained rate and the nanoparticles remained on the skin surface for longer thus high efficacy is obtained coupled with reduced dosing frequency.

The TDD route of drug administration exhibits a number of advantages over the oral or parenteral drug administration including the reduction of side effects, elimination of first-pass metabolism, less frequent drug administration, sustained (controlled) drug delivery, and better patient compliance (Sahoo et al., 2008; Kala and Sundeeep, 2012). The use of polymeric colloidal drug delivery systems improves solubility of drugs including hydrophobic drugs like steroids in inflammatory skin disorders (Kayser et al., 2005; Shi et al., 2010). The potential use a nanocarrier system was further proved to be effective in TDDS without using any chemical penetration enhancers by Phatak and Chaudhari (2012). Despite these advantages some drugs may not be suitable for the TDD route because the skin normally allows for the permeation of particles less than 500 Da. This limits the number of likely drug candidates that can be employed (Phatak and Chaudhari, 2012). Furthermore there is a lack of empirical

evidence regarding the mechanism of release (Samah and Heard, 2013), therefore more investigations considering this form of drug delivery is necessary to overcome these limitations in TDD.

There is a growing interest in the development of efficient drug delivery systems targeted to the physiological sites of the body system. Several attempts have been investigated and ongoing research strives to develop the transdermal formulations of nanoparticles for the treatment of various skin diseases. In dermatology, nanosized particles have been widely studied resulting in many formulations entering clinical trials and some are still awaiting for approval (Onoue et al., 2014). A number of biodegradable, biocompatible and non-toxic synthetic and semi-synthetic polymers have been investigated for their efficiencies as TDD systems. Examples of successfully studied polymers are highlighted (Table 2.1).

Table 2.1: Specialized polymeric nanogel systems in transdermal drug delivery.

A. Improved drug permeation studies		
Polymer	Loaded drug/protein/gene	Reference
Poly(lactic-co-glycolic acid) (PLGA)-Chitosan	Spantide II and Ketoprofen	(Shah et al., 2012)
Poly(<i>N</i> -isopropylacrylamide-copolymerized-acrylic acid) (polyNIPAM)	Methotrexate (MTX)	(Warheit et al., 2008)
Tyrosine-derivative (PEG5K-b-oligo(desaminotyrosyl-tyrosine octyl ester suberate)-b-PEG5K triblock copolymer)	Sodium diclofenac	(Batheja et al., 2011)
Chitosan	Fluconazole	(Mohammed et al., 2013)
Eudragit RL 100 and Eudragit RS 100	Aceclofenac	(Barry, 1987)
Chitin	Curcumin	(Sabitha et al., 2013)
B. Improved drug efficacy with reduced side effects studies		
Celullose [hydroxypropylmethylcellulose] (HPMC), sodium carboxymethylcellulose	Chlorpheniramine maleate (CPM)	(Tas et al., 2003)

(NaCMC) and methyl cellulose (MC)		
N-isopropylacrylamide (NIPAM) and butylacrylate (BA)	MTX	(Murphy et al., 2011)
C. Optimisation of polymeric nanogel properties studies		
Polymethacrylic acid (PMA) and polyglutamic acid (PGA)	Doxorubicin	(Band and Bronich, 2014)
Chitosan	Bovine serum albumin (protein)	(Brunel et al., 2009, Schütz et al., 2011)
Poly [2-(dimethylamino) ethyl methacrylate],PDMAEMA,	No drug/protein/gene	(Meléndez-Ortiz et al., 2014)
D. Stimuli responsive studies		
Polyacrylic acid	Temozolodine	(Wu et al., 2010)
Poly(N-isopropylacrylamide)	Indomethacin drug	(Shi et al., 2010)
	5-fluorouracil	(Wang et al., 2008)
poly(N-isopropylacrylamide-co-acrylamide) (poly (NIPAM-co-AAc))	Curcumin	(Wang et al., 2014)
Chitosan	Bovine serum albumin (protein)	(Yu et al., 2006)
	Doxorubicin	(Oh et al., 2010)
Poly[2-(N,N-diethylamino)methacrylate] core and PEG	Procaine hydrochloride	(Oishi et al., 2007)
Poly(N-isopropylacrylamide- co-acrylic acid	Caffeine	(Samah and Heard, 2013)

From the work highlighted (Table 2.1) research has shown that nanogels have the ability to potentiate drug penetration through all the skin layers as well as the blood circulation. Based on both *in vivo* and *in vitro* skin penetration, drug loading and entrapment of the nanogel

formulations was significantly enhanced, hence nanogels are considered safe and effective for TDD especially in dermatological conditions treatment. Also the pharmacokinetics of the drugs was improved and according to the *in vitro* cytotoxicity tests of the nanogels very low cytotoxicity resulted from these gel preparations. The prepared nanogel formulation showed better skin penetration mostly due to the enhanced contact between the drug and the skin resulting from more surface area and hydration. The formulation showed stability over the study period and showed substantial increase in the efficacy in animal studies. DPCNs formulations proved to be the better alternative for TDD of most drugs especially for chronic conditions treatment and eliminate the limitations of the TDDS. Although in most of these formulations chemical enhancers were used some of them had better skin penetration without the use of the enhancers, but by utilizing the occlusive and nano-carrier properties. During *in vivo* drug delivery covalently crosslinked nanogels present improved stability compared to the non-crosslinked nanogels, ensuring better controlled drug release (Liu and An, 2014). Nonetheless, the chemical crosslinking also raises safety concerns regarding its potential for toxicity due to either the covalent crosslinking remnants or the unpredicted side effects associated with drugs loaded during the chemical crosslinking procedure (Liu and An, 2014). Thus more studies are still required to assess the effect of nanogels in evaluating the gel's *in vitro* stability, *in vivo* fate and cellular toxicity.

2.6. Recent Advances in Polymeric Colloidal Nanogels

Although the synthesis of nanogels has been extensively studied a number of challenges exist with the development of advanced colloidal nanogels where novel applications in various medical fields are being developed. This is evident from recent work of Raemdonck et al. (2009) which focused on new technologies for the formulation of nanogels with superior molecular structures which is a necessity for *in vivo* optimized drug delivery systems (Raemdonck et al., 2009). Furthermore examples of the advancements are described below and they include application of liposomal nanogel, enzymatically crosslinked colloidal nanogels and stimuli sensitive (dual/multiple responsiveness) (Liu and An, 2014).

2.6.1. Stimuli responsive polymeric colloidal nanogels / Targeted polymeric colloidal nanogels

Stimuli sensitive nanogels may be termed as 'intelligent nanogels' or 'smart nanogels'. The design of these nanogels is in such a way that they recognize their microenvironment, process and transmit a stimulus, and respond by producing a useful effect, and in doing so they mimic

living organisms' responsiveness (Yan and Tsujii, 2005; Lu et al., 2013; Mura et al., 2013; Meléndez-Ortiz et al., 2014). Figure 2.4 shows how a stimuli sensitive nanogel behaves. Nanogels respond to the environment by changing their chemical or/and physical behavior, hence release of the drug encapsulated in the polymeric matrix in a controlled fashion (Oh et al., 2007; du Toit et al., 2014).

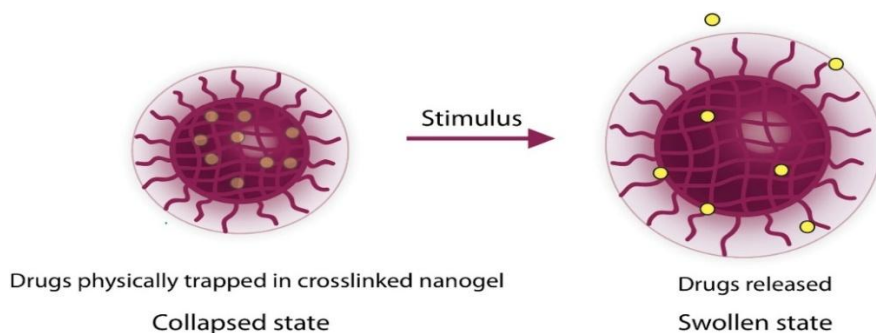


Figure 2.4: Proposed drug release from a nanogel in response to a stimulus applied. The model shows that the stimulus triggers physical changes in structure of the nanogel, resulting in swelling, erosion and ultimately releases the drug. (Adapted with the permission from Chacko et al. (2012). Copyright (2012) Elsevier).

Intelligent drug delivery occurs either through exogenous stimuli i.e. light, ultrasound, electric fields and temperature or endogenous stimuli i.e. redox potential, pH, and enzymes concentration. The various types of stimuli with the ability to activate drug release at the desired time and location, allows for the flexibility of designing intelligent systems, therefore much research is directed towards the design of more sensitive specific stimuli with discrete variations. A specific sensitivity can be achieved by the incorporation of functional groups into the gels, enabling a response of the network structure to external triggers (Klinger and Landfester, 2012)] and so far a number of “smart” polymeric nanoparticle based drug delivery systems have been extensively studied and proved to significantly enhance the overall therapeutic outcome in various conditions (Oishi et al., 2007; Oh et al., 2010; Singka et al., 2010; Murphy et al., 2011; Shah et al., 2012; Samah and Heard, 2013; Shang et al., 2013). These studies have shown that this type of TDDS may be applied to a variety of drugs including chemotherapeutics which are cytotoxic, as the polymeric film provides protection from the drug toxic effects and also targets only the affected tissues. Stimuli responsive polymeric nanogels are different from the other drug delivery systems and they possess a high application potential specifically due to the following reasons (Zha et al., 2011):

- I. They have higher stability for prolonged drug release once they are absorbed into the skin because of the hydrophilic polymer and their chemically crosslinked structure.
- II. They have the ability to selectively enhance the uptake of the therapeutic drug into the pathological site.
- III. As drug release is modulated by stimuli, the drug loading capacity and bioavailability of the drug may be greatly enhanced as the therapy is targeted towards specific sites and also few side effects are expected from drug loaded stimuli responsive nanogels.
- IV. As nanogels are flexible carriers, they are capable of retaining any shape, they may enter the vascular surface and be attached to multiple places, they may also be applicable in different shapes of bone cavities, and hence they have a better chance of specific retention in the targeted disease site.

Cumulative permeation profiles for caffeine loaded-poly (NIPAM-co-AAc) nanogels at 2–4 °C (Figure 2.5a), and room temperature (RT) (Figure 2.5b), with and without the addition of citric acid (CA) which is a pH modulator were investigated (Samah and Heard, 2013). This system comprised of NIPAM which is a temperature responsive monomer and AAc which is a pH (change in charges) responsive co-monomer. The *in vitro* TDDS permeation data of the caffeine-loaded poly (NIPAM-co-AAc) confirmed that, the nanogel significantly improved the delivery of caffeine across the epidermal membrane, compared to the saturated solution of the caffeine (Samah and Heard, 2013). The highest TDDS permeation was exhibited by the nanogel prepared at lower temperatures, hence, the thermal stimulus was the main factor determining the release of the drug (Samah and Heard, 2013). This is therapeutically significant in TDDS because nanogels prepared at lower temperatures can easily be delivered through the skin due to the greater pressure (change in gel conformity) as the temperature increases from 2-4 to 32°C which is the temperature of the skin. The acidic environment of the skin (pH 4-7) would not be as strong as in the presence of the pH modulator, CA, thus, the pH change had no significant impact in this study (Samah and Heard, 2013).

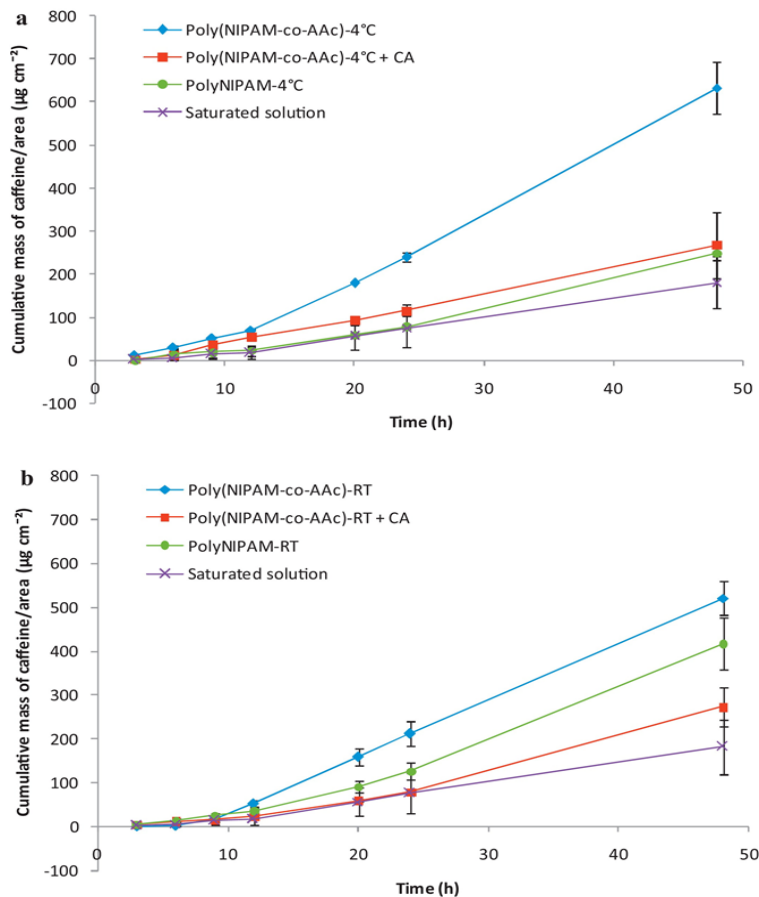


Figure 2.5: Cumulative permeation profiles of a caffeine-loaded nanogel at (a) 2–4 °C, and (b) room temperature (RT). A loaded polyNIPAM nanogel and a saturated caffeine solution was used as a control (Adapted with the permission from Samah and Heard (2013). Copyright (2013) Elsevier).

According to Mura et al. (2013) recent advances are geared towards the design of superior smart nanotechnological drug delivery systems. However only a few have been tested using *in vivo* preclinical models, very few have reached the clinical stage and a number of *in vitro* studies have been done to confirm their efficacy. These stimuli-responsive drug release strategies rely on the changes in specific physical or chemical properties of the environmental medium which are sometimes limited for *in vivo* applications, hence there are inadequate *in vivo* studies (Dorwal, 2012; Wang et al., 2014). This poses a challenge in the whole chain of the study of stimuli responsive DPCNs in TDDS; hereafter strategies on how to effectively characterize these systems are among the issues deserving a more comprehensive research attention.

2.6.2. Multiple (dual) stimuli responsive polymeric colloidal nanogels

Multi-stimuli responsive polymeric nanogels are nanoparticulate based drug delivery platforms releasing a drug in response to two or more external/internal signals, these signals may either occur concurrently or sequentially from gel preparation to its delivery into the targeted cells (Chiang et al., 2012; Cheng et al., 2013). These nanogels may be formulated from two or more polymers (copolymers) grafted together (Mahmoud et al., 2011;Chiang et al., 2012). Currently multi-stimuli-responsive nanoparticles have indicated significant *in vitro* and/or *in vivo* drug release profiles improvements (Pasparakis and Vamvakaki, 2011; Cui et al., 2012; Cheng et al., 2013) these nanoparticulate based drug formulations may have tremendous potential for targeted TDDS. Recently a polymer backbone of poly thioether ketal's has been functionalized with dual stimuli responsive counterparts and has been employed by Mahmoud and co-workers (Mahmoud et al., 2011) for the delivery of proteins. The results obtained with this polymer showed an enhanced delivery system directed towards inflammation responsiveness. This polymer consists of a pH and oxidative sensitive components that undergoes programmed degradation in the presence of inflammatory reactions (H_2O_2 and acidic pH). Since the skin is one of the organs prone to inflammation due to a number of causes from genetic disorders to general hypersensitivity reactions, this approach may be modified and applied in TDDS either for local or systemic effects. Figure 2.6 demonstrates a nanogel complex with a dual stimuli response, in response to low pH this complex changes its features i.e. charge changes from negative to positive (Zhuang et al., 2014). The nanogel has the ability of sequentially releasing the hydrophobic guest molecules i.e. drug molecules in response to redox stimuli. The polyelectrolyte detaches from the nanogel, allowing reduction occurrence, which is followed by concomitant targeted release of the guest molecules from the nanogel (Zhuang et al., 2014). This dual sensitivity ensures that both stimulus are concurrently present for drug release to occur, ensuring further improved site specific drug delivery (Zhuang et al., 2014).

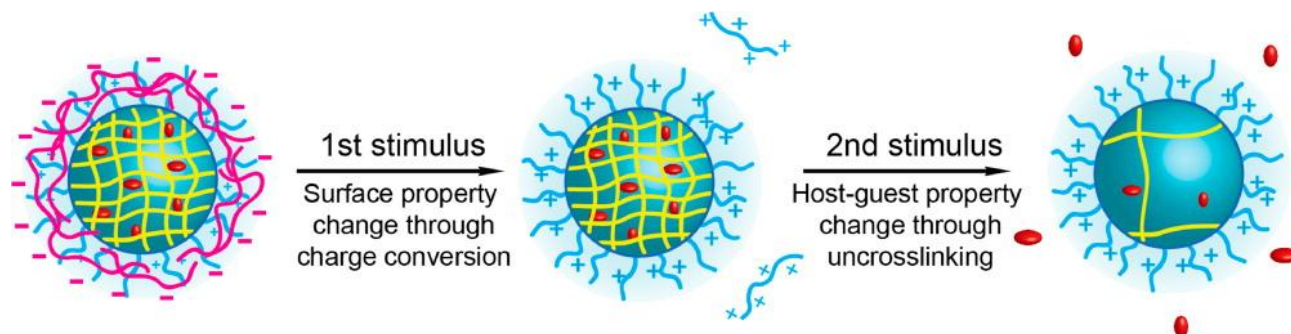


Figure 2.6: This nanogel-polyelectrolyte complex is modified with two stimuli responsive functionalities. (Adapted with the permission from Zhuang et al. (2014). Copyright (2014) American Chemical Society).

Although various multiple intelligent nanogels have been successful in showing the predictions of these systems for various TDD applications, detailed research on the functional aspects of these systems is still required. Full details on how to maximize their potential, how they are affected by the presence of other compounds (i.e. preservatives) and the working formulas for their preparation using diverse stimuli responsive groups in TDDS are also required.

2.6.3. Nanogels as carriers for liposomes / liposomal nanogels

Liposomes are drug carriers that are used to enhance drug permeation through the skin in TDDS. By combining the advantages of both liposomes and nanoparticle-based gel vehicle (Kermany, 2010; Murphy et al., 2011) a liposomal nanogel with superior properties is formulated. A liposomal nanogel may be described as lipid-coated drug loaded nanoparticles dispersed in a gel system (Murphy et al., 2011). The liposomes are formed by the self-assembly of amphiphilic lipid molecules into a lipid bilayer membrane surrounding the aqueous media (Zhang et al., 2013a) amphiphilic substances such as phospholipids and cholesterol are incorporated in the liposomes (Zhang et al., 2013a). These carriers may be used for both hydrophilic and lipophilic drugs molecules (Cevc, 2004; Honeywell-Nguyen and Bouwstra, 2005), therefore the synergistic effect of the gels and liposomes may be applicable in the drug delivery for a variety of drugs in TDDS. In TDDS the use of chemical enhancers may be avoided as the lipid coating enhances penetration of sufficient amount of drug molecules through the skin. A number of studies where nanogels have been used with liposomes, have been reported for delivery of drugs in the treatment conditions such of microbials and wounds (Fang, 2006). The release and entrapment efficacy of an antimicrobial drug chloramphenicol from a liposomal gel was studied and the penetration of the drug through the mucous membrane was greatly improved. The gel-liposomes (GLs) were prepared using a thermo-responsive gel as the

aqueous inner core of the liposome. The lipid bilayer of the delivery system was destroyed to confirm the stimuli responsiveness and sustainability of the gel (Zhang et al., 2013a). Moreover an example of a lipid coated nanogel was investigated and proved to be superior to the use of either liposome or nanogel on their own in TDDS (Murphy et al., 2011). Figure 7 shows a liposome formulation with a high bilayer melting temperature (T_m) and sodium alginate is encapsulated in the liposomal core. To prove their hypothesis the liposomes were placed in an aqueous buffer containing calcium chloride, and the temperature was raised up to T_m , allowing the permeation of Ca^{2+} ions through the bilayer and into the core, whereupon these ions resulted into the gelation of the encapsulated alginate. The GL showed an improved trans-bilayer permeability near the T_m (Zhang et al., 2013a). The lipid bilayer is expected to enhance the nanogel penetration, after passing through the skin the gelled alginate is unrestricted by the lipid layer, it may release the drug in a controlled manner as expected (Zhang et al., 2013a). From this study it is established that employing both a stimuli sensitive polymer/monomer and lipid bilayer in a single system has the potential of drastically improving TDD of drug loaded colloids.

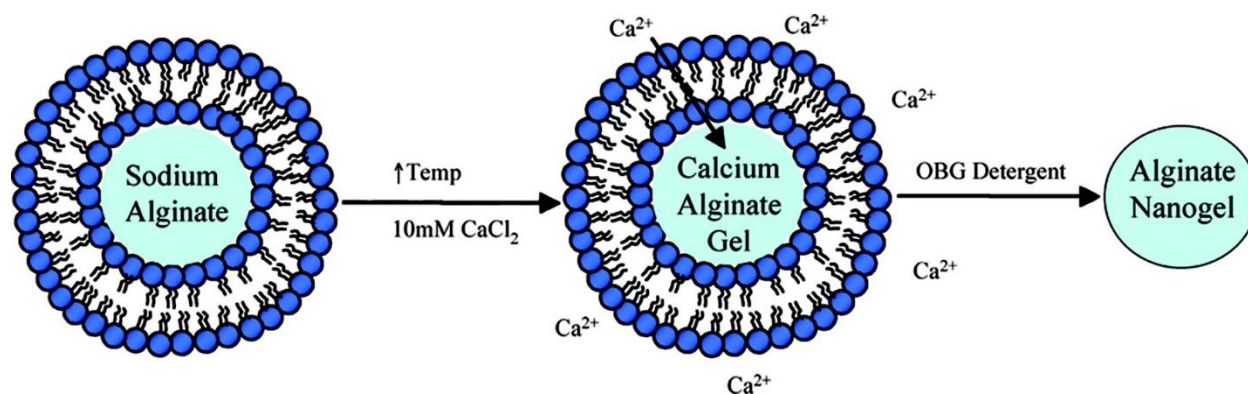


Figure 2.7:Route to the preparation of alginate nanogel liposomal templates. Reaction involves treating liposomes encapsulating sodium alginate to a 10 mmol/L $CaCl_2$ solution at temperatures near the T_m of the lipid. The increased transmembrane permeability permits Ca^{2+} to diffuse into the liposomes and ionically cross-link the alginate to form a nanogel. Upon removal of the lipid shell, alginate nanogels are isolated (Adapted with the permission from Hong et al. (2008). Copyright (2008) American Chemical Society).

According to Kermany (2010) the liposome mechanism of action as a penetration enhancer in TDDS through the skin is not clearly defined, but some researchers propose that liposomes disrupt the skin resulting in drug absorption into the skin (Fang, 2006). The composition of the lipid in liposomes and the concentration of the liposomes used to formulate the GLs are critical factors in determining the rheological gel properties, thus the drug release from the delivery

system, such as the release of a lipophilic drug, is greatly affected by lipid concentration (Mourtas et al., 2008). However, research on liposomal nanogel is still at its early stages of growth, hence fundamental studies on interactions between nanogels and liposomes, as well as their interaction with the skin layers in TDDS are yet to be discovered.

2.6.4. Enzymatically crosslinked nanogels

In this application enzymes are used as biological catalysts to mediate the formation of the nanogel by utilizing a few advantages such as the reduced need to use toxic polymers as crosslinkers, as they have a high selectivity and achieve crosslinking under mild conditions (Singh et al., 2013; Klinger and Landfester, 2012). Very few research advances have been reported on enzyme-mediated hydrogelation, especially in TDDS. One example is natural gelation process of fibrin, where they replaced a chemical crosslinker with a naturally occurring protein (fibrin) in the body to improve the gel characteristic of a DPCN (Singh et al., 2013). An ongoing study was carried out by utilizing dextran as a polysaccharide that is cleaved with dextranase upon incubation (Klinger and Landfester, 2012). Nanogels consisting of polyacrylamide (PAAm), crosslinked with dextran methacrylate (Dex-MA), were designed to be partially biodegradable by enzymatic cleavage of the methacryl-functionalized polysaccharide chains. It was established that the sensitivity of nanogels towards enzymes is of great advantage for release applications and it gives a chance for the development of more dual sensitive nanogels, hence improving the efficacy of DPCNs (Klinger and Landfester, 2012). Even though dextran nanogels are presently used for slow intracellular delivery of proteins, future research may explore the potential of increasing their application for other therapeutics. Although this nanogel advancement is not yet fully investigated it seems to be a better intervention, releasing the drug at site specific enzymatic responses. It allows the reduction of the toxicity of chemical crosslinkers while releasing the drug in a controlled manner. It also creates more research in drug delivery field for generating further specialized nanogels in TDDS biomedical application.

2.7. Concluding Remarks

It has been elucidated that physicochemical modifications of DPCNs in drug delivery systems have provided various advantages to TDD technology. The most common limitations associated with conventional transdermal based drug delivery systems are skin irritations, toxicities and unfavorable pharmacokinetics, whereas with the application of modified DPCNs the therapeutic outcomes of various drug molecules could be drastically improved. Even though various

investigations have been done to prove the effectiveness of DPCNs there are still some gaps in the explanation of the nanogels and their advanced developments as there are less preclinical development studies involving their application in TDDS. Hence there is still some necessity for research directed towards the improvement of their *in vitro*, *ex vivo* and *in vivo* studies of drugs delivered using the DPCNs via the transdermal route of drug administration. These advantageous properties associated with DPCNs have created a unique research expansion, diagnostic and pharmaceutical science research and development opportunities in transdermal application.

CHAPTER 3

A NOVEL BIOACTIVE COPPER COMPLEX WITH PREDNISOLONE SUCCINATE AND GLYCYLGLYCINE: SYNTHESIS, CHARACTERIZATION AND BIOLOGICAL EVALUATION FOR TRAPS MANAGEMENT

3.1. Introduction

Tumor Necrosis Factor Receptor Associated Periodic Syndrome (TRAPS) is among inherited genetic auto-inflammatory disorders caused by mutations in the TNF receptor, coded by the TNFRSF1A gene (Meiorin et al., 2013; Standing et al., 2013). TRAPS disorder is characterized by seemingly unprovoked recurrent episodes of fever and severe localised skin inflammation (McDermott et al., 1999; Kastner and O'Shea, 2001; Vitale et al., 2013; Meiorin et al., 2013). It is a lifelong condition and usually begins in early childhood with symptomatic episodes lasting between 1-3 weeks (Meiorin et al., 2013). Therefore the efficacy and the overall therapeutic outcome of the current agents are the basic concern in the treatment of TRAPS. There is still no proven treatment for this disorder and oral corticosteroids are being used as first line treatment to relieve the inflammatory symptoms. However with long-term use of the present corticosteroids may lead to serious side effects.

Corticosteroids exert their effect through the suppression of the immune system and the various inflammatory pathways. Hence they are used for the genetic auto inflammatory disorder TRAPS (Edwards, 2014). Currently, for the treatment of TRAPS, oral corticosteroids are preferred over topical corticosteroids, due to their high efficacy in the management of TRAPS. However, oral corticosteroids exhibit more serious side effects such as the suppression of the hypothalamic-pituitary-adrenal axis and erratic absorption kinetics. Hence, in this research, a metal-drug complex with superior properties compared to conventional corticosteroids such as improved anti-oxidant/ant-inflammatory efficacy and permeation through the skin was formulated.

Metal-drug complexation involves the co-ordination of metal ions to a ligand (drug) and in this study Copper (II) (Cu^{2+}) was complexed to prednisolone succinate (model drug). Cu^{2+} complexes are widely used in cancer treatment as therapeutic drugs (Gokhale et al., 2001; Malon et al., 2001; Singh et al., 2011; Chemik, 2013; Ng et al., 2014), and various observations have indicated that Cu^{2+} complexation enhances the anti-inflammatory effect of a number of drugs, resulting in more potent coordination compounds compared to the free ligands (Cini et

al., 1990; Sorenson, 1976). The therapeutic effects of Cu^{2+} complexes have been well studied and were found to be beneficial. One of its advantages is the ability to penetrate through the stratum corneum of the skin, reaching both the epidermis and dermis layers of the skin and becoming available for systemic and local effects (Hostynek et al., 2006; Szymanski et al., 2012). Therefore, the copper complex may be an alternative anti-inflammatory bioactive via the transdermal route.

Copper is depleted during inflammation and the body inevitably transports the copper to the inflamed tissue (Hostynek et al., 2011). The degradation and elimination of copper is managed by the body, as it is one of the essential micro-elements for human life and in contrary to other transition metals, like ruthenium it is considered less toxic (Szyman'ski et al., 2012; Chemik, 2013). Although Cu compounds in therapeutic formulations are much higher than the normal daily requirements, it was established by Sorenson (1976) that patients with chronic inflammation require more than the normal requirements for the anti-inflammatory activity of the compounds, henceforth the risks of toxicity are minimized with the formulations (Sorenson, 1976). Addition recent and historical data has shown that all forms of copper are safe for use in humans either in the form of metal, drug or complex (Roy et al., 2006; Hostynek et al., 2011; Stevenson et al., 2013). Hence the medicinal uses and applications of Cu complex are of increasing clinical importance.

The objective of the current study was to employ the Cu(II) coordination strategy to link PS in the presence of a modulating glycyglycine (glygly) ligand to give a $[\text{Cu}(\text{glygly})(\text{PS})]$ complex with improved anti-inflammatory/anti-oxidant activity relative to the free PS. The success of the coordination was confirmed using NMR, IR, mass spectrometry and UV-visible absorption spectroscopy. Furthermore additional studies were carried out, such as thermal analysis (TGA/DSC), X-ray diffraction, antioxidant activity assay, *in vitro* permeation studies, and a cytotoxicity assay.

3.2. Materials and Methods

3.2.1. Materials

Copper (II) nitrate, glycyglycine (glygly), triethylamine, DPPH (1, 1-diphenyl-2-picrylhydrazyl), lipoxygenase enzyme linoleic acid, and prednisone succinate (PS) salt, deuterated methanol (CD_3OD) were all purchased from Sigma-Aldrich (St. Louis, MO, USA). Buffering constituents: potassium chloride, potassium dihydrogen phosphate, disodium hydrogen phosphate, sodium

chloride, sodium hydroxide pellets, and hydrochloric acid, as well as D-methanol, dimethyl sulfoxide (DMSO), and boric acid were purchased from Merck (Wadeville). Deionised water was obtained from a Milli-Q system (Milli-Q, Millipore, Johannesburg) and methanol from Rochelle Chemicals (Johannesburg, South Africa). The pig skin tissue was obtained from the University of the Witwatersrand animal unit (South Africa, Johannesburg).

3.2.2. Synthesis of the [Copper(glycylglycine)(prednisolone succinate)] complex

The metal complex was prepared using methods adapted with modifications from Feng et al. (2014) and Sorenson (1976). PS salt (0.22mmol) in methanol was stirred continuously, adding a solution of glycylgly (0.22mmol) in deionised water. A drop of triethylamine was added to the reaction mixture, which was stirred for 30minutes before the addition of copper (II) nitrate (0.26mmol) (the reaction was done in a controlled pH of 7). The resulting blue solution was stirred for 2hours. Thereafter [Cu(glycylgly)PS] complex was precipitated using diethylether, filtered and washed with double deionised water three times and dried *in vacuo*.

Molecular simulation of the free PS drug and [Cu(glycylgly)(PS)] was performed using ChemBio3D Ultra 11.0 (CambridgeSoft Corporation, UK), where the structures of the PS and complex were visualised in their geometric preferences.

3.2.3. Chemical structural analysis of the [Copper(glycylglycine)(prednisolone succinate)] complex

Fourier transform infrared (FTIR) spectrum was generated on [Cu(glycylgly)(PS)] compared to the native PS. FT-IR Spectrometer (PerkinElmer Inc., Waltham, Massachusetts, USA) was used to assess the vibrational transitions in the chemical structures of these compounds. Samples were placed on a single bounce diamond crystal and processed by a universal attenuated total reflectance (ATR) polarization accessory, at a resolution of 4cm^{-1} , with the spectrum ranging from 4000 to 650cm^{-1} .

3.2.4. Analysis of the chemical shifts of the [Copper(glycylglycine)(prednisolone succinate)] complex

The magnetic properties of the [Cu(glycylgly)(PS)] complex compared to the native PS was analysed using the nuclear magnetic resonance (NMR) spectroscopy (^1H and ^{13}C spectra) (Bruker BioSpin GmbH, Germany). All ^1H NMR spectra were recorded on a Bruker Avance spectrometer operated at 300.13 MHz and all ^{13}C NMR spectra were recorded on a Bruker

Avance spectrometer operation at 75.48 MHz. The samples were analysed by preparing 15mg/mL of each sample in deuterated methanol (CD₃OD).

3.2.5. Analysis of the UV-visible absorption spectrometry of the[Copper(glycylglycine)(prednisolone succinate)] complex

The UV-visible absorption of [Cu(glygly)(PS)] and PS was determined using the double-beam UV-Vis spectrophotometer (PerkinElmer Spectrum 100, Llantrisant, Wales, UK) at room temperature. The spectrometric measurements were carried out over the UV-visible excitation wavelength range of 200-700nm for native PS and [Cu(glygly)(PS)] complex.

3.2.6. Identification of the molecular fragmentations of the [Copper(glycylglycine)(prednisolone succinate)] complex

Molecular fragmentations of the PS and [Cu(glygly)(PS)] were identified using a quadrupole ion trap mass spectroscopy (Finnigan-MAT model LCQ, San Jose, CA, USA), equipped with electrospray ionization (ESI). Samples were dissolved in methanol (1mg/L) and introduced to the mass spectrometer at a flow rate of 3.0µL/min through the ESI. The major isotopic ions from PS and [Cu(glygly)(PS)] complex were mass selected with a 5m/z window and subjected to collision-induced dissociation (CID), to examine the fragmentation reactions of the isotopic ions.

3.2.7. Evaluation of the degree of structural order of the the [Copper(glycylglycine)(prednisolone succinate)] complex

The X-ray Diffraction (XRD) pattern of the [Cu(glygly)(PS)] complex compared to the the drug was investigated with the X-ray diffractometer (ULTIMA-III, Rigaku, Japan), using nickel-filtered Cu K α radiation (a voltage of 40kV and a current of 30mA) for pure drug and formulated complex. The X-ray diffractograms were attained at the scanning rate of 5°/min with the scanning scope of 2 θ from 5° to 90° at room temperature.

3.2.8. Determination of thermal properties of the [Copper(glycylglycine)(prednisolone succinate)] complex

A differential scanning calorimeter (DSC) (Mettler Toledo, DSC1, STAR^e System, Schwerzenback, Switzerland) was used to determine the thermal properties of the [Cu(glygly)(PS)] complex compared to the drug. The analysis was conducted using the basic DSC and alternating DSC (ADSC) at a temperature range of 25-350°C, ramped at 10°C/min

under a N₂ atmosphere. All samples were weighed (10mg) on perforated 40μL aluminum crucibles.

3.2.9. Determination of thermal properties of the [Copper(glycylglycine)(prednisolone succinate)] complex

Thermogravimetric analysis (TGA) was performed using a Toleda TC15 TA controller (Mettler). It was used to measure how the changes in the chemical and physical properties of the [Cu(glygly)(PS)] complex compared to the drug. Dried sample measurements of 5mg were analysed after tarring the empty crucibles. The analysis was carried out from 25 to 800°C, using a heating rate of 10°C/min under a constant nitrogen gas flow. The percentage weight losses incurred during the heating cycle were estimated using the associated software (STARe).

3.2.10. Evaluation of the antioxidant/ antiinflammatory activities of the Copper(glycylglycine)(prednisolone succinate)] complex

3.2.10.1. DPPH free radical scavenging assay

The DPPH free radical scavenging assays of [Cu(glygly)(PS)] complex compared to the free drug (PS) and ascorbic acid were determined by dissolving these samples in a methanolic solution (1mmol/L). Sample solutions were allowed to react for 30min with DPPH (1mmol/L) in the absence of light, thereafter the decrease in absorbance of these samples was measured at 517nm using UV-Vis spectroscopy (PerkinElmer Spectrum 100, Llantrisant, Wales, UK). The percentage inhibition of radical scavenging activity was calculated using the following formula:

$$\% \text{Inhibition} = \left(\frac{A_b - A_s}{A_b} \right) \times 100 \quad \text{Equation 3.1}$$

Where A_s is the absorbance of the sample after reacting with DPPH and A_b is the absorbance of the blank sample (DPPH in methanolic solution) (Awah et al., 2012; Hong and Yang, 2013; Jothy et al., 2011).

3.2.10.2. 5-lipoxygenase inhibition assay

The 5-lipoxygenase (5-Lox) inhibition assays of [Cu(glygly)(PS)] complex, free drug (PS) and ascorbic acid were determined. Each of the solutions used to measure the percentage 5-Lox inhibition assay was prepared using 0.05mL of the inhibitor (0.125mmol/L), 1.95mL of the enzyme (5-Lox) solution (10 000 units/mL) and 2mL of the substrate solution (0.125mmol/L), all of which were made in borate buffer (0.2M). The reaction solutions were left to react for 15min

at room temperature and subsequently the absorbance was measured using UV-Vis spectroscopy (PerkinElmer, Lambda 25 UV/Vis spectrometer, UK) at 234nm. A blank sample was prepared in a manner omitting the inhibitor from solution. The percentage inhibition of [Cu(glygly)(PS)] compared to the drug and ascorbic acid was determined using an equation adapted from Feng et al. (2014) as follows:

$$\%5 - \text{Lox inhibition} = \left(\frac{A'}{A_0} \right) \times 100 \quad \text{Equation 3.2}$$

Where A' is the absorbance of the reaction mixture and A_0 is the absorbance of the blank sample (Maiga et al., 2006 and Helle Wangensteen, Samuelsen, Malterud, 2004).

3.2.11. *In vitro* permeation studies

Full-thickness of a pig's ear skin was separated from cartilage using a scalpel and dermis was wiped with isopropyl alcohol to remove any residual adhering fat. The skin was washed with deionised water, wrapped in aluminum foil and stored in a freezer at -20°C until required. Prior to the diffusion experiment the epidermis was thawed at room temperature and cut to a cross-sectional area of 4cm^2 .

The permeation studies were performed according to method adapted with modifications from Wissing and Muller (2002). These studies were carried out using the Franz diffusion cell with a diffusional area of 3.14cm^2 and a receptor chamber with 12mL volume capacity. This chamber was filled with phosphate buffer saline (PBS) pH 7.4 and maintained at 37°C in order to ensure a surface skin temperature of 32°C . Weighed samples (5mg) of the drug and complex, which were dispersed in 3mL of PBS and evenly distributed on the surface of donor compartment. At hourly time intervals 0.2mL samples were taken from diffusion medium and the volume of the diffusion medium then replaced with PBS. Sampling was done every hour for the first 10h and at 24h. The samples were diluted with 2.8mL of PBS before analysis and PBS was used as the reference. Absorbance was determined using the UV-Vis spectrophotometry (PerkinElmer Spectrum 100, Llantrisant, Wales, UK) at 248nm and 242nm for the PS and complex (Figure 3.1) respectively. Calibration curves were constructed for concentration calculations. The flux and permeation coefficient (Pk) were calculated using the following equations:

$$J_s = \frac{Q_s}{AT} \quad \text{Equation 3.3}$$

$$Pk = \frac{J_s}{C_{\text{donor}}} \quad \text{Equation 3.4}$$

Where J_s is the flux ($\mu\text{g}/\text{cm}^2/\text{hr}$), Q_s is the amount of drug (μg) and AT is the area (cm^2) by time (hr). C_{donor} Concentration in the donor compartment.

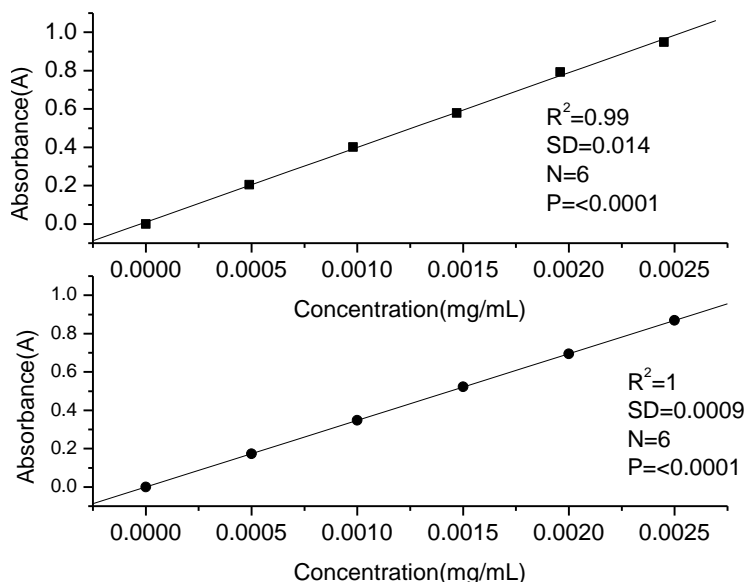


Figure 3.1: The calibration curve of (a) PS at 248nm and (b) [Cu(glygly)PS] complex at 242nm.

3.2.12. *In vitro* cytotoxicity analysis

Human Dermal fibroblast adult (HDFa) cells (Cell Applications Inc. (CAI), San Diego, USA) were seeded in culture flasks with complete media consisting of GIBCO®-Dulbecco's Modified Eagle Medium (DMEM) supplemented with 10% fetal bovine serum, 2mM glutamine and 100U/ml penicillin/streptomycin (Sigma-Aldrich; St. Louise, MO, USA). The flasks used for the culturing were coated with poly-L-lysine (Sigma-Aldrich; St. Louise, MO, USA) 24h before cell culture was initiated. During cell culture the cells were then maintained in an incubator (RS Biotech Galaxy, Irvine, UK) with a humidified atmosphere of 5% CO_2 at 37°C.

Cultured HDFa cells were seeded at a concentration of 15000 cells/well. After culturing for 48h in complete media, PS, and [Cu(glygly)PS] were added at a concentration of 1, 2, 10, 20, 100, and 200 $\mu\text{g}/\text{ml}$ drug (PS) equivalent concentrations and the cells were further incubated for 48h. At the end of the incubation the medium was removed and 100 μL of MTT (3-(4,5-dimethylthiazol-2-yl)-2,5-diphenyltetrazolium bromide) solution (diluted in a culture media with a final concentration of 0.5mg/mL) was added and incubated for another 4h. Following incubation the medium was removed through centrifuging (Optima® LE-80 K, Beckman, California, USA) at 3000rpm for 5 min. Next the remaining formazan crystals were dissolved by incubation for 30

min in 100 μ L of dimethyl sulfoxide (DMSO) and analysed with microplate reader (FilterMax™ F5 Multi-Mode Microplate Reader, Molecular Devices, USA)

The number of viable cells is directly proportional to the quantity of formazan product formed as quantified by absorbance at 570nm (Mohanty et al., 2012), using a microplate reader. Results are presented as %cell viability (CV) (mean \pm standard deviation), the percentage of viable cells was calculated using the following equation:

$$\%CV = \frac{\text{absorbance read in treated cells}}{\text{absorbance read in control(untreated)cells}} \quad \text{Equation 3.5}$$

3.3. Results and Discussions

3.3.1. Characterisation and evaluation of the formulations

The [Cu(glygly)(PS)] complex was synthesised by the by reacting a PS with Cu (NO₃)₂ and glycyglycine as a ligand in a 1:1.2:1 ratio respectively. The resulting [Cu(glygly)(PS)] complex was obtained as a blue-green fine powder and percentage yield was 60- 69%. Shown in Figure 3.2(a) are the 3D visualization models of the geometrical preferences of the PS and [Cu(glygly)(PS)] after molecular simulation, and in Figure 3.2(a) the reaction scheme for the preparation of the [Cu(glygly)PS] complex.

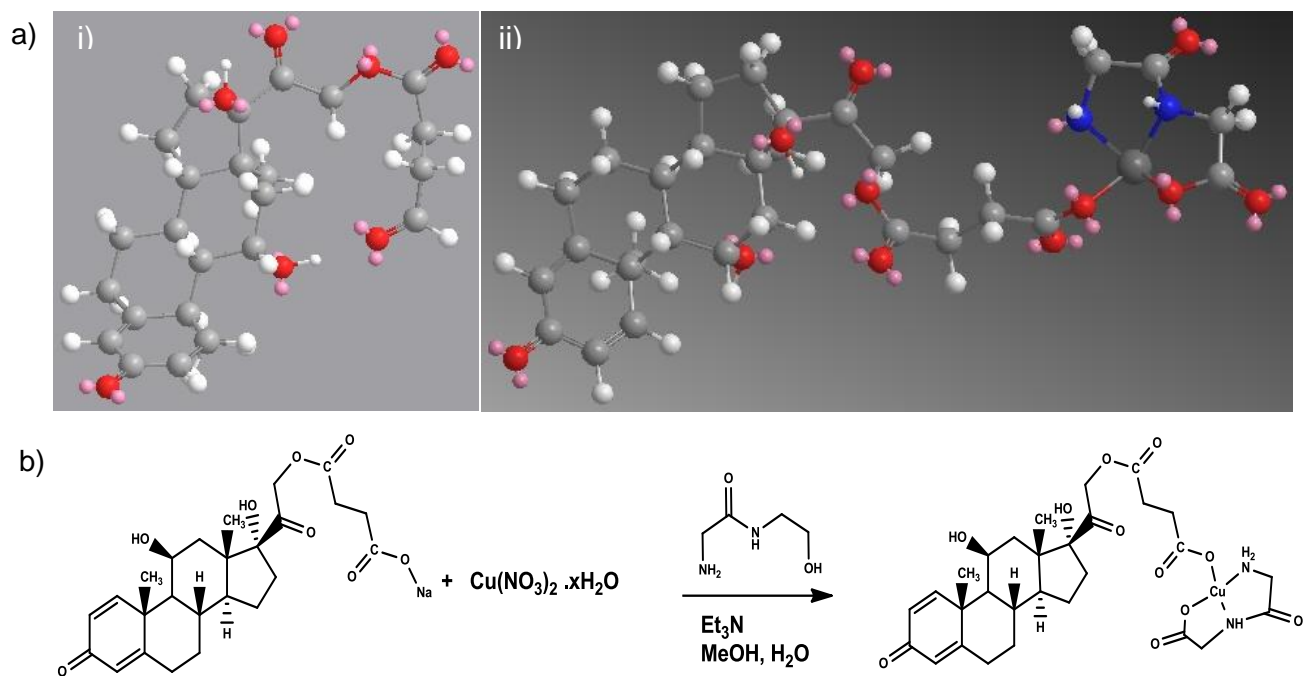


Figure 3.2: Visualization of geometrical preferences of (i) PS and (ii) [Cu(glygly)PS] complex after molecular simulation. Color codes: C (grey), O (red), N (white), H (pink) and Cu (blue), and b) reaction scheme for the preparation of the [Cu(glygly)PS] complex.

The complex is expected to exert its anti-inflammatory effects through a number of pathways (Lewis, 1984). The different pathways of its anti-inflammatory effects are shown in Figure 3.3, most of the [Cu(glygly)PS] complex is expected to dissociate once inside the body system. The drug and /or the [Cu(glygly)PS] complex may exert their own anti-inflammatory effects, while the Cu^{2+} binds to amino acids readily available in blood, or remain with the modulating ligand glygly (amino acid). The anti-inflammatory activity of the amino acid bound Cu^{2+} may be to the Cu-amino acid complex or its metabolised residue.

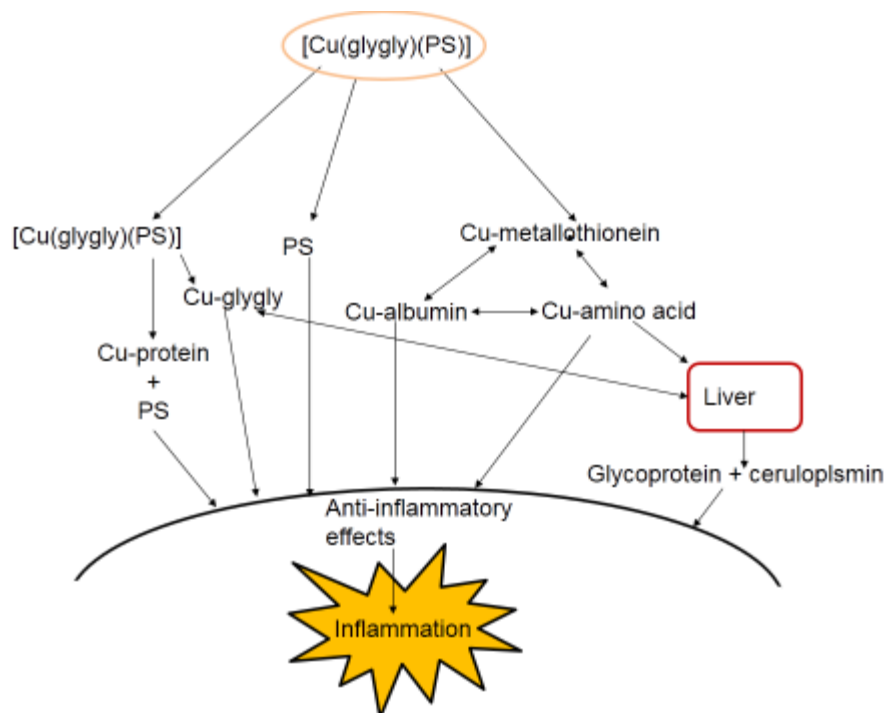


Figure 3.3: The proposed anti-inflammatory effects caused by [Cu(glygly)(PS)] complex (Adapted with modifications from Lewis, 1984).

3.3.2. Chemical structural evaluation of the the [Copper(glycylglycine)(prednisolone succinate)] complex

In order to investigate the coordination mode of PS to the metal in the complex, the FTIR spectrum of the parent ligand was evaluated in relation to the complex. The FTIR spectra of glycylglycine, PS and [Cu(glygly)(PS)] are shown in Figure 3.4 a,b and c, respectively. The absorption bands are discussed as marked in Figure 3.4 (inserted boxes). PS shows characteristic absorption bands in the region of 2929, 1719, 1654 and 1571 cm^{-1} which were assigned to C-H (alkanes), C=O (alkyl ketone), C=O (ring ketone), and C=O (sodium hemisuccinate) vibrations, respectively. Most of the bands seen in PS are also present in the complex, with an important change in the shift of the $\nu_{\text{asym}}\text{COO}^-$ upon complexation with copper. The absorption band at $\nu_{\text{asym}}\text{COO}^-$ 1572 cm^{-1} and $\nu_{\text{sym}}\text{COO}^-$ 1370 cm^{-1} in the ligand spectrum was shifted to 1590 and 1320 cm^{-1} respectively. These shifts are a result of the withdrawal of electron density from the C-O bond due to coordination of the “O” donor to the copper ion.

Relative to the spectrum of the free drug there are new molecular vibrations in the spectrum of the complex which infers the presence of the glycylglycine. Glycylglycine (glygly) contains three potential donors namely the N-amino, NH-peptido and O-carboxylate group. Additionally

glygly has a zwitterion ionic structure evident by the presence of the protonated N-amino and ionised O-carboxylate group (NH_3^+ and COO^-) groups respectively. The $\nu_{\text{as}}(\text{NH}_3^+)$, and $\delta(\text{NH}_3^+)$ bands at 3015cm^{-1} in free glygly are red shifted to 3260 and 3249cm^{-1} in FTIR spectrum of the complex. This indicates that the NH_3^+ groups are deprotonated after coordination to the metal center. Notably the stretching band corresponding to 1134cm^{-1} for free glygly is shifted to $\nu(\text{C4}'\text{-N-amino})$ ($\sim 1132\text{cm}^{-1}$) in the spectrum of the complex.

The $\nu(\text{NH})$ peptide band at 3284cm^{-1} assigned to free glygly appeared at 3329cm^{-1} in the spectrum of the complex and this implies that the NH-peptide remains protonated and possibly interacts as a donor to the copper metal center. The shift in the wavenumber of 1602 for $\nu(\text{COO}^-)$ asymmetric stretching O-carboxylate group of free glygly to higher wavenumber ($\Delta\nu\text{COO}^-$ of $\Delta 50\text{cm}^{-1}$) is indicative of coordination to the metal center (Mandal et al., 2015). Both predicted and experimental results reported for copper (glygly) complexes give relative higher wavenumber of when coordination via the O-carboxylate group occurs. However the FTIR of the complex contained several overlapping bands in the regions of $1600\text{-}1500\text{ cm}^{-1}$ of which rendered it difficult to make an accurate characterisation. On closer evaluation of the FTIR spectrum there was a slight change to the ν symmetric (COO^-) stretch at 1403 to 1393cm^{-1} , which implies that copper may be coordinated to O-carboxylate donor of glygly. Therefore it may be established that in the copper (II) complex, the dipeptide acts as a tridentate ligand (N-amino, NH-peptide donors and O-carboxylate) in the presence of PSA.

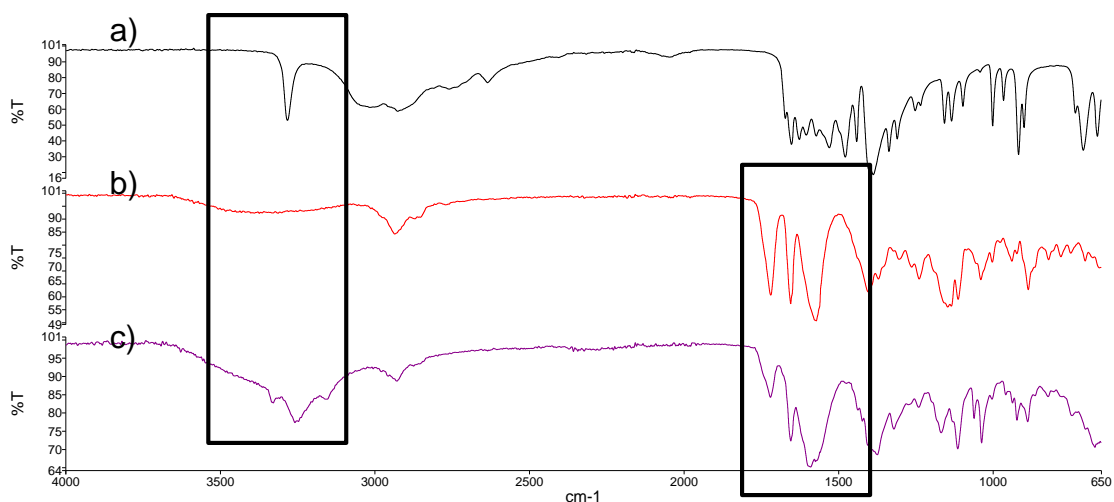


Figure 3.4: The FTIR spectra of a) Glycylglycine, b) PS, c) $[\text{Cu}(\text{glygly})(\text{PS})]$.

With all these shifts and new bands appearing in the complex spectrum it may be established that the [Cu(glygly)(PS)] complex was successfully formed. The nature of metal–ligand bonding is confirmed by the newly formed band at ~ 510 and $\sim 440\text{cm}^{-1}$ in the spectra of the complex (Figure 3.5) which is tentatively assigned to Cu–N and Cu–N vibrations, a comparable band was observed in the studies of copper complexes by Baran (2005) and Zhang et al. (2010).

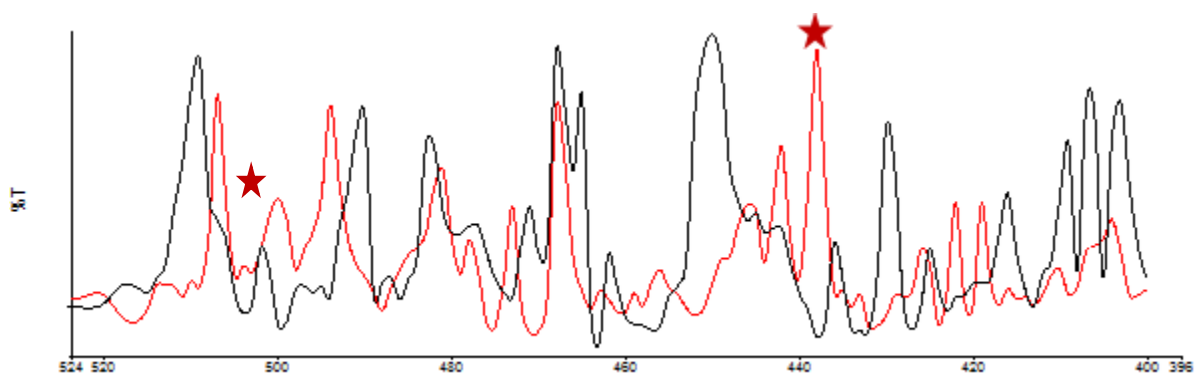


Figure 3.5: The FTIR of the complex and drug at lower wavelengths, the red spectrum being the [Cu(glygly)(PS)] complex.

3.3.3. Evaluation of the chemical shifts of the [Copper(glycylglycine)(prednisolone succinate)] complex

The comparative ^1H NMR spectra of PS and [Cu(glygly)(PS)] are shown in Figure 3.6a and b, respectively. To be noted were the broad ^1H NMR bands of the [Cu(glygly)(PS)] complex, in comparison to the ^1H NMR spectrum of free PS. The NMR spectrum of the Cu (II) complex shows a slightly upfield chemical shift (δ), relative to the free PS. For example ^1H signals at $\delta 2.49$ and 2.68 were assigned to the methylene protons at C23 and 24 in the free ligand and these peaks appeared relatively up field values (2.33 and 2.61) indicative of metal coordination. It is possible that the copper complexation creates a shielding effect, as copper (II) is known to be paramagnetic, resulting in protons experiencing an overall lower effective magnetic environment, with these signals appearing upfield. Similar observations for copper (II) complexes have been reported (Tella and Obaleye, 2009). Overall the chemical shifts were relatively small, implying that delocalization of spin density from the metal into molecular orbitals of ligands was marginal (Ramadan et al., 2004).

Similar slight upfield shifts are also noted in ^{13}C NMR spectrum of PS and [Cu(glygly)(PS)] (Figure 3.7a and b, respectively). There is a significant shift for the C18 of adjacent carbon C17

hydroxy group undergoing some weak interactions after metal coordination. Additionally, C23 and 24 show light movement to upfield values (24.84, 31.68 to 24.79 and 30.69).

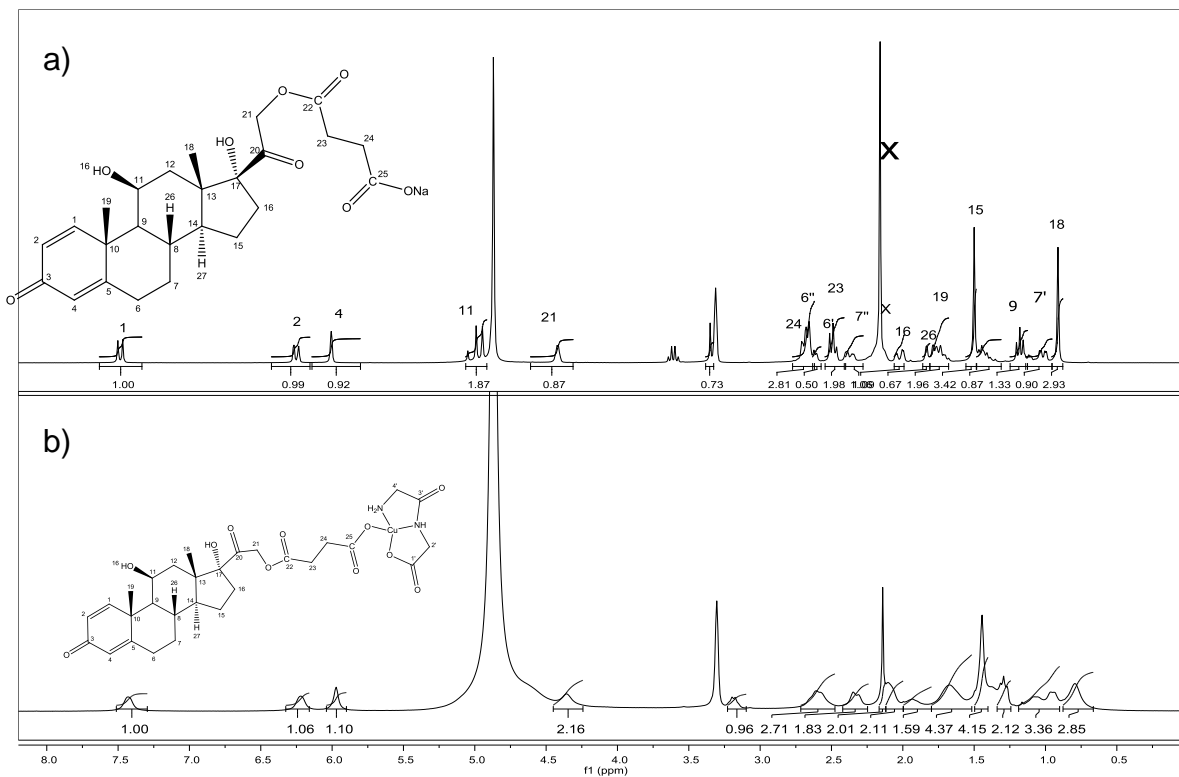


Figure 3.6: Comparison of ¹H NMR for (a) PSA and (b) the [Cu(glygly)(PS)] complex in CD₃OD.

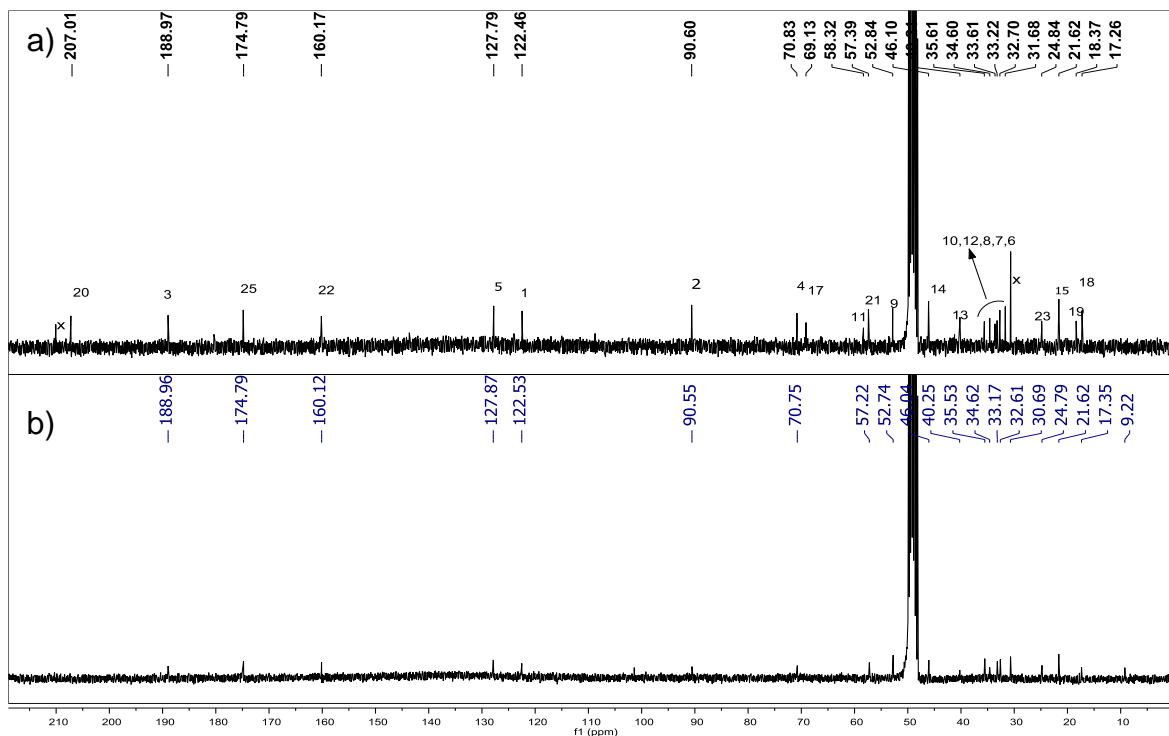


Figure 3.7: Comparison of ^{13}C NMR for (a) PSA and (b) the $[\text{Cu}(\text{glygly})(\text{PS})]$ complex in CD_3OD

Based on the characterisation data it is indicated that the PS ligand is monodentate, glygly is tridentate and the binding sites are dipeptide nitrogen, amino and carboxylato oxygen atoms in the $[\text{Cu}(\text{glygly})(\text{PS})]$ complex. The proposed structure of $[\text{Cu}(\text{glygly})(\text{PS})]$ complex is shown along with the ^1H NMR spectra (Figure 3.6b) with chemical formula of $\text{C}_{29}\text{H}_{37}\text{CuN}_2\text{O}_{11}$ and a molecular weight of 653.16m/z.

3.3.4. Evaluation of the UV-visible absorption spectrometry of the $[\text{Copper}(\text{glycylglycine})(\text{prednisolone succinate})]$ complex

The UV-VIS spectrum of the complex shows maximum absorption at 242nm (Figure 3.8a) which is lower than that seen in the free drug which is at 248nm and this is due to the charge transfer transitions that occur during the complexation which is indicative of metal complexation (Ahmed et al. 2012). Since the $[\text{Cu}(\text{glygly})(\text{PS})]$ complex is blue-green in color the expected absorption is at 650-750nm. This is evident by the observation of a very weak and broad band at $\sim 700\text{nm}$ (Figure 3.8b) which is due to d-d transitions (metal-to-ligand charge transfer). This absorption band suggests that this complex may be tetrahedral in structure, as presented in the proposed structure (Ahmed et al. 2012). Moreover, these absorption band patterns are compatible with absorption spectra of reported copper complexes (Azzellini et al., 2010; Dias et al., 2010).

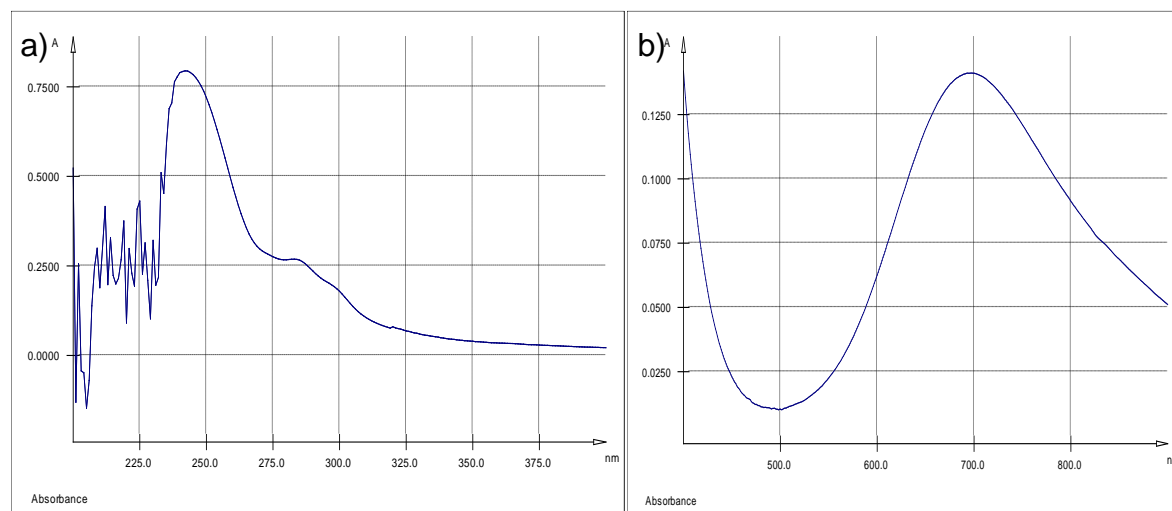


Figure 3.8: The UV/Visible of complex at (a) 200-300nm and (b) 400-800nm in methanol.

3.3.5. Identification of the molecular fragmentations of the [Copper(glycylglycine)(prednisolone succinate)] complex

The mass analysis can play an important role in confirming the monomeric Cu(II) complex. In the free ligand $[M^+]$ loss of succinate to give prednisolone was assigned to m/z 383 for the fragment $[M\text{-succinate} + Na^+]$. No $[M^+]$ ion was observed. Additional m/z for dimeric ions were observed at m/z 943 $[2M+2\text{succinate} + Na^+]$ and 949 $[2M+2\text{succinate} + 2Na^+]$.

The molecular ion peak of $[Cu(\text{glygly})(PS)]$ was observed at m/z 690.7845 $[M+K]$, with a fragment for the free prednisolone succinate ester observed at m/z 459.2015 $[PS]^+$. Mass spectra the complex are well agreed with their proposed structures, with similar studies that undertaken by (Kowcun et al., 2012). Based on the characterisation data, it is indicated that the PS ligand is monodentate, glygly is tridentate and the binding sites are dipeptide nitrogen and carboxylato oxygen atoms, in the $[Cu(\text{glygly})(PS)]$ complex. The proposed structure of $[Cu(\text{glygly})(PS)]$ complex is shown along with the 1H NMR spectra (Figure 3.6b), with a chemical formula of $C_{29}H_{38}CuN_2O_{11}$ and a molecular weight of 691 m/z was obtained via HR-ESI-MS.

3.3.6. Evaluation of the degree of structural order of the [Copper(glycylglycine)(prednisolone succinate)] complex

The XRD analysis was performed to evaluate any changes in the crystalline nature of the complex compared to the free ligand. Figure 3.9a and b illustrates the XRD patterns for complex and free ligand PS. One sharp characteristic peaks is observed around $2\theta = 18\text{-}22^\circ$ for both samples and the intensity of the peak is reduced in the complex compared to the free drug. This peak is less pronounced in the complex, it is attributed to the PS structure. Both spectra show that the compounds are amorphous and this result are in alignment with the findings of Palanisamy and Khanam (2011) and Gup et al. (2015, where the XRD of prednisolone and Copper (II) complex have been studied, respectively. The amorphous state of the complex made the growing of a crystal for the complex impossible. These results confirm the interaction of PS and Cu during complexation, as seen in FTIR and NMR results.

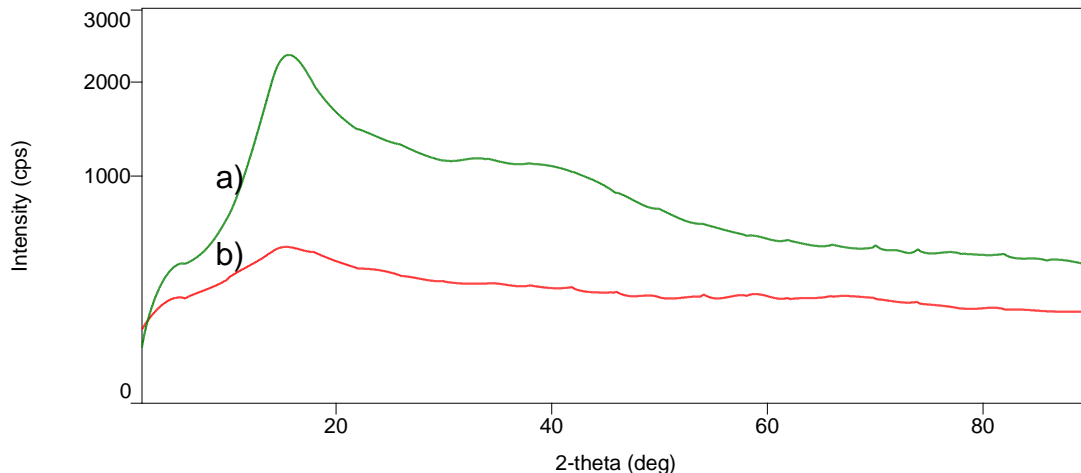


Figure 3.9: The powder XRD of (a) pristine PS and (b) the [Cu(glygly)(PS)] complex is show.

3.3.7. Evaluation of thermal properties of the [Copper(glycylglycine)(prednisolone succinate)] complex

The PSA trace indicates endothermic reaction peaks at 108°C and 170°C (melting process begins), and exothermic peak at 191°C (crystallization) specific to pure substances and an exothermic reaction >300°C attributed to the decomposition and combustion of PS organic structure (Figure 3.10a).

Absence of dehydration peaks (100-125°C) supports the proposal of an anhydrous complex. The complex showed both an endothermic peaks at 380°C and exothermic peak at 385°C suggestive of melting and crystallization. The complex shows a two-stage decomposition at temperature >400°C (Figure 3.10b). The first decomposition would result from loss of organic components and final decomposition would lead to CuO as seen in a study done by Joseyphus and Nair (2010). Overall this analysis implies greater thermal stability of complex relative to PS.

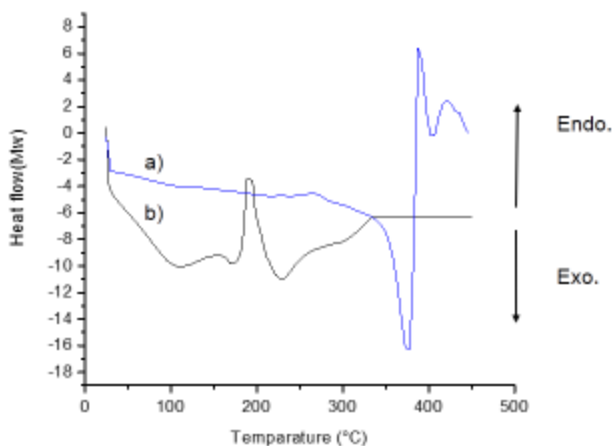


Figure 3.10: The DSC spectrometry of the (a) free PS and (b) [Cu(glygly)(PS)] complex.

3.3.8. Evaluation of thermal properties of the [Copper(glycylglycine)(prednisolone succinate)] complex

Thermogravimetric (DT/TGA) analysis of the [Cu(glygly)(PS)] complex was employed to provide quantitative information on mass losses due to thermal decomposition as a function of temperature. The thermal analyses data of PS drug and Cu(glygly)(PS)] complex and PS drug were are shown in Figure 3.11a and b respectively. From DT/TGA curve shown in Figure 3.11a the decomposition of PS presented with the initial mass loss (12.3%) occurring at 90-97°C with $T_{\text{peak DTA}} = 95^{\circ}\text{C}$ which may be the loss of the Na^+ in the PS salt. The second step of decomposition is in the 211–720°C range (total mass loss) which is attributed to the loss of the organic compounds. There is no further mass loss beyond 720°C and a plateau is obtained.

The thermogram (Figure 3.11b) for [Cu(glygly)(PS)] shows the presence of an anhydrous complex containing no water of crystallization, and no coordinated water molecules as evident by the plateau from 100 to 200°C. From DT/TGA curve, it is clear that thermal decomposition of the [Cu(glygly)(PS)] complex occurs in three major steps. The initial mass loss occurs within the temperature range 319–325°C, $T_{\text{peak DTA}} = 323.5^{\circ}\text{C}$ with a mass loss of 14.5% possibly due to elimination of the glygly ligand. The second mass loss was represented by two $T_{\text{peak DTA}}$ at 373 and 385°C occurring in the temperature range of 370-390°C (mass loss = ~15.5%), respectively, possibly due to initial loss of PS. The third step corresponds to the thermal decomposition and complete elimination of the remaining part of the PS drug molecule starting from 500°C on the thermogram of the complex with final mass loss ~83% at DTA = 740-760°C leaving the CuO residue. Comparable findings were obtained in a study done by Maravalli and

Goudar (1999) on thermal analysis of a copper complex. The findings of the DT/TG analysis were also in accordance with the above DSC and XRD results, providing evidence that the amorphous structure of PS was re-organised into another amorphous state ([Cu(glygly)(PS)] complex), with strong interaction bonds, hence increased melting and decomposition temperatures are observed in the DT/TGA and DSC analysis.

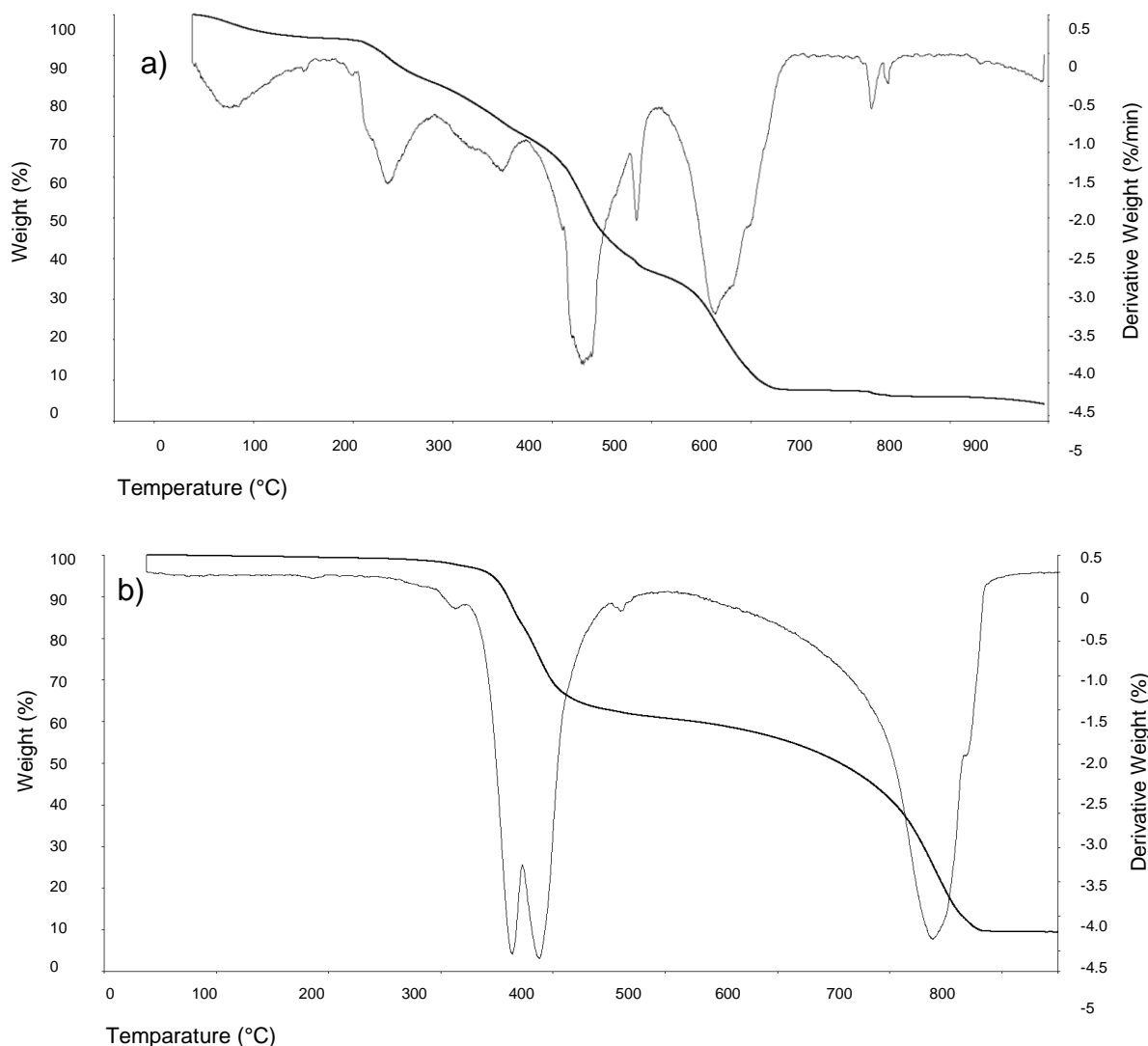


Figure 3.11: TG/DTGA) analysis of the (a) PS, and (b) [Cu(glygly)(PS)] complex.

3.3.9. Antioxidant/anti-inflammatory activities of the [Copper(glycylglycine)(prednisolone succinate)] complex

Compounds that may be useful in the treatment of TRAPS should have anti-inflammatory/antioxidant activity exhibiting free radical scavenging activity (Psomas and Kessissoglou, 2013).

Hence DPPH is a stable free radical used for rapid screening of antioxidant activity and it is related to the ability of the compounds present in the extracts to donate electrons/hydrogen to free radicals, thus being used to determine the scavenging activity (Tolia et al., 2013). Anti-inflammatory activity of copper complex has been shown to be effective by a number of researchers (Sorenson, 1976; Roy and Srivastava, 2006; Hostynek et al., 2011). Some of this research included various NSAIDS and steroidal complex (Dimiza et al., 2011, Psomas and Kessissoglou, 2013), with results demonstrating that copper complexes are more effective in the inhibition of inflammation compared to the free ligands (drugs).

According to *in vitro* antioxidant activity evaluation of [Cu(glygly)(PS)] using DPPH, [Cu(glygly)(PS)] exhibited excellent antioxidant activities, which were comparable to the standard ascorbic acid with the a corresponding concentration. The DPPH scavenging activity of the [Cu(glygly)(PS)] complex was higher ($60.13 \pm 1.20\%$) than that of the corresponding free PS ($4.41 \pm 1.40\%$).

Considering that lipoxygenase plays a role in regulating inflammation by producing pro-inflammatory mediators (Wisastra and Dekker, 2014) the development of modulators targeting the Lox-5 pathway have the potential of providing a better approach in the treatment of TRAPS disorder. Lox-5 inhibitors have the ability to reduce the total oxidative stress resulting from the pathogenesis of inflammation. In this study it has been established that complexing the drug to the metal copper drastically improves the Lox-5 inhibition properties of free PS drug. The [Cu(glygly)(PS)] complex exhibit approximately 6 times ($36.65 \pm 1.30\%$) the percentage inhibition compared to the parent PS($6.14 \pm 2.60\%$), wherethe overall antioxidant effect was compared to a standard ascorbic acid, which is known to be a highly effective antioxidant compound (Choy et al., 2000 and Barrita and Sanchez, 2013).

According to the anti-radical activity and lipid peroxidation outcomes, as summarized in Table 3.2 and shown in Figure 3.12, the synthesised complex showed increased antiradical activities in the DPPH radical scavenging assay and also improved lipid peroxidation in the presence of lipoxidase enzyme. It can be concluded that the complexation of the Cu^{2+} to PS significantlyimproves the anti-inflammatory and antioxidant efficacy of the PS. The results described here, show that copper complex may be an alternative ant-inflammatory bioactive in TRAPS.

Table 3.1: Antioxidant/anti-inflammatory activity

Inhibitor	DPPH assay % Inhibition	% 5-Lox assay % Inhibition
Ascorbic acid	94.73 ± 0.30	54.11 ± 0.50
PS	4.41 ± 1.40	6.14 ± 2.60
[Cu(glygly)(PS)]	60.13 ± 1.20	36.65 ± 1.30

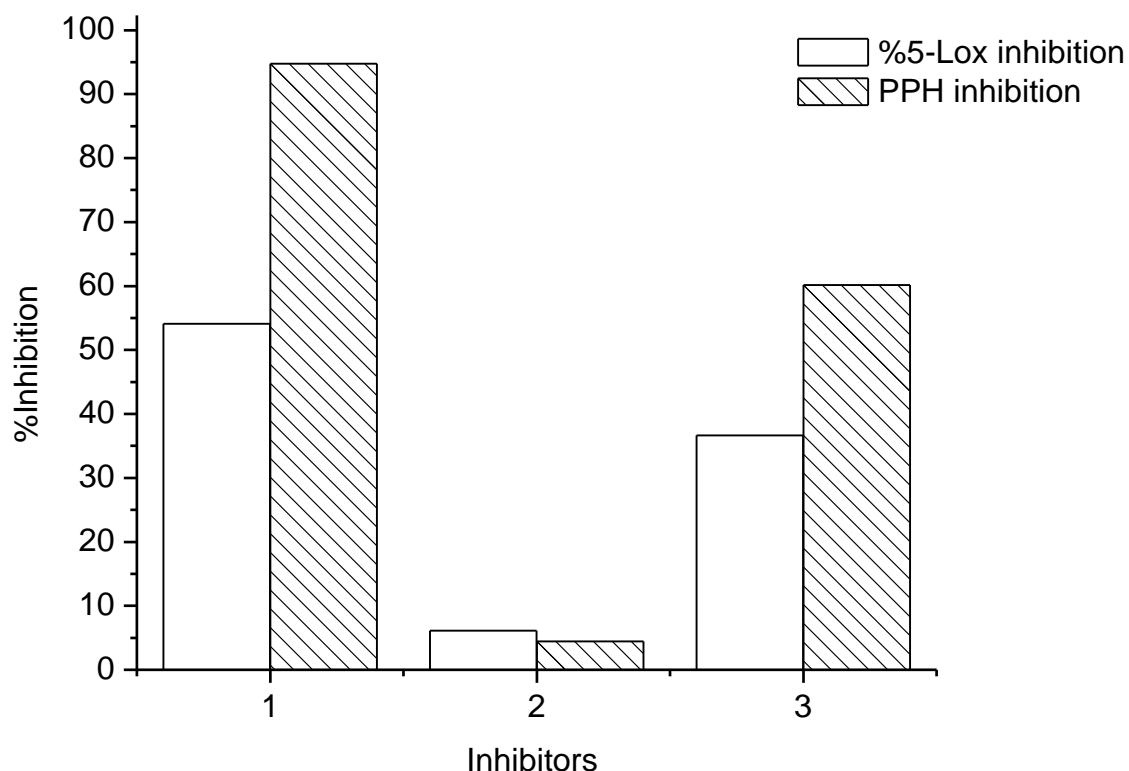


Figure 3.12: The percentage lipid peroxidation and antiradical activities of ascorbic acid (1) as the control, and the free PS drug (2), compared to [Cu(glygly)(PS)] complex (3)

3.3.10. *Ex vivo* permeation studies

The permeability of the drug and complex was quantified in terms of cumulative amount of the drug that permeated per unit time and per unit area and the permeability was plotted against the time. The concentrations and flux values obtained from the permeability study are presented in Figure 3.13 and summarized in Table 3.2. According to the concentration in the donor compartment, the steady state was achieved after 7h for both formulations. The permeation rate of the complex through the skin is slightly elevated compared to the free drug and the peak concentrations were obtained after 24h. This is consistent with a study that was done by

Hostynek et al. (2011), where an increase in permeability of about 100-fold was found in a complete dermatomed skin with a copper (II) complex. Skin permeability coefficients (P_k) for the [Cu(glygly)PS] complex rang went up to 1.93 while the P_k value of PS was 1.60 and the overall flux value of PS was increased from $1.09\mu\text{gcm}^2/\text{h}$ to $1.78\mu\text{gcm}^2/\text{h}$ in the Cu complex form, which is slightly significant. These results suggest that the complex slightly improves *in vitro* skin permeation compared to parent drug.

Table 3.2: The ex vivo studies concentration and flux values (n=3)

Time(h)	[Cu(glygly)(PS)] complex	
	PS Concentration ($\mu\text{g/ml}$)	Concentration ($\mu\text{g/ml}$)
1	4.09 \pm 1.10	4.92 \pm 2.10
1	5.00 \pm 2.40	10.63 \pm 2.80
2	6.44 \pm 1.90	8.55 \pm 0.80
3	8.38 \pm 3.10	13.43 \pm 3.10
4	11.35 \pm 3.60	16.86 \pm 2.90
5	11.02 \pm 2.20	17.58 \pm 1.90
6	11.94 \pm 1.90	18.41 \pm 4.00
7	12.84 \pm 2.70	18.06 \pm 1.90
8	14.36 \pm 4.10	23.54 \pm 4.50
9	14.32 \pm 3.80	22.60 \pm 0.90
10	18.87 \pm 0.90	20.64 \pm 2.00
24	4.09 \pm 1.10	4.92 \pm 2.10

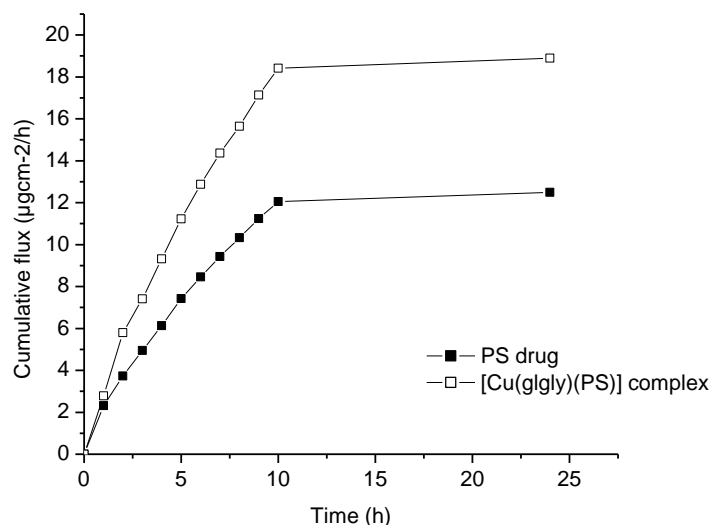


Figure 3.13: The permeability of the drug or/and Cu^{2+} was quantified in terms of cumulative amount permeated per unit time and per unit area and the permeability was plotted against the time.

The results described here, show that a copper complex may be an alternative ant-inflammatory bioactive using the transdermal route as the Cu (II) ions complexed to a drug assist the hydrophilic drug across the stratum corneum. However, the permeation enhancement mechanism of this complex through skin still needs further discussion as it is not fully understood. Also the skin permeation may be further improved with the use of a nanocarrier system, which may include the use of skin permeating polymers.

3.3.11. Cytotoxic potential of the [Copper(glycylglycine)(prednisolone succinate)] complex

The potential cytotoxicity of the PS, and [Cu(glygly)PS] were assessed by exposing cultured HDFa to different concentrations of these compounds, and by evaluating and comparing the change in the mitochondrial metabolic activity of those cells using the MTT assay. The results obtained from the MTT assays are presented in Figure 4. The results showed that [Cu(glygly)PS] complex did not significantly reduce the viability of HDFa when compared to the free drug (PS) and control (untreated cells). Hence it can be established that [Cu(glygly)PS] is non-toxic and the results confirm the findings of Roy et al. (2006); Hostynek et al. (2011) and Stevenson et al. (2013) suggesting that copper complexes have the potential for use without any toxicity concerns in humans.

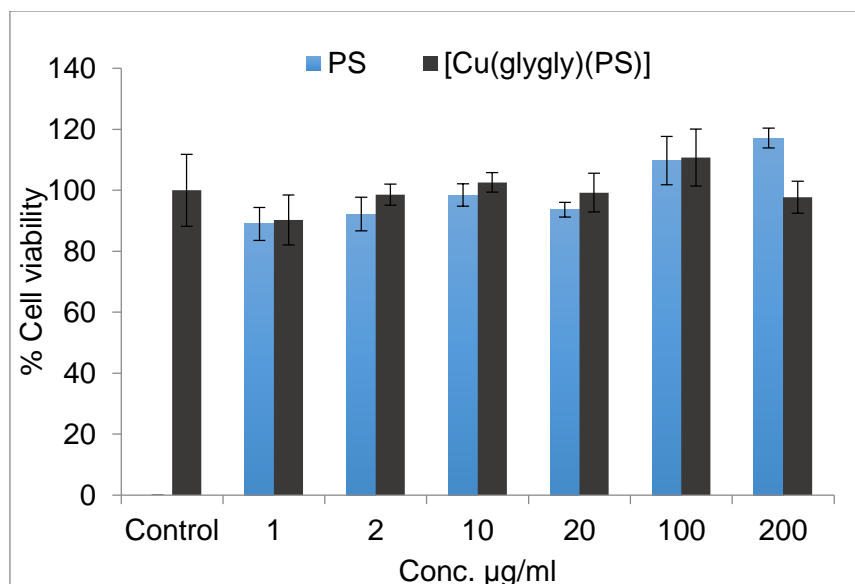


Figure 3.14: The % Cell viability of the PS and complex with MTT assay

3.4. Concluding Remarks

In this study, it has been established that [Cu(glygly)PS] exhibited improved *in vitro* anti-inflammatory/ anti-oxidant activity compared to the parent drug, and also its skin penetration efficacy was slightly improved in TDDS. Furthermore it appeared to be non-toxic in HDFa cells at a concentration equivalent to that of the parent drug. Based on these results, it can be concluded that the coordination of this corticosteroid drug to Cu^{2+} has the potential of reactivating the drug into a more potent coordination compound with improved pharmacokinetics/dynamics that can be advantageous in the treatment of TRAPS through the transdermal route. Although this complex shows a positive outcome in TDDS, the unclear ligand exchange (change in oxidation state) of Cu^{2+} during the diffusion through the skin and its less understood mechanism of action warrant further research directed towards this system. Furthermore the permeation of the complex could be improved by using specific polymeric drug delivery platforms, which have been proved to be highly effective in TDDS while utilizing the improved antioxidant effect of the complex at the site of action.

CHAPTER 4

***IN VITRO* EVALUATION OF NOVEL REDOX/PH DUAL STIMULI-RESPONSIVE NANOLIPOSOMES LOADED WITH COPPER-LIGANDED BIOACTIVE COMPLEX**

4.1. Introduction

Currently there is no ultimate treatment confirmed for prevention or cure for Tumor Necrosis Factor Receptor Associated Periodic Syndrome (TRAPS) disease (Ozen and Bilginer, 2014). This condition is modulated by oxidative stress and redox inflammatory process (Zhu et al., 2012), therefore non-specific anti-inflammatory agents, including steroids are used to reduce the severity and duration of related symptoms. Since the disease symptoms may be prolonged lasting from 1-3 weeks and normally beginning at an early childhood stage (Meiorin et al., 2013). Long term steroidal therapy is a major concern, they become less effective over time, requiring increased dosages and serious side effects may result (Masson et al., 2004). Therefore in this study targeted dual stimuli responsive nanoliposomes (NLs) were formulated for the delivery of [Cu(glygly)(PS)] which have the potential to improve TRAPS symptom management even in prolonged therapy. Based on the vast studies highlighting the benefits of nanotechnologies, liposomes especially have been proven to reduce toxicity and improve the pharmacokinetics of a number of drugs (Kaiser et al., 2013).

Among many kinds of nanocarriers, drug loaded NLs have been extensively studied as an effective type of drug delivery system due to their unique properties (Ozpolat et al., 2014). NLs possess the same physical and chemical properties as liposomes, except that they are presented in a nanoscale diameter range (Khosravi-Darani and Mozafari, 2010), hence allowing improved loading efficiency and their nanosize also allows for easy penetration through skin compared to ordinary liposomes. NLs can be designed to deliver drugs at specific and selective sites by modifying the carrier system, for instance conjugating carriers sensitive to different stimuli including redox and pH stimuli (Khosravi-Darani and Mozafari, 2010). Targeted nanocarriers have the potential to increase solubility, reduce toxicity, enhance bioavailability, improve time-controlled release and enable precision targeting of the entrapped bioactives to a greater extent due to increased surface area (Khosravi-Darani and Mozafari, 2010; Mura, Nicolas and Couvreur, 2013).

Liposomes were initially reported as skin penetration enhancers for transdermal drug delivery in 1980. Since then, liposomes have been shown to be a promising drug-delivery system through the skin (Zhao et al., 2013). It has been determined that NLs up to 600nm in diameter penetrate through skin rather easily and more are retained in the stratum corneum, hence NLs may be significant for the TDD in TRAPS (Schramlova et al., 1997). TDDS provide a convenient route of drug administration for a variety of indications; diseases such as skin cancer, depression and post-menopausal bone loss already have drugs designed to suite TDDS (Patel et al., 2009). NLs delivering drugs through a TDDS can decrease systemic absorption and minimize collateral symptoms due to a reservoir effect and Phospholipid-containing liposomal formulations may act as penetration enhancers and facilitate dermal delivery (Pierre and Costa, 2011; Zhao et al., 2013). In addition, liposomes are generally biodegradable, making them ideal candidates for the delivery of active agents to the body using different routes of administration including TDD (Bowey et al., 2014).

Recently, there has been a growing interest in the development of improved intelligent polymeric drug nanocarrier systems. These systems may have the ability to respond to more than one stimuli, thus assuring controlled drug release under specific pathological conditions (Lu et al., 2014). As a result numerous studies on nanocarriers with dual or multi-sensitivities, such as pH/temperature, pH/redox, pH/glucose, pH/enzyme, dual enzyme, and enzyme/light (Ganta et al., 2008; Cheng et al., 2013; Mura, Nicolas and Couvreur, 2013), have been developed. Even though extensive work has been reported on dual stimuli sensitive nanocarriers, the full potential of these nanocarriers have not yet been reached, hence the aim of this study is to further explore the use of dual stimuli responsive in nanoliposomes and its application in TRAPS treatment.

In the present work, a dual stimuli-responsive Eudragit® E100-cystamine (EuE100-cyst) polymer for pH and redox responsiveness was developed for anti-inflammatory drug delivery in patients with TRAPS. EuE100 is a cationic (pH dependent) polymer that has been widely exploited for its effects in tablet coating (Joshi, Kevadiya and Bajaj, 2010), taste masking (Shishu and Kapoor, 2009; Malik, Arora, and Singh, 2011) and few instances where it is used as an actual drug carrier system (Liu et al., 2007; Kalimuthu and Yadav, 2009; Guzmán, Manzo and Olivera, 2012) and in TDD (Hu et al., 2011). In the present work the EuE100 polymer was developed into a dual sensitive carrier system by coupling it with a sulphide containing agent

(cystamine dihydrochloride) into EuE100-Cyst, the amino groups representing the pH-sensitive component and redox-sensitivity represented by the disulfide bonds (Figure 4.1).

The synthesised EuE100-Cyst polymer was prepared to target the oxidative stress areas of inflammation, as it is well established that the pathological consequences of TRAPS, have pro-inflammatory effects (Touitou et al., 2013) leading to prolonged inflammation. During TRAPS disorder (inflammatory disorder), reactive oxygen species (ROS) are formed when oxygen undergoes a partial one-electron reduction to the super-oxide anion, and subsequently forms hydrogen peroxide and other oxidants causing an oxidative imbalance (stress) (Trachootham et al., 2009). ROS often induces redox adaptation in response to the continued oxidative stress, leading to an up regulation of glutathione (GSH) and other antioxidant molecules (Zhu et al., 2012). Hence the formulated NLs are triggered by both GSH increase (redox sensitivity) and low pH which are typically significant in inflamed tissues (Mahmoud et al., 2011). The underlying mechanism for redox sensitivity is based on the disulfide/GSH exchange reactions (Lopez-Mirabal and Winther 2008). Figure 4.1 below shows the structure of the inflammatory sensitive EuE100-cyst and how it breaks down in the presence of GSH which is excessively increased in the intracellular matrix (ICM) of inflamed cells.

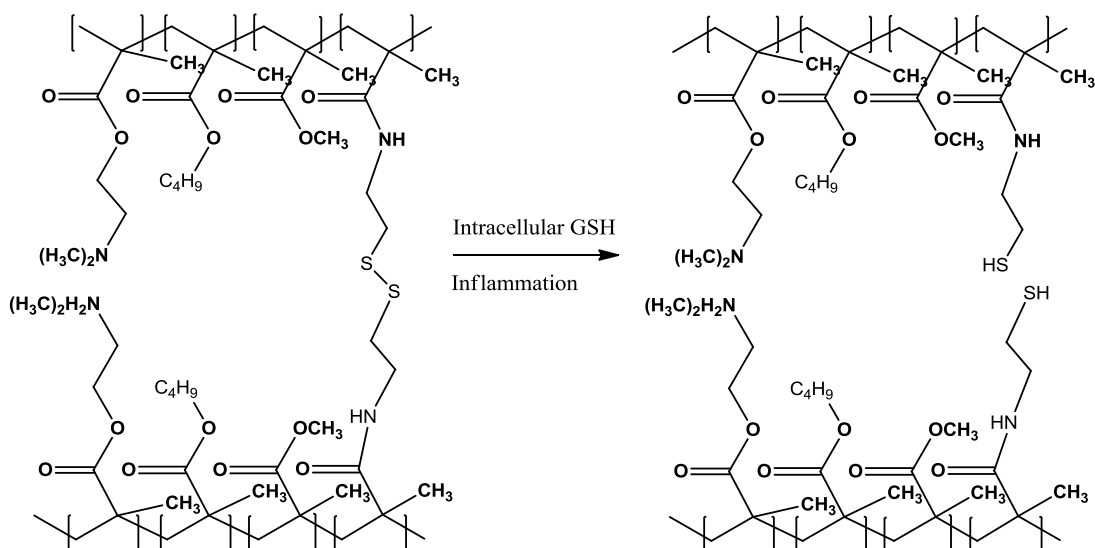


Figure 4.1: Proposed chemical structure of EuE100-cyst and its ICM degradation through the disulfide link in the presence of a reducing agent (GSH).

In this study, intelligent nanocarriers were formulated using EuE100-cyst, loaded with [Cu(glygly)(PS)] complex giving [Cu(glygly)(PS)]-loaded intelligent NLs. Firstly the EuE100 was

modified using cystamine hydrochloride and the formation of EuE100-cyst was confirmed using FTIR, COSY NMR and ^1H NMR. Thereafter the $[\text{Cu}(\text{glygly})(\text{PS})]$ complex was loaded into the prepared NLs and the loading was confirmed using FTIR, the complex entrapment efficacy was also measured. The formation of the NLs was confirmed using TEM and Zetasizer analysis, while the pH/redox sensitivity of the NLs was established by the change in particle size using the size analysis and drug release studies. Furthermore cytotoxicity studies were performed on both the loaded and non-loaded NLs.

4.2. Materials and methods

4.2.1. Materials

Eudragit® E100 (EuE100) was purchased from Evonik Degussa Africa (Midrand, Gauteng, South Africa). Cystamine dihydrochloride (Cyst-2HCl), 1-Ethyl-3-(3dimethylaminopropyl) carbodiimide hydrochloride (EDC), N-hydroxysuccinimate (NHS, cystamine hydrochloride, and 5, 5' dithiobis(nitrobenzoic acid) (Ellman's agent, DTNB), phospholipids included L- α -Phosphatidylcholine (PC), cholesterol (CHOL), and 1,2-distearoyl-sn-glycero-3-phosphatidyl-ethanolamine (DSPE). Phosphate buffer saline (PBS) tablets, Prednisone Succinate (PS) salt, copper (II) nitrate were purchased from Sigma–Aldrich (St. Louise, MO, USA). Sodium hydroxide (NaOH) pellets and dimethylformamide (DMF), ammonium sulphate ($\text{NH}_4(\text{SO}_4)_2$), sodium acetate and glacial acetic acid were purchased from Merck (Wadeville). Dimethylsulfoxide (DMSO) was purchased from Saarchem (Pty) Ltd. (Brakpan, South Africa) and liquid nitrogen was obtained from Afrox (Pty) Ltd. (Industria West, Germiston, South Africa). Double deionised water (ddw) was obtained from a Milli-Q system (Milli-Q, Millipore, Johannesburg) and methanol from Rochelle Chemicals (Johannesburg, South Africa). All other solvents and reagents were of analytical grade and were used as received.

4.2.2. Formulation of dual pH/redox responsive $[\text{Cu}(\text{glygly})\text{PS}]$ -loaded nanoliposomes

4.2.2.1. Synthesis of the $[\text{Cu}(\text{glygly})(\text{PS})]$ complex

$[\text{Cu}(\text{glygly})(\text{PS})]$ complex was prepared as previously detailed in Chapter 3, section 2.2.

4.2.2.3. Coupling of the Eudragit® E100

EuE100 (1mmol) was dissolved in ethanol, while excess NaOH (1.5mmol) was added, and the reaction mixture was left to stir at 60°C for 12h. The resulting brown-yellow solution was

dialyzed using a dialysis membrane of 12kDa against deionised water three times. The purified solution product was freeze-dried, resulting in a water soluble, light brown fine powder.

The powdered dry product (0.5mmol) was dissolved in dimethylformamide(DMF) with EDC (0.6mmol) and NHS (0.6mmol) added immediately to the solution and left to stir for 30min. Cyst-2HCl (0.6mmol) was thereafter added to couple the polymer, carrying out the reaction at room temperature for 6h while stirring continuously. The resulting solution was dialyzed using a dialysis membrane of 12kDa against double deionised water three times, firstly time with 1%w/v NaCl₂ to remove any unreacted cyst-2HCl (Li et al., 2011). Thereafter the purified solution was also freeze-dried to produce a water soluble caramel colored fine product (EuE100-Cyst). The thiol group on the side chain of E100-Cyst was determined using Ellman's method.

4.2.2.2. Determination of thiol groups

The amount of thiol groups present on EuE100-Cyst was determined spectrophotometrically using ellmas reagent DTNB [5,5'-dithiobis-(2-nitrobenzoic acid)], which is also known as the Ellman's method. Briefly, 250µL of 5 mg EuE100-Cyst sample dissolved in 2.5mL PBS at pH 8, then 250µL of PBS at pH 8 and 500µL of 10 mM (4mg/mL) solution of DTNB. The mixture was incubated for 15min at room temperature. The absorbance was determined by the double-beam UV-Vis spectrophotometry (PerkinElmer Spectrum 100, Llantrisant, Wales, UK) at 415nm which is DTNB's maximum absorption. The quantity of thiol was determined using a standard cystamine calibration curve of thiol concentration against absorbance (Robb et al., 2007 and Nguyen et al., 2011).

4.2.2.3. Preparation of the nanoliposomes

The [Cu(glygly)(PS)]-loaded NLs were prepared by adapting a method from Esfahani et al. (2014). In brief, 75:25:10 molar ratios of PC, cholesterol, and DSPE respectively were dissolved in a chloroform/methanol mixture (1:1% v/v) in a round bottom flask. Two phospholipid mixtures were formulated in different flasks. In one formulation the solution of [Cu(glygly)(PS)] complex was added in 0.2:1 ratio of complex to phospholipid (Abraham et al., 2002) and stirred at room temperature for 2h. The mixtures were dried *in vacuo* overnight. The thin phospholipid films remaining on the walls of both flasks were hydrated with 2mM suspension of EuE100-cyst in double deionised water. Final phospholipid concentrations (10mg/ml) (Castile and Taylor, 1999) were subjected to probe sonication (Sonics VibraCell Inc. Danbury, CT, USA) in ice baths. Dual pH/redox responsive [Cu(glygly)(PS)]-loaded NLs and unloaded NLs were produced. In

the loaded NLs unencapsulated [Cu(glygly)(PS)], easily precipitated out of the double deionised water suspension, being easily separated from loaded NLs. The NLs were stored at 4°C until further usage.

4.2.3. Chemical structural analysis of EuE100, EuE100-Cyst, [Cu(glygly)(PS)]-loaded and unloaded NLs using Fourier transform infrared spectroscopy

Fourier transform infrared (FTIR) spectra were performed on EuE100, EuE100-Cyst, [Cu(glygly)(PS)]-loaded and unloaded NLs. FT-IR Spectrometer (PerkinElmer Inc., Waltham, Massachusetts, USA) was used to assess the vibrational transitions in the chemical structures of these compounds, as described in chapter 3, section 3.2.3.

4.2.4. Analysis of the chemical shifts of EuE100 and EuE100-cyst using Nuclear magnetic resonance spectroscopy

The magnetic properties of EuE100 and EuE100-cyst were analysed using the nuclear magnetic resonance (NMR) spectroscopy (¹H, ¹³C and correlated spectroscopy (COSY) spectra) operating at 500 MHz (Bruker Avance BioSpin, Germany), as detailed in Chapter 3, section 3.2.4.

4.2.5. X-ray diffraction Analysis of EuE100 and EuE100-cyst

The XRD pattern of EuE100 and EuE100-cyst was investigated with the X-ray diffractometer (ULTIMA-III, Rigaku, Japan), as detailed in chapter 3, section 3.2.7.

4.2.6. Determination of the thermal properties of EuE100 and EuE100-cyst

4.2.6.1. Differential scanning calorimeter analysis

A differential scanning calorimeter (DSC) (Mettler Toledo, DSC1, STAR^e System, Schwerzenback, Switzerland) was used to determine the thermal properties of the EuE100 and EuE100-cyst as detailed in chapter 3, section 3.2.9.

4.2.6.2. Thermogravimetric analysis

Thermal analysis was performed using thermogravimetric analysis (TGA) (Toleda TC15 TA controller, Mettler). It was used to measure the thermally induced changes in chemical and physical properties of EuE100 and EuE100-cyst as detailed in chapter 3, section 3.2.9.

4.2.7. Determination of particle size and zeta potential of [Cu(glygly)(PS)]-loaded intelligent nanoliposomes

The zeta sizer was employed to determine the typical particle size and polydispersity index (PDI) of the NLs, also zeta potential analysis was performed to establish the surface charge and physical stability of the NLs. These procedures were carried out using a Zetasizer NanoZS (Malvern Instruments, Worcestershire, UK).

4.2.8. Transmission electron microscopy of the [Cu(glygly)(PS)]-loaded intelligent nanoliposomes

The structural morphology of the [Cu(glygly)(PS)]-loaded NLs was carried out using transmission electron microscopy (TEM) (Jeol 1200 EX, Japan). The NLs were suspended in double deionised water (0.5mg/mL) and a pipette was used to place a drop of the suspension on a 200 mesh thick formvar copper grid (TABB Laboratories Equipment, Berks, UK). The NLs were allowed to be adsorbed on the surface of the copper grid, thereafter a drop of 2%w/v uranyl acetate in double deionised water was added on the adsorbed NLs and left to dry for an hour at room temperature (Ruozi et al., 2011).

4.2.9. Investigation of redox/pH Sensitivity of the [Cu(glygly)(PS)]- loaded intelligent nanoliposomes

The significant concentration difference of GSH between the extracellular matrix (ECM) (~0.002 to 0.02mM) and ICM (~10mM) environment has been widely utilized as an ideal trigger for the redox responsive delivery systems, as the disulphide bond is cleaved in the presence of GSH and drug release occurs (Lv et al., 2014; Ashwinkumar et al., 2014). Additionally during inflammatory diseases there is a significant decrease of pH in the ECM, hence the effect of pH is also used as a response mechanism for drug release. To mimic these responses the [Cu(glygly)(PS)]-loaded NLs were soaked in PBS (pH 7.4) and acetate buffer (pH 5), at room temperature with or without 10mM of GSH. The NLs were incubated for 30min ensuring that swelling equilibrium was reached (Aydın and Pulat, 2012). Particle size evaluation was undertaken after incubation of the NLs in different mediums, using a Zetasizer Nano Z (Malvern, UK).

4.2.10. Determination of entrapment efficiency of [Cu(glygly)(PS)]-loaded intelligent NLS

Entrapment efficiency (EE) was calculated to account for the ratio of [Cu(glygly)(PS)] encapsulated in the NLS to that of the total [Cu(glygly)(PS)] in the NLS dispersion. To disrupt the structure of the NLS, the NLS were suspended in methanol (5mg/mL) and centrifuged at 1000rpm for 20min to separate drug from phospholipids and polymer. The %EE was determined by measuring the absorbance of the supernatant using UV-Vis spectroscopy (PerkinElmer Spectrum 100, Llantrisant, Wales, UK) at wavelength 242nm. A concentration versus absorbance calibration curve was employed for the quantification of the [Cu(glygly)(PS)] entrapped. The %EE was calculated using the following equation:

$$\%EE = \left(\frac{\text{Amount of [Cu(glygly)(PS)] in liposomes}}{\text{Amount of total [Cu(glygly)(PS)]}} \right) \times 100 \quad \text{Equation 4.1}$$

4.2.11. *In vitro* drug release from the NLS

In vitro drug release from [Cu(glygly)(PS)]-loaded NLS was carried out in PBS (pH 7.4) and acetate buffer (pH 5) with and without GSH (10mM) at 37°C using dialysis membranes (MWCO: 1.2kDa). The medium of pH 7.4 without GSH corresponds to the condition in which NLS will encounter during circulation after administration, while medium of pH 7.4 with 10mM GSH corresponds to the ICM condition. At pH 5 ECM conditions were mimicked with insignificant GSH (KC, Thapa, Xu, 2012). Equivalent amounts of [Cu(glygly)(PS)]-loaded NLS were placed in dialysis bags and immersed in 50mL of different buffer mediums. At predetermined time intervals (0.5, 1, 2, 4, 6 and 24h), 1mL of each buffer medium was removed for analysis and replaced with the same quantity of fresh buffer medium, to maintain sink conditions. Samples were kept at 8°C until they were analysed using the UV-vis spectroscopy at a wavelength of 242nm using calibration curve as described in chapter 3, section 3.2.11.

4.2.12. *In vitro* cytotoxicity studies

In vitro cytotoxicity Studies of the [Cu(glygly)(PS)]-loaded and unloaded NLS were carried out using Human Dermal fibroblast adult (HDFa) cells (Cell Applications Inc. (CAI), San Diego, USA) as described in Chapter 3, section 3.2.12.

4.2.13. Statistical analysis

Results are presented as average \pm SD of triplicate experiments unless otherwise mentioned.

4.3. Results and Discussion

4.3.1. Synthesis and Characterisation of EuE100-Cyst

The 3D structure of the EuE100 and EuE100-cyst in the visualization of geometrical preferences is shown in Figure 4.2(a), and b) reaction scheme for the preparation of the EuE100-cyst.

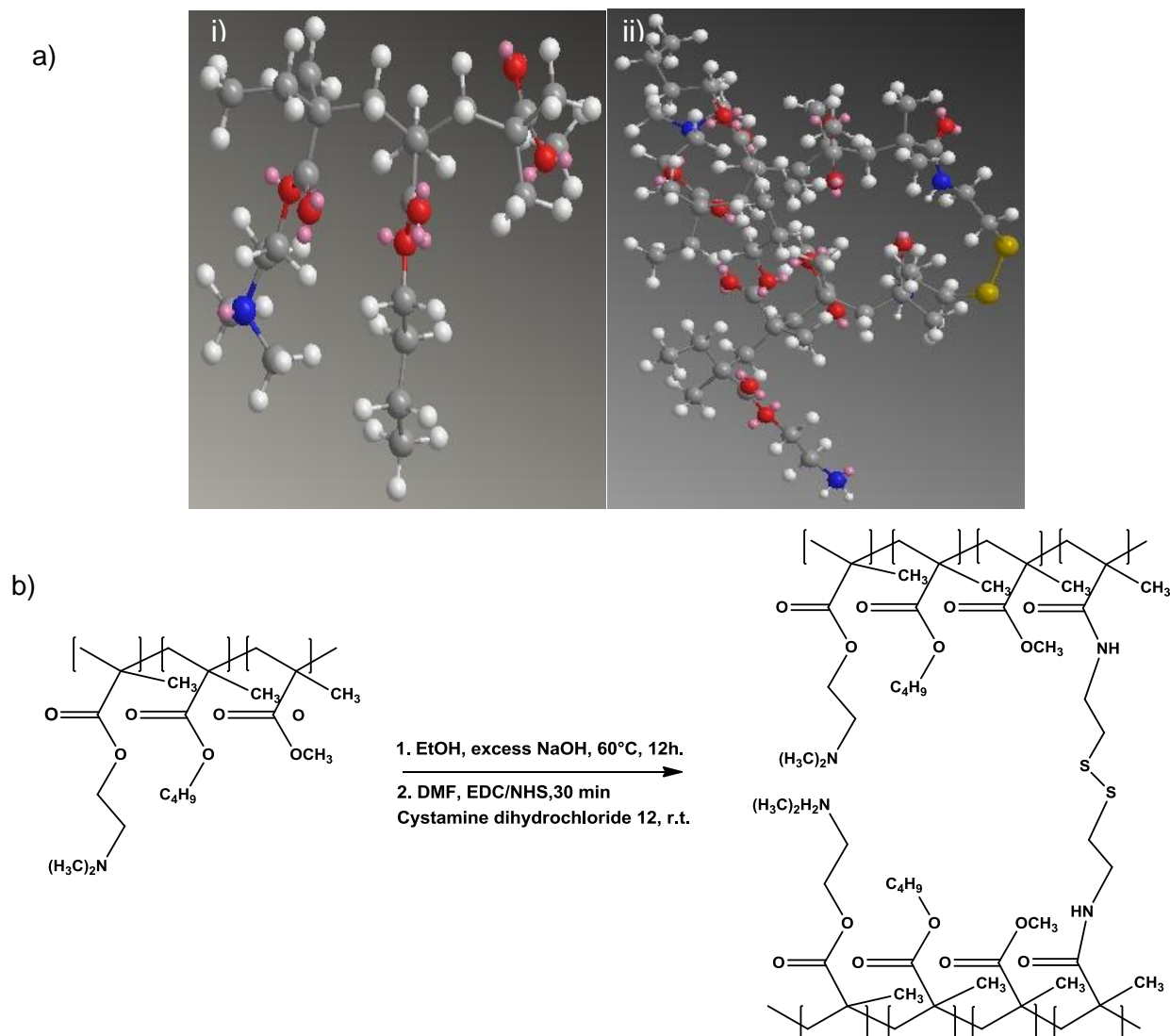


Figure 4.2: Visualization of geometrical preferences of (i) EuE100 and (ii) EuE100-cyst after molecular simulation. Color codes: C (grey), O (red), N (white), H (pink) and S-S (yellow), and b) reaction scheme for the preparation of the EuE100-cyst.

The dual pH/redox responsive NLs were loaded with [Cu(glygly)(PS)] complex. These NLs were prepared by conjugating a pH/redox responsive EuE100-cyst polymer with a phospholipid bilayer. The EuE100-cyst polymer was prepared by coupling a cationic EuE100 polymer with a cystamine compound producing a 20-28% cystamine (thiol) group substitution on the EuE100-cyst. Due to the hydrophilicity of this polymer it is expected to attach itself on the outer

hydrophilic layer of the phospholipid bilayer while the hydrophobic [Cu(glygly)(PS)] complex is embedded within the bilayer. As a result of the EuE100-cyst conjugation, the NLs are predicted to degrade in a sequential manner (Figure 4.3). As the NLs penetrate through inflamed cells they will first encounter a low pH in the ECM where they will undergo an initial degradation (slight swelling). Upon reaching the ICM cytosol, the NLs will fully degrade in the presence of GSH and release the complex to the cell nucleus (site of action). This specific approach is expected to modify the release of the complex molecules under low pH values and high GSH concentrations, allowing the NLs molecules to move freely via normal diffusion and eventually be excreted if no inflammation occurs.

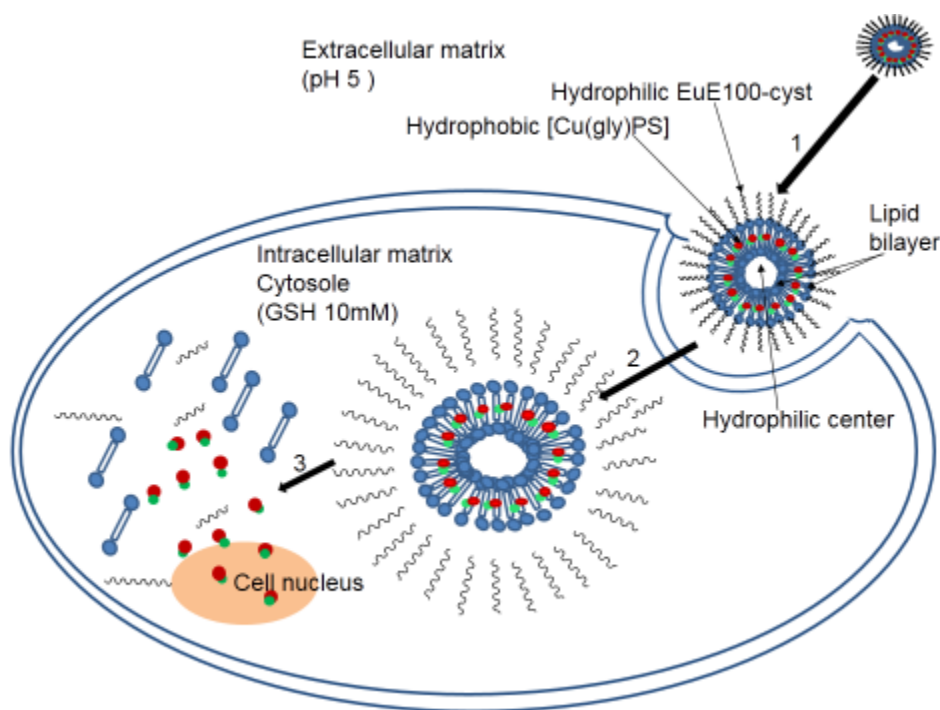


Figure 4.3: The expected sequential degradation of the NLs in the inflamed tissue: 1. The initial degradation; as the NL passes through the extracellular matrix into the cell it encounters a reduced pH up to pH 5, and it swells. 2. The NL passes through the cell into the ICM (cytosol) where there is increased GSH concentration up to 10mM during inflammation, the NL undergoes full degradation. 3. The complex is finally released to the nucleus of the cell where it exert its improved ant-inflammatory effects.

4.3.2. Chemical structural evaluation using Fourier transform infrared (FTIR) spectroscopy

An FTIR spectrum is a unique technique that may be utilized in drug delivery to identify the presence or absence of certain chemical functional groups in molecules (Parida et al., 2012). The vibrations of IR spectra may be used to characterize the possible interactions of the different molecules used to formulate the NLs. The FT-IR spectra of EuE100-cys and EuE100

are shown in Figure 4.4a, and b, respectively. Only the noteworthy absorption bands are discussed (inserted boxes). Figure 4.4a shows a new strong N-H stretch band at 3285cm^{-1} , the one and two amide absorption bands are also seen at 1644 and 1555cm^{-1} respectively, and all these bands are due to the coupling of the amino group from the cystamine to the COO^- of the EuE100 resulting in $-\text{COONH}-$. It is also observed that the band at 1098cm^{-1} , which is the ester stretch from RCOCH_3 of the EuE100 is not seen in the EuE100-cyst spectra, hence thiolation of the polymer occurred.

Furthermore other major absorption bands were noted to be present in both spectra for instance the alkyl carboxylic acid R-COO-R band at 1721cm^{-1} , aliphatic C-H stretch absorption band at $2949-59\text{cm}^{-1}$, the methyl ($-\text{CH}_3$) C-H stretch band at 1453cm^{-1} and isopropyl CH_3 doublet at 1370 and 1380cm^{-1} , thus the backbone of EuE100 was maintained.

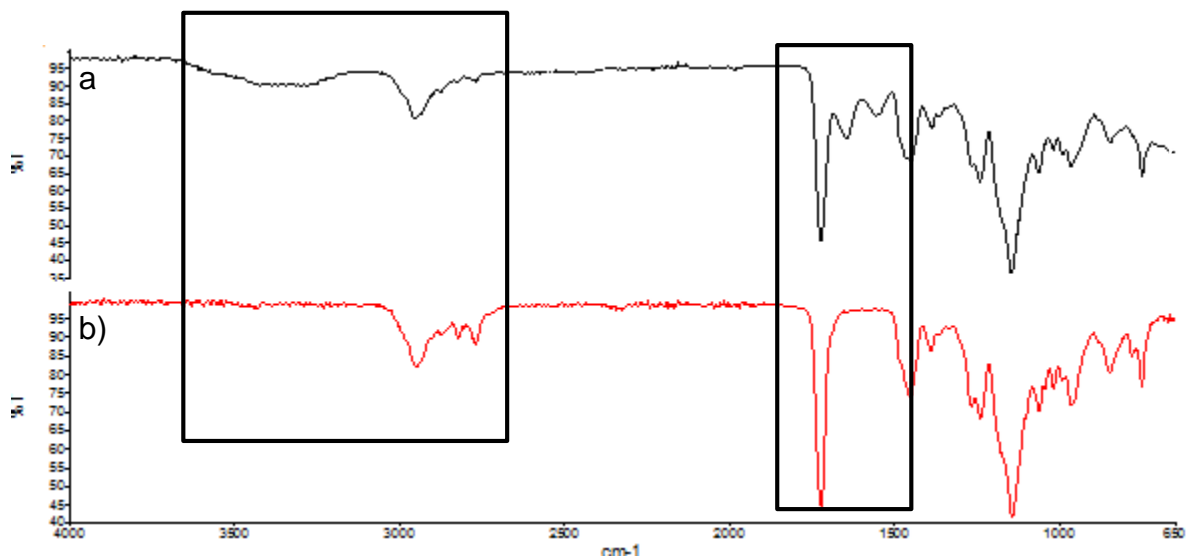


Figure 4.4: The FTIR spectra of EuE100 and its derivatives are shown. (a) EuE100-Cyst. (b) EuE100.

FTIR spectra were used to validate the covalent conjugation of complex into the NLs. Figure 4.5a, b and c shows a typical FTIR spectrogram of unloaded NLs, complex-loaded NLs the complex, respectively. The FTIR spectra of the complex loaded NLs and unloaded NLs indicate that characteristic peaks of the unloaded NLs were not altered and had no changes in their positions after $[\text{Cu}(\text{glygly})(\text{PS})]$ encapsulation. However there was one new significant $\text{C}=\text{O}$ (aryl ketone) vibration which is the $[\text{Cu}(\text{glygly})(\text{PS})]$ characteristic peak at 1653cm^{-1} and 1656cm^{-1} (inserted box in figure 4.6) for $[\text{Cu}(\text{glygly})(\text{PS})]$ and $[\text{Cu}(\text{glygly})(\text{PS})]$ -

loaded NLS, respectively, indicating complex loading was achieved. The novel [Cu(glygly)(PS)]-loaded NLS were thus successfully formulated.

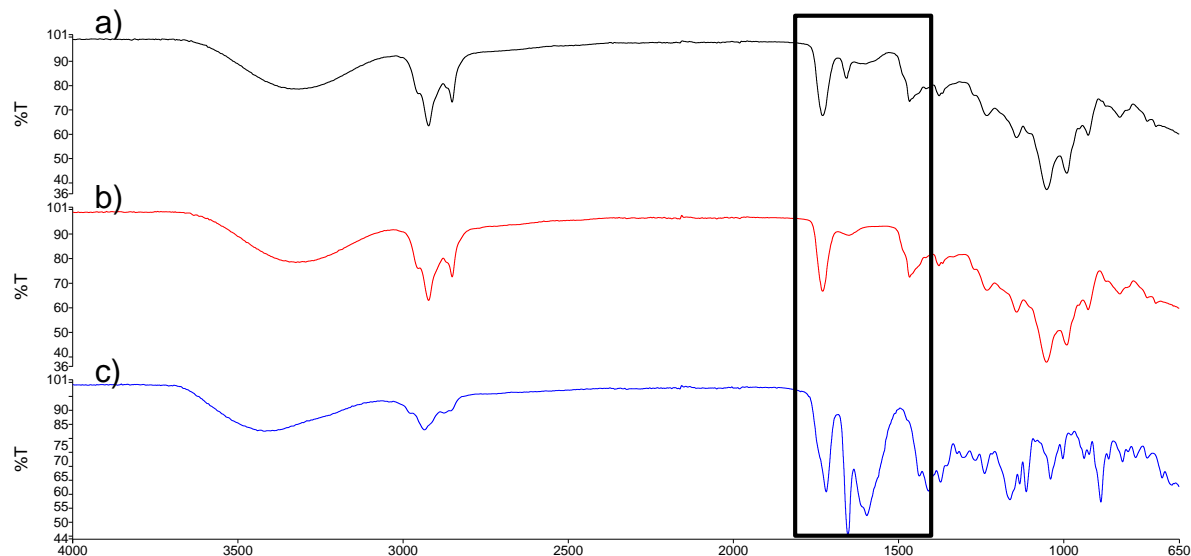


Figure 4.5: FTIR spectroscopic analysis of (a) [Cu(glygly)(PS)]- loaded NLS, (b) unloaded NLS and (c) complex.

4.3.3. Evaluation of the magnetic properties using Nuclear magnetic resonancespectroscopy

The ^1H NMR comparative spectra of EuE100 and EuE100-cyst indicate that the polymer (EuE100) and cystamine successfully coupled into EuE100-cyst (Figure 4.6). It can be found that the peak at 7.99ppm is associated with the amide bond (-CONH-) where the cystamine interacts with the EuE100 in coupling reaction. The rest of the peaks from 0.92-4.18ppm in the EuE100-cyst are corresponding to the EuE100 peaks from 0.92-4.14. The only difference being the shifting of the peak at from 4.13 in EuE100 to 4.18 in EuE100-cyst which shows the bonding of the COO^- to the amide instead of the carbon (methyl group). This also demonstrates that the backbone of the EuE100 chain is maintained.

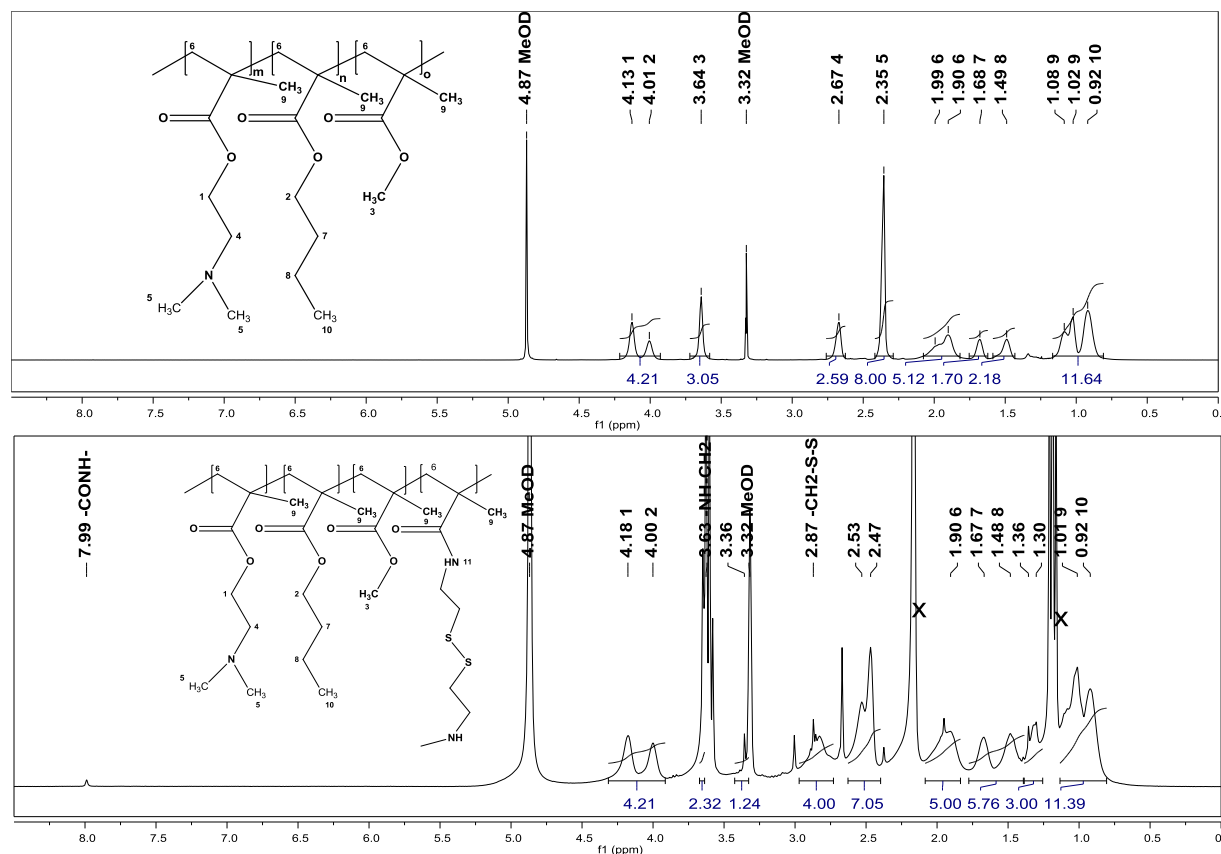


Figure 4.6: Comparative ¹H NMR in MeOD.

Additionally COSY is important in structure elucidation as it shows the correlation or coupling between two adjacent protons. From the COSY spectrum (Figure 4.7), the coupling between protons at [1] and [4] (blue dotted line) and [2] and [7] (red dotted line) is observed. When compared to the EUD cyst similar interactions are observed and there are some new CH₂-CH₂ interactions as well (green dotted line) coming from the cyst moiety. These new interactions confirm the coupling reaction.

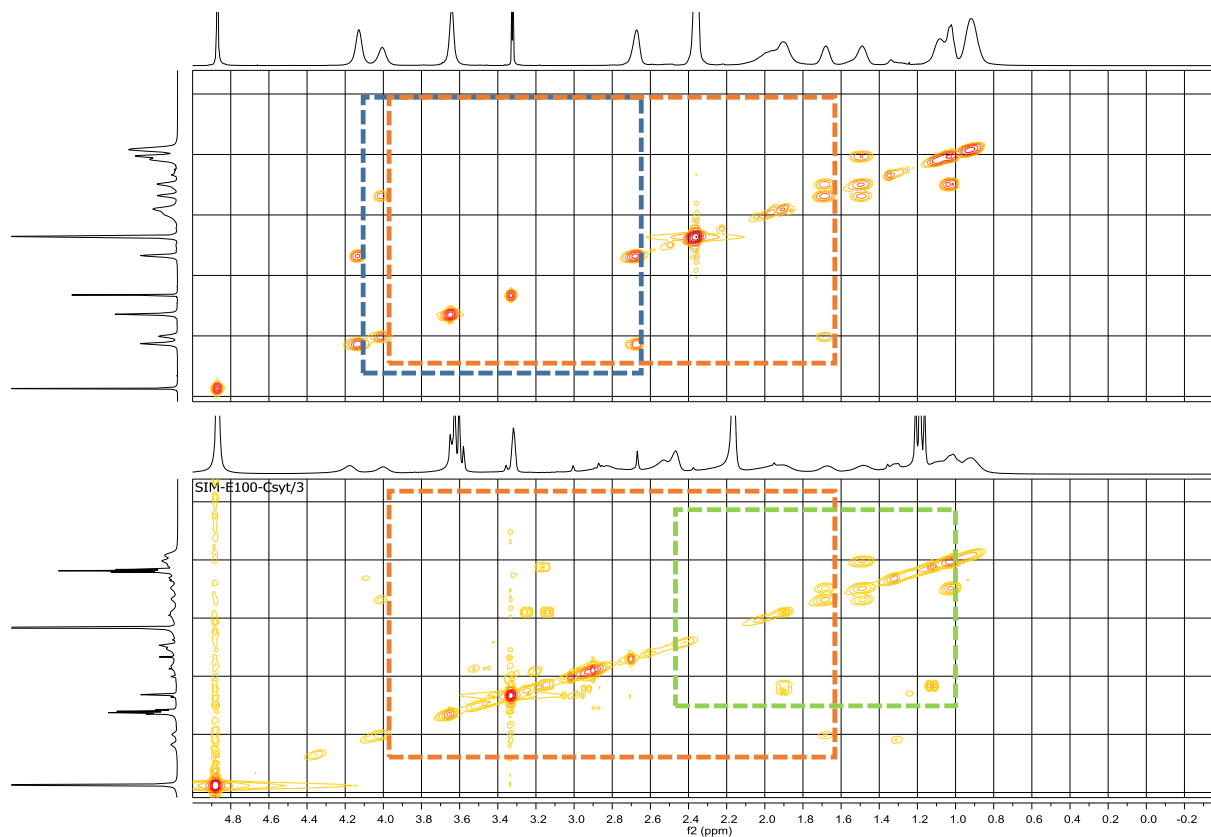


Figure 4.7: Comparative COSY NMR in MeOD.

4.3.4. Evaluation of the thermal properties of EuE100 and EuE100-Cyst using differential scanning calorimeter analysis

Figure 4.8 shows the DSC thermograms of EuE100 and EuE100-Cyst. All the graphs represent endothermic melting peaks, Figure 4.8a shows EuE100 with the onset at: 260.03°C, maximum peak at: 301.13°C, and recovery (endset) at: 333.13°C, Figure 4.8b shows EuE100-Cyst with the onset at: 210.28°C, maximum peak at: 254.23°C, recovery (endset) at: 288.32°C. Additionally there is a small peak at ~272°C on the EuE100-cytgraph which may be attributed to the decomposition of the cystamine group on the EuE100.

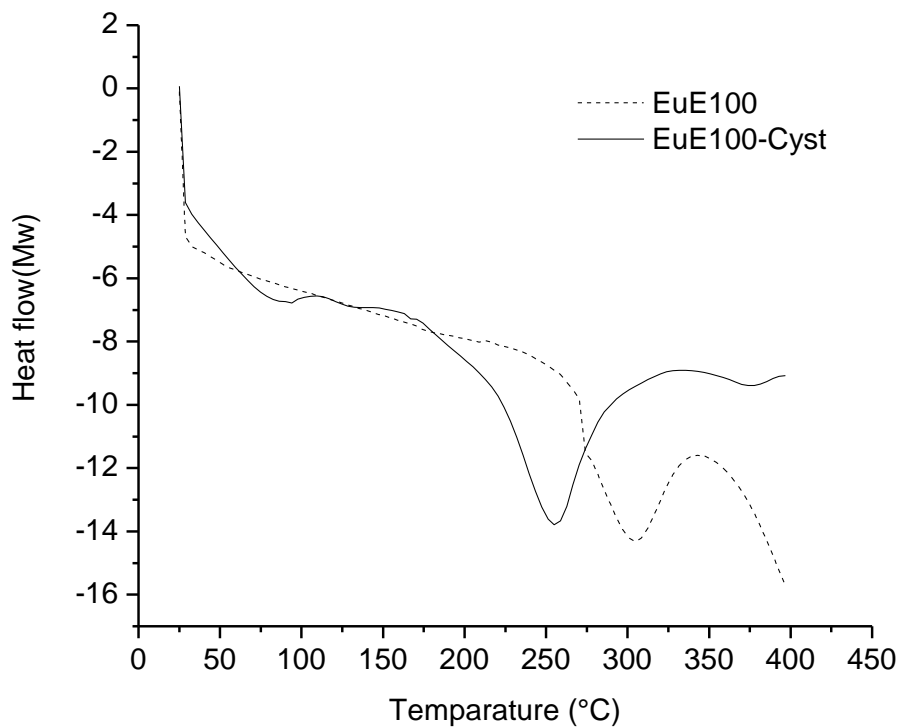


Figure 4.8: The DSC graphs, a) EuE100, b) EuE100-cyst.

4.3.5. Evaluation of the thermal properties using thermogravimetric analysis (TGA)

The simultaneous TG/DTA thermal analysis of EuE100 and EuE100-Cyst are observed in Figure 4.9a and b. The graphs show that the weight losses from EuE100 and EuE100-Cyst in the temperature range of 300–400°C are approximately 46-74% and 46-76%, respectively. The total weight loss occurred at 425°C and 470°C for EuE100 and EuE100-Cyst, respectively, which shows the decomposition of the compounds. The shift to a higher temperature in the thermal degradation of the thiolated EuE100 indicated an increase in the organization of the compound mostly due to the interaction between the cyst and EuE100 during the coupling resulting into EuE100-cyst. Additionally there is a small peak between 350°C and 400°C in the TG/DTA graph which may be attributed to the decomposition of the Cystamine group on the EuE100. This also agrees with the DSC results where the EuE100 has a higher melting point compared to the EuE100-cyst.

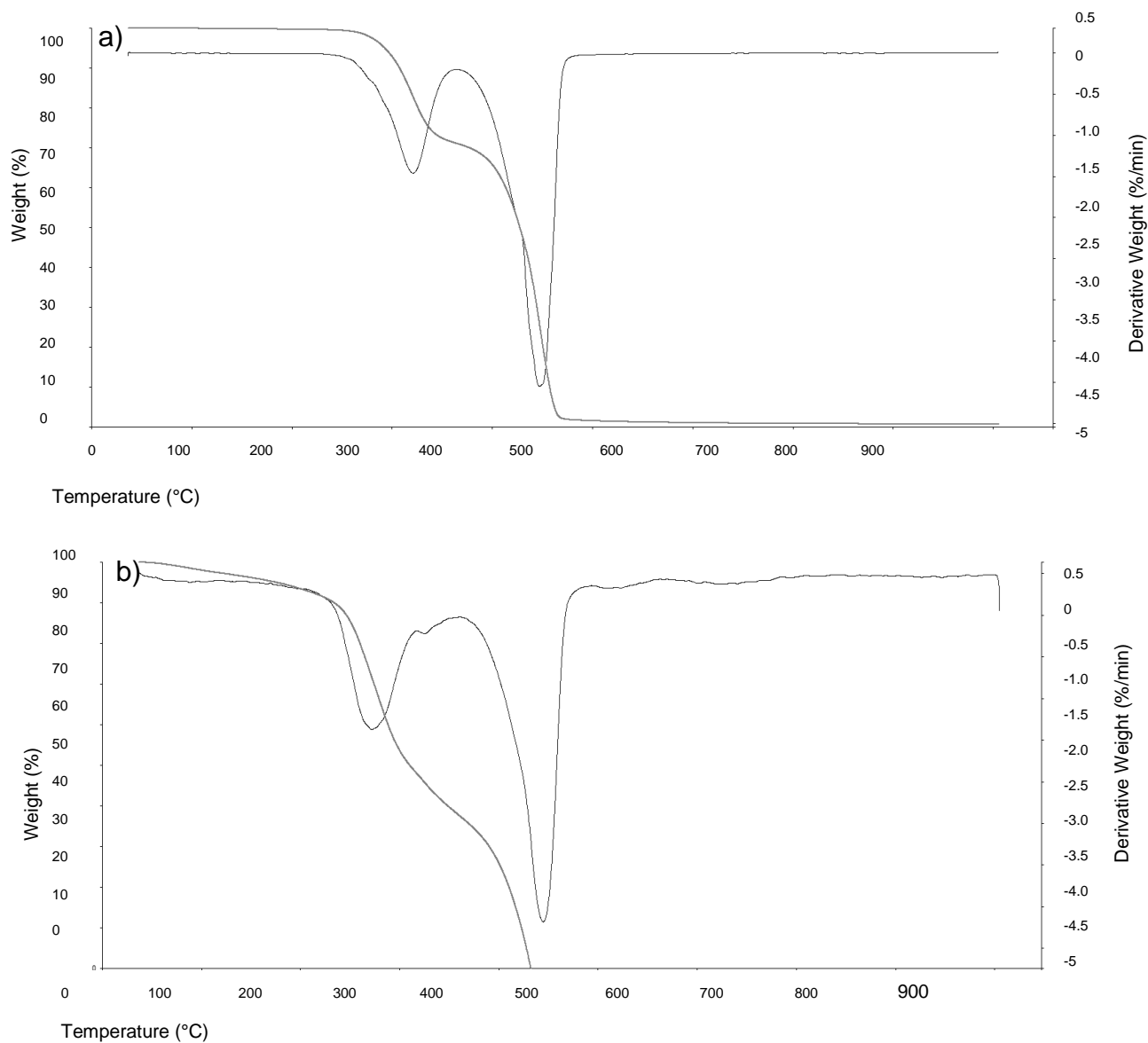


Figure 4.9: (a) TG/DTA of the EuE100 and (b) TG/DTA of EuE100-cyst.

4.3.6. Assessment of the degree of structural order using X-ray Diffraction

The powder X-ray diffraction patterns for the pure EuE100 and functionalized EuE100 (EuE100-cyst) are given in Figure 4.10. In the XRD profiles of the powder, EuE100 is in a crystalline state with the main diffraction peaks observed at $2\theta = 9.3$ and 19.1 , whereas in the EuE100-cyst these two corresponding amorphous peaks still exist, but their intensities are reduced. These results demonstrate that the functionalization of EuE100 by coupling with cyst destroyed the original amorphous state of the EuE100. In addition these results confirm the

interaction of the EuE100 carbonyl group and amino group of the cyst, which then resulted in an amorphous structure of the polymer complex (EuE100). According to Prabakaran and Gong (2008) the amorphous nature of the thiolated EuE100, may be attributed to the improved biodegradability and mucoadhesive properties of the EuE100-cyst. The findings of the XRD analysis were also in accordance with the above DSC and TGA results, providing evidence that the crystalline structure of EuE100 was converted to an amorphous state (EuE100-cyst).

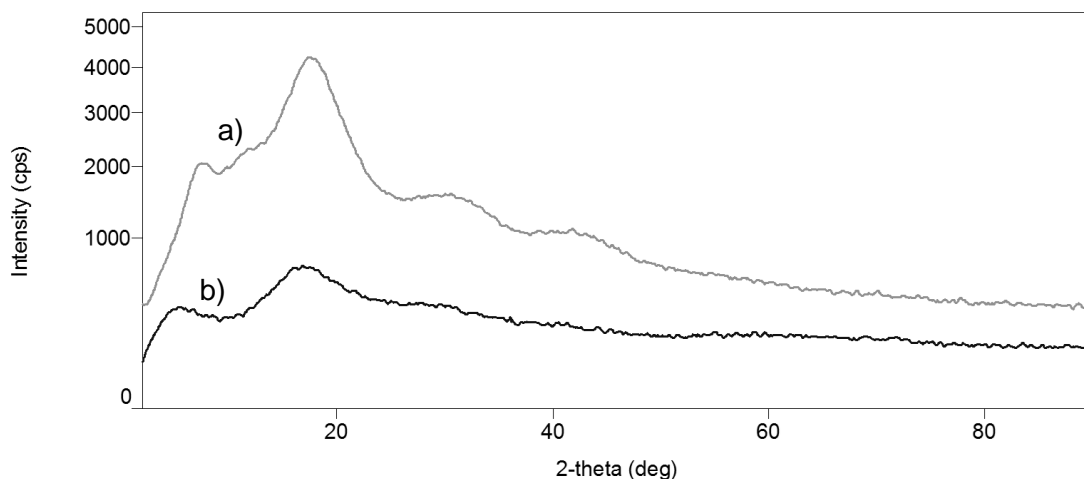


Figure 4.10: The X-ray diffraction of the (a) EuE100-Cyst powder and (b) EuE100.

4.3.7. Determination of particle size in functionalised nanoliposomes

The size distribution and average of three different batches of nanoliposome suspensions were analysed using the Zeta sizer. The size distribution profile of all the batches was narrow (Pdl 0.199 ± 0.148) with a particle range of $100 \pm 47\text{nm}$ (Figure 4.11). The zeta potential analysis (Figure 4.12), show that the [Cu(gly)(PS)]-loaded NLs had a charge of +17mV which is significantly more positive compared to the surface charge of the non-loaded NLs which is +5mV. The strong positive charge on [Cu(gly)(PS)]-loaded NLs may be due to the complex which is on the lipid bilayer of the NLs.

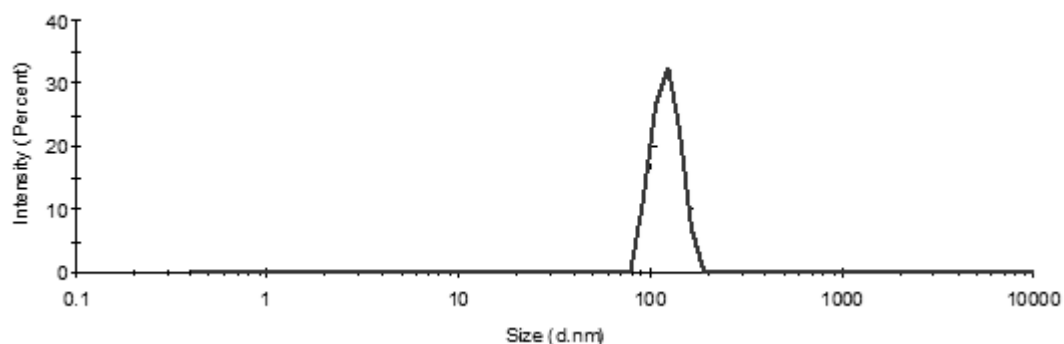


Figure 4.11: Size distribution of the [Cu(gly)(PS)]-loaded intelligent NLs is shown.

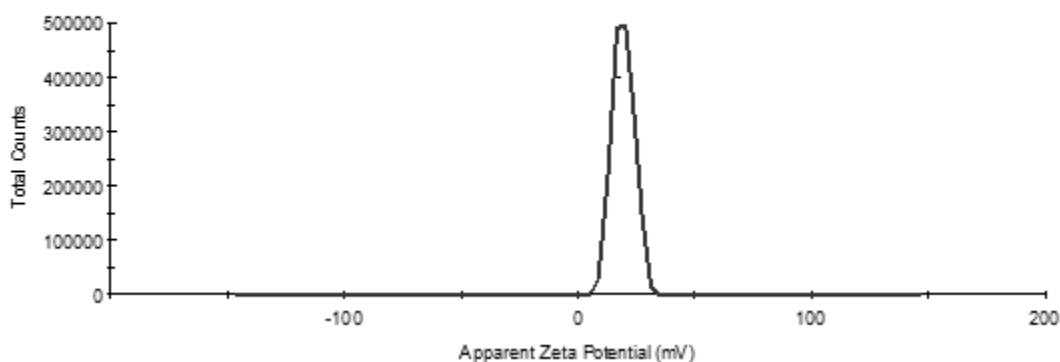


Figure 4.12: Surface charge (zeta potential) of the [Cu(gly)(PS)]-loaded intelligent NLs

4.3.8. Transmission electron microscopy of the [Cu(gly)(PS)]-loaded intelligent nanoliposomes

The morphology and presence of the NLs were confirmed by TEM which established the existence of predominantly spherical-shaped unilaminar vesicles with a size range less than 200nm (Figure 4.13). The NLs existed homogenously dispersedly in the system, in a non-aggregated form. The sizes of the NLs observed in the TEM micrographs were typically of a similar size as the results obtained by the measurement of the particle size.

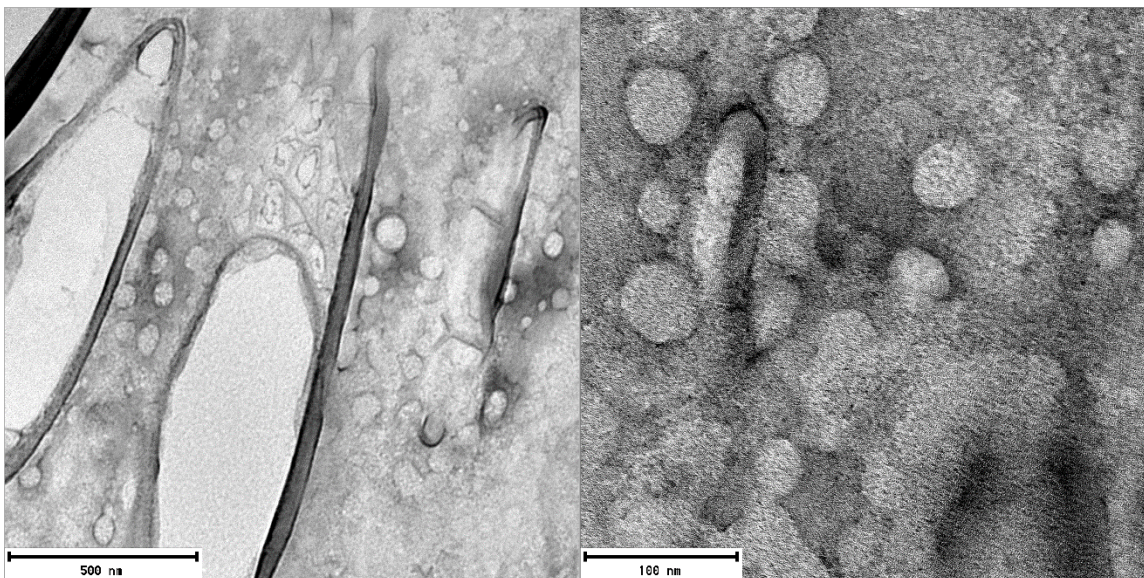


Figure 4.13: The TEM micrographs of [Cu(gly)(PS)]-loaded intelligent nanoliposomes in uranyl acetate (negative stain).

4.3.9. Investigation of redox/pH sensitivity of nanoliposomes

As the EuE100-cyst network contains a pH-ionizable group, and a disulphide bond that is broken in the presence of GSH/pH, soaking the NLs in a medium with GSH, low pH or both mimics the inflamed environment conditions thus elicits the swelling behavior. Therefore the change in mean size of the pH/redox sensitive EuE100 NLs was determined. According to the graphs in Figure 4.14, particle size sharply increased when pH was reduced from 7.4 to 5 and in the presence of GSH; the GSH has a major impact on the particle size, hence as swelling and drug release, as confirmed by a sharp increase in its presence compared to low pH. This GSH-responsive behavior could be ascribed to cleavage of the disulphide bonds in the ICM environment of inflamed cells, but firstly NL penetrates through the cell from ECM to the ICM where the complex is partially released in the low pH and once in the cytosol complete drug release occurs in the presence of GSH (Aydın and Pulat, 2012). This will ensure a controlled release of the complex.

These results concluded that particle size of the NLs is very sensitive to the changing pH/redox values of the aqueous environment they are in. The particle size is increased from 100nm up to 357nm at low pH 5 and 900nm in the presence of GSH. In this study, the swelling and shrinking mechanism with regard to swinging pH values has been investigated in terms of smart responsive nanoparticle systems for localised drug delivery.

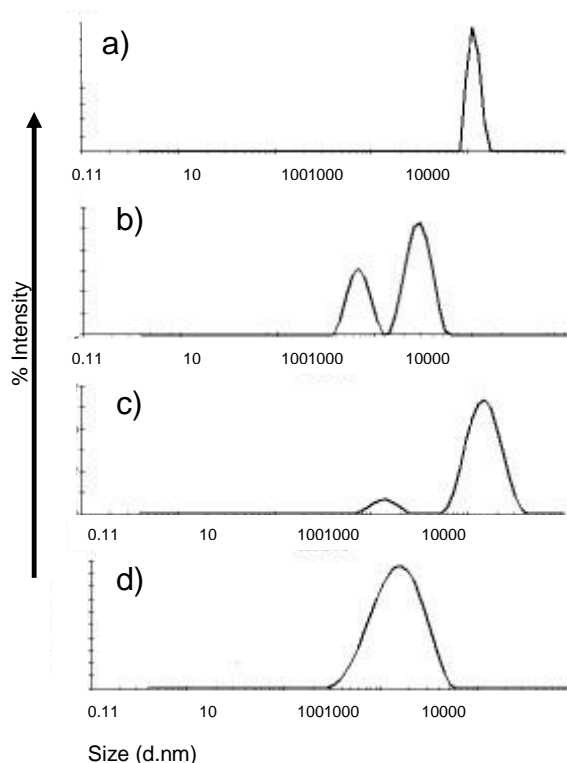


Figure 4.14: The particle size of NLs: (a) at pH 5 with 10mM GSH, (b) at pH 5 without any GSH, (c) at pH 7.4 with 10mM GSH and (d) at pH 7.4 without any GSH.

4.3.10. Entrapment efficiency and *in vitro* [Cu(glygly)PS] release studies

An ultimate stimuli responsive nanocarrier system should have properties of slow drug release during circulation while it targets the affected cells and release the drug rapidly in the affected cells. This ensures fewer side effects from the drug, as less drug molecules are expected to be present in blood circulation. The %EE was $85 \pm 8\%$ and the percentage *in vitro* release was calculated using the established %EE values. *In vitro* complex release from the dual pH/redox sensitive NLs was assessed and the results are summarized in Figure 4.15. As anticipated, the release rate of [Cu(glygly)(PS)] in pH 5 was faster than that in pH 7.4, 65.2 ± 4.9 and 78.9 ± 3.7 of the complex was released within 6h in pH 7.4 and 5 respectively, with 10mM of GSH. The % release in pH 5 and 7.4 without GSH was 65.6 ± 4.2 and $27.6 \pm 5.4\%$, respectively. The slow release of [Cu(glygly)(PS)] in PBS pH 7.4 without GSH indicates that the functionalized NLs are mostly stable at physiological environments, hence minimising side effects in the unaffected tissues and cells. It should be noted that the effects of the GSH are more pronounced compared to the acidic pH effects in the swelling, degradation and release of the drug; this could be due to the direct coupling of the disulphide bond on the EuE100 polymer (high percentage of

substitution). This concludes that the incorporation of the redox/pH polymer controls the degradation and the release of [Cu(glygly)(PS)]. This finding is also consistent with the swelling of the NLs in Figure 4.14 with NLs incubated in GHS at both PBS (pH 7.4) and acetate buffer (pH 5), with and without 10mM GSH. This concludes that the incorporation of the redox/pH polymer controls the degradation and the release of the complex. These results agree with the findings established by number investigators(Remant et al., 2012; Lu et al., 2014; Kang et al., 2015).

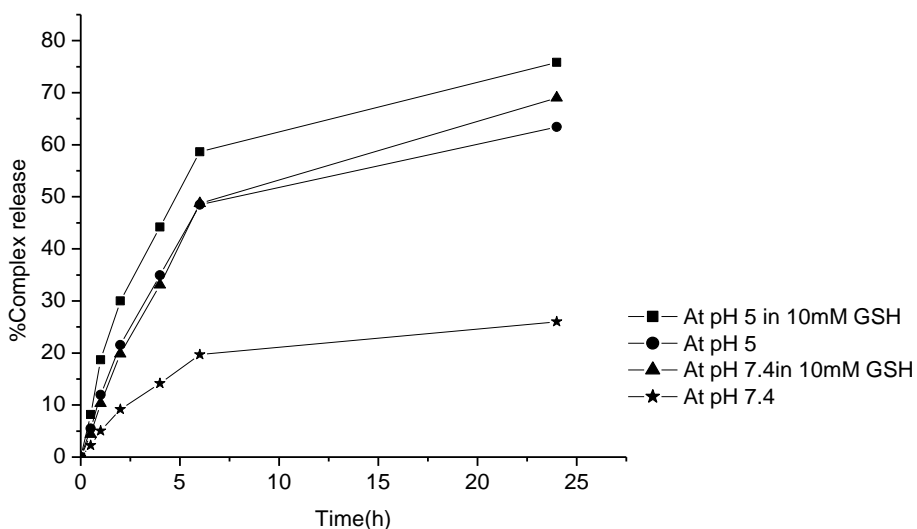


Figure 4.15: Drug-release profile of [Cu(glygly)(PS)] from pH/redox sensitive NLs at pH 7.4 and 5, with and without 10mM GSH.

4.3.11. Evaluation of *in vitro* cytotoxicity

The potential cytotoxicity of the [Cu(glygly)PS]-loaded and unloaded NLs were assessed by exposing cultured HDFa to different concentrations of these compounds. The CV observed (Figure 4.16) was consistent throughout all the concentrations and slightly dependent on the concentration, the CV was increased with an increase in both the loaded and unloaded NLs concentration. These results show no significant difference in CV of the HDFa cells when compared to the the control (untreated cells). According to Sharma et al. (2012) a cell viability of 80% or greater shows a good cytotoxicity compatibility of the tested formulations, hence establishing that these formulations have the potential for use without toxicity concerns.

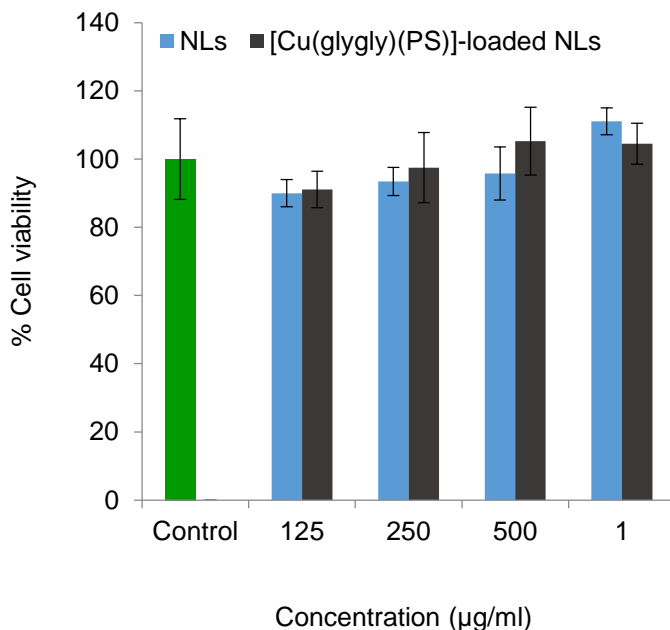


Figure 4.16:The % Cell viability of the [Cu(glygly)(PS)]-loaded and unloded NLS with MTT assay.

4.4. Concluding Remarks

In conclusion, a nanoliposome vehicle for controlled [Cu(glygly)(PS)] delivery in TRAPS which is based on dual pH/redox responsive NLS were successfully formulated. The NLS are responsive to inflammatory mediators due to the hydrophilic redox/ pH sensitive layer of EuE100-cyst coating the phospholipids. The dual responsive [Cu(glygly)(PS)] release from the NLS have been successfully demonstrated. Further, an MTT assay was performed to observe the cell viability using HDFa cells in the presence of the unloaded and [Cu(glygly)(PS)] loaded NLS. The good biocompatibility and efficient drug release of these functionalized NLS establish a promising future pharmaceutical/biomedical application. To be noted is that the combination of the use of metal-drug complex as a bioactive and the targeting pH/redox-triggered quick drug release system could significantly increase the intracellular bioactive concentration and efficiently during inflammation inhibition with reduced drug (steroids) side effects. However *in vivo* studies are necessary to support the established *in vitro* findings.

CHAPTER 5

APPLICATION OF BOX-BEHNKEN DESIGN IN THE FORMULATION AND OPTIMISATION OF DUAL RESPONSIVE [COPPER-GLYCYLGLYCINE-PREDNISOLONE SUCCINATE] LOADED NANOLIPOSOMAL SLUDGE FOR TRANSDERMAL DRUG DELIVERY

5.1. Introduction

Management of tumor necrosis factor receptor-associated periodic syndrome (TRAPS) using corticosteroids is mainly limited by long-term side effects from oral drug delivery (Aróstegui, 2011) mainly due to high systemic drug exposure. This may result in poor bioavailability of drugs at the site of action, which may be circumvented by using an intelligent metal-drug complex loaded nanocarrier design for transdermal drug delivery system (TDDS). Even though the TDDS have many advantages over other drug administration routes, the stratum corneum forms a strong barrier to most topically applied formulations (Prausnitz and Langer, 2008). However by combining the advantages of both a liposomal nanocarrier and a gel-based vehicle, a liposomal nanogel with superior properties is formulated. A liposomal nanogel may be described as a lipid-coated drug loaded nanoparticulates dispersed in a gel matrix (Kermany, 2010; Murphy et al., 2011), the gel matrix further enhances the overall drug delivery outcome of the design.

In the development of a gel system hydroxypropyl methylcellulose (HPMC) was used due to its gel forming, hydration (Karavas et al., 2006) and skin permeating properties (Batheja et al., 2011) and poly(*N*-vinylpyrrolidone) (PVP) was added to promote the bio-adhesiveness (Karavas et al., 2006) and the stability (Qiu and Bae, 2006) of the nanogel as previously assessed (Fang et al., 1999; Darwhekar et al., 2011). The main aim of the study was to formulate a liposomal nanogel termed a nanoliposomal sludge with optimal mechanical properties, good bioadhesion and acceptable viscosity which may attribute to increased patient compliance and clinical efficacy of the formulation. Previously a gel matrix based on a blend of HPMC and PVP has been designed for enhanced transdermal drug delivery (Fang et al., 1999; Darwhekar et al., 2011) and it was established that combining the chemical bonds between these two polymers may be an ideal TDDS design for TRAPS management.

In the present study, a dual pH/redox responsive cationic polymer Eudragit E100-cystamine (EuE100-cyst) and phospholipids were conjugated into pH/redox responsive nanoliposomes (NLs). NLs have previously been investigated as promising drug delivery systems for various applications in TDDS (El-Nabarawi et al., 2013; Ghanbarzadeh and Arami, 2013; Sun et al., 2015). Herein the NLs were loaded with the previously formulated [Copper-glycylglycine-prednisolone succinate] complex (Chapter 3) and optimised using the design of experiments by employing a 3-factor, 3-level Box-Behnken statistical design method. Independent variables studied were the different ratios of lipids, cholesterol and sonication time. The dependent variables studied were the Z-Average size, Polydispersity Index (pdi), zeta potential, entrapment efficiency (%EE) and % drug loading (%DL). Response surface plots were drawn, statistical validity of the polynomials was established, and an optimised formulation was selected by feasibility and grid search. The optimised formulation was characterized using FTIR, DSC and SEM. Lastly the optimized formulation was dispersed in a blend of HPMC/PVA gel resulting into a ([Cu(glygly)(PS)]) loaded nanoliposomal sludge with desired viscosity for TDDS. Furthermore the sludge was characterized using *ex vivo* permeation and *in vitro* release studies compared to the conventional and marketed prednisolone formulations.

5.2. Materials and methods

5.2.1. Materials

Eudragit E100-cystamine (EuE100-cyst) was synthesised as described in Chapter 4. Phospholipids included L- α -Phosphatidylcholine (PC), cholesterol, and 1,2-distearoyl-sn-glycero-3-phosphatidyl-ethanolamine (DSPE) which were purchased from Sigma–Aldrich (St. Louise, MO, USA). Phosphate buffer saline (PBS) tablets, Prednisone Succinate (PS) salt and copper (II) nitrate, were also purchased from Sigma–Aldrich (St. Louise, MO, USA). Sodium hydroxide (NaOH) pellets and dimethylformamide (DMF), ammonium sulphate (NH₄ (SO₄)₂), sodium acetate and glacial acetate acid were purchased from Merck (Wadeville). Dimethylsulfoxide (DMSO) was purchased from Saarchem (Pty) Ltd. (Brakpan, South Africa) and liquid nitrogen was obtained from Afrox (Pty) Ltd. (Industria West, Germiston, South Africa). Double deionised water (ddw) was obtained from a Milli-Q system (Milli-Q, Millipore, Johannesburg) and methanol from Rochelle Chemicals (Johannesburg, South Africa). Prednisolone tablets and syrup were commercially available. All other solvents and reagents were of analytical grade and were used as received.

5.2.2. Preparation of dual pH/redox [Cu(glygly)(PS)]-loaded nanoliposomes

5.2.2.1. Optimisation using a Box–Behnken design

A three-factor, three-level BB design was applied for the optimization procedure with the independent factors and the dependent variables used in this design listed in Table 5.1. The amounts of PC, cholesterol, DSPE and sonication time used to prepare each of the 27 formulations are given in Table 5.2. These high, middle, and low levels were selected from the preliminary experimentation.

Table 5.1: The Box–Behnken design independent and dependent variables are shown

Independent variables	Low	Middle	High
X1: L- α -Phosphatidylcholine (PC)	50	87.5	125
X2: Cholesterol (CHOL)	0	37.5	75
X3: 1,2-distearoyl-sn-glycero-3-phosphatidyl-ethanolamine (DSPE)	0	25	50
X4: Sonication Time	5	17.5	30
Dependent variables	Goal		
Y1: Z-Average size (nm)	Minimise		
Y2: Polydispersity Index (pdi)	Minimise		
Y3: Zeta potential (Mv)	In range		
Y4: % drug loading (%DL)	Maximise		
Y5: % Entrapment Efficiency (%EE)	Maximise		

Table 5.2: The BB design formulations

Formulation	X1 (mg)	X2 (mg)	X3 (mg)	X4 (min)
1	50	37.5	0	17.5
2	50	37.5	25	30
3	87.5	0	25	5
4	87.5	37.5	25	17.5
5	87.5	37.5	0	5
6	125	37.5	50	17.5
7	125	0	25	17.5
8	87.5	75	50	17.5
9	87.5	0	25	30
10	50	0	25	17.5
11	50	37.5	50	17.5
12	87.5	0	0	17.5
13	125	37.5	0	17.5
14	125	75	25	17.5
15	87.5	37.5	50	5
16	87.5	75	25	30
17	50	75	25	17.5
18	87.5	37.5	25	17.5
19	87.5	37.5	0	30
20	87.5	37.5	50	30
21	87.5	75	25	5
22	87.5	37.5	25	17.5
23	87.5	75	0	17.5
24	125	37.5	25	5
25	50	37.5	25	5
26	125	37.5	25	30
27	87.5	0	50	17.5

*X1: L- α -Phosphatidylcholine (PC); X2: Cholesterol (CHOL); X3: 1,2-distearoyl-sn-glycero-3-phosphatidyl-ethanolamine (DSPE) and X4: Sonication Time.

5.2.2.2. Formulation of the [Cu(glygly)(PS)]-loaded nanoliposomes

NLs were prepared as described in chapter 4 (Section 4.2.2.3). The NLs were frozen at -80°C for 2h and then lyophilised for 24h to maintain the stability for longer storage (Chen et al., 2010; Wieberet al., 2012) and to prevent them from aggregation. Sucrose (1%w/v) was used as a cyroprotectant (Zhou et al., 2013).

5.2.3. Dermal sludge preparation

The dermal sludge formulation was composed of 76%w/v[Cu(glygly)(PS)]-loaded NLs (equivalent to 1%w/vPS), 4%w/vHPMC/PVA (1:1 ratio), 10%v/vglycerol and 76%v/vdouble

deionised water. For the preparation of the sludge, deionised water and glycerol were mixed using magnetic stirrer, HPMC and PVA were added slowly until a clear gel was formed. The gel was left for 24h to form while stirring. Subsequently, [Cu(glygly)(PS)]-loaded NLs were added to the vortex of agitated gel, the NLs were not soluble in the formulation, they remained suspended and the dermal sludge was formed. The dermal nanoliposomal sludge was stored at 4°C until further usage (Prasad and Kishore, 2012; Darwhekar et al., 2011 and Shah et al., 2012).

5.2.4. Preparation of Conventional prednisolone Gel

Conventional prednisolone gel was as per the method described by Shakeel et al. (2007) with modifications where 1g of the Carbopol® 940 was dispersed in a sufficient quantity of deionised water. The carbopol 940 solution was left in the dark while stirring overnight for complete settling of the gel. Thereafter 1g of prednisolone was dissolved in deionised water. This solution of drug was added slowly to the aqueous dispersion of Carbopol® 940. Subsequently additional ingredients like isopropyl alcohol 10%w/w, propylene glycol 10%w/w, and triethanolamine 0.5%w/w were added to obtain a homogeneous neutral gel.

5.2.5. Determination of entrapment efficiency and drug loading of the nanoliposomes

For the quantitative determination of [Cu(glygly)(PS)] within the NLs, the loading and encapsulation efficacy of the NLs was determined. Drug loading capacity (DL) was calculated as [Cu(glygly)(PS)] complex analysed and determined as detailed in chapter 4, section 4.2.9. The % entrapment efficiency (%EE) of [Cu(glygly)(PS)] in NLs was determined, being the ratio between actual and theoretical loading, using the following equation:

$$\%EE = \frac{[\text{Cu(glygly)(PS)}] \text{ added in NLs}}{\text{total } [\text{Cu(glygly)(PS)}] \text{ added}} * 100 \text{ Equation 5.1}$$

The %DL and EE were both determined using the UV/Vis spectrometry (PerkinElmer Spectrum 100, Llantrisant, Wales, UK), the detection wavelength was 242nm.

5.2.6. Chemical structural analysis of [Cu(glygly)(PS)] complex, optimised [Cu(glygly)(PS)]-loaded and unloaded NLs using Fourier transform infrared (FTIR) spectroscopy

Fourier-transform infrared (FTIR) spectroscopy was generated using A Perkin Elmer Spectrum 2000 FTIR spectrometer with a MIRTGS detector, (PerkinElmer Spectrum 100, Llantrisant,

Wales, UK). FTIR analysis was performed on the dried [Cu(glygly)(PS)] complex, optimised [Cu(glygly)(PS)]-loaded and unloaded NLs, NLs loaded nanoliposomal sludge and unloaded HPMC/PVP gel as described in chapter 3, section 3.2.3.

5.2.7. Determination of the thermal properties of the [Cu(glygly)(PS)] complex, optimised [Cu(glygly)(PS)]-loaded and unloaded NLs

5.2.7.1. *Differential scanning calorimeter analysis*

The differential scanning calorimeter (DSC) analysis of the dried [Cu(glygly)(PS)] complex, optimised [Cu(glygly)(PS)]-loaded and unloaded NLs was performed as detailed in Chapter 3, section 3.2.8.

5.2.7.2. *Thermogravimetric analysis*

Thermal analysis was performed using thermogravimetric analysis (TGA) (Toleda TC15 TA controller, Mettler). It was used to measure how the changes in chemical and physical properties of the [Cu(glygly)(PS)], optimised[Cu(glygly)(PS)]-loaded and unloaded NLs, as detailed in chapter 3, section 3.2.9.

5.2.8. Determination of the size and zeta potential of the nanoliposomes

The particle size was analysed to determine the typical diameter and Pdl of the NLs, also zeta potential analysis was performed to establish the surface charge and physical stability of the NLs. These procedures were carried out using a Zetasizer NanoZS (Malvern Instruments, Worcestershire, UK).

5.2.9. Analysis of the surface and structure morphology of the optimised dual pH/redox responsive nanolipoosomes

5.2.9.1. Scanning electron microscopy

The surface morphology of the cryo-protected [Cu(glygly)(PS)]-loaded NLs were analysed using a scanning electron microscopy (SEM) (Jeol JSM-120, Tokyo, Japan) . A small quantity of the cryo-protected lyophilized NLs, was sputter coated using gold isotope while being mounted on an aluminum spud, with an EPI coater (SPI Module TM sputter-coater and control unit, Chester, PA, USA). After coating the NLs for 60s, under constant nitrogen gas conditions, the sample was analysed using a FEI Quanta 400F (FEITM, Hillsboro, OR, USA) electron microscope. To

produce high image resolution of the particles an electron acceleration charge of 20kV was used.

5.2.9.2. Transmission electron microscopy

The structural morphology of the [Cu(glygly)(PS)]-loaded NLs was determined using a transmission electron microscopy (TEM) (Jeol 1200 EX, Japan), as described in chapter 4, section 4.2.7.

5.2.10. Analysis of the rheological behaviour of the nanoliposomal sludge

The storage modulus (G'), loss modulus (G'') and dynamic viscosity (η) of the sludge were determined using a Haake Modular Advanced Rheometer (Thermo Electron Corp., Karlsruhe, Germany). These rheological tests were determined over a frequency of 1Hz. In the oscillatory mode, a parallel plate of 40mm diameter, the geometry measuring system was employed, and the gap was set to 1mm. The G' and G'' was employed to determine the viscoelasticity of the sludge, applying a small oscillatory stress and measuring the resulting strain. This was used to determine the deformation energy and flow, while the η was used to analyse the flow properties of the sludge. The G' , G'' and η tests were all undertaken at 37°C, recorded and each test was run in triplicate (Kantaria, Rees and Lawrence, 1999).

5.2.11. Analysis of the textural properties of the optimizednanoliposomal sludge

A Texture Analyser (TA.XT *plus*. *Textureanalyser*, Stable Microsystems®, Surrey, UK) was used to determine the textural properties of the optimizednanoliposomal sludge. The textural properties of the sludge were performed using a Force (N)-Time (Sec) profile, as a measure of the sludge hardness, cohesiveness and adhesiveness after a compressive stress was applied by the textural probe. Three replicate analyses were performed at room temperature for the sludge and the parameter employed for the textural properties are shown in Table 5.3.

Table 5.3: Textural analysis parameter settings for determining the nanoliposomal sludge textural properties.

Parameter	Setting
Test Mode	Compression
Pre-Test Speed	1.0mm/sec
Test Speed	1.5mm/sec
Post-Speed	1.5mm/sec
Target Mode	Force
Force	4N
Trigger Type	Auto Force
Trigger Force	0.05N
Probe type	10mm cylinder

5.2.12. *In vitro* drug release studies of the PS, [Cu(glygly)(PS)]-loaded NLs and [Cu(glygly)(PS)]- loaded nanoliposomal sludge

In vitro drug release from conventional oral PS, [Cu(glygly)(PS)]-loaded NLs and [Cu(glygly)(PS)]- loaded nanoliposomal sludge was performed in buffers (PBS pH 7.4 and acetate buffer at pH 5) with and without GSH (10mM) at 37°C using dialysis membranes (MWCO: 1.2kDa). It has been reported that the concentration of GSH in ECM fluid is less than 0.01mM, while ICM GSH is significantly higher, in the range of ~10mM. The medium of pH 7.4 without GSH corresponds to the condition in which NLs will encounter during circulation after administration, while the medium of pH 7.4 with 10mM GSH corresponds to the ICM condition, and pH 5 mimics the ECM condition which has insignificant GSH (RB KC, B Thapa, P Xu, 2012). These three formulations were placed in dialysis bags and immersed into 30mL buffer solutions in the different media. At a predetermined time (0.5, 1, 2, 4, 6, 8 and 24h) 1.0mL of the buffer was taken out and the same amount of fresh buffer was added to make up the constant volume of the release medium.

Absorbance using the UV-Vis spectrophotometry (PerkinElmer Spectrum 100, Llantrisant, Wales, UK) at 248nm and 242nm for the PS and complex was used to quantify the release, concentration versus absorbance calibration curves were employed as shown in chapter 3, section 3.3.

5.2.13. Ex vivo permeation studies of the [Cu(glygly)(PS)]-loaded nanoliposomal sludge compared to conventional formulations

The full-thickness of a pig's ear skin was separated from cartilage using a scalpel and dermis was wiped with isopropyl alcohol to remove any residual adhering fat. The skin was washed with deionised water, wrapped in aluminum foil and stored in a freezer at -20°C , and was used within a month. Prior to the diffusion experiment the epidermis was thawed at room temperature and cut to appropriate size (2 by 2cm). The *ex vivo* studies were performed on prednisolone cream, conventional prednisolone gel, [Cu(glygly)(PS)]-loaded HPMC/PVP gel, and [Cu(glygly)(PS)]-loaded nanoliposomal sludge in PBS pH 7.4. These studies were performed according to method adapted from Wissing and Muller (2002), as detailed in chapter 3, section 3.2.11.

Furthermore, the skin membrane integrity was evaluated before and after each exposure to the different formulations being tested by measuring the skin surface electrical conductivity according to a method described by Klimova et al. (2012) with modifications. A simple dual pH/conductivity meter (Mettler-Toledo, Zürich, Switzerland) was used to measure the conductivity in order to determine if the skin remained intact while in contact with the formulations.

5.2.13.1. Determination of complex and drug retention in the Skin

At the end of the permeation experiments, the skin was carefully removed from the Franz cell and the skin surface was swabbed and washed twice with PBS pH 7.4 ensuring that no traces of formulation were left on the skin surface. The permeation area of the skin was excised and cut into small pieces to extract the drug/complex content present in the skin with methanol. The resulting solutions were centrifuged at 5000rpm for 30min using and drug/complex retained was expressed as percent of the initially applied formulation (Ghanbarzadehand Arami, 2013).

5.3. Results and discussions

5.3.1.1. The results of optimization using the Box–Behnken design

All 27 formulations from the design template produced NLs of variable z-average size, zeta potential, drug loading, and entrapment efficacy (Table 5.4). The results showed that the DEE ranged from 86.0 to 98.2% and DL ranged from 16 to 21%. The maximum DEE value (98.2%) was found in conditions of $X_1 = 87.5\text{mg}$, $X_2 = 37.5\text{mg}$, $X_3 = 50\text{mg}$ and $X_4 = 30\text{min}$. The measured z-average size for the different formulations showed wide variation, the particles

ranged from 88 to 933nm. The minimum particle size was found in conditions X1 = 87.5mg, X2 = 37.5mg, X3 = 50mg and X4 = 17.5min, which are the same conditions as the formulation with highest DEE, the only difference being the sonication time. It was also seen that the highest DL% is attributed to formulations in which the ratio of PC is the highest.

These results clearly indicate that the responses values are strongly affected by the variables selected for the study. Further it was established that there was a correlation between particle size and amount of drug incorporated, the smaller the particle size the more drug was loaded mainly because of the increase in surface area with the reduction in particle size. Additionally with the wide lipid compositions used there was significant influence of the lipid on the particle size as well as amount of drug incorporated. Increasing the ratio of cholesterol in comparison with the other lipid constituents significantly increased the particle size, which resulted in reduced % DEE and DL as observed by Patel et al. (2012) as well. This may be due to increased rigidity and packing density caused by the cholesterol/phospholipid molecules assembled into bilayer vesicles, which reduces the encapsulation of the drug on the hydrophobic [Cu(glygly)(PS)] by the lipid bilayer (Semple et al., 1996).

Table 5.4: Responses measured for the Box–Behnken design

Formulation	Y1 (nm)	Y2 (Pdl)	Y3 (Mv)	Y4 (%)	Y5 (%)
1	394± 0	0.428±0.008	22.4±5.6	17.86	89.3±3.2
2	252±18	0.44±0.002	12.6±5.2	20.1	95.4±2.1
3	132± 2	0.363±0.004	27.5±0.5	17.56	87.8±6.1
4	249±76	0.403±0.084	15.8±1.2	18.14	90.7±2.9
5	181±24	0.319±0.009	8.89±5.14	17.2	86.0±1.8
6	256±23	0.408±0.06	23.9±4.03	19.9	96.2±2.7
7	257±22	0.380±0.09	5.6±0.9	18.82	94.1±3.3
8	88±43	0.295±0.120	17.9±2.1	19.1	95.5±1.2
9	275±80	0.295±0.09	18.8±6.2	18.98	94.9±2.0
10	178±46	0.340±0.05	26.4±1.4	18.76	93.8±0.9
11	315±40	0.245±0.01	6.61±25	16.7	83.5±3.9
12	119±51	0.240±0.075	26±8	18.84	94.2±2.2
13	131±53	0.288±0.088	15.5±7	17.8	89±3.8
14	176±90	0.399±0.099	0.625±0.6	18.82	94.1±0.8
15	609±29	0.375±0.022	22.6±4.5	17.6	88±3.1
16	160±29	0.423±0.003	4.1±2.2	19.3	96.5±2.8
17	617±50	0.529±0.023	19.9±5	17.42	87.1±3.0
18	249±76	0.403±0.084	15.8±1.2	18.14	90.7±2.9
19	383±11	0.519±0.031	24.5±1.6	17.98	89.9±2.6
20	342±20	0.361±0.012	20.7±2.4	20.64	98.2±0.8
21	880±36	0.188±0.006	4.86±0.9	17.84	89.2±4.1
22	249±76	0.403±0.084	15.8±1.2	18.14	90.7±2.9
23	772±46	0.459±0.099	14.6±5.71	17.62	88.1±3.3
24	933±23	0.487±0.007	22.1±6	18.94	94.7±1.6
25	250±47	0.482±0.004	21±4.1	17.86	89.3±2.0
26	241±44	0.342±0.034	4.72±1.1	21.02	95.1±0.7
27	252±24	0.424±0.022	31.5±1.5	17.68	88.4±3.9

* Y1: Z-Average size (nm); Y2: Polydispersity Index (pdi); Y3: Zeta potential (Mv); Y4: % drug loading (%DL) and Y5: % Entrapment Efficiency (%EE).

The obtained results were inputted into the MINITAB®(V14, State College, Pennsylvania, USA)software to yield four possible optimized formulations and the most appropriate optimized formulation had a composite desirability (D) of 1.000. The optimal formulation had independent

parameters as follows; sonication time of 30min and PC: Chol: DSPE ratio of 50: 75: 50 which gave predicted NLs responses of; z-average size 52.1667nm (Y1), % DL of 19.6967 (Y4) and %EE of 95.650 (Y5) (Figure 5.1). The independent and dependent variables relationship generated using MINITAB® is also described in a study done by Ailiesei et al. (2014) and Lu et al. (2014), where the size of the NLs increases with increase in cholesterol ratio compared to PC, while the sonication time also plays a major role in reducing the particle size.

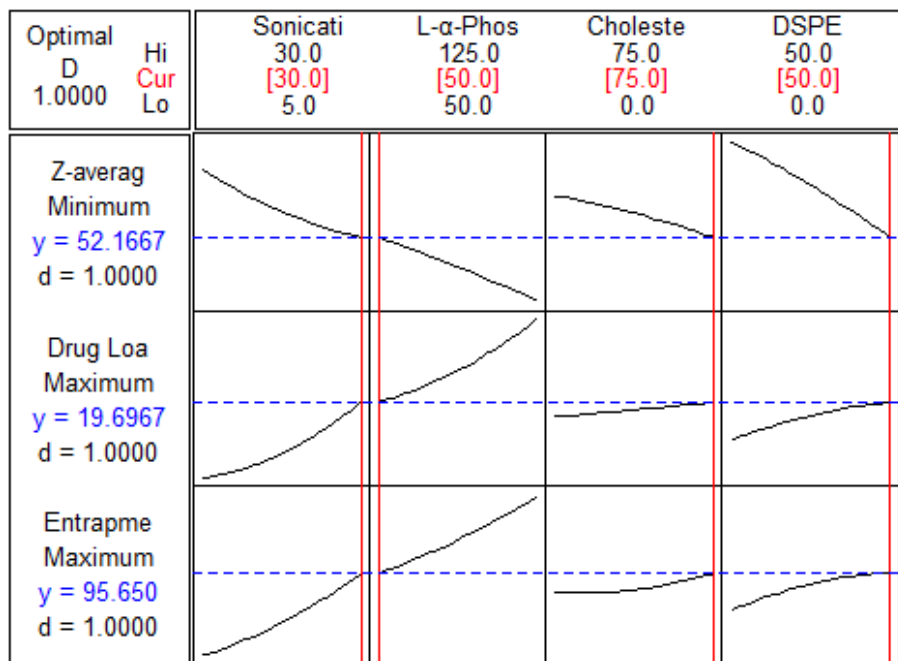


Figure 5.1: The resulted generated using MINITAB® for the optimized formulation, the desirable results are also shown.

5.3.1.2. Statistical validity of the optimized formulation

The suitability of the model was assessed by additional experimental data that was derived using the optimized formulation. The predicted values were approximately a size of 52.2nm, %DL of 19.7% and %EE of 95.7% and in the experimental the data it was 138 ± 32.34 nm, 21.2 ± 0.5 % and 93.8 ± 0.8 % for Y1, Y4 and Y5, respectively (Table 5.5). Although the particle size of the optimized NLs was not within the same range as the predicted value the generated model was considered to be adequately valid. According to Lu et al. (2014) it was stated that the bulky nature of lipids may not be suitable for smaller particle range especially in cases where the cholesterol ratio is high compared to the rest of the lipids, and also a particle size below 200nm is considered sufficient for penetration through the dermis and hair follicles for a TDDS (Tomoda et al., 2012; Gomes et al., 2014).

Table 5.5: The predicted responses versus the actual responses from the optimized formulation.

Responses	Y1 (nm)	Y4 (%)	Y5 (%)
Predicted	52.2	19.70	95.7
Actual	138±18	21.2±0.5	93.8±0.8

5.3.1.3. Dermal sludge formulation

The optimized Cu(glygly)(PS)-loaded NLs were intended for a TDDS, therefore an adequate permeation efficacy, skin adhesiveness and rheology was achieved by preparing a nanoliposomal sludge of desired properties. The sludge would be applied dermally and degrade in an inflammatory-responsive manner as described previously described in chapter 4 (section 4.3.1) and shown in Figure 5.2.

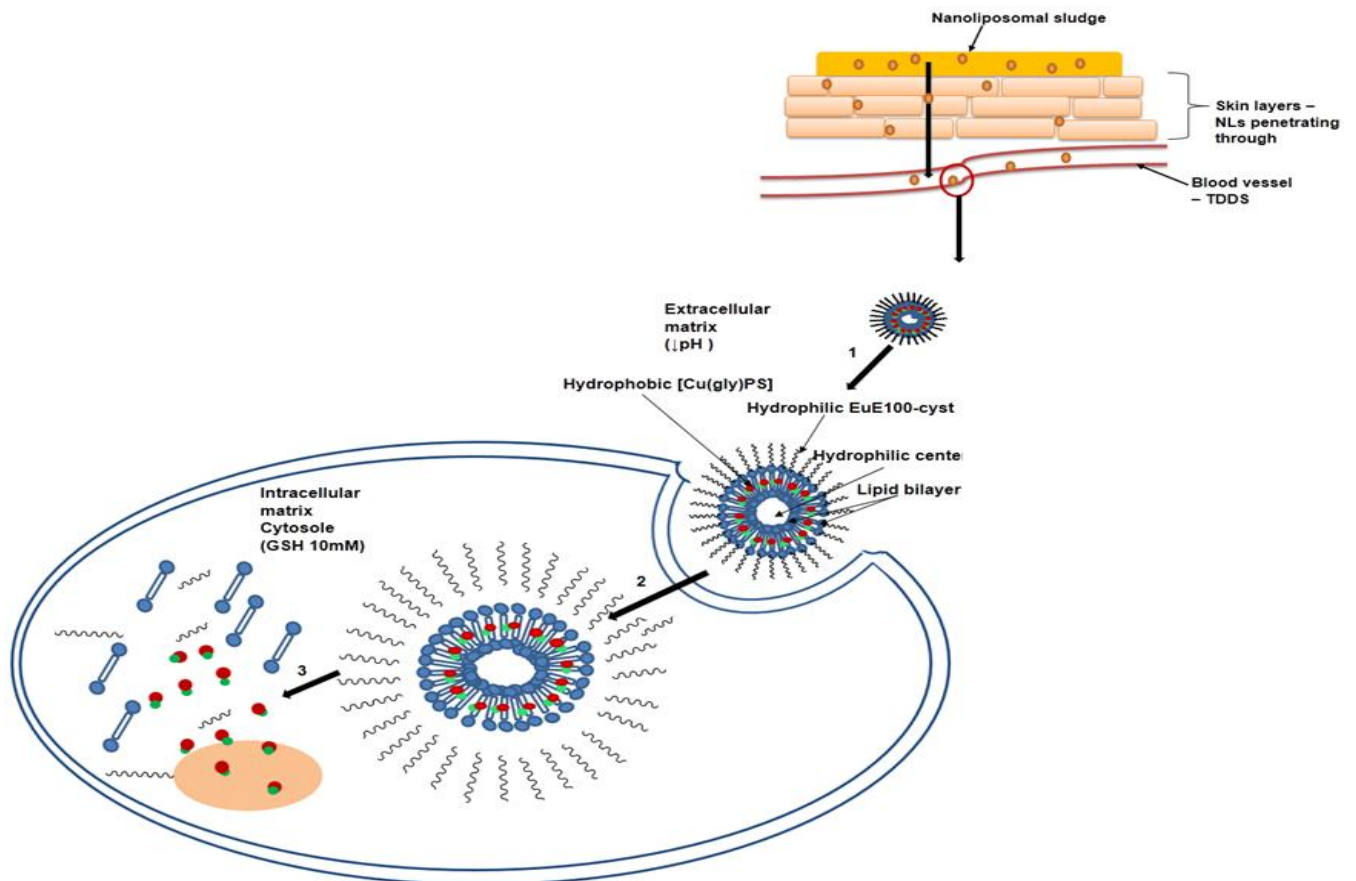


Figure 5.2: (a) The expected penetration of the nanoliposomal sludge through the skin and (b) thereafter its sequential degradation of the inflamed site occurs as described in Chapter 3, Figure 4.3.

5.3.2. Structural characterisation of the optimized nanoliposomes and sludge

The FTIR spectra of the complex loaded-NLs and unloaded NLs indicate that characteristic peaks of the unloaded NLs were not altered and had no changes in their positions after [Cu(glygly)(PS)] encapsulation, as detailed in chapter 3 section 3.3.2. The similarities and differences are seen in Figure 5.3 where the spectra are superimposed. From these results it can be established that complex encapsulation within the optimised NLs was achieved.

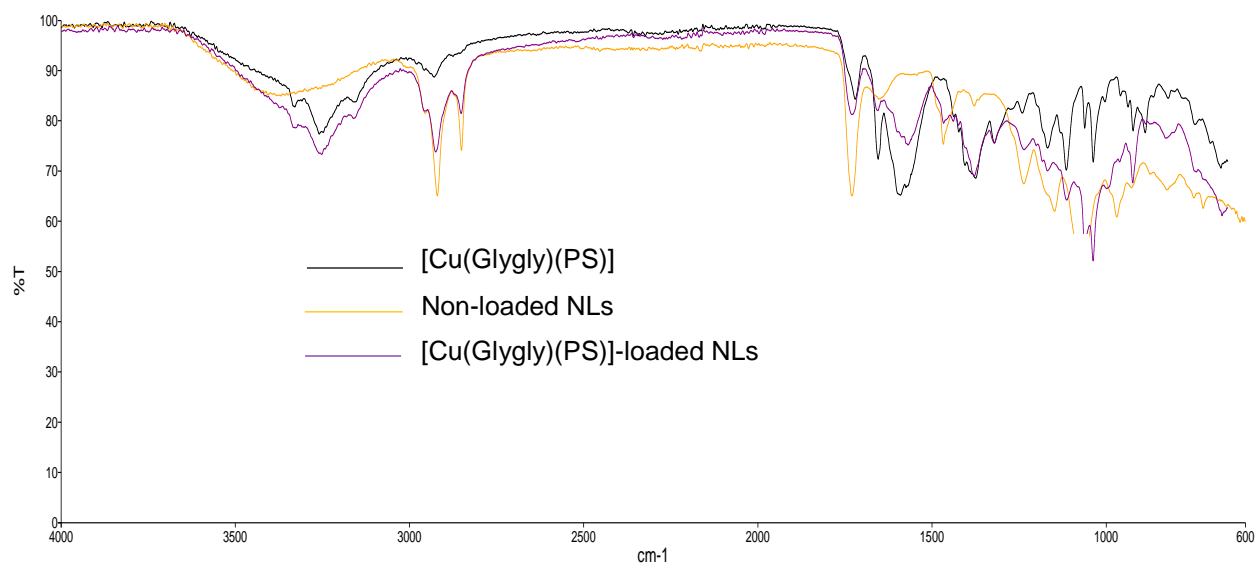


Figure 5.3: Superimposed FTIR spectra of [Cu(glygly)(PS)], [Cu(glygly)(PS)]-loaded NLs and unloaded NLs

Figure 5.4 shows the FTIR spectroscopic analysis of the unloaded gel compared to nanoliposomal sludge which also showed no remarkable chemical interaction occurring between the complex and the polymers used to formulate the gel. Notably the nanoliposome characteristic peak is seen (box in figure 5) at 1729.29cm^{-1} and 1728.9cm^{-1} for [Cu(glygly)(PS)]-loaded NLs and nanoliposomal sludge. These FTIR spectra shows that the [Cu(glygly)(PS)]-loaded NLs were successfully adsorbed into the HPMC/PVP gel matrix. FTIR spectroscopy is one of the most powerful chemical analytical techniques used for analyzing, vibration, and characteristics of chemical functional groups of phospholipids, similar results were demonstrated by Mufamadi et al. (2013) and Jin et al. (2014). Overall the absence of significant chemical interaction within the loaded NLs and nanoliposomal gel has an added advantage since the respective phospholipids and polymeric functions of the NLs and gel are retained, hence the site-specific function of the NLs is not altered by the loading within the gel.

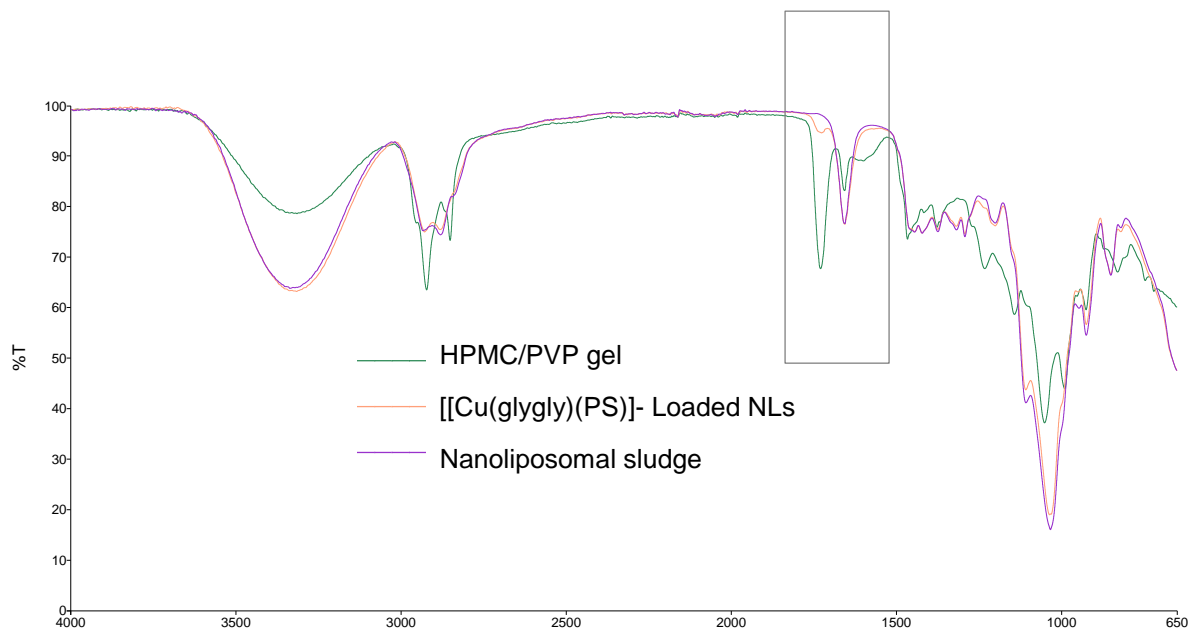


Figure 5.4: The comparative FTIR spectroscopic analysis of the placebo gel and loaded NLs compared to the nanoliposomal sludge which is the combination of the two.

5.3.3. Evaluation of the thermal properties of the optimized nanoliposomes and sludge

The DSC tracings for [Cu(glygly)(PS)], unloaded NLs and [Cu(glygly)(PS)]-loaded NLs are presented in Figure 5.5. The complex showed an endothermic peaks at 380°C and an exothermic peak at 385°C, which corresponds to its melting and glass transition temperature. The endothermic peaks for unloaded NLs are observed at 194.3 and 280°C indicating glass transition and melting temperatures, respectively. The endothermic peaks for the [Cu(glygly)(PS)]-loaded NLs were observed at 185.3, 237.3, 285 and 358.7°C in which the temperatures have relatively shifted with an additional peak at 358.7°C compared to the unloaded NLs. These changes in the endothermic peaks may be attributed to the physical and morphological changes of NLs after [Cu(glygly)(PS)] loading. Additionally the absence of the significant [Cu(glygly)(PS)] peaks and shifting of the lipid bilayer components endotherm suggested significant interaction of [Cu(glygly)(PS)] with the bilayers. Similar findings were previously noted by Hathout et al. (2007).

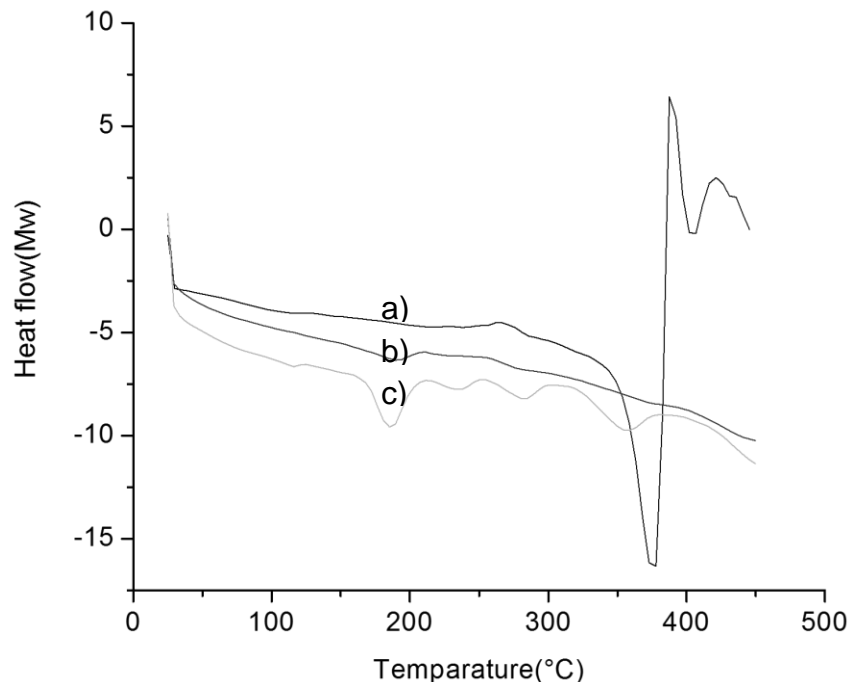


Figure 5.5: DSC analysis of [Cu(glygly)(PS)] complex, (b) unloaded NLs and (c) [Cu(glygly)(PS)]-loaded NLs

Thermogravimetric (TG/DTG) analysis of the [Cu(glygly)(PS)] complex was employed to provide quantitative information on mass losses due to thermal decomposition as a function of temperature. The thermal analyses data of [Cu(glygly)(PS)], [Cu(glygly)(PS)]-loaded and unloaded NLs are shown in figure 5.6a, b and c respectively. The thermogram (Figure 5.6a) for [Cu(glygly)(PS)] shows the presence of an anhydrous complex containing no water of crystallization, and no coordinated water molecules as evident by the plateau from 100 to 200°C. From the DTG/TGA curve, it is clear that the thermal decomposition of the Cu(glygly)(PS)] complex occurs in three steps. The initial mass loss occurs within the temperature range of 319–325°C, T_{peak} DTG of 323.5°C, with a mass loss of 14.5% possibly due to elimination of the glygly ligand. The second mass loss has a split peak with the T_{peak} DTG of 373 and 385°C occurring in the temperature range of 370-390°C (mass loss = ~15.5%, respectively) possibly due to initial loss of PS. The third step corresponds to the thermal decomposition and complete elimination of the remaining part of the PS drug molecule starting from 500°C on the thermogram of the complex with final mass loss of ~83% at DTG between 740-760°C for the leaving CuO residue. Comparable findings were obtained in a study done by Maravalli and Goudar (1999) on thermal analysis of copper complexes.

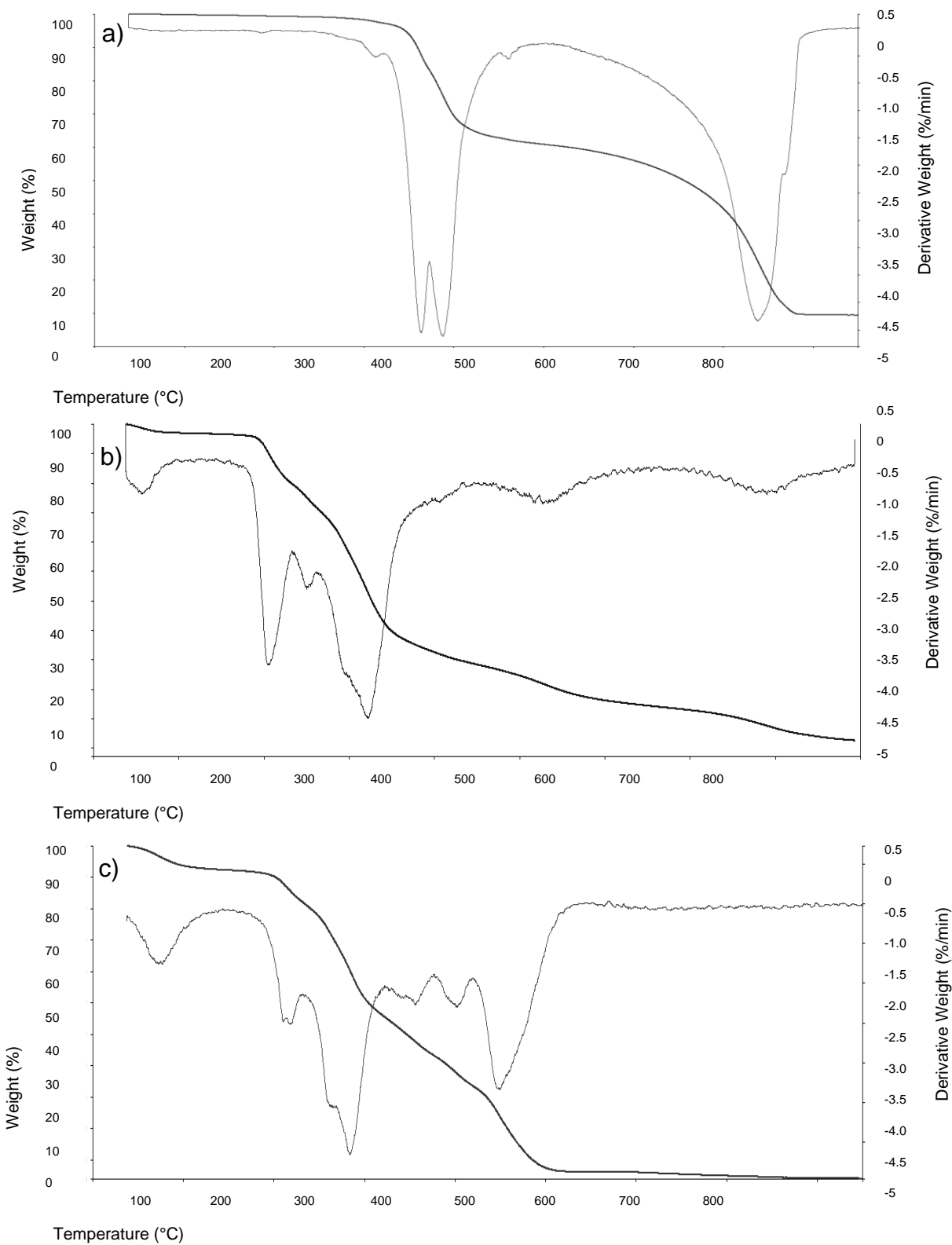


Figure 5.6: TG/DTG) analysis of the (a) [Cu(glygly)(PS)], (b) [Cu(glygly)(PS)]-loaded and (b) unloaded NLs

5.3.4. Particle size and zeta potential of the optimised nanoliposomes

The size distribution is generally used as a characterisation tool to evaluate the stability of NLs, and vesicle size is a relevant characteristic regarding both the organ distribution and encapsulation or adsorption efficiency of liposomal drug carriers. Polydispersity is an indicator of particle diameter distribution in colloidal systems. The smaller the value of polydispersity index (Pdl), the more likely the particle diameter distribution is narrower, and thus particles show better uniformity in diameter (Ding et al., 2011). The ideal nanoliposome particle size was obtained using the sonication procedure, the average particle size of the unloaded NLs was $99.14 \pm 48.7 \text{ nm}$ with a Pdl of 0.24 (Figure 5.7a). The particle size was slightly increased after [Cu(glygly)(PS)] was loaded into the NLs to $138.0 \pm 32.34 \text{ nm}$ with PDI of 0.20 (Figure 5.7c). The particle size does not match the predicted size (52.1667 nm) according to the BB design due to the bulky nature of the lipids, complex and EuE100-cyst combined. However it has been reported that a mean particle size of 200 nm or less is sufficient for penetrating through the dermis and hair follicles (Tomoda et al., 2012; Gomes et al., 2014), hence these nanoliposomes are considered appropriate for TDDS.

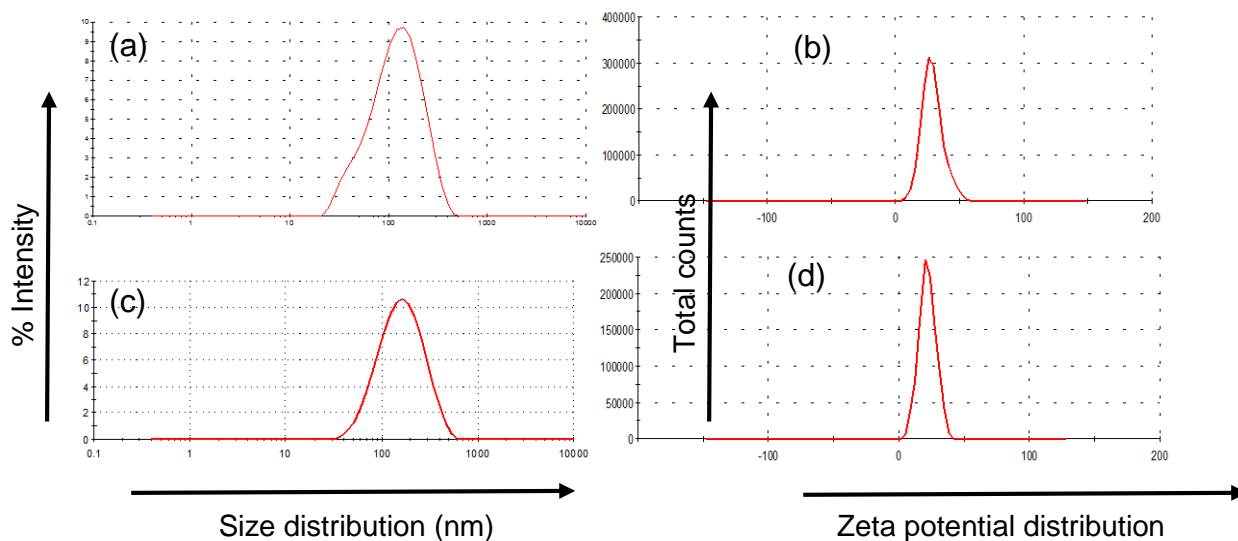


Figure 5.7: The size (a+c) and zeta potential (b+d) distribution of the unloaded (a+b) and loaded (b+d) NLs

The zeta potential of NLs was $28.0 \pm 3.81 \text{ mV}$ and $21.9 \pm 6.47 \text{ mV}$ before and after [Cu(glygly)(PS)] loading, respectively. Figure 5.7b and d shows the zeta potential for the unloaded and loaded NLs, respectively. The NLs showed a positive zeta potential, in agreement with the observations

of previous studies where chitosan, which is also a cationic polymer, was used to coat liposomes (Mady et al., 2010). This potential can be attributed to the cationic EuE100-Cyst adsorbed to the liposomal surface. Since the [Cu(glygly)(PS)] complex has a neutral charge and is hydrophobic it is adsorbed on the surface of the NLs (Xu et al., 2007); the adsorption of the [Cu(glygly)(PS)] appears to have reduced the density of positive charge in the loaded NLs. The magnitude of the zeta potential indicates the potential stability of the colloidal system, as zeta potential increases the colloidal stability also increases (Mady et al., 2010). As a rule of thumb described by Honary et al. (2013), zeta potential values of around 20mV or higher and lower than -20mV can provide sufficient stabilization, therefore the nanoliposome zeta potential in this study is desirable.

5.3.5. The electron micrographs of the optimized [Cu(glygly)(PS)]-Loaded nanoliposomes

The physical morphology of the Cu(glygly)(PS)]-Loaded NLs was evaluated using TEM. Figure 5.8a reveals that the NLs have a mean particle size of 100–200 nm, and most of them appeared spherical in shape. The particles existed dispersedly on the copper grid, and they were not agglomerated. Further seen in the inserted figure is that the NLs were unilaminar and these results agree with previous studies (Mufamadi et al., 2012; Fonte et al., 2014 and Mohan et al., 2014).

The surface morphology of the cyroprotected NLs was assessed using SEM (Figure 5.8b). The powder obtained by lyophilization of the NLs containing 1% sucrose cryoprotectant indicates that fusion of the phospholipid nanoparticulates did not occur. The lyophilized NLs are visible in the micrographs as spherical structures and they are clearly incorporated into the excess mass of sucrose. According to Yokota, Moraes and Pinho (2012) the addition of cryoprotectants prevents leakage or fusion and plays an essential role in cake formation by creating an amorphous matrix in and around the phospholipid vesicles. Similar studies were undertaken by Moretton et al. (2011) and Zhoua et al. (2013) where the addition of a cryoprotectant enhanced the separation of nanoparticulates without altering the size and morphology of the phospholipid nanoparticulates.

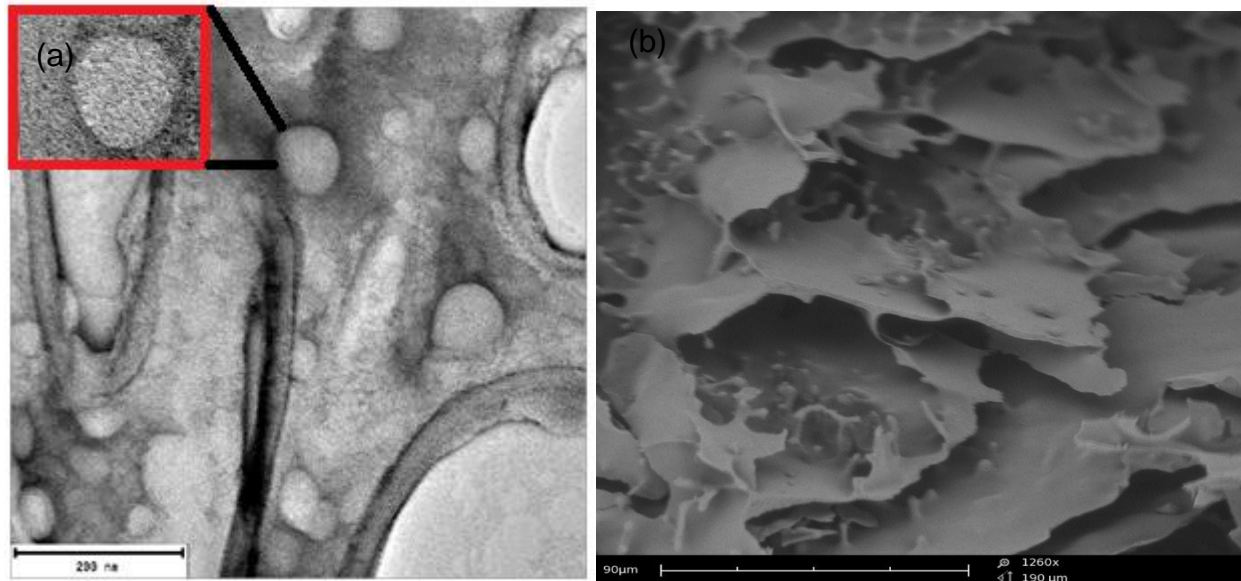


Figure 5.8:a) The TEM analysis of the [Cu(glygly)(PS)]- Loaded NLs in a negative stain (uranyl acetate) and b) SEM evaluation of the cryoprotected freeze dried NLs at 1260X

5.3.6. Rheological evaluation of the optimized nanoliposomal sludge

The nanoliposomal sludge was monitored by the dynamic small-amplitude oscillatory shear measurements using the time sweep mode at 1 rad s⁻¹ of angular frequency and 1 strain. The storage modulus (G') and loss modulus (G'') were presented as functions of time as shown in Figure 5.9. In general, it can be seen that the behavior of the sludge can be divided into three zones. First, there was a short period where viscosity and elasticity were alternatively seen, of which when stress was applied there is an increase in G' (decrease in G'') resulting in increase in viscosity. While when stress was removed there was an increase in G'' (decrease in G') resulting in the gel retaining its elasticity. At the end of the first zone the frequency dropped to almost zero as G' increased rapidly while G'' decreased rapidly as well when the transition stage was reached. During the final zone the sludge reached its fluidity zone, as the G' increased and G'' decreased reaching their final equilibrium value. Additionally η^* decreased with an increase in applied frequency, similar results are seen where solid lipid nanoparticles gel were formulated (Khurana et al., 2013). These results show that the sludge possesses shear-thinning properties (pseudoplastic behavior) as it has the ability to thin during application (shear stress application) (Batheja et al., 2011) and reform following application of shear stress (Kumar et al., 2005). Therefore it was established that the sludge had desirable properties for topical application with ideal cohesiveness, adhesiveness and spreadability.

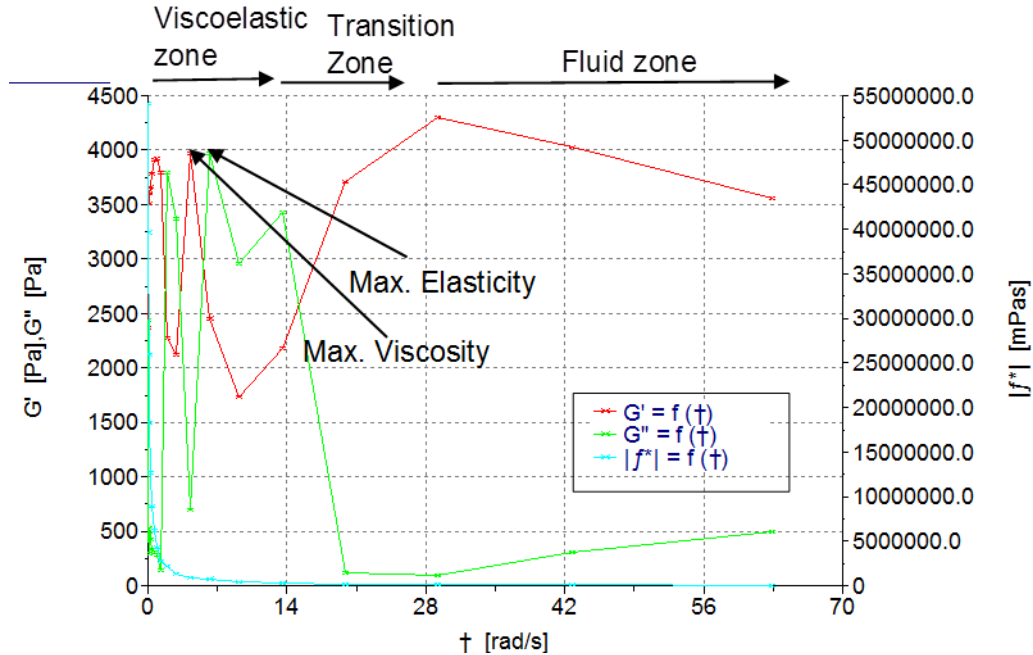


Figure 5.9: The rheological analysis of the nanoliposomal sludge

5.3.7. Determination of the texture properties of the optimized nanoliposomal sludge

Textural analyses properties i.e. hardness, compressibility, cohesiveness and adhesiveness are directly correlated with *in vivo* sensory parameters. Therefore, they are valuable in designing an optimal transdermal formulation with desirable characteristics that contribute to patient acceptability and compliance (Hurler et al., 2012 and Gratieri et al., 2010). Figure 5.10 shows the texture analysis profile of the nanoliposomal sludge, where the maximum compressing force, cohesiveness, adhesiveness and minimum retracting forces are displayed.

The maximum compressing force hereby present the hardness of the nanoliposomal sludge, which is related to the maximum work required to spread the product over a certain skin surface area. After the sludge has been applied on the skin it is desirable for the sludge to form a homogeneous layer on the skin surface. An ideal nanoliposomal sludge, particularly in relation to prolonged retention time on the skin, for the treatment of inflammatory disorders, a balance between the sludge adhesiveness and cohesiveness should be maintained. Cohesiveness relates to the work required to spread the sludge over a certain skin surface (Hurler et al., 2010), while adhesiveness relates to the work necessary to overcome the attractive forces between the surface of the sludge and the surface of the skin (Gratier et al., 2012). A formulation designed for transdermal use should present with good spreadability on the skin surface and adhere to the mucous layer without disintegrating, in order to prolong retention

time. A higher adhesiveness value imply greater adhesion at the skin surface and increase the retention time and based on the results presented (Figure 5.10), the nanoliposomal sludge confers these desirable properties, and they are in agreement with its storage modulus values. Similar findings were observed by Tamburic and Craig (1997).

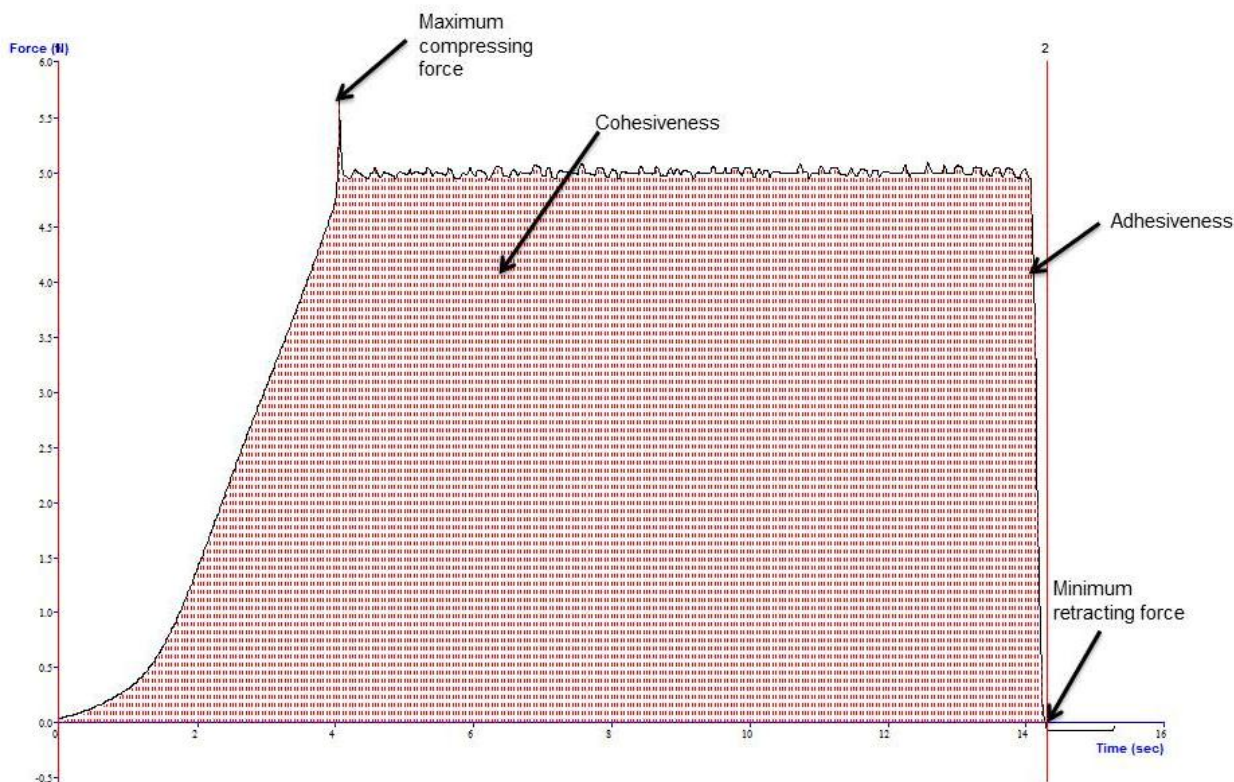


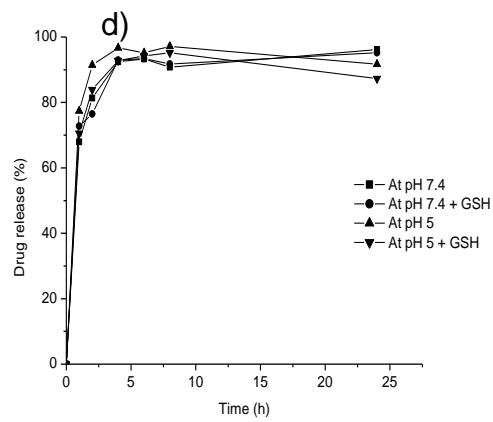
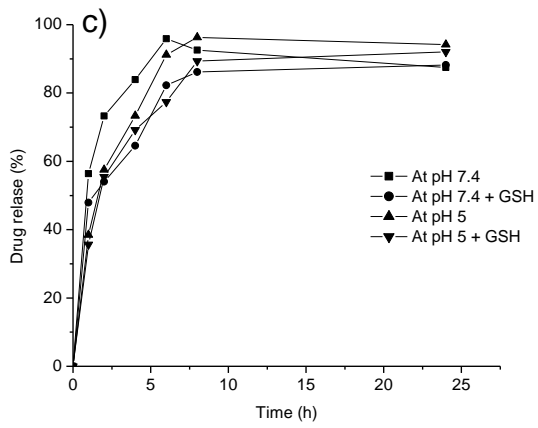
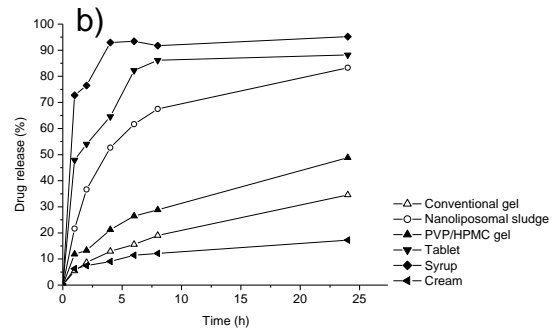
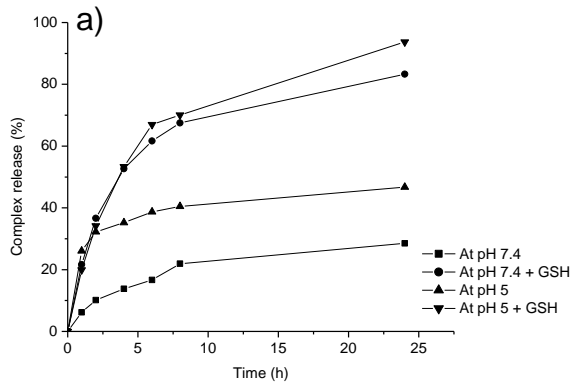
Figure 5.10: Typical force versus time plot of the nanoliposomal sludge.

5.3.8. Drug release analysis of PS, [Cu(glygly)(PS)]-loaded NLs and [Cu(glygly)(PS)]-loaded nanoliposomal sludge

The drug release profile of the [Cu(glygly)(PS)]-loaded nanoliposomal sludge, PS conventional gel, PS tablet and PS syrup upon acid and redox gradient was assessed in phosphate-buffered saline (PBS, pH 7.4) and acetate buffer (pH 5) with and without GSH (10mM) at 37°C. The nanoliposomal sludge results are summarized in Figure 5.11a. As expected, the release rate of [Cu(glygly)(PS)] in PBS pH 7.4 was much slower than that in acetate buffer pH 5.0, about 21.9±1.1% and 40.4±2.1% of [Cu(glygly)(PS)] was released respectively in the first 8h. However the amount of [Cu(glygly)(PS)] released from the NLs was promptly increased when it was incubated in the medium complemented with 10mM GSH. At pH 7.4 and 5.0 with GSH a

release of $67.5 \pm 1.5\%$ and $70.1 \pm 0.9\%$ was achieved respectively, over the same time period. It is worth noting that even though the release of the [Cu(glygly)(PS)] is low at pH 7.4 but with the supplementation of GSH the released is notably enhanced such that more [Cu(glygly)(PS)] was release compared to pH 5, indicating the superiority of the redox-sensitivity of the nanoliposomal sludge, which could be attributed to the direct incorporation of disulfide bonds to the polymeric backbone of the EuE100 used in the nanocarrier preparation, the cleavage of which highly promoted drug release (Lu et al., 2014). Similar finding are observed in studies are observed in cancer targeted drug delivery which is also characterized as an inflammatory disease (Pan et al., 2012; Lu et al., 2014; Lv et al., 2014).The nanoliposomal sludge slowed down the release rate of the [Cu(glygly)(PS)] complex as compared to the release from the NLS described in (Chapter 4, section 4.3.10), this delay is advantageous to the system as it has to first penetrate through the skin before reaching the site of release. The nanoliposomal sludge is expected to effectively enhance the penetration of the NLS through the skin, while the NLS will deliver the [Cu(glygly)(PS)] complex, reducing the undesired drug loss during blood circulation and hence reducing the drug-related side effect and preferentially release the drugs under the inflammatory-relevant conditions. Further there is improved anti-inflammatory/antioxidant properties of the complex compared to parent, which will altogether lead to the enhanced anti-inflammatory efficacy in TRAPS.

Comparative *in vitro* skin release studies were performed to compare the release of drug from [Cu(glygly)(PS)] loaded nanoliposomal sludge, [Cu(glygly)(PS)] loaded gel, PS conventional gel, PS cream, tablet and syrup, all having the same quantity (1% w/w) of PS in the medium of pH 7.4 with 10mM GSH corresponds to the ICM condition. The release was highest from the PS tablet and syrup (Figures 5.11b), however to be noted is that the release of both these formulations is not controlled (Figure 5.11c and d for tablet and syrup, respectively) as their release remain constant at about $90 \pm 5\%$ at 8h all the drug is released within the first 6h in both formulations at all mediums. The sludge showed improved release compared to the conventional gel which also releases the drug in a non-controlled manner (Figure 5.11e), where approximately $30 \pm 6\%$ is release at 8h in all the media. The complex loaded gel showed an intermediate release profile (Figure 5.11f) of approximately $30 \pm 5\%$ of the complex in all media. The cream had the lowest % release profile (Figure 11g). Overall the [Cu(glygly)(PS)]-loaded nanoliposomal sludge significantly improved the *in vitro* % release profile of the [Cu(glygly)(PS)] complex by delaying the release rate of the [Cu(glygly)(PS)] complex, this is mainly due to gel matrix.



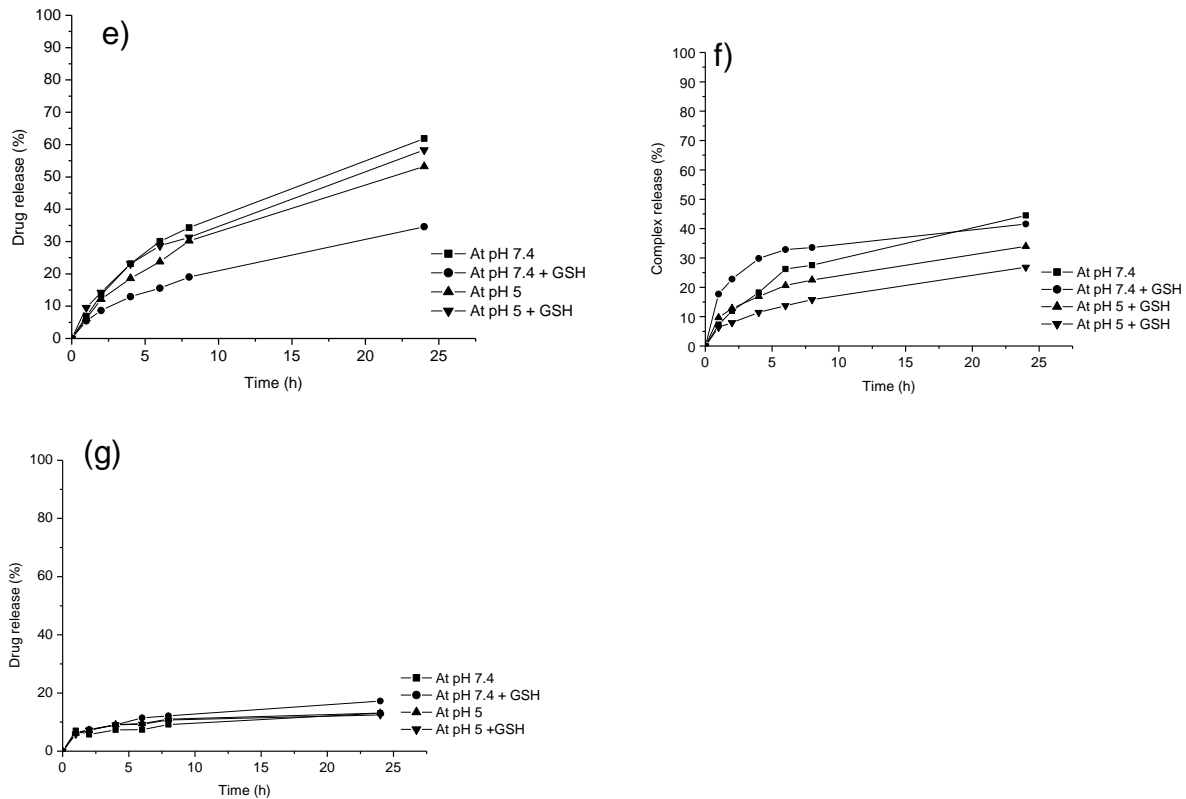


Figure 5.11: (a) The % [Cu(glygly)(PS)] release from the nanolipoosomal sludge treated with GSH (10 mM) in acid (pH 5.0) and normal pH 7.4 at 37 °C. (b) The comparative combined data of all the marketed PS formulations (cream, tablet and syrup), conventional gel and novel [Cu(glygly)(PS)] loaded nanolipoosomal sludge formulation. (c) The % PS release from the tablet treated with GSH (10 mM) in acid (pH 5.0) and normal pH 7.4 at 37 °C. (d) The % PS release from the syrup treated with GSH (10 mM) in acid (pH 5.0) and normal pH 7.4 at 37 °C. (e) The PS release from the conventional gel treated with GSH (10 mM) in acid (pH 5.0) and normal pH 7.4 at 37 °C. (f) The [Cu(glygly)(PS)] release from the PVP/HPMC gel treated with GSH (10 mM) in acid (pH 5.0) and normal pH 7.4 at 37 °C. (g) The PS release from the cream treated with GSH (10 mM) in acid (pH 5.0) and normal pH 7.4 at 37 °C. (Data represent mean \pm S.D. (n=3)).

5.3.9. Skin Permeation evaluation

Transdermal cumulative flux for the marketed formulation (cream), conventional gel, [Cu(glygly)(PS)] loaded PVP/HPMC gel and [Cu(glygly)(PS)] loaded nanolipoosomal sludge across the excised pig skin was 10.9 ± 0.9 , 11.3 ± 1.6 , 18.9 ± 2.2 and $26.6 \pm 1.2 \mu\text{g}/\text{cm}^2/\text{h}$, respectively after 8h in PBS pH 7.4 at 37°C (Figure 5.12).

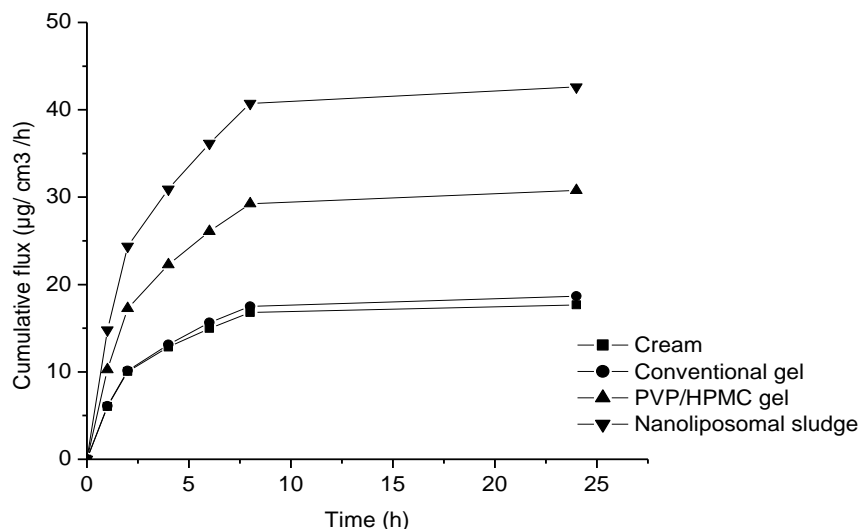


Figure 5.12: Comparative permeation studies through the pig skin in PBS pH7.4 at 37 °C.

The flux from the nanoliposomal sludge was significantly higher (approximately 2.1 ± 0.6 -fold higher) than that obtained after application of either the conventional gel or cream in PBS pH 7.4 and approximately 0.4 ± 0.5 -fold higher than the HPMC/PVP gel in PBS pH 7.4. The data indicates that the transdermal flux of [Cu(glygly)(PS)] was enhanced and this may be attributed to the vesicle size (138.0 ± 52.34 nm) as it has been established that particle size < 200 nm results into an improved permeation (Mavuso et al., 2015). Furthermore, better permeation of [Cu(glygly)(PS)] from the sludge compared to either the [Cu(glygly)(PS)] complex (Chapter 3, section 3.3.3) and HPMC/PVP gel alone suggested some kind of synergistic mechanism between nanoliposomal vesicles, the gel matrix, and skin lipids. Results also revealed that, some of the drug and complex were retained in the skin layers, the amount of drug or/and complex retained was 4.2 ± 1.1 , 4.5 ± 0.9 , 5.8 ± 0.5 and $11.5 \pm 0.7 \mu\text{g}/\text{cm}^3$ for the cream, conventional gel, HPMC/PVP gel and sludge, respectively. Compared to the rest of the formulation, incorporation of the vesicular formulation into the HPMC/PVP gel preparation significantly increased flux. It can be concluded from the results that the nanoliposomal sludge could penetrate and deposit the bioactive 2-3 times more than the conventional and other formulations. High deposition percent indicated that the sludge could provide a drug reservoir in skin to prolong the effect of bioactive and for its local effects. Similar findings were also recorded in other studies (Ghanbarzadeh and Arami, 2013). Moreover the skin integrity was maintained (Table 5.6) as there is only a slight change in conductivity from before and 24h after formulation application, and this was considered insignificant. Hence it was concluded that the permeation was not altered by the skin's integrity.

Table 5.6: Comparative skin conductivity values before and after *ex vivo* studies.

Formulation	Conductivity (mV)	
	Before exposure	After exposure
Cream	141.7±1.2	142.8±1.6
Conventional gel	141.8±0.9	142.1±1.3
HPMC/PVP gel	145.2±2.0	146.0±0.8
Nanoliposomal sludge	145.0±2.7	145.9±1.1

5.4 . Concluding Remarks

The dual pH/redox responsive [Cu(glygly)(PS)]-loaded NLs were successfully formulated and the design of the NLs was optimised using the Box-Behnken experimental design. The dependent responses were the Z-Average size, %DL and %DEE, and, for diverse combinations of independent variables, which were the different ratios of lipids, cholesterol and sonication time. The quantitative effect of independent variables at different levels on the dependent response was investigated by using polynomial equations generated by the model. This study revealed that the relative ratios of the phospholipids significantly influenced the size of the NLs, which alters the %DL and %DEE. On the basis of desirable constraints, the point predication technique of Box-Behnken design proposed an optimized formulation combination. The optimal formulation had independent parameters of sonication time of 30min and PC: Chol: DSPE ratio of 50: 75: 50 which gave predicted NLs responses of; z-average size 52.167nm (Y1), % DL of 19.697 (Y4) and %EE of 95.650 (Y5). It can be concluded that [Cu(glygly)(PS)]-loaded NLs were successfully optimized and developed using the Box-Behnken design.

The [Cu(glygly)(PS)]-loaded NLs showed a dual pH/redox responsive release pattern with a promptly increased release in an environment mimicking inflammation while a sustained release was achieved in a normal physiological environment. Further the flux from the nanoliposomal sludge was significantly higher (about 2.1±0.6-fold higher) than that obtained after application of either the conventional gel or cream. Moreover, more [Cu(glygly)(PS)] was retained in the skin layers compared to other formulations and the integrity of the skin was maintained throughout the *ex vivo* studies. In conclusion this platform has shown the potential for use in the management of TRAPS inflammatory disorder, however further *in vivo* evaluation studies are necessary to confirm the superiority of this design.

CHAPTER 6

***IN VIVO* EVALUATION OF A [COPPER(GLYCYLGLYCINE)(PREDNISOLONE SUCCINATE)]- LOADED NANOLIPOSOMAL SLUDGE IN SPRAGUE-DAWLEY RATS FOR TRANSDERMAL DRUG DELIVERY**

6.1. Introduction

Numerous transdermal drug delivery system (TDDS) containing drugs such as nitroglycerin, scopolamine, clonidine, fentanyl, oxybutynin, nicotine and estradiol are already available in the market (Wokovich et al., 2006). However, the use of TDDS is limited due to a number of reasons such as tremendously low drug release rate from the matrix and the low permeability of the drug through the skin (Im et al., 2010). Generally, specific regulations over the quantity of the drug and its rate of release are necessary in optimizing the overall drug therapy. The main hypothesis of this study was to optimize the overall drug therapy in TNF receptor associated periodic syndrome (TRAPS) which is a genetic auto-inflammatory disorder through TDDS. This may be attained by designing a drug nanocarrier system that responds to internal or external cues and releases the drug-metal complex in a predictable fashion.

A dual stimuli responsive nanoliposomal sludge loaded with a Copper (II) liganded bioactive complex which is the [Copper(glycylglycine)(prednisolone)] ([Cu(glyg)(PS)]) complex that has been established to have improved *in vitro* anti-inflammatory/anti-oxidant activities (Chapter 3, section 3.3.10). Herein the objective is to show that these properties are enhanced as suggested by the *in vitro* studies. Additionally the nanoliposomal sludge was intended to achieve both systemic and local effects via skin application for TDD, as nanoliposomes (NLs) are believed to improve the complex deposition within the skin at the site of action where the goal is to reduce systemic absorption and thus minimize side effects (El Maghraby et al., 2008). Hence the efficacy of the NLs as carrier systems would be evaluated for both local and systemic effects.

In the present study the delivery of the [Cu(glyg)(PS)] complex from the nanoliposomal sludge for TDD was tested over a period of 24 hours in the rat model. The rat model has been selected as the ideal model as it shares physiological and anatomical similarity to humans which makes them the ideal models for conduction of *in vivo* testing (Spanagel, 2000). Various studies of nanocarriers in TDD and its effects have been carried out in rat models (Akhter et al., 2008; Nal

et al., 2008; Pillai and Panchagnula, 2003). Additionally the size of rats allows for great manipulation and Sprague-Dawley rats are particularly docile and easy to handle (Suckow et al., 2006). *In vivo* studies using the rats were aimed at providing information on the preclinical efficacy of the nanoliposomal sludge and the anti-inflammatory/ antioxidant activity of the complex *in vivo* for correlation with *in vitro* studies. Additionally the kinetics of drug release was evaluated to determine PS concentration in the blood so that it can be established that the dual stimuli responsive delivery device increases the anti-inflammatory efficacy of the PS at the site of action, while it reduces the systemic availability of the drug, hence less steroidal side effects.

The amount of [Cu(glyg)(PS)] complex released was analysed using Ultra Performance Liquid Chromatography (UPLC), as depicted in Chapter 3, section 3.3.1 (Figure 3.3). After the complex is released, the drug and metal coordination is broken (Lewis, 1984), as a result free PS may be detected in blood serum. A similar quantification procedure was carried out previously in a study done by Martins et al., 2015, where the release of a copper–naproxen metallodrug was done using High Performance Liquid Chromatography (HPLC). The molar concentration of PS is expected to be equivalent to that of Cu^{2+} as proposed in chapter 3.

6.2. Materials and methods

6.2.1. Materials

The Sprague Dawley rats utilized in this study were obtained according to the Central Animal Services (CAS) protocols at the University of the Witwatersrand. Prednisolone succinate, dexamethasone and copper (II) nitrate and glycyglycine were purchased from Sigma Aldrich (St. Louis, MO, USA). Double de-ionized water was obtained from a Milli-Q system, (Milli- Q, Millipore, Johannesburg). Acetonitrile, prednisolone syrup and tablets were commercially available. All solvents utilized for UPLC-UV detection were of UPLC grade and all other reagents were of analytical grade. The preparation of the optimized nanoliposomal sludge was discussed earlier in this dissertation in Chapter 5, Section 5.2.2.

6.2.2. Nanoliposomal sludge sterilization and lyophilisation

A suspension (10mg/ml) of NLs was diluted to a concentration of 10mg/5mL with water and sterilized by filtration through sterile disposable syringe filters (0.20 μm Millipore filter) into 5mL glass vials (Darole et al., 2008). All glasswares were sterilized by autoclaving and the entire procedure was performed in a laminar flow hood (Esco. Singapore). The NLs were then frozen at -80°C for overnight, for long term stability the NLs were lyophilised in the presence of a

cryoprotectant (1% sucrose) and the samples were kept at -20°C (Chaudhury et al., 2012). The gel was sterilized under UV light overnight (Karunakaran et al., 2011; Luo et al., 2008) and NLs were then dispersed into it under the laminar flow hood unit. The sterility of the gel was validated by incubating the sludge in an agar plate at 37°C for 24h.

6.2.3. Experimental design

Sprague Dawley rats weighing 250 to 300g were housed in a room that was automatically maintained on a 12h light/dark cycle at 25°C and properly humidified. Animals were handled in accordance with the University of the Witwatersrand CAS guidelines. The 110 rats (5 for pilot and 105 for main study) were housed singly at the CAS and were allowed one week to adjust to the surroundings. They were fed with standard rodent pellet and supplied with water *ad-libitum* under strict hygienic conditions. The rats receiving an oral administration of the prednisolone were fasted from solid food for 12h before the experiments but habituated with a diet of jelly for sustenance and to ensuring that their energy levels were upheld (Pang et al., 2008). Prior to the main study a pilot study was conducted using five additional rats with the aim of assessing inflammation induction using carrageenan and to test the efficacy of the open glass chamber to hold the formulation in place, Figure 6.1 shows the flow diagram of the procedure.

Rats were assigned in groups of five ($n=5/\text{group}$, except at 0h where $n=1/\text{group}$), one rat was euthanized at each specific time point per group and all studies were done in triplicate. Each group underwent administration of the relevant formulation as well as blood sampling. To ensure that formulations remained in place, treated rats were covered with a layer of Tegaderm (3 M, St. Paul, MN), a layer of dry non-adherent gauze (Telfa, Kendall Company, Manfield, MA), and an elastic bandage was wrapped around the dorsum and abdomen of the rats. Prior to the application of all the formulations the rats were anesthetized with xylazine (5mg/kg) and ketamine (100mg/kg).

This was an interventional study where 105 rats with an initial mass of 250g-300g were randomly assigned to 5 groups (21 rats per group) (refer to Flow diagram, Figure 6.2), the steps of the procedure are also summarised (Figure 6.3).

Group 1: This was the placebo group where inflammatory challenged rats received a dermal application of placebo nanoliposomal sludge that was applied evenly on the dorsal portion (3.14cm^2) of the rats.

Group 2: This was the test group where inflammatory challenged rats received a dermal application of [Cu(glyg)(PS)]-loaded nanoliposomal sludge that was applied evenly on the dorsal portion (3.14cm²) of the rats.

Group 3: This was the comparison group where inflammatory challenged rats received an oral formulation of the PS drug

Group 4: This was the comparison group where inflammatory challenged rats received the model drug, a dermal application of prednisolone, which was applied on the dorsal portion (3.14cm²) of the rats.

Group 5: This was the comparison group where healthy rats received a dermal application of [Cu(glyg)(PS)]-loaded nanoliposomal sludge, which was applied evenly on the dorsal portion (3.14cm²) of the rats.

Group 2 is the experimental group and groups 1, 3, 4 and 5 are the control groups. In all groups inflammation was induced except group 5.

At the end of both the pilot and main study the rats were euthanized through the cardiac puncture and sodium pentobarbital (200mg/kg). This was done in order to determine the concentration of the drug/ complex in the system of the animals a large volume of blood was needed (Parasuraman et al., 2010) and due to the small size of the animal, the animals were sacrificed in order to obtain the blood volume of 5mL (Beeton et al., 2007). Additionally histopathological skin samples were required in order to grade the induced inflammation.

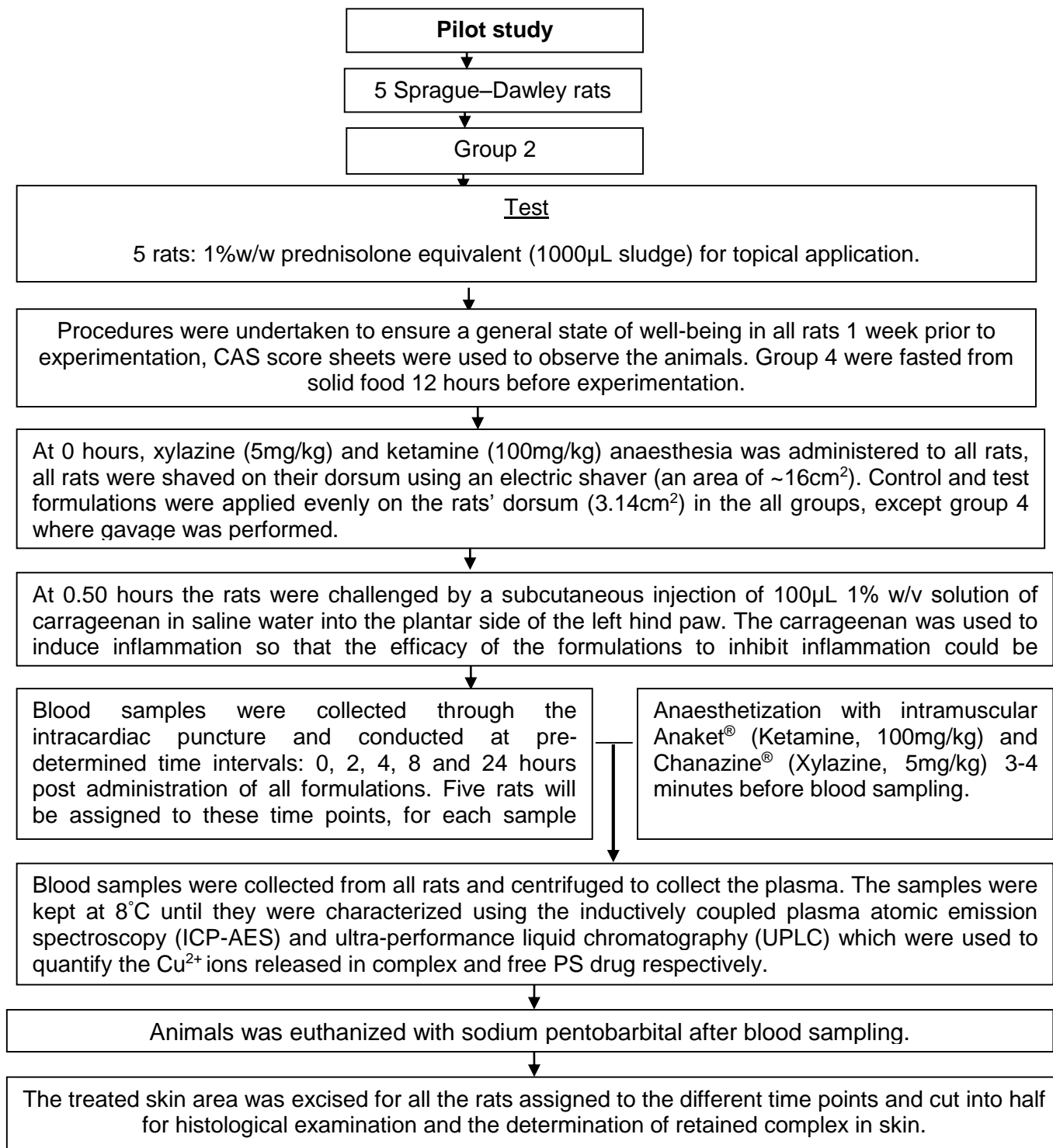


Figure 6.1: The flow diagram showing the steps involved in the pilot of the in vivo studies using sprague-dawley rats.

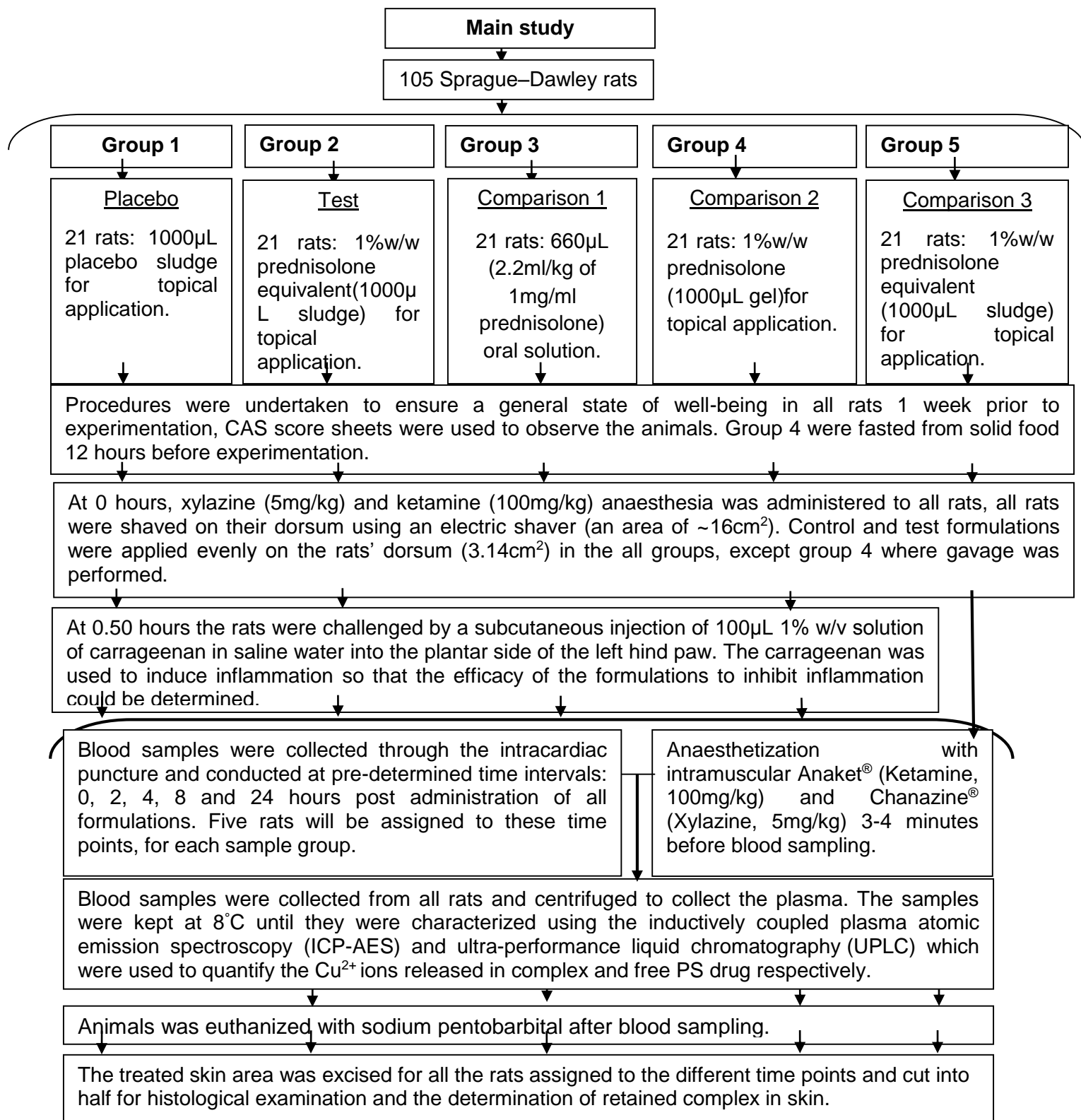


Figure 6.2: The flow diagram showing the steps involved in the main in vivo studies using sprague–dawley rats.

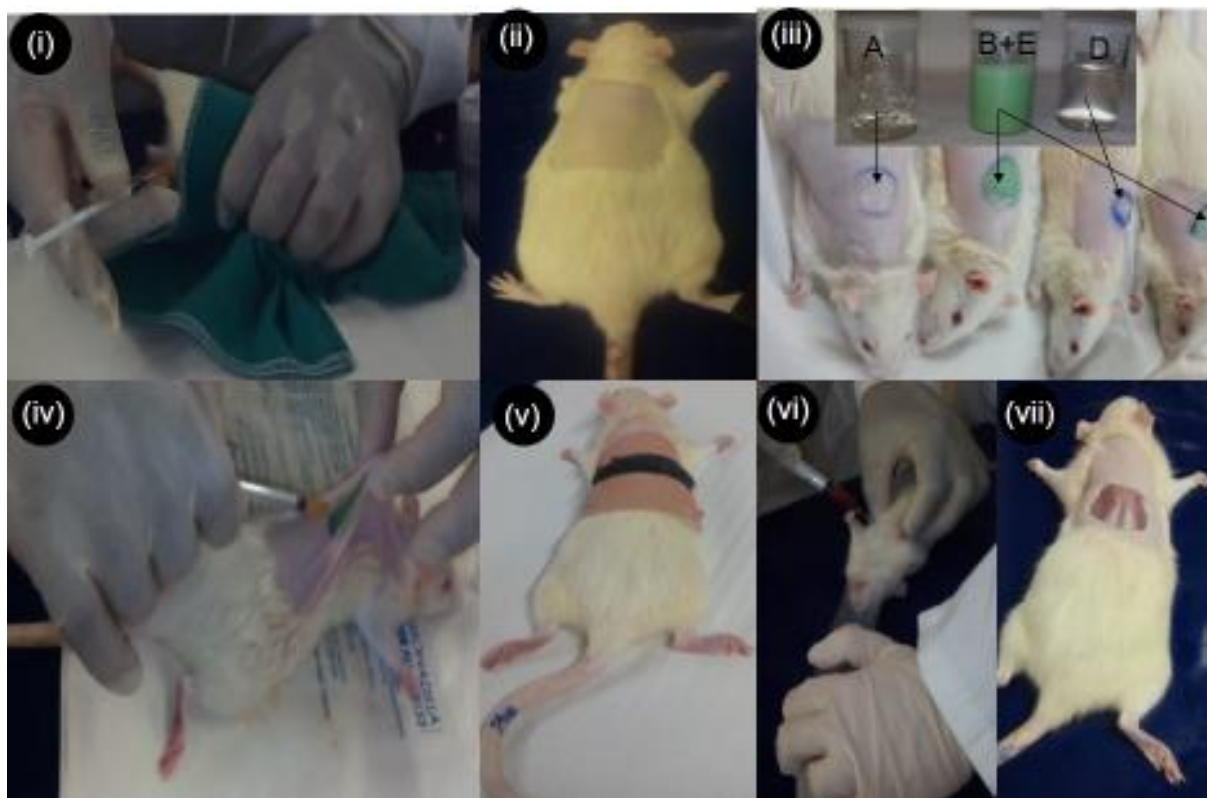


Figure 6.3: The photographic procedure of the *in vivo* studies using rats. Wherein (i) An anesthesia was administered to all rats, (ii) all rats were shaved on their dorsum and shaved area wiped with water, (iii) at 0h different gels were applied on an area of 1.44cm² of the shaved portion, while group 3 rats were gavaged, (iv) all rats except group 5 rats received an SC injection at 0.5h after gel application, (v) all rats were bandaged to keep the formulations in place, (vi) blood was collected through cardiac puncture, (vii) and rats were euthanized immediately after blood collection and skin was excised.

6.2.4. Histological assessment

For histological assessment, immediately after the rats were euthanized the treated skin area was excised for all the rats assigned to the different time points and stored in 10% formalin. A skin section of 5µm thickness was cut from each sample and stained with hematoxylin–eosin for microscopic examination (Pillai and Panchagnula, 2003). The treated skin sections were observed under a light microscope and a scoring system was used to assess the changes in the skin. The intensity of the inflammatory response was graded from 0 to 3, where: 0, represents the absence of any inflammatory cells (no infiltration); 1, represents the presence of less than 10% of inflammatory cells (mild infiltration); 2, represents the presence of 10 to 50% of

inflammatory cells (moderate infiltration); and 3, represents the presence of more than 50% of inflammatory cells (severe infiltration) within the total population cells (Riella et al., 2012). All histological assessments were performed in triplicate.

6.2.5. Determination of retained complex in skin

Complex/drug retained in the skin were determined according to a method described by Lei et al. (2013). The skin layers were separated by removing the stratum corneum using a tape stripping and 10 strips were collected. The remained skin was frozen at -80°C and separated into epidermis and dermis horizontally. The parts of skin layers were chopped and extracted in methanol with homogenization. The samples were kept refrigerated for 12h and then centrifuged to obtain a supernatant for analysis of complex content using UPLC.

6.2.6. Prednisolone analysis using Ultra-performance liquid chromatography (UPLC)

6.2.6.1. The chromatographic system

The PS released was analysed using an ultra-performance liquid chromatography (UPLC) system after an appropriate extraction procedure. UPLC chromatographic separations were performed with an ACQUITY UPLC®BEH Shield RP 18 column (1.7µm, 100mm × 2.1mm) (Waters, Milford, MA, USA), equipped with array detector(PDA), Empower® Pro software (Waters, Milford, MA, USA), autosampler and 515 dual pumps. The mobile phase was pumped at a flow rate of 0.05mL/min and consisted of the combination water: Acetonitrile 40:60% v/v. Detection was by UV absorption at 248nm at room temperature. The prepared mobile phase was filtered through a 0.22µm Millipore filter before use. The injection volume for all UPLC analyses was 10µL.

6.2.6.2. Internal standard

The internal standard used was dexamethasone where 25µg/mL (25µl) concentration of the drug in methanol was added to the plasma for generation of calibration standards and samples from rats.

6.2.6.3. Calibration curve standards

Standard solutions of PS (50µg/ml) and dexamethasone (0.025µg/µL) in ethanol were prepared. From these solutions, calibration standards were prepared in 150µL of blood plasma so that each contained 25, 50, 75, 100, 125 or 150µL of PS (0.050µg/µL) and 150µL of dexamethasone (0.025µg/µL) as the internal standard. The mixtures were sonicated for 5min before the

extraction procedure. A standard calibration was constructed with the area under the curve (AUC) of the standard solutions and internal standard using the following equation:

$$y = \frac{\text{AUC of standard solution}}{\text{AUC of internal standard}} \quad \text{Equation 6.1}$$

6.2.6.4. Liquid-liquid extraction procedure

Plasma (150 μ L) was extracted by shaking on a vortex mixer for 5min with 1mL ethyl acetate in a 2.5mL centrifuge tube and then centrifuging for 10min at 5000rpm. The supernatant organic phase was transferred to a glass vial and evaporated in a vacuum oven to dryness under inert conditions at 60°C. The residue was reconstituted with 1mL of mobile phase and vortex mixed for 2min. The solution was filtered through a 0.22 μ m millipore filter (Morrison et al., 1977) before being injected into UPLC column. The total percentage of PS extracted was determined using the AUC of the plasma and standard solution as follows:

$$\text{Percentage yield} = \frac{\text{AUC plasma}}{\text{AUC standard}} \quad \text{Equation 6.2}$$

6.2.6.5. Plasma sample handling and preparation from rats

Rats' blood samples were collected into glass tubes and centrifuged at 3000rpm for 15 min and the plasma separated. The plasma was kept frozen at -80°C until analysis. In all the plasma samples (1mL) 50 μ L of methanol and 50 μ L of naproxen sodium in methanol (1mg/mL) were added and extracted as described above.

6.2.6.6. Method validation

Method validity was assessed as validated by AbuRuz et al. (2003) and Kurakula et al. (2011) using the linearity, accuracy and precision. The linearity was investigated from the squared correlation coefficient (R^2 value). Five calibrators were included in the curve and were required to meet all qualitative identification and quantification criteria. The quantitative accuracy required was within 20% of target. Linearity was achieved with a minimal R^2 value of 0.99. Accuracy was expressed as percent recovery after analyzing drug-spiked serum and comparing this to the added amounts; precision was expressed as the relative standard deviations (RSDs) of the determined concentrations.

6.3. Results and Discussion

6.3.1. Validity of the sterility procedure

The incubated plate with a streak of the sterilized sludge revealed that there was no bacterial growth from the sludge, hence it was established that the sludge was sterile before its application in the *in vivo* studies, Figure 6.4 demonstrates the plate with no bacterial growth.

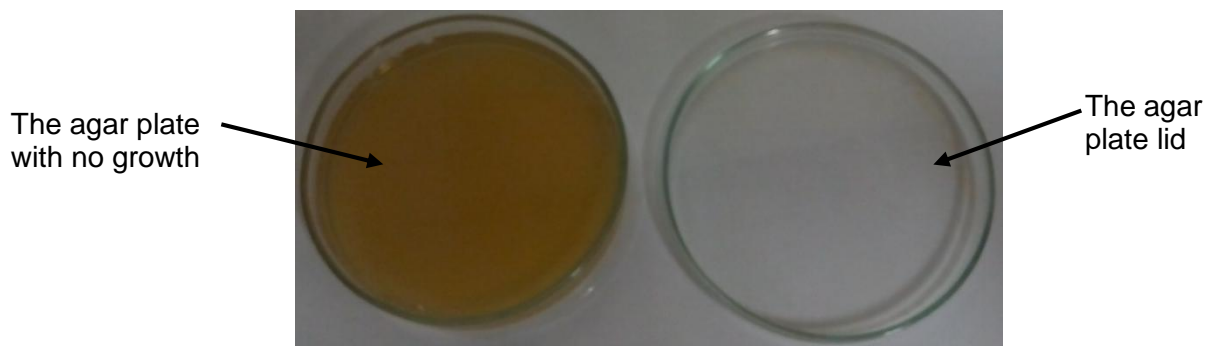


Figure 6.4: the agar plate streaked with sludge, after it has been incubated for 24h at 37°C

6.3.2. Pilot study using five rats from group B

The pilot study was performed as shown in Figure 6.1, where each rat was euthanized 0, 2, 4, 8 and 24h. According to the histopathology results (Figure 6.5), inflammation was successfully induced with inflammatory cells comprising of neutrophils and lymphocytes. Figure 6.5 shows the inflammatory cells of the subcutaneous and dermis regions, at 2h with moderate (grade 2) to mild inflammation at 4h (grade 1). There was an immediate slight increase of edema and erythema due to inflammation, similar observations were also reported previously (Tsuji et al., 1998; Mei et al., 2003; Fouad et al., 2013). Worth noting is a study done by Khurana et al. (2013) where there was no obvious skin erythema and edema observed in the animals, yet the histology of the animals skin proved that inflammation occurred after inflammation was induced using carrageenan, thus the slight edema observed in this pilot study may be justified. As the pilot study was carried out, it was established that the Teflon rings were not necessary as the gel was viscous enough to stick on the designated area, henceforth they were not used in the main study.

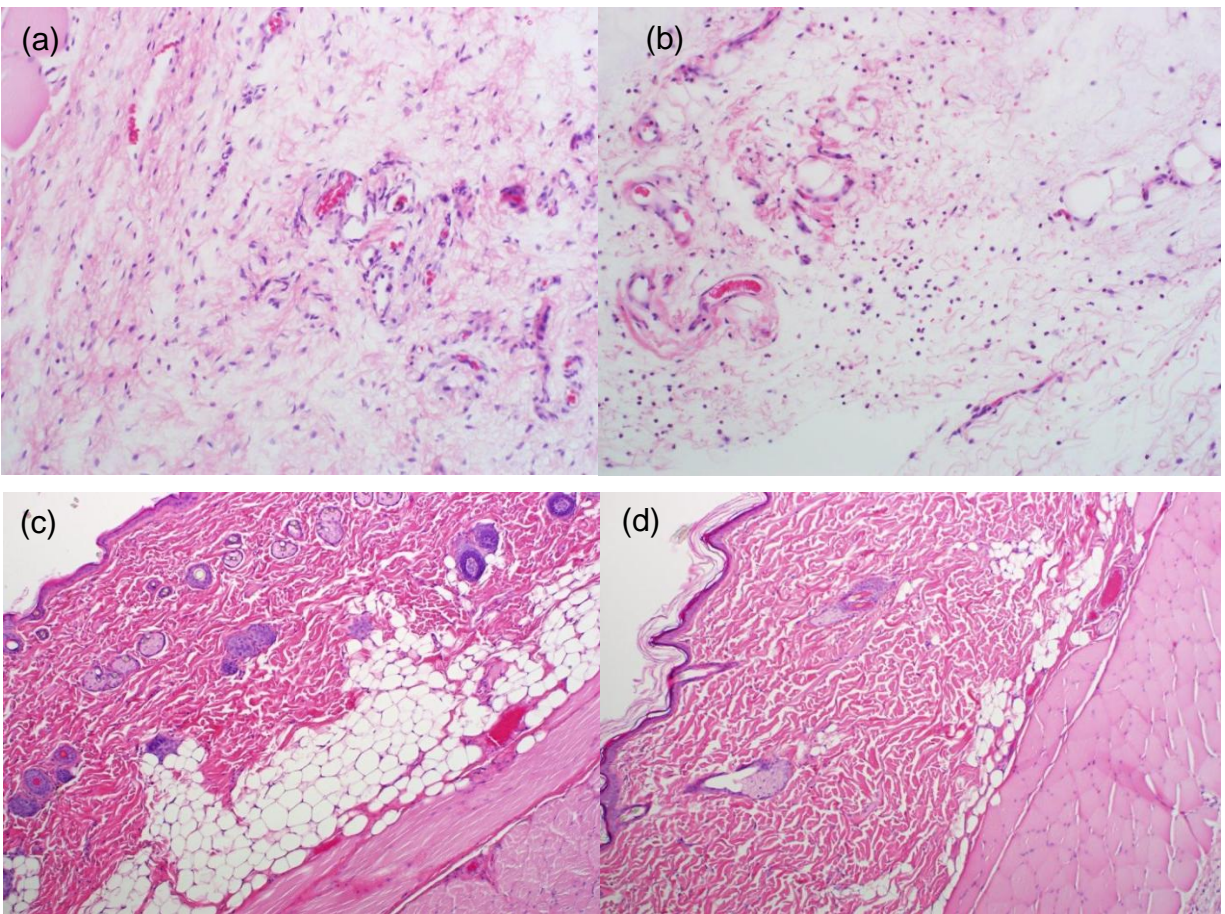


Figure 6.5: The light microscope images of the H&E stained slides showing the pilot study images (a) the subcutaneous region at 2h, (b) the subcutaneous region at 4h, (c) the dermis region at 2h, and (d) the dermis region at 4h.

6.3.3. *In vivo* evaluation of the anti-inflammatory/anti-oxidant activity of the [Cu(glyg)(PS)] delivered from the sludge

The anti-inflammatory/anti-oxidant activity of the [Cu(glyg)(PS)] delivered from the sludge was evaluated and compared to other formulations using histopathology, results are summarized in table 6.1 and discussed as follows:

Group 1

The histopathology results showed that mild inflammation was observed at 2h and moderate inflammation was observed at 4h which subsided to mild inflammation at 8 and 24h post-exposure. The inflammation challenged rats showed constant inflammation with no discernible effect of the placebo nanoliposomal sludge, detailed results are described as follows:

- (i) **At 2h:** A focus of mild dermal oedema was noted along with very mild mononuclear infiltration in the subcutis below the cutaneous skeletal muscle. The epidermis, subcutis and cutaneous skeletal muscle were within normal limits.
- (ii) **At 4h:** Moderate perivascular to interstitial neutrophilic infiltration was noted in the subcutis below the cutaneous skeletal muscle and was associated with mild haemorrhage. Scattered lymphocytes, plasma cells and macrophages were also present. The epidermis, dermis and cutaneous skeletal muscle appear within normal limits.
- (iii) **At 8h:** Mild dermal oedema was noted along with a mild increase in interstitial leukocytes which included a few neutrophils as well as mononuclear cells. Mild subcutaneous fibroplasia was noted along with mild oedema and a very mild increase in neutrophils and spindle cells below the cutaneous skeletal muscle. The epidermis and cutaneous skeletal muscle appear within normal limits.
- (iv) **At 24h:** Mild increase in interstitial leukocytes, mostly mononuclear cells with a few scattered lymphocytes and were noted in the subcutis below the cutaneous skeletal muscle. Mild acanthosis was observed in the epidermis. The dermis and cutaneous skeletal muscle appear within normal limits.

Group 2

The histopathology results showed that no inflammation was observed at 2h which increased to very mild inflammation at 4 and 8h with reduction to no inflammation at 24h. This would suggest that the test substance may have an anti-inflammatory effect, detailed results are described as follows:

- (i) **At 2h:** The epidermis, dermis, follicles, subcutis and cutaneous skeletal muscle were all within normal limits. No inflammatory cells were observed.
- (ii) **At 4h:** Very mild eosinophilic and mononuclear infiltration was observed in the subcutis below the cutaneous skeletal muscle. The epidermis, dermis and cutaneous skeletal muscle appear normal limits.
- (iii) **At 8h:** Very mild scattered neutrophilic and eosinophilic infiltration along with a few lymphocytes and plasma cells were noted in the subcutis below the cutaneous skeletal muscle. The epidermis, dermis and cutaneous skeletal muscle appear within normal.
- (iv) **At 24h:** The epidermis, dermis, follicles, subcutis and cutaneous skeletal muscle were all within normal limits. No inflammatory cells were observed.

Group 3

The histopathology results showed that no inflammation was observed at 2h but mild inflammation was observed at 4h. This was reduced to very mild inflammation at 8 and 24h. The anti-inflammatory was comparatively more notably in group 2 animals as the inflammatory grade of 2 was not reached. This would indicate that oral prednisolone treatment may have had some anti-inflammatory effect, detailed results are described as follows:

- (i) **At 2h:** One hair follicle showed only mild intramural mononuclear infiltration. Very mild oedema and scattered mononuclear cells were observed in the subcutis below the cutaneous skeletal muscle. The remaining epidermis, dermis and cutaneous skeletal muscle were within normal limits.
- (ii) **At 4h:** A mild increase in the number of neutrophils and lesser numbers of eosinophils was observed in the subcutis below the cutaneous skeletal muscle along with mild focal haemorrhage, oedema and an increase in spindle cells. The epidermis, dermis and cutaneous skeletal muscle appear within normal limits
- (iii) **At 8h:** Mild dermal oedema was observed along with very mild, scattered lymphocytes and plasma cells in the subcutis below the cutaneous skeletal muscle as well as mild oedema. The epidermis showed focal areas of mild acanthosis. The cutaneous skeletal muscle appears within normal limits.
- (iv) **At 24h:** Mild dermal oedema was noted and one sample also showed very mild scattered mononuclear cell infiltration in the dermis. Very mild, scattered eosinophilic and mononuclear infiltration was present in the subcutis below the cutaneous skeletal muscle along with mild oedema. The cutaneous skeletal muscle appears within normal limits.

Group 4

The histopathology results showed that very mild inflammation was observed at 2h while mild inflammation was observed at 4h which subsided to very mild inflammation at 8h and again increased at 24h. This would indicate the epicutaneous application of prednisolone may have had some anti-inflammatory effect, detailed results are described as follows:

- (i) **At 2h:** Mild haemorrhage was noted in the subcutis below the cutaneous skeletal muscle and this was associated with mild oedema and very mild, scattered mononuclear infiltration with a few neutrophils and eosinophils. Mild acanthosis was

noted in the epidermis. The dermis and cutaneous skeletal muscle appear within normal limits. No inflammatory cells were observed.

- (ii) **At 4h:** Mild dermal oedema with just a few scattered interstitial neutrophils were observed, primarily in the superficial dermis. One section did show a mild accumulation of non-degenerate heterophils in the subcutis just below the cutaneous skeletal muscle. The epidermis and cutaneous skeletal muscle appear within normal limits.
- (iii) **At 8h:** Very mild, scattered mononuclear cells were observed in the subcutis below the level of the cutaneous skeletal muscle along with mild oedema. The epidermis, dermis and cutaneous skeletal muscle appear within normal limits.
- (iv) **At 24h:** A single focus of mild infiltration with non-degenerate neutrophils, eosinophils as well as lymphocytes and plasma cells and the occasional Mott cell were noted in the subcutis below the cutaneous skeletal muscle. A few segments of skeletal muscle degeneration with mild interstitial neutrophilic and lymphoplasmacytic infiltration was observed just adjacent to the area of inflammation in the subcutis. The epidermis and dermis appear within normal limits.

Group 5

The histopathology results showed that very mild inflammation was observed at 2 and 4h with no inflammation at 8h and 24h. This would suggest that the [Copper(glycylglycine)(prednisolone)]-loaded nanoliposomal had an anti-inflammatory effect. It was noted that the cutaneous skeletal muscle showed degeneration in association with the inflammation and may represent an injection tract injury, detailed results are described as follows:

- (i) **At 2h:** Very mild, scattered eosinophilic as well as mononuclear infiltration was noted in the subcutis below the cutaneous skeletal muscle along with mild oedema. The epidermis, dermis and cutaneous skeletal muscle appear within normal limits.
- (ii) **At 4h:** Very mild perivascular to interstitial neutrophilic infiltration was noted in the subcutis below the cutaneous skeletal muscle and was associated with very mild haemorrhage. Scattered lymphocytes, plasma cells and macrophages were also present. The epidermis, dermis and cutaneous skeletal muscle appear within normal limits.
- (iii) **At 8h:** The epidermis, dermis, follicles, subcutis and cutaneous skeletal muscle were all within normal limits. No inflammatory cells were observed.

(iv) **At 24h:** The epidermis, dermis, follicles, subcutis and cutaneous skeletal muscle were all within normal limits. No inflammatory cells were observed.

Table 6.1: Grading of the anti-inflammatory effects of the formulations applied on the different groups of rats.

Time (h)	INFLAMMATION GRADING				
	Group 1	Group 2	Group 3	Group 4	Group 5
0	0	0	0	0	0
2	1	0	0	1	1
4	3	1	2	2	1
8	2	1	1	1	0
24	2	0	1	2	0

*Where 0 is no infiltration, 1 is mild infiltration, 2 is moderate infiltration, and 3 is severe infiltration.

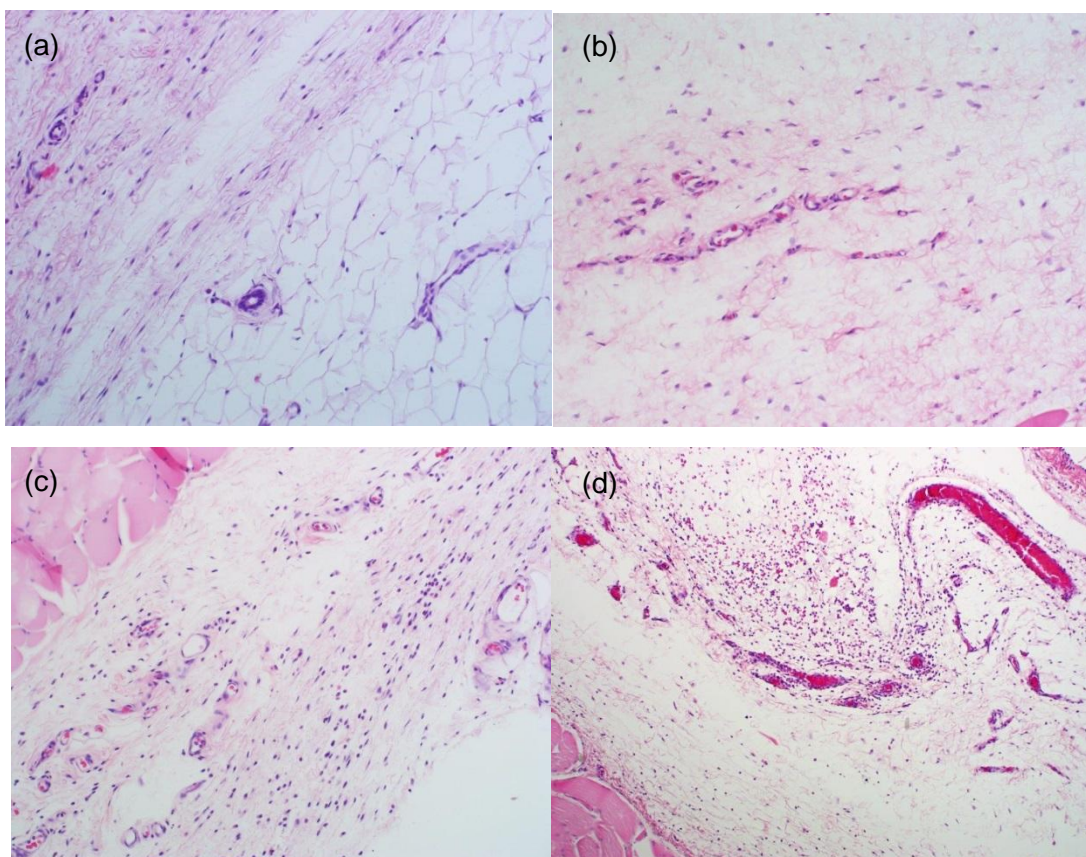


Figure 6.6: The light microscope images of the H&E stained slides showing some of the main study images (a) the subcutaneous region with no infiltration (grade 0), (b) the subcutaneous region with mild infiltration (grade 1), (c) the subcutaneous region with moderate infiltration (grade 2), and (d) the subcutaneous region with severe infiltration (grade 3).

Examples of the histopathology grading are shown in Figure 6.6, where grade 0 and 1 were the skin samples from group 2 rats, grade 2 and grade 3 were the skin samples from group 3 and 1, respectively. The [Copper(glycylglycine)(prednisolone)]-loaded nanoliposomal sludge appeared to have an anti-inflammatory effect comparable to oral prednisolone but this will have to be proven with appropriate statistical testing as the lesions are mostly mild to begin with. These samples have no relation to timing of exposure and may likely indicate chronic trauma or injury in these sections.

6.3.4. *In vivo* evaluation of the [Cu(glyg)(PS)] complex delivery from the sludge

6.3.4.1. Validation of the extraction procedure

The liquid-liquid extraction method was considered to be valid as the recovery and purity of PS were optimum. Average recoveries were calculated for four plasma analytes concentrations of 1.25-7.5µg/µL (n=3) as summarized in Table 6.2, the recovery percentage ranged from ~87 to 95%.

Table 6.2: Average and relative standard deviations (RSDs) of PS recoveries from spiked plasma blanks.

PS concentration (µg/µL)	1.25	2.5	6.25	7.5
Recovery (%)	87.3	94.7	94.5	90.5
RSDs (%)	4.4	12.1	9.6	8.9

6.3.4.2. Chromatographic separation and validation assay

Figure 6.7 shows calibration curve properties for the PS analytical method in the mobile phase (a) and blood serum (b). The PS and dexamethasone (internal standard) spiked in the analytes were effectively eluted within 10min, with an observed PS retention time (R_t) of 4.496 and 4.137min, and dexamethasone R_t of 6.150 and 5.977min in mobile phase and blood serum, respectively. The calibration curve was found to be linear in the range of 1.25-7.5µg/µL, with five calibrators and $R^2 = 0.945$. The acceptance criteria to fulfill the requirements for therapeutic drug monitoring were: $\pm 10\%$ for accuracy and $RSD \leq 10\%$; for the lowest concentration on the calibration curve the RSD was $\leq 20\%$, which is in accordance with US Food and Drug Administration (FDA) and ICH requirements (Frahner et al., 2003).

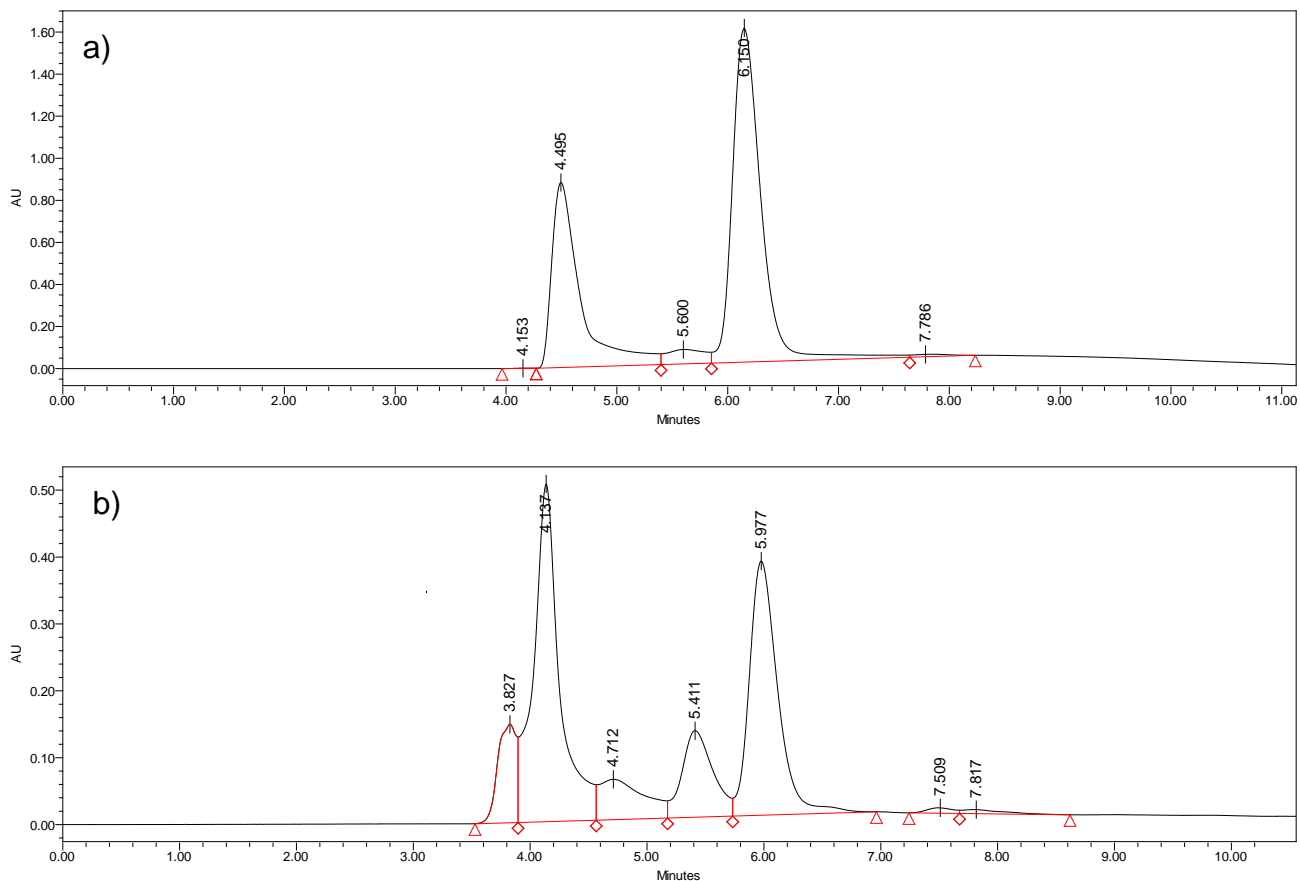


Figure 6.7: The UPLC PS and dexamethasone (internal standard),(a) in the mobile phase and (b) blood serum

6.3.4.3. Determination of the [Cu(glyg)(PS)] concentrations in the rats blood plasma

To complement the anti-inflammatory effects that indirectly assess the ability of the dermal sludge to deliver [Cu(glyg)(PS)] across skin, the plasma PS concentrations were directly measured using UPLC. The plasma PS concentration versus time profiles following the application of the different formulations are shown in Figure 6.8. The time to reach maximum serum concentration (C_{max}) of PS released was different for all formulations, however it was noted that the PS released from the formulation in group B rats was significantly higher and released in a controlled manner compared to the rest of the groups. The pharmacokinetic parameters of PS after the oral administration were significantly different from the parameters obtained after the transdermal application of sludge formulation. After the oral administration of PS, the C_{max} of PS was reached within 4h, and a sharp decay was observed afterwards as shown in the graph (Figure 6.8). The AUC of PS after the application of dermal sludge was increased immediately after application of formulation in group 2, which indicates the improved bioavailability of PS through the TDD route. The bioavailability of PS with reference to orally

administered PS was found to increase by 2.4 times within 2h when the sludge formulation was applied in inflammatory challenged rats. Greater PS plasma levels were achieved immediately and were maintained till the last sample, where a C_{max} of $3.611 \pm 0.405 \mu\text{g/mL}$ was achieved at 24h. With this type of release the anti-inflammatory activity of the sludge formulation is expected to be maintained for longer period of time as the drug is released in a sustained manner and this was attributed to the NLs presence in gel structure and the surface-active properties of the gel. Additionally the release of the PS from the sludge in group 2 is maintained within the minimum and maximum therapeutic range (0.5-2mg/kg).

According to the AUC of PS from the sludge in Group 2 and 5 it is observed that the NLs circulated in the blood for a long period of time in Group 5 where inflammation was not induced compared to Group 2. In Group 5 there is a slight increase of the PS release as the sludge was applied on the skin, the release was maintained at 0.959, 1.695 and $1.397 \mu\text{g/mL}$ at 2, 4 and 8h, and eventually the PS release was abruptly reduced to $0.409 \mu\text{g/mL}$ at 24h. Comparing the release in Group 2 and 5, this mechanism of release is attributed to the inflammatory responsive release system that was designed in this study. The AUC of PS retained in the skin of the Group 5 rats was significantly higher compared to inflammatory challenged rats (Group 2) as shown in Figure 6.9, hence it was established that less NLs degrade in an inflammatory free environment while more NLs are retained within the skin resulting in low bioavailability and reduced cytotoxicity as the NLs slowly degrade. Further it was noted that the sludge released the drug in a single steady peak rather than fluctuating peaks which may be observed from repeated oral (Group 3) administration of PS, hence the sludge may have less side effects associated with drug compared to conventional oral formulation.

In the conventional gel formulation (Group 4 rats) a PS C_{max} of $1.153 \mu\text{g/mL}$ was achieved at 8h which is below the minimum therapeutic effective dose of 0.5mg/kg ($\sim 125\text{-}150 \mu\text{g}$ in each rat considering their weight), therefore this gel was not as effective as the sludge. Also be noted was the low amount of drug retained in the skin with this gel compared to the sludge (Figure 6.9). The AUC decreased in the following order Group 5 > 2 > 4 for skin retained PS. In the present studies, the skin of the rats after a 24h application of the formulations in the different groups did not show any visible skin reaction.

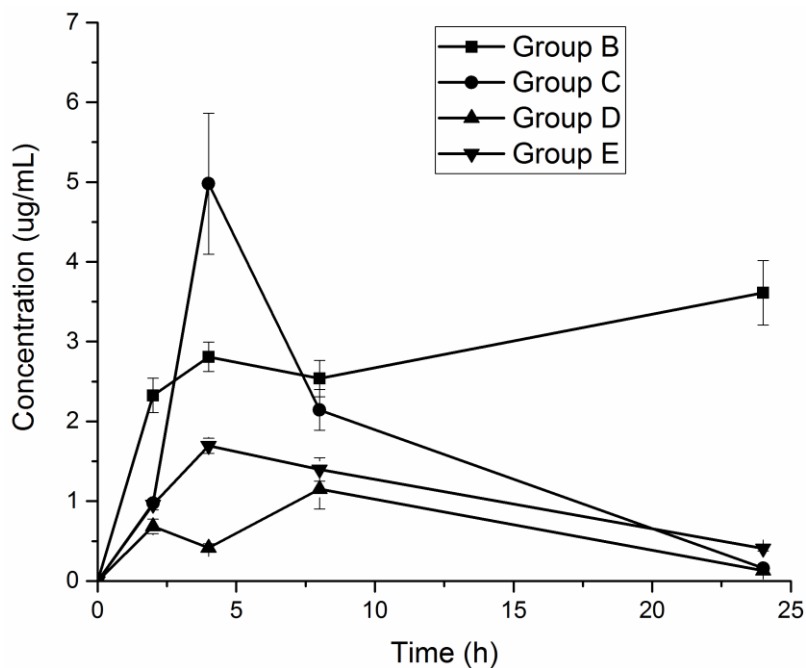


Figure 6.8: The plasma levels of PS in Sprague-Dawley rats after the application of the different formulations in all the groups (standard deviations (n=3)).

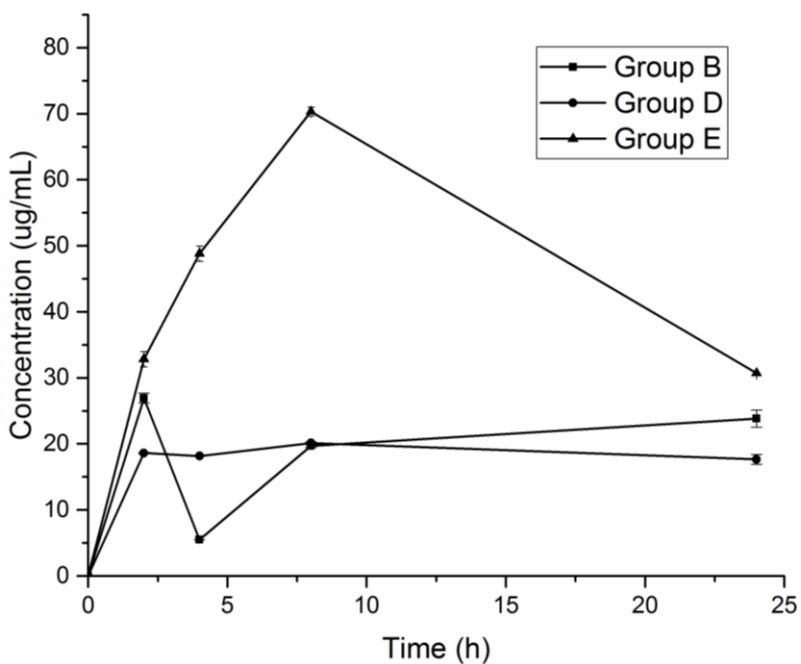


Figure 6.9: The AUC of the formulations applied on the different groups of rats at various time intervals with the standard deviations (n=3).

Considering the *in vivo* release studies in this chapter and *in vitro* release studies covered in chapter 5 of the PS from the dermal sludge, it is indicated that even though the release rates

were higher in the *in vitro* studies there is still some correlation in the release pattern. In the literature, *in vivo-in vitro* correlations have been performed for other drugs and the correlation between *in vitro* and *in vivo* studies were generally poor, *in vitro* studies gave higher rates than *in vivo* results (Kararli et al., 1995). Therefore the correlation perceived in this study was considered significant, as the relationship observed between the *in vivo* and *in vitro* studies indicate a consistency between *in vitro* study and *in vivo* study.

6.4. Concluding Remarks

In conclusion, *in vitro* and *in vivo* studies indicated that the management of the inflammatory symptoms during TRAPS could be enhanced by the novel nanoliposomal dermal sludge. According to the *in vivo* studies the [Copper(glycylglycine)(prednisolone)]-loaded nanoliposomal sludge showed anti-inflammatory effects comparable to the oral prednisolone and this formulation is capable of overcoming the shortcomings of the oral administration of PS, such as high first pass metabolism, while maintaining the required therapeutic dose of the drug. Therefore, it was established that the dermal sludge may be a promising system to be used in the treatment of inflammation in TRAPS.

CHAPTER 7

CONCLUSIONS AND RECOMMENDATIONS

7.1. Conclusions

Tumour necrosis factor receptor (TNFR) associated periodic syndrome (TRAPS) is found worldwide, and is a key representative of Genetic auto-inflammatory inflammatory skin disorders (GAISDs)(Stojanov and McDermott, 2005). The clinical presentation is typically associated with recurrent fever episodes and systemic inflammation involving skin and serosal linings (Yao et al., 2012). The use of this novel transdermal drug delivery system (TDDS) may be beneficial in the management of these symptoms. This system may have an advantage over the currently used oral corticosteroids as it has the ability to reduce side effects associated with corticosteroids while increasing the efficacy of the drug.

In this study, it has been established that a novel copper-liganded bioactive complex with prednisolone succinate as the corticosteroid drug exhibited improved *in vitro* anti-inflammatory/anti-oxidant activity, in comparison to the parent drug, and also its skin penetration efficacy was slightly improved in TDDS. The complex appeared to be non-toxic in human dermal fibroblast adult (HDFa) cells in a concentration equivalent to that of parent drug. Based on these results, it can be concluded that the coordination of this corticosteroid drug to copper (II) has the potential of reactivating the drug into a more potent coordination compound with improved pharmacokinetics/dynamics that can be advantageous in the treatment of TRAPS through the transdermal route.

To further enhance the TDDS of the copper-liganded bioactive complex, the complex was successfully loaded into a dual pH/redox responsive nanoliposomal system, allowing the complex to be released in an inflammatory responsive manner. The complex loaded nanoliposomes (NLs) were optimized and developed successfully using the Box-Behnken design. The overall designed system displayed the synergistic effects of the metal-drug complex as a bioactive, dual pH/redox-responsive NLs as the complex nanocarrier and gel matrix which promoted the skin penetration of the complex loaded NLs. The combined gel-based vehicle resulted in a liposomal nanogel with an ideal TDDS design for TRAPS management which was termed the nanoliposomal dermal sludge. According to the *in vitro*, *ex vivo*, and *in vivo* results, which were collected in this study it was concluded that this system could significantly increase

the intracellular bioactive concentration and efficiency for TRAPS inflammation inhibition, with reduced drug (steroids) side effects through the transdermal route of delivery.

7.2. Recommendations

TRAPS may result from consequences of the abnormally retained TRAPS mutant TNFR1 (Lobito et al., 2006). The TRAPS therapy proposed in this dissertation indirectly treat the inflammatory symptoms without correcting the underlying molecular abnormality. Therefore further research is required for therapies directed at inhibiting expression or aiding the correction of the folded mutant receptors, which may be additional targets for therapy in TRAPS.

The novel copper-liganded bioactive complex conceptualised in this study shows a tremendous inflammation inhibitory outcome, however it remains unclear how the ligand exchange (change in oxidation state) of Cu^{2+} occurs during diffusion after its application. Its mechanism of action is still not entirely understood, and this warrants further research towards this system. Various studies have proved that metal complexes may have properties other than their anti-inflammatory effects, such as anti-malaria, antimicrobial and anticancer effects (Chohan et al., 2004; Chohan et al., 2005; Bruijninx and Sadler, 2008; Salas, Herrmann and Orvig, 2013), these advantageous properties associated with complexes may create unique research expansion in pharmaceutical science research with the use of the copper-liganded bioactive complex.

The sludge in this study could be upgraded to allow for a longer duration as it was observed that the maximum drug release was achieved at 24h. The increase in duration may be achieved by means of using a more sustainable system that would release the bioactive at a slower rate; such a system that may be considered may be an implant, which would also offer better patient compliance as well. With the use of nanocarriers responsive to inflammatory cues and their designing as an implant, it may result in an improved system with enhanced efficacy and increased device functional duration in comparison to the sludge.

REFERENCES

- Abe, A., Yamashita, S. and Noma, A., 1989. Sensitive, direct colorimetric assay for copper in serum. *Clinical chemistry*, 35(4), 552-554.
- Abraham, S.A., Edwards, K., Karlsson, G., MacIntosh, S., Mayer, L.D., McKenzie, C. and Bally, M.B., 2002. Formation of transition metal–doxorubicin complexes inside liposomes. *Biochimica et Biophysica Acta (BBA)-Biomembranes*, 1565(1), 41-54.
- AbuRuz, S., Millership, J., Heaney, L. and McElnay, J., 2003. Simple liquid chromatography method for the rapid simultaneous determination of prednisolone and cortisol in plasma and urine using hydrophilic lipophilic balanced solid phase extraction cartridges. *Journal of Chromatography B*, 798(2), 93-201.
- Ahmed, A. and Lal, R.A., 2012. Synthesis, characterization and electrochemical studies of copper (II) complexes derived from succinoyl-and adipoyldihydrazones. *Arabian Journal of Chemistry*. Available at: <http://www.sciencedirect.com/science/article/pii/S1878535212003176>[accessed 20 Oct. 2015].
- Ailiese, I., Cinteza, L.O., Orbesteanu, A.M., Cojocar, V. and Anuta, V., 2014. Development and optimization of alendronate loaded liposomes for oral administration by using response surface methodology. *Studia Universitatis "Vasile Goldis" Arad. Seria Stiintele Vietii (Life Sciences Series)*, 24, p.73.
- Akhter S, Jain G, Ahmad F, Khar R, Jain N, Khan Z and Talegaonkar S, 2008. Investigation of Nanoemulsion System for Transdermal Delivery of Domperidone: *Ex-vivo* and *in vivo* Studies. *Current Nanoscience*, 4, 381-390.
- Akiyoshi, K., Deguchi, S., Moriguchi, N., Yamaguchi, S. and Sunamoto, J., 1993. Self-aggregates of hydrophobized polysaccharides in water. Formation and characteristics of nanoparticles. *Macromolecules*, 26(12), 3062-3068.
- Akiyoshi, K., Kang, E.C., Kurumada, S., Sunamoto, J., Principi, T. and Winnik, F.M., 2000. Controlled association of amphiphilic polymers in water: thermosensitive nanoparticles formed by self-assembly of hydrophobically modified pullulans and poly (N-isopropylacrylamides). *Macromolecules*, 33(9), 3244-3249.

- Akiyoshi, K., Sasaki, Y. and Sunamoto, J. 1999. Molecular Chaperone-Like Activity of Hydrogel Nanoparticles of Hydrophobized Pullulan: Thermal Stabilization with Refolding of Carbonic Anhydrase B. *Bioconjugate Chemistry*, 10, 321-324.
- Alexander, A., Dwivedi, S., Giri, T.K., Saraf, S., Saraf, S. and Tripathi, D.K., 2012. Approaches for breaking the barriers of drug permeation through transdermal drug delivery. *Journal of Controlled Release*, 164(1), 26-40.
- Almeida, H., Amaral, M. H. & Lobão, P. 2012. Temperature and pH stimuli-responsive polymers and their applications in controlled and self regulated drug delivery. *J App Pharm Sci*, 2, 1-10.
- Alvarez-Lorenzo, C. and Concheiro, A. eds., 2013. Smart Materials for Drug Delivery. *Royal Society of Chemistry*, 1, 7743-7765.
- Alvarez-Lorenzo, C. and Concheiro, A., 2008. Intelligent drug delivery systems: polymeric micelles and hydrogels. *Mini reviews in medicinal chemistry*, 8(11), 1065-1074.
- Aparna, P., Divya, L., Bhadrappa, K. and Subrahmanyam, C.V., 2013. Formulation and *In vitro* Evaluation of Carvedilol Transdermal Delivery System. *Tropical Journal of Pharmaceutical Research*, 12(4), 461-467.
- Aróstegui, J.I., 2011. Hereditary systemic autoinflammatory diseases. *Reumatología Clínica (English Edition)*, 7(1), 45-50.
- Asadi, H., Rostamizadeh, K., Salari, D. & Hamidi, M. 2011. Preparation and characterization of tri-block poly(lactide)–poly(ethylene glycol)–poly(lactide) nanogels for controlled release of naltrexone. *International Journal of Pharmaceutics*, 416, 356-364.
- Asadi, H., Rostamizadeh, K., Salari, D. and Hamidi, M., 2011. Preparation and characterization of tri-block poly (lactide)–poly (ethylene glycol)–poly (lactide) nanogels for controlled release of naltrexone. *International journal of pharmaceutics*, 416(1),356-364.
- Ashwinkumar, N., Maya, S. and Jayakumar, R., 2014. Redox-responsive cystamine conjugated chitin–hyaluronic acid composite nanogels. *RSC Advances*, 4(91), 49547-49555.
- Awah, F.M., Uzoegwu, P.N., Ifeonu, P., Oyugi, J.O., Rutherford, J., Yao, X., Fehrmann, F., Fowke, K.R. and Eze, M.O., 2012. Free radical scavenging activity, phenolic contents and cytotoxicity of selected Nigerian medicinal plants. *Food Chemistry*, 131(4), 1279-1286.

- Aydin, R. and Pulat, M., 2012. 5-Fluorouracil encapsulated chitosan nanoparticles for pH-stimulated drug delivery: evaluation of controlled release kinetics. *Journal of Nanomaterials*, 2012, 42.
- Azzellini, M.A.A., Abbott, M.P., Machado, A., Miranda, M.T.M., Garcia, L.C., Caramori, G.F., Gonçalves, M.B., Petrilli, H.M. and Ferreira, A., 2010. Interactions of di-imine copper (II) complexes with albumin: competitive equilibria, promoted oxidative damage and DFT studies. *Journal of the Brazilian Chemical Society*, 21(7), 1303-1317.
- Bajaj, S., Whiteman, A. & Brandner, B. 2011. Transdermal drug delivery in pain management. *Contin Educ Anaesth Crit Care Pain*, 11, 39-43.
- Band, H. and Bronich, T., 2014. *Mechanism-based enhanced delivery of drug-loaded targeted nanoparticles for breast cancer therapy*. Nebraska univ medical center omaha.
- Baran, E.J., 2005. Structural data and vibrational spectra of the copper (II) complex of L-selenomethionine. *Zeitschrift für Naturforschung B*, 60(6), 663-666.
- Barrita, J.L.S. and Sánchez, M.D.S.S., 2013. Antioxidant role of ascorbic acid and his protective effects on chronic diseases. *Oxidative stress and chronic degenerative diseases—A role for antioxidants*, Morales-Gonzalez JA, Ed, *InTech*, 449-484.
- Barry, B. W. 1987. Mode of action of penetration enhancers in human skin. *Journal of Control Release*, 6, 85-97.
- Batheja, P., Sheihet, L., Kohn, J., Singer, A. J. and Michniak-Kohn, B. 2011. Topical drug delivery by a polymeric nanosphere gel: Formulation optimization and *in vitro* and *in vivo* skin distribution studies. *Journal of Controlled Release*, 149, 159-167.
- Beeton, C., Garcia, A. and Chandy, K.G., 2007. Drawing blood from rats through the saphenous vein and by cardiac puncture. *JoVE (Journal of Visualized Experiments)*, (7), e266-e266.
- Behl, G., Sharma, M., Sikka, M., Dahiya, S., Chhikara, A. and Chopra, M. 2012. Gallic acid loaded disulfide cross-linked biocompatible polymeric nanogels as controlled release system: synthesis, characterization, and antioxidant activity. *Journal of Biomaterials Science, Polymer Edition*, 24, 865-881.
- Beratu M., Mosekilde E., Westerhoff H.V., 2008. Biosimulation in Drug Development, [Online] Wiley-VCH Verlag GmbH & Co. KGaA, Page. Available

from:<http://onlinelibrary.wiley.com/book/10.1002/9783527622672>. [Accessed: 6th May 2015].

- Bharadwaj, S., Gupta, G.D. and Sharma, V.K., 2012. Journal of Chemical, Biological and Physical Sciences, 2, 856-867.
- Binions, R., 2012. Thermochromic Thin Films and Nanocomposites for Smart Glazing. *Intelligent Nanomaterials: Processes, Properties, and Applications*, 251-316.
- Biruss, B., Kählig, H. and Valenta, C., 2007. Evaluation of an eucalyptus oil containing topical drug delivery system for selected steroid hormones. *International journal of pharmaceutics*, 328(2), 142-151.
- Bissett, D. L., Kydonieus, A. F. and Berner, B. (eds.) 1987. Anatomy and biochemistry of the skin- Transdermal delivery of drugs: CRC Press Inc Boca Raton
- Bowey, K., Tanguay, J.F. and Tabrizian, M., 2014. 2-Dioleoyl-sn-glycero-3-phosphocholine-based nanoliposomes as an effective delivery platform for 17 β -estradiol. *European Journal of Pharmaceutics and Biopharmaceutics*, 86(3), 369-375.
- Brazzini, B. and Pimpinelli, N., 2002. New and established topical corticosteroids in dermatology. *American journal of clinical dermatology*, 3(1), 47-58.
- Bruijninx, P.C. and Sadler, P.J., 2008. New trends for metal complexes with anticancer activity. *Current opinion in chemical biology*, 12(2), 197-206.
- Brunel, F., Véron, L., Ladaviere, C., David, L., Domard, A. and Delair, T., 2009. Synthesis and structural characterization of chitosan nanogels. *Langmuir*, 25(16), 8935-8943.
- Bulua, A.C., Mogul, D.B., Aksentijevich, I., Singh, H., He, D.Y., Muenz, L.R., Ward, M.M., Yarboro, C.H., Kastner, D.L., Siegel, R.M. and Hull, K.M., 2012. Efficacy of etanercept in the tumor necrosis factor receptor-associated periodic syndrome: A prospective, open-label, dose-escalation study. *Arthritis & Rheumatism*, 64(3), 908-913.
- Castile, J.D. and Taylor, K.M., 1999. Factors affecting the size distribution of liposomes produced by freeze-thaw extrusion. *International journal of pharmaceutics*, 188(1), 87-95.

- Celia, C., Trapasso, E., Cosco, D., Paolino, D. and Fresta, M., 2009. Turbiscan Lab® Expert analysis of the stability of ethosomes® and ultradeformable liposomes containing a bilayer fluidizing agent. *Colloids and Surfaces B: Biointerfaces*, 72(1), 155-160.
- Cevc, G., 2004. Lipid vesicles and other colloids as drug carriers on the skin. *Advanced drug delivery reviews*, 56(5), pp.675-711.
- Chacko, R.T., Ventura, J., Zhuang, J. and Thayumanavan, S., 2012. Polymer nanogels: a versatile nanoscopic drug delivery platform. *Advanced drug delivery reviews*, 64(9), 836-851.
- Chaudhury, A., Das, S., Lee, R.F., Tan, K.B., Ng, W.K., Tan, R.B. and Chiu, G.N., 2012. Lyophilization of cholesterol-free PEGylated liposomes and its impact on drug loading by passive equilibration. *International journal of pharmaceuticals*, 430(1), 167-175.
- Chen, C., Han, D., Cai, C. and Tang, X., 2010. An overview of liposome lyophilization and its future potential. *Journal of Controlled Release*, 142(3), 299-311.
- Chen, Y., Quan, P., Liu, X., Wang, M. and Fang, L., 2014. Novel chemical permeation enhancers for transdermal drug delivery. *Asian Journal of Pharmaceutical Sciences*, 9(2), 51-64.
- Cheng, K. and Mahato, R.I. eds., 2013. *Advanced delivery and therapeutic applications of RNAi*. John Wiley & Sons.
- Cheng, R., Meng, F., Deng, C., Klok, H.A. and Zhong, Z., 2013. Dual and multi-stimuli responsive polymeric nanoparticles for programmed site-specific drug delivery. *Biomaterials*, 34(14), 3647-3657.
- Chiang, W.H., Ho, V.T., Huang, W.C., Huang, Y.F., Chern, C.S. and Chiu, H.C., 2012. Dual stimuli-responsive polymeric hollow nanogels designed as carriers for intracellular triggered drug release. *Langmuir*, 28(42), 15056-15064.
- Chohan, Z.H., Khan, K.M. and Supuran, C.T., 2005. In-vitro antibacterial, antifungal and cytotoxic properties of sulfonamide-derived Schiff's bases and their metal complexes. *Journal of enzyme inhibition and medicinal chemistry*, 20(2), 183-188.
- Choy, C.K.M., Benzie, I.F.F. and Cho, P., 2000. Ascorbic acid concentration and total antioxidant activity of human tear fluid measured using the FRASC assay. *Investigative ophthalmology & visual science*, 41(11), 3293-3298.

- Cini, R., Giorgi, G., Cinquantini, A., Rossi, C. and Sabat, M., 1990. Metal complexes of the antiinflammatory drug piroxicam. *Inorganic Chemistry*, 29(26), 5197-5200.
- Cui, W., Lu, X., Cui, K., Niu, L., Wei, Y. and Lu, Q., 2012. Dual-responsive controlled drug delivery based on ionically assembled nanoparticles. *Langmuir*, 28(25), 9413-9420.
- Dainichi, T., Hanakawa, S. and Kabashima, K., 2014. Classification of inflammatory skin diseases: A proposal based on the disorders of the three-layered defense systems, barrier, innate immunity and acquired immunity. *Journal of dermatological science*, 76(2), 81-89.
- Darole, P.S., Hegde, D.D. and Nair, H.A., 2008. Formulation and evaluation of microemulsion based delivery system for amphotericin B. *AAPS PharmSciTech*, 9(1), 122-128.
- Darwhekar, G., Jain, D.K. and Patidar, V.K., 2011. Formulation and evaluation of transdermal drug delivery system of clopidogrel bisulfate. *Asian Journal of Pharmacy and Life Science ISSN*, 2231, 4423.
- De Sanctis, S., Nozzi, M., Del Torto, M., Scardapane, A., Gaspari, S., de Michele, G., Breda, L. and Chiarelli, F., 2010. Autoinflammatory syndromes: diagnosis and management. *Italian journal of pediatrics*, 36(1), 57.
- Dhole, S.M., Amnerkar, N.D. and Khedekar, P.B., 2012. Comparison of UV spectrophotometry and high performance liquid chromatography methods for the determination of repaglinide in tablets. *Pharmaceutical Methods*, 3(2), 68-72.
- Dias, P.M., Kinouti, L., Constantino, V.R., Ferreira, A.M., Gonçalves, M.B., Nascimento, R.R.D., Petrilli, H.M., Caldas, M. and Frem, R.C., 2010. Spectroscopic characterization of schiff base-copper complexes immobilized in smectite clays. *Química Nova*, 33(10), 2135-2142.
- Dimiza, F., Fountoulaki, S., Papadopoulos, A.N., Kontogiorgis, C.A., Tangoulis, V., Raptopoulou, C.P., Psycharis, V., Terzis, A., Kessissoglou, D.P. and Psomas, G., 2011. Non-steroidal antiinflammatory drug-copper (II) complexes: Structure and biological perspectives. *Dalton Transactions*, 40(34), 8555-8568.
- Ding, B., Zhang, X., Hayat, K., Xia, S., Jia, C., Xie, M. and Liu, C., 2011. Preparation, characterization and the stability of ferrous glycinate nanoliposomes. *Journal of food engineering*, 102(2), 202-208.

- Diwan, P. V. Estimation of Prednisolone in Proliposomal formulation using RP HPLC method. Vol. 2(4) Oct - Dec 2011. Available at: www.ijrpbsonline.com [accessed 21 Aug. 2015].
- Donnelly, R.F., Singh, T.R.R., Garland, M.J., Migalska, K., Majithiya, R., McCrudden, C.M., Kole, P.L., Mahmood, T.M.T., McCarthy, H.O. and Woolfson, A.D., 2012. Hydrogel-Forming Microneedle Arrays for Enhanced Transdermal Drug Delivery. *Advanced functional materials*, 22(23), 4879-4890.
- Dorwal, D., 2012. Nanogels as novel and versatile pharmaceuticals. *Int J Pharm Pharm Sci*, 4(3), 67-74.
- Du Toit, L.C., Carmichael, T., Govender, T., Kumar, P., Choonara, Y.E. and Pillay, V., 2014. *In vitro*, *in vivo*, and *in silico* evaluation of the bioresponsive behavior of an intelligent intraocular implant. *Pharmaceutical research*, 31(3), 607-634.
- Edwards S.H., 2014. The Merck Veterinary Manual. Available from http://www.merckvetmanual.com/mvm/pharmacology/anti-inflammatory_agents/overview_of_anti-inflammatory_agents.html [accessed 9 Aug. 2015].
- Egbaria, K. and Weiner, N., 1990. Liposomes as a topical drug delivery system. *Advanced Drug Delivery Reviews*, 5(3), 287-300.
- El Maghraby, G.M., Barry, B.W. and Williams, A.C., 2008. Liposomes and skin: from drug delivery to model membranes. *European journal of pharmaceutical sciences*, 34(4), 203-222.
- El Maghraby, G.M., Williams, A.C. and Barry, B.W., 2006. Can drug-bearing liposomes penetrate intact skin?. *Journal of Pharmacy and Pharmacology*, 58(4), 415-429.
- El-Kattan, A.F., Asbill, C.S. and Michniak, B.B., 2000. The effect of terpene enhancer lipophilicity on the percutaneous permeation of hydrocortisone formulated in HPMC gel systems. *International journal of pharmaceuticals*, 198(2), 179-189.
- El-Nabarawi, M.A., Bendas, E.R., El Rehem, R.T.A. and Abary, M.Y., 2013. Transdermal drug delivery of paroxetine through lipid-vesicular formulation to augment its bioavailability. *International journal of pharmaceuticals*, 443(1), 307-317.
- Escobar-Chávez, J.J., 2012. Nanocarriers for transdermal drug delivery. *skin*, 19, 22.

- Esfahani, M.K.M., Alavi, S.E., Akbarzadeh, A., Ghassemi, S., Saffari, Z., Farahnak, M. and Chiani, M., 2014. Pegylation of Nanoliposomal Paclitaxel Enhances its Efficacy in Breast Cancer. *Tropical Journal of Pharmaceutical Research*, 13(8), 1195-1198.
- Fang, J., 2006. Nano-or submicron-sized liposomes as carriers for drug delivery. *Chang Gung medical journal*, 29(4), 358.
- Fang, J.Y., Sung, K.C., Lin, H.H. and Fang, C.L., 1999. Transdermal iontophoretic delivery of diclofenac sodium from various polymer formulations: *in vitro* and *in vivo* studies. *International journal of pharmaceutics*, 178(1), 83-92.
- Farag, R.K. and Mohamed, R.R., 2012. Synthesis and characterization of carboxymethyl chitosan nanogels for swelling studies and antimicrobial activity. *Molecules*, 18(1), 190-203.
- Feng, J., Du, X., Liu, H., Sui, X., Zhang, C., Tang, Y. and Zhang, J., 2014. Manganese-mefenamic acid complexes exhibit high lipoxigenase inhibitory activity. *Dalton Transactions*, 43(28), pp.10930-10939.
- Ferreira, S.A., Gama, F.M. and Vilanova, M., 2013. Polymeric nanogels as vaccine delivery systems. *Nanomedicine: Nanotechnology, Biology and Medicine*, 9(2), pp.159-173.
- Fonte, P., Soares, S., Sousa, F., Costa, A., Seabra, V., Reis, S. and Sarmiento, B., 2014. Stability Study Perspective of the Effect of Freeze-Drying Using Cryoprotectants on the Structure of Insulin Loaded into PLGA Nanoparticles. *Biomacromolecules*, 15(10), 3753-3765.
- Frahnert, C., Rao, M.L. and Grasmäder, K., 2003. Analysis of eighteen antidepressants, four atypical antipsychotics and active metabolites in serum by liquid chromatography: a simple tool for therapeutic drug monitoring. *Journal of Chromatography B*, 794(1), 35-47.
- Ganta, S., Devalapally, H., Shahiwala, A. and Amiji, M., 2008. A review of stimuli-responsive nanocarriers for drug and gene delivery. *Journal of Controlled Release*, 126(3), 187-204.
- Ghanbarzadeh, S. and Arami, S., 2013. Enhanced transdermal delivery of diclofenac sodium via conventional liposomes, ethosomes, and transfersomes. *BioMed research international*, 2013.

- Gokhale, N.H., Padhye, S.S., Padhye, S.B., Anson, C.E. and Powell, A.K., 2001. Copper complexes of carboxamidrazone derivatives as anticancer agents. 3. Synthesis, characterization and crystal structure of [Cu (apcc) Cl 2],(apcc= N 1-(2-acetylpyridine) pyridine-2-carboxamidrazone). *Inorganica Chimica Acta*, 319(1), 90-94.
- Gomes, M.J., Martins, S., Ferreira, D., Segundo, M.A. and Reis, S., 2014. Lipid nanoparticles for topical and transdermal application for alopecia treatment: development, physicochemical characterization, and *in vitro* release and penetration studies. *International journal of nanomedicine*, 9,1231.
- Gonçalves, C., Pereira, P. and Gama, M., 2010. Self-assembled hydrogel nanoparticles for drug delivery applications. *Materials*, 3(2), pp.1420-1460.
- Gonçalves, C., Pereira, P. and Gama, M., 2010. Self-assembled hydrogel nanoparticles for drug delivery applications. *Materials*, 3(2), 1420-1460.
- Görög, S., 2004. Recent advances in the analysis of steroid hormones and related drugs. *Analytical sciences*, 20(5), 767-782.
- Grateau, G., 2004. Clinical and genetic aspects of the hereditary periodic fever syndromes. *Rheumatology*, 43(4), 410-415.
- Gratieri, T., Gelfuso, G.M., Rocha, E.M., Sarmiento, V.H., de Freitas, O. and Lopez, R.F.V., 2010. A poloxamer/chitosan in situ forming gel with prolonged retention time for ocular delivery. *European Journal of Pharmaceutics and Biopharmaceutics*, 75(2), 186-193.
- Greaves, M.W., 1976. Anti-inflammatory action of corticosteroids. *Postgraduate medical journal*, 52(612), 631-633.
- Gup, R., Gökçe, C. and Aktürk, S., 2015. Copper (II) complexes with 4-hydroxyacetophenone-derived acylhydrazones: Synthesis, characterization, DNA binding and cleavage properties. *Spectrochimica Acta Part A: Molecular and Biomolecular Spectroscopy*, 134, 484-492.
- Guzman, M.L., Manzo, R.H. and Olivera, M.E., 2012. Eudragit E100 as a drug carrier: the remarkable affinity of phosphate ester for dimethylamine. *Molecular pharmaceutics*, 9(9), 2424-2433.
- Hans, M. L. & Lowman, A. M. 2002. Biodegradable nanoparticles for drug delivery and targeting. *Current Opinion in Solid State and Materials Science* 6, 319-327.

- Hathout, R.M., Mansour, S., Mortada, N.D. and Guinedi, A.S., 2007. Liposomes as an ocular delivery system for acetazolamide: *in vitro* and *in vivo* studies. *AAPS PharmSciTech*, 8(1), e1-e12.
- Honary, S. and Zahir, F., 2013. Effect of zeta potential on the properties of nano-drug delivery systems-a review (Part 2). *Tropical Journal of Pharmaceutical Research*, 12(2), 265-273.
- Honeywell-Nguyen, P.L. and Bouwstra, J.A., 2005. Vesicles as a tool for transdermal and dermal delivery. *Drug Discovery Today: Technologies*, 2(1), 67-74.
- Hong, J.S., Vreeland, W.N., DePaoli Lacerda, S.H., Locascio, L.E., Gaitan, M. and Raghavan, S.R., 2008. Liposome-templated supramolecular assembly of responsive alginate nanogels. *Langmuir*, 24(8), 4092-4096.
- Hong, Y.J. and Yang, K.S., 2013. Anti-inflammatory activities of crocetin derivatives from processed Gardenia jasminoides. *Archives of pharmacal research*, 36(8), 933-940.
- Hostýnek, J.J., Dreher, F. and Maibach, H.I., 2006. Human stratum corneum penetration by copper: *in vivo* study after occlusive and semi-occlusive application of the metal as powder. *Food and chemical toxicology*, 44(9), 1539-1543.
- Hostynek, J.J., Dreher, F. and Maibach, H.I., 2010. Human skin retention and penetration of a copper tripeptide *in vitro* as function of skin layer towards anti-inflammatory therapy. *Inflammation research*, 59(11), 983-988.
- Hostynek, J.J., Dreher, F. and Maibach, H.I., 2011. Human skin penetration of a copper tripeptide *in vitro* as a function of skin layer. *Inflammation research*, 60(1), 79-86.
- Hu, Y., Wu, Y.Y., Xia, X.J., Wu, Z., Liang, W.Q. and Gao, J.Q., 2011. Development of drug-in-adhesive transdermal patch for α -asarone and *in vivo* pharmacokinetics and efficacy evaluation. *Drug delivery*, 18(1), 84-89.
- Huppertz, T. & de Kruif, C. G. 2008. Structure and stability of nanogel particles prepared by internal cross-linking of casein micelles. *International Dairy Journal*, 18, 556-565.
- Hurler, J., Engesland, A., Poorahmary Kermany, B. and Škalko-Basnet, N., 2012. Improved texture analysis for hydrogel characterization: gel cohesiveness, adhesiveness, and hardness. *Journal of Applied Polymer Science*, 125(1), 180-188.

- Im, J.S., Bai, B.C. and Lee, Y.S., 2010. The effect of carbon nanotubes on drug delivery in an electro-sensitive transdermal drug delivery system. *Biomaterials*, 31(6), 1414-1419.
- Inal, O., Kiliçarslan, M., Ari, N. and Baykara, T., 2007. *In vitro* and *in vivo* transdermal studies of atenolol using iontophoresis. *Acta poloniae pharmaceutica*, 65(1), 29-36.
- Iordanskii, A.L., Feldstein, M.M., Markin, V.S., Hadgraft, J. and Plate, N.A., 2000. Modeling of the drug delivery from a hydrophilic transdermal therapeutic system across polymer membrane. *European Journal of Pharmaceutics and Biopharmaceutics*, 49(3), 287-293.
- Isaac, M. and Holvey, C., 2012. Transdermal patches: the emerging mode of drug delivery system in psychiatry. *Therapeutic advances in psychopharmacology*, 2(6), 255-263.
- Jesus, A.A., Oliveira, J.B., Aksentijevich, I., Fujihira, E., Carneiro-Sampaio, M.M., Duarte, A.J. and Silva, C.A., 2008. TNF receptor-associated periodic syndrome (TRAPS): description of a novel TNFRSF1A mutation and response to etanercept. *European journal of pediatrics*, 167(12), 1421-1425.
- Jin, Y., Pan, H., Li, Y. and Dai, Z., 2014. Chitosan modified cerasomes incorporating poly (vinyl pyrrolidone) for oral insulin delivery. *RSC Advances*, 4(102), 58137-58144
- Joseyphus, R.S. and Nair, M.S., 2010. Synthesis, characterization and biological studies of some Co (II), Ni (II) and Cu (II) complexes derived from indole-3-carboxaldehyde and glycyglycine as Schiff base ligand. *Arabian Journal of Chemistry*, 3(4), 195-204.
- Joshi, G.V., Kevadiya, B.D. and Bajaj, H.C., 2010. Controlled release formulation of ranitidine-containing montmorillonite and Eudragit® E-100. *Drug development and industrial pharmacy*, 36(9), 1046-1053.
- Jothy, S.L., Zuraini, Z. and Sasidharan, S., 2011. Phytochemicals screening, DPPH free radical scavenging and xanthine oxidase inhibitory activities of Cassia fistula seeds extract. *J Med Plants Res*, 5, 1941-1947.
- Kabanov, A.V. and Vinogradov, S.V., 2009. Nanogels as pharmaceutical carriers: finite networks of infinite capabilities. *Angewandte Chemie International Edition*, 48(30), 5418-5429.
- Kadajji, V.G. and Betageri, G.V., 2011. Water soluble polymers for pharmaceutical applications. *Polymers*, 3(4), 1972-2009.

- Kadam, R.S., Bourne, D.W. and Kompella, U.B., 2012. Nano-advantage in enhanced drug delivery with biodegradable nanoparticles: contribution of reduced clearance. *Drug Metabolism and Disposition*, 40(7), 1380-1388.
- Kählig, H., Valenta, C., Dampfhart, U. and Auner, B.G., 2005. Rheology and NMR self-diffusion experiments as well as skin permeation of diclofenac-sodium and cyproterone acetate of new gel preparations. *Journal of pharmaceutical sciences*, 94(2), 288-296.
- Kaiser, J.M., Imai, H., Haakenson, J.K., Brucklacher, R.M., Fox, T.E., Shanmugavelandy, S.S., Unrath, K.A., Pedersen, M.M., Dai, P., Freeman, W.M. and Bronson, S.K., 2013. Nanoliposomal minocycline for ocular drug delivery. *Nanomedicine: Nanotechnology, Biology and Medicine*, 9(1), 130-140.
- Kala N, Sundeep A, inventor; V.B. Medicare Pvt. Ltd. assignee. Carrier based nanogel formulation for skin targeting. Patent application No PCT/IN2012/000130. 2012 Dec.
- Kalimuthu, S. and Yadav, A.V., 2009. Formulation and evaluation of carvedilol loaded Eudragit E 100 nanoparticles. *International Journal of PharmTech Research*, 1, 179-183.
- Kanazawa, N. and Furukawa, F., 2007. Autoinflammatory syndromes with a dermatological perspective. *The Journal of dermatology*, 34(9), 601-618.
- Kanazawa, N. and Furukawa, F., 2007. Autoinflammatory syndromes with a dermatological perspective. *The Journal of dermatology*, 34(9), 601-618
- Kantaria, S., Rees, G.D. and Lawrence, M.J., 1999. Gelatin-stabilised microemulsion-based organogels: rheology and application in iontophoretic transdermal drug delivery. *Journal of controlled release*, 60(2), 355-365.
- Kararli, T.T., Kirchoff, C.F. and Penzotti, S.C., 1995. Enhancement of transdermal transport of azidothymidine (AZT) with novel terpene and terpene-like enhancers: *in vivo-in vitro* correlations. *Journal of controlled release*, 34(1), 43-51.
- Karavas, E., Georgarakis, E. and Bikiaris, D., 2006. Application of PVP/HPMC miscible blends with enhanced mucoadhesive properties for adjusting drug release in predictable pulsatile chronotherapeutics. *European Journal of Pharmaceutics and Biopharmaceutics*, 64(1), 115-126.

- Karunakaran, C., Vijayabalan, A., Manikandan, G., & Gomathisankar, P. (2011). Visible light photocatalytic disinfection of bacteria by Cd–TiO₂. *Catalysis Communications*, 12(9), 826-829.
- Kastner, D.L. and O'Shea, J.J., 2001. A fever gene comes in from the cold. *Nature genetics*, 29(3), 241-242.
- Kastner, D.L., Aksentijevich, I. and Goldbach-Mansky, R., 2010. Autoinflammatory disease reloaded: a clinical perspective. *Cell*, 140(6), 784-790.
- Kayser, O., Lemke, A. & Hernández-Trejo, N. 2005. The impact of nanobiotechnology on the development of new drug delivery systems. *Current Pharmaceutical Biotechnology*, 6, 3-5.
- Kayser, O., Lemke, A. and Hernandez-Trejo, N., 2005. The impact of nanobiotechnology on the development of new drug delivery systems. *Current pharmaceutical biotechnology*, 6(1), 3-5.
- KC, R.B., Thapa, B. and Xu, P., 2012. pH and redox dual responsive nanoparticle for nuclear targeted drug delivery. *Molecular pharmaceutics*, 9(9), 2719-2729.
- Kermany, B. P. 2010. Carbopol hydrogels for topical administration: treatment of wounds. Degree master of pharmacy, University of Tromsø.
- Kettel, M.J., Schaefer, K., Groll, J. and Moeller, M., 2014. Nanogels with high active β -cyclodextrin content as physical coating system with sustained release properties. *ACS applied materials & interfaces*, 6(4), 2300-2311.
- Khmelnitsky, Y. L., Neverova, I. N., Gedrovich, A. V., Polyakov, V. A., Levashov, A. V. and Martinek, K. 1992. Catalysis by α -chymotrypsin entrapped into surface-modified polymeric nanogranules in organic solvent. *European Journal of Biochemistry*, 210(3), 751-757.
- Khosravi-Darani, K. and Mozafari, M.R., 2010. Nanoliposome potentials in nanotherapy: A concise overview. *International Journal of Nanoscience and Nanotechnology*, 6(1), 3-13.
- Khurana, S., Bedi, P.M.S. and Jain, N.K., 2013a. Preparation and evaluation of solid lipid nanoparticles based nanogel for dermal delivery of meloxicam. *Chemistry and physics of lipids*, 175, 65-72.

- Khurana, S., Jain, N.K. and Bedi, P.M.S., 2013b. Nanoemulsion based gel for transdermal delivery of meloxicam: physico-chemical, mechanistic investigation. *Life sciences*, 92(6), 383-392.
- Kim, J.O., Oberoi, H.S., Desale, S., Kabanov, A.V. and Bronich, T.K., 2013. Polypeptide nanogels with hydrophobic moieties in the cross-linked ionic cores: synthesis, characterization and implications for anticancer drug delivery. *Journal of drug targeting*, 21(10), 981-993.
- Kiran, K.R., 2014. Synthesis, characterization and antibacterial activity of Cu(II), Zn(II) ternary complexes with maltol and glycylglycine. *Chemical Science Transactions*, 3, 592-601
- Klimová, Z., Hojerová, J., Lucová, M. and Pažoureková, S., 2012. Dermal exposure to chemicals-evaluation of skin barrier damage. *Acta Chimica Slovaca*, 5(1), 70-74.
- Klinger, D. and Landfester, K., 2012. Enzymatic-and light-degradable hybrid nanogels: Crosslinking of polyacrylamide with acrylate-functionalized Dextrans containing photocleavable linkers. *Journal of Polymer Science Part A: Polymer Chemistry*, 50(6), 1062-1075.
- Kowcun, K., Frańska, M. and Frański, R., 2012. Binuclear copper complexes with non-steroidal anti-inflammatory drugs as studied by electrospray ionization mass spectrometry. *Open Chemistry*, 10(2), 320-326.
- Kumar, R. and Katare, O.P., 2005. Lecithin organogels as a potential phospholipid-structured system for topical drug delivery: a review. *AAPS pharmscitech*, 6(2), e298-e310.
- Kuroda, K., Fujimoto, K., Sunamoto, J. and Akiyoshi, K., 2002. Hierarchical self-assembly of hydrophobically modified pullulan in water: gelation by networks of nanoparticles. *Langmuir*, 18(10), 3780-3786.
- Lee, R.W., Shenoy, D.B. and Sheel, R., 2010. Micellar nanoparticles: applications for topical and passive transdermal drug delivery. *Handbook of Non-Invasive Drug Delivery Systems*. Burlington, MA: Elsevier Inc, 37-58.
- Lei, W., Yu, C., Lin, H. and Zhou, X., 2013. Development of tacrolimus-loaded transfersomes for deeper skin penetration enhancement and therapeutic effect improvement *in vivo*. *asian journal of pharmaceutical sciences*, 8(6), 336-345.
- Lewis A. J., 1984. The role of copper in inflammatory disorders. *Agents Actions* 15:513–519 15

- Liang, Y. and Kiick, K.L., 2014. Multifunctional lipid-coated polymer nanogels crosslinked by photo-triggered Michael-type addition. *Polymer Chemistry*, 5(5), 1728-1736.
- Liska, S.K., Kerkay, J. and Pearson, K.H., 1985. Determination of zinc and copper in urine using Zeeman effect flame atomic absorption spectroscopy. *Clinica chimica acta*, 151(3), 231-236.
- Liu, G. and An, Z., 2014. Frontiers in the design and synthesis of advanced nanogels for nanomedicine. *Polymer Chemistry*, 5(5), 1559-1565.
- Liu, Y., Fang, L., Zheng, H., Zhao, L., Ge, X. and He, Z., 2007. Development and *in vitro* evaluation of a topical use patch containing diclofenac diethanolamine salt. *Asian Journal of Pharmaceutical Sciences*, 2(3), 106-113.
- Lobito, A.A., Kimberley, F.C., Muppidi, J.R., Komarow, H., Jackson, A.J., Hull, K.M., Kastner, D.L., Screatton, G.R. and Siegel, R.M., 2006. Abnormal disulfide-linked oligomerization results in ER retention and altered signaling by TNFR1 mutants in TNFR1-associated periodic fever syndrome (TRAPS). *Blood*, 108(4), 1320-1327.
- López-Mirabal, H.R. and Winther, J.R., 2008. Redox characteristics of the eukaryotic cytosol. *Biochimica et Biophysica Acta (BBA)-Molecular Cell Research*, 1783(4), 629-640.
- Lu, N., Yang, K., Li, J., Weng, Y., Yuan, B. and Ma, Y., 2013. Controlled drug loading and release of a stimuli-responsive lipogel consisting of poly (N-isopropylacrylamide) particles and lipids. *The Journal of Physical Chemistry B*, 117(33), 9677-9682.
- Lu, Q., Lu, P.M., Piao, J.H., Xu, X.L., Chen, J., Zhu, L. and Jiang, J.G., 2014. Preparation and physicochemical characteristics of an allicin nanoliposome and its release behavior. *LWT-Food Science and Technology*, 57(2), 686-695.
- Lu, Y., Mo, R., Tai, W., Sun, W., Pacardo, D.B., Qian, C., Shen, Q., Ligler, F.S. and Gu, Z., 2014. Self-folded redox/acid dual-responsive nanocarriers for anticancer drug delivery. *Chemical Communications*. 50, 15105-15108
- Lull, M.E., Carkaci-Salli, N., Freeman, W.M., Myers, J.L., Midgley, F.M., Thomas, N.J., Kimatian, S.J., Vrana, K.E. and Ündar, A., 2008. Plasma biomarkers in pediatric patients undergoing cardiopulmonary bypass. *Pediatric research*, 63(6), 638-644.
- Luo L., Miao L., Tanemura S., Tanemura M., 2008. Photocatalytic sterilization of TiO₂ films coated on Al fibre. *Materials Science and Engineering: B*, 148 (1–3), 183–186.

- Lv, S., Tang, Z., Zhang, D., Song, W., Li, M., Lin, J., Liu, H. and Chen, X., 2014. Well-defined polymer-drug conjugate engineered with redox and pH-sensitive release mechanism for efficient delivery of paclitaxel. *Journal of Controlled Release*, 194, 220-227.
- Mady, M.M. and Darwish, M.M., 2010. Effect of chitosan coating on the characteristics of DPPC liposomes. *Journal of Advanced Research*, 1(3), 187-191.
- Maggi, F., Ciccarelli, S., Diociaiuti, M., Casciardi, S. and Masci, G., 2011. Chitosan nanogels by template chemical cross-linking in polyion complex micelle nanoreactors. *Biomacromolecules*, 12(10), 3499-3507.
- Mahmoud, E.A., Sankaranarayanan, J., Morachis, J.M., Kim, G. and Almutairi, A., 2011. Inflammation responsive logic gate nanoparticles for the delivery of proteins. *Bioconjugate chemistry*, 22(7), 1416-1421.
- Maiga, A., Malterud, K.E., Diallo, D. and Paulsen, B.S., 2006. Antioxidant and 15-lipoxygenase inhibitory activities of the Malian medicinal plants *Diospyros abyssinica* (Hiern) F. White (Ebenaceae), *Lannea velutina* A. Rich (Anacardiaceae) and *Crossopteryx febrifuga* (Afzel) Benth.(Rubiaceae). *Journal of ethnopharmacology*, 104(1), 132-137.
- Malik, K., Arora, G. and Singh, I., 2011. Taste masked microspheres of ofloxacin: formulation and evaluation of orodispersible tablets. *Scientia pharmaceutica*, 79(3), 653-672.
- Maloň, M., Trávníček, Z., Maryško, M., Zbořil, R., Mašláň, M., Marek, J., Doležal, K., Rolčík, J., Kryštof, V. and Strnad, M., 2001. Metal complexes as anticancer agents 2. Iron (III) and copper (II) bio-active complexes with N 6-benzylaminopurine derivatives. *Inorganica Chimica Acta*, 323(1), 119-129.
- Mandal, S., Lyngdoh, R.H.D., Askari, H. and Das, G., 2015. Metalation of Glycylglycine: An Experimental Study Performed in Tandem with Theoretical Calculations. *Journal of Chemical & Engineering Data*, 60(3),659-673.
- Mangalathillam, S., Rejinold, N.S., Nair, A., Lakshmanan, V.K., Nair, S.V. and Jayakumar, R., 2012. Curcumin loaded chitin nanogels for skin cancer treatment via the transdermal route. *Nanoscale*, 4(1), 239-250.
- Maravalli, P.B. and Goudar, T.R., 1999. Thermal and spectral studies of 3-N-methyl-morpholino-4-amino-5-mercapto-1, 2, 4-triazole and 3-N-methyl-piperidino-4-amino-5-mercapto-1,

2, 4-triazole complexes of cobalt (II), nickel (II) and copper (II). *Thermochimica acta*, 325(1), 35-41.

Martins, D.D.J., Ur-Rehman, H., Rico, S.R.A., Costa, I.D.M., Santos, A.C.P., Szesudlowski, R.G. and de Oliveira Silva, D., 2015. Interaction of chitosan beads with a copper–naproxen metallodrug. *RSC Advances*, 5(109), 90184-90192.

Masson, C., Simon, V., Hoppé, E., Insalaco, P., Cissé, I. and Audran, M., 2004. Tumor necrosis factor receptor-associated periodic syndrome (TRAPS): definition, semiology, prognosis, pathogenesis, treatment, and place relative to other periodic joint diseases. *Joint Bone Spine*, 71(4), 284-290.

McAllister, K., Sazani, P., Adam, M., Cho, M.J., Rubinstein, M., Samulski, R.J. and DeSimone, J.M., 2002. Polymeric nanogels produced via inverse microemulsion polymerization as potential gene and antisense delivery agents. *Journal of the American Chemical Society*, 124(51), 15198-15207.

McDermott, M.F., Aksentijevich, I., Galon, J., McDermott, E.M., Ogunkolade, B.W., Centola, M., Mansfield, E., Gadina, M., Karenko, L., Pettersson, T. and McCarthy, J., 1999. Germline mutations in the extracellular domains of the 55 kDa TNF receptor, TNFR1, define a family of dominantly inherited autoinflammatory syndromes. *Cell*, 97(1), 133-144.

Medeiros, S.F., Santos, A.M., Fessi, H. and Elaissari, A., 2010. Synthesis of biocompatible and thermally sensitive poly (N-vinylcaprolactam) nanogels via inverse miniemulsion polymerization: Effect of the surfactant concentration. *Journal of Polymer Science Part A: Polymer Chemistry*, 48(18), 3932-3941.

Meiorin, S.M., Espada, G. and Rosè, C., 2013. Enfermedades autoinflamatorias en pediatría. *Archivos argentinos de pediatría*, 111(3), 237-243.

Meléndez-Ortiz, H.I., Peralta, R.D., Bucio, E. and Zerrweck-Maldonado, L., 2014. Preparation of stimuli-responsive nanogels of poly [2-(dimethylamino) ethyl methacrylate] by heterophase and microemulsion polymerization using gamma radiation. *Polymer Engineering & Science*, 54(7), 1625-1631.

Messenger, L., Portecop, N., Hachet, E., Lapeyre, V., Pignot-Paintrand, I., Catargi, B., Auzély-Velty, R. and Ravaine, V., 2013. Photochemical crosslinking of hyaluronic acid

confined in nanoemulsions: towards nanogels with a controlled structure. *Journal of Materials Chemistry B*, 1(27), 3369-3379.

Mitra, S., Gaur, U., Ghosh, P.C. and Maitra, A.N., 2001. Tumour targeted delivery of encapsulated dextran–doxorubicin conjugate using chitosan nanoparticles as carrier. *Journal of Controlled Release*, 74(1), 317-323.

Mohammed, N., Rejinold, N.S., Mangalathillam, S., Biswas, R., Nair, S.V. and Jayakumar, R., 2013. Fluconazole loaded chitin nanogels as a topical ocular drug delivery agent for corneal fungal infections. *Journal of biomedical nanotechnology*, 9(9), 521-1531.

Mohan, A., Narayanan, S., Sethuraman, S. and Krishnan, U.M., 2014. Novel resveratrol and 5-fluorouracil coencapsulated in PEGylated nanoliposomes improve chemotherapeutic efficacy of combination against head and neck squamous cell carcinoma. *BioMed research international*, 2014.

Mohanty, S., Mishra, S., Jena, P., Jacob, B., Sarkar, B. and Sonawane, A., 2012. An investigation on the antibacterial, cytotoxic, and antibiofilm efficacy of starch-stabilized silver nanoparticles. *Nanomedicine: Nanotechnology, Biology and Medicine*, 8(6), 916-924.

Moretton, M.A., Chiappetta, D.A. and Sosnik, A., 2011. Cryoprotection–lyophilization and physical stabilization of rifampicin-loaded flower-like polymeric micelles. *Journal of The Royal Society Interface*, p.rsif20110414.

Morrison, P. J., Bradbrook, I. D., & Rogers, H. J. (1977). Plasma prednisolone levels from enteric and non-enteric coated tablets estimated by an original technique. *British journal of clinical pharmacology*, 4(5), 597-603.

Mourtas, S., Haikou, M., Theodoropoulou, M., Tsakiroglou, C. and Antimisiaris, S.G., 2008. The effect of added liposomes on the rheological properties of a hydrogel: A systematic study. *Journal of colloid and interface science*, 317(2), 611-619.

Moyo, B., Oyedemi, S., Masika, P.J. and Muchenje, V., 2012. Polyphenolic content and antioxidant properties of Moringa oleifera leaf extracts and enzymatic activity of liver from goats supplemented with Moringa oleifera leaves/sunflower seed cake. *Meat science*, 91(4), 441-447.

- Mufamadi, M.S., Choonara, Y.E., Kumar, P., Modi, G., Naidoo, D., Ndesendo, V.M., du Toit, L.C., Iyuke, S.E. and Pillay, V., 2012. Surface-engineered nanoliposomes by chelating ligands for modulating the neurotoxicity associated with β -Amyloid aggregates of Alzheimer's disease. *Pharmaceutical research*, 29(11), 3075-3089.
- Mufamadi, M.S., Choonara, Y.E., Kumar, P., Modi, G., Naidoo, D., van Vuuren, S., Ndesendo, V.M., du Toit, L.C., Iyuke, S.E. and Pillay, V., 2013. Ligand-functionalized nanoliposomes for targeted delivery of galantamine. *International journal of pharmaceuticals*, 448(1), 267-281.
- Muhammad, N. and Guo, Z., 2014. Metal-based anticancer chemotherapeutic agents. *Current opinion in chemical biology*, 19, 144-153.
- Mura, S., Nicolas, J. and Couvreur, P., 2013. Stimuli-responsive nanocarriers for drug delivery. *Nature materials*, 12(11), 991-1003.
- Murphy, E.A., Majeti, B.K., Mukthavaram, R., Acevedo, L.M., Barnes, L.A. and Cheresch, D.A., 2011. Targeted nanogels: a versatile platform for drug delivery to tumors. *Molecular cancer therapeutics*, 10(6), 972-982.
- Murray, M.J. and Snowden, M.J., 1995. The preparation, characterisation and applications of colloidal microgels. *Advances in colloid and interface science*, 54, 73-91.
- Nadanasabapathi, S., Rufia, J. and Manju, V., 2013. In vitro free radical scavenging activity and bioavailability of dietary compounds caffeine, caffeic acid and their combination. *International Food Research Journal*, 20(6), 3159-3165.
- Nagarwal, R. C., Kant, S., Singh, P. N., Maiti, P. & Pandit, J. K. 2009. Polymeric nanoparticulate system: A potential approach for ocular drug delivery. *Journal of Controlled Release*, 136, 2-13.
- Nair, J., Sone, H., Nagao, M., Barbin, A. and Bartsch, H., 1996. Copper-dependent formation of miscoding etheno-DNA adducts in the liver of Long Evans cinnamon (LEC) rats developing hereditary hepatitis and hepatocellular carcinoma. *Cancer research*, 56(6), 1267-1271.
- Nair, M.S., 1982. Effect of copper (II) ternary complex formation on the co-ordination behaviour of dipeptides in aqueous solution. *Journal of the Chemical Society, Dalton Transactions*, (3), 561-566.

- Ng, C.H., Kong, S.M., Tiong, Y.L., Maah, M.J., Sukram, N., Ahmad, M. and Khoo, A.S.B., 2014. Selective anticancer copper (II)-mixed ligand complexes: targeting of ROS and proteasomes. *Metallomics*, 6(4), 892-906.
- Nguyen, D.H., Joung, Y.K., Choi, J.H., Moon, H.T. and Park, K.D., 2011. Targeting ligand-functionalized and redox-sensitive heparin-Pluronic nanogels for intracellular protein delivery. *Biomedical Materials*, 6(5), 055004.
- Nicoletti, C.R., Marini, V.G., Zimmermann, L.M. and Machado, V.G., 2012. Anionic chromogenic chemosensors highly selective for fluoride or cyanide based on 4-(4-Nitrobenzylideneamine) phenol. *Journal of the Brazilian Chemical Society*, 23(8), 1488-1500.
- Nishikawa, T., Akiyoshi, K. and Sunamoto, J., 1996. Macromolecular complexation between bovine serum albumin and the self-assembled hydrogel nanoparticle of hydrophobized polysaccharides. *Journal of the American Chemical Society*, 118(26), 6110-6115.
- Nochi, T., Yuki, Y., Takahashi, H., Sawada, S.I., Mejima, M., Kohda, T., Harada, N., Kong, I.G., Sato, A., Kataoka, N. and Tokuhara, D., 2010. Nanogel antigenic protein-delivery system for adjuvant-free intranasal vaccines. *Nature materials*, 9(7), 572-578.
- Nukolova, N.V., Oberoi, H.S., Cohen, S.M., Kabanov, A.V. and Bronich, T.K., 2011. Folate-decorated nanogels for targeted therapy of ovarian cancer. *Biomaterials*, 32(23), 5417-5426.
- O'Donnell, J., 1989. Adverse effects of corticosteroids. *Journal of Pharmacy Practice*, 256-266.
- Oh, J.K., Siegwart, D.J., Lee, H.I., Sherwood, G., Peteanu, L., Hollinger, J.O., Kataoka, K. and Matyjaszewski, K., 2007. Biodegradable nanogels prepared by atom transfer radical polymerization as potential drug delivery carriers: synthesis, biodegradation, *in vitro* release, and bioconjugation. *Journal of the American Chemical Society*, 129(18), 5939-5945.
- Oh, N.M., Oh, K.T., Baik, H.J., Lee, B.R., Lee, A.H., Youn, Y.S. and Lee, E.S., 2010. A self-organized 3-diethylaminopropyl-bearing glycol chitosan nanogel for tumor acidic pH targeting: *in vitro* evaluation. *Colloids and surfaces B: Biointerfaces*, 78(1), 120-126.

- Oishi, M., Miyagawa, N., Sakura, T. and Nagasaki, Y., 2007. pH-responsive PEGylated nanogel containing platinum nanoparticles: Application to on–off regulation of catalytic activity for reactive oxygen species. *Reactive and Functional Polymers*, 67(7), 662-668.
- Onoue, S., Yamada, S. and Chan, H.K., 2014. Nanodrugs: pharmacokinetics and safety. *International journal of nanomedicine*, 9, 1025-1037
- Ozen, S. and Bilginer, Y., 2014. A clinical guide to autoinflammatory diseases: familial Mediterranean fever and next-of-kin. *Nature Reviews Rheumatology*, 10(3), 135-147.
- Ozpolat, B., Sood, A.K. and Lopez-Berestein, G., 2014. Liposomal siRNA nanocarriers for cancer therapy. *Advanced drug delivery reviews*, 66, 110-116.
- Palanisamy, M. and Khanam, J., 2011. Cellulose-based matrix microspheres of prednisolone inclusion complex: preparation and characterization. *Aaps Pharmscitech*, 12(1), 388-400.
- Pan, G., Guo, Q., Cao, C., Yang, H. & Li, B. 2013. Thermo-responsive molecularly imprinted nanogels for specific recognition and controlled release of proteins. *Soft Matter*, 9, 3840-3850.
- Pan, Y.J., Chen, Y.Y., Wang, D.R., Wei, C., Guo, J., Lu, D.R., Chu, C.C. and Wang, C.C., 2012. Redox/pH dual stimuli-responsive biodegradable nanohydrogels with varying responses to dithiothreitol and glutathione for controlled drug release. *Biomaterials*, 33(27), 6570-6579.
- Pang, Q.F., Zhou, Q.M., Zeng, S., Dou, L.D., Ji, Y. and Zeng, Y.M., 2008. Protective effect of heme oxygenase-1 on lung injury induced by erythrocyte instillation in rats. *Chinese medical journal*, 121(17), 1688-1692.
- Parasuraman, S., Raveendran, R. and Kesavan, R., 2010. Blood sample collection in small laboratory animals. *Journal of pharmacology & pharmacotherapeutics*, 1(2), 87-93.
- Parida, L., Neogi, S. and Padmanabhan, V., 2014. Effect of Temperature Pre-Exposure on the Locomotion and Chemotaxis of *C. elegans*. *PLoS one*, 9(10), e111342.
- Pasparakis, G. and Vamvakaki, M., 2011. Multiresponsive polymers: nano-sized assemblies, stimuli-sensitive gels and smart surfaces. *Polymer Chemistry*, 2(6), 1234-1248.

- Patel, H.K., Shah, C.V., Shah, V.H. and Upadhyay, U.M., 2012. Design, development and *in vitro* evaluation of controlled release gel for topical delivery of quetiapine using box-behnen design. *International Journal of Pharmaceutical Sciences and Research*, 3(9), 3384.
- Patel, S., Gheewala, N., Suthar, A. and Shah, A., 2009. In-vitro cytotoxicity activity of Solanum nigrum extract against Hela cell line and Vero cell line. *Int J Pharm Pharm Sci*, 1(1), 38-46.
- Pattan, S.R., Pawar, S.B., Vetat, S.S., Gharate, U.D., Bhawar S.B., 2012. The scope of metal complexes in drug design. *Indian drugs*, 49, 5-12.
- Pedrosa, S.S., Gonçalves, C., David, L. and Gama, M., 2014. A novel crosslinked hyaluronic acid nanogel for drug delivery. *Macromolecular bioscience*, 14(11), 1556-1568.
- Pedrosa, S.S., Gonçalves, C., David, L. and Gama, M., 2014. A novel crosslinked hyaluronic acid nanogel for drug delivery. *Macromolecular bioscience*, 14(11), 1556-1568.
- Phatak Atul, A. and Chaudhari Praveen, D., 2012. Development and evaluation of nanogel as a carrier for transdermal delivery of aceclofenac. *Asian J. Pharm. Tech*, 2(4), 125-132.
- Phatak Atul, A. and Chaudhari Praveen, D., 2012. Development and evaluation of nanogel as a carrier for transdermal delivery of aceclofenac. *Asian J. Pharm. Tech*, 2(4), 125-132.
- Pierre, M.B.R. and Costa, I.D.S.M., 2011. Liposomal systems as drug delivery vehicles for dermal and transdermal applications. *Archives of dermatological research*, 303(9), 607-621.
- Pillai, O and Panchagnula, R. (2003). Transdermal delivery of insulin from poloxamer gel: *ex vivo* and *in vivo* skin permeation studies in rat using iontophoresis and chemical enhancers. *Journal of controlled release*, 89(1), 127-140.
- Piret, J.P., Vankoningsloo, S., Mejia, J., Noël, F., Boilan, E., Lambinon, F., Zouboulis, C.C., Masereel, B., Lucas, S., Saout, C. and Toussaint, O., 2012. Differential toxicity of copper (II) oxide nanoparticles of similar hydrodynamic diameter on human differentiated intestinal Caco-2 cell monolayers is correlated in part to copper release and shape. *Nanotoxicology*, 6(7), 789-803.
- Płotek, M., Dudek, K. and Kyzioł, A., 2013. Wybrane związki kompleksowe miedzi (I) jako potencjalne czynniki przeciwnowotworowe. *Chemik*, 67(12).

- Poorahmary Kermany, B., 2010. Carbopol hydrogels for topical administration: treatment of wounds.
- Prabaharan, M. and Gong, S., 2008. Novel thiolated carboxymethyl chitosan-g- β -cyclodextrin as mucoadhesive hydrophobic drug delivery carriers. *Carbohydrate Polymers*, 73(1), 117-125.
- Prasad, S.R. and Kishore, V.S., 2012. Enhancement of skin permeation of diltiazem hydrochloride gels through mouse skin by using olive oil as permeation enhancers. *International journal of pharmaceutical, chemical and biological sciences*. 2012, 2(3), 348-353.
- Prausnitz, M. R and Langer, R. 2008. Transdermal drug delivery. *Nat Biotech*, 26, 1261-1268.
- Prow, T.W., Chen, X., Prow, N.A., Fernando, G.J., Tan, C.S., Raphael, A.P., Chang, D., Ruutu, M.P., Jenkins, D.W., Pyke, A. and Crichton, M.L., 2010. Nanopatch-Targeted Skin Vaccination against West Nile Virus and Chikungunya Virus in Mice. *Small*, 6(16), 1776-1784.
- Psomas, G. and Kessissoglou, D.P., 2013. Quinolones and non-steroidal anti-inflammatory drugs interacting with copper (II), nickel (II), cobalt (II) and zinc (II): Structural features, biological evaluation and perspectives. *Dalton Transactions*, 42(18), 6252-6276.
- Pujana, M. A., Pérez-Álvarez, L., Iturbe, L. C. C. & Katime, I. 2014. Water soluble folate-chitosan nanogels crosslinked by genipin. *Carbohydrate Polymers*, 101, 113-120.
- Pujana, M. A., Pérez-Álvarez, L., Iturbe, L. C. C. & Katime, I. 2014. Water soluble folate-chitosan nanogels crosslinked by genipin. *Carbohydrate Polymers*, 101, 113-120.
- Pujana, M.A., Pérez-Álvarez, L., Iturbe, L.C.C. and Katime, I., 2014. Water soluble folate-chitosan nanogels crosslinked by genipin. *Carbohydrate polymers*, 101, 113-120.
- Qiu, L.Y. and Bae, Y.H., 2006. Polymer architecture and drug delivery. *Pharmaceutical research*, 23(1), 1-30
- Rabe, K.F., Bateman, E.D., O'Donnell, D., Witte, S., Bredenbröcker, D. and Bethke, T.D., 2005. Roflumilast—an oral anti-inflammatory treatment for chronic obstructive pulmonary disease: a randomised controlled trial. *The Lancet*, 366(9485), 563-571.

- Raemdonck, K., Demeester, J. and De Smedt, S. 2009. Advanced nanogel engineering for drug delivery. *Soft Matter*, 5, 707-715.
- Ramadan, S., Hambley, T.W., Kennedy, B.J. and Lay, P.A., 2004. NMR spectroscopic characterization of copper (II) and zinc (II) complexes of indomethacin. *Inorganic chemistry*, 43(9), 2943-2946.
- Rancan, F., Blume-Peytavi, U. and Vogt, A., 2014. Utilization of biodegradable polymeric materials as delivery agents in dermatology. *Clinical, cosmetic and investigational dermatology*, 7, 23.
- Richtering, W. and Pich, A., 2012. The special behaviours of responsive core-shell nanogels. *Soft Matter*, 8(45), pp.11423-11430.
- Riella, K.R., Marinho, R.R., Santos, J.S., Pereira-Filho, R.N., Cardoso, J.C., Albuquerque-Junior, R.L.C. and Thomazzi, S.M., 2012. Anti-inflammatory and cicatrizing activities of thymol, a monoterpene of the essential oil from *Lippia gracilis*, in rodents. *Journal of ethnopharmacology*, 143(2), 656-663.
- Rigogliuso, S., Sabatino, M.A., Adamo, G., Grimaldi, N., Dispenza, C. and Ghersi, G., 2012. Polymeric nanogels: Nanocarriers for drug delivery application. *Chemical engineering*, 27, 247-252.
- Robb, S.A., Lee, B.H., McLemore, R., Vernon, B.L., 2007. Simultaneously physically and chemically gelling polymer system utilizing a poly(NIPAAm-co-cysteamine)-based copolymer. *Biomacromolecules* 8, 2294-2300.
- Roy, P. and Srivastava, S.K., 2006. Hydrothermal growth of CuS nanowires from Cu-dithiooxamide, a novel single-source precursor. *Crystal growth & design*, 6(8), 1921-1926.
- Roy, S., Banerjee, R. and Sarkar, M., 2006. Direct binding of Cu (II)-complexes of oxicam NSAIDs with DNA backbone. *Journal of inorganic biochemistry*, 100(8), 1320-1331.
- Ruozi, B., Belletti, D., Tombesi, A., Tosi, G., Bondioli, L., Forni, F. and Vandelli, M.A., 2011. AFM, ESEM, TEM, and CLSM in liposomal characterization: a comparative study. *International journal of nanomedicine*, 6, 557.

- Ryu, J.H., Chacko, R.T., Jiwanich, S., Bickerton, S., Babu, R.P. and Thayumanavan, S., 2010. Self-cross-linked polymer nanogels: a versatile nanoscopic drug delivery platform. *Journal of the American Chemical Society*, 132(48), 17227-17235.
- Sabitha, M., Rejinold, N.S., Nair, A., Lakshmanan, V.K., Nair, S.V. and Jayakumar, R., 2013. Development and evaluation of 5-fluorouracil loaded chitin nanogels for treatment of skin cancer. *Carbohydrate polymers*, 91(1), 48-57.
- Sahoo, S.K., Dilnawaz, F. and Krishnakumar, S., 2008. Nanotechnology in ocular drug delivery. *Drug discovery today*, 13(3), 144-151.
- Salas, P.F., Herrmann, C. and Orvig, C., 2013. Metalloantimalarials. *Chemical reviews*, 113(5), 3450-3492.
- Samah, N.H.A. and Heard, C.M., 2013. Enhanced *in vitro* transdermal delivery of caffeine using a temperature-and pH-sensitive nanogel, poly (NIPAM-co-AAc). *International journal of pharmaceutics*, 453(2), 630-640.
- Sanson, N. and Rieger, J., 2010. Synthesis of nanogels/microgels by conventional and controlled radical crosslinking copolymerization. *Polymer Chemistry*, 1(7), 965-977.
- Scheuplein, R. J. 1965. Mechanism of percutaneous adsorption. I. Routes of penetration and the influence of solubility. *Journal of Investigative Dermatology*, 45, 334-346.
- Schramlova, J., Blazek, K., Bartackova, M., Otova, B., Mardesicova, L., Zizkovský, V. and Hulinska, D., 1996. Electron microscopic demonstration of the penetration of liposomes through skin. *Folia biologica*, 43(4), 165-169.
- Schütz, C.A., Juillerat-Jeanneret, L., Käuper, P. and Wandrey, C., 2011. Cell response to the exposure to chitosan–TPP//alginate nanogels. *Biomacromolecules*, 12(11), 4153-4161.
- Semple, S.C., Chonn, A. and Cullis, P.R., 1996. Influence of cholesterol on the association of plasma proteins with liposomes. *Biochemistry*, 35(8), 2521-2525.
- Senyigit, T. and Ozer, O., 2012. Corticosteroids for Skin Delivery: Challenges and New Formulation Opportunities. INTECH Open Access Publisher.
- Shah, P. P., Desai, P. R., Patel, A. R. & Singh, M. S. 2012. Skin permeating nanogel for the cutaneous co-delivery of two anti-inflammatory drugs. *Biomaterials*, 33, 1607-1617.

- Shah, P.P., Desai, P.R., Patel, A.R. and Singh, M.S., 2012. Skin permeating nanogel for the cutaneous co-delivery of two anti-inflammatory drugs. *Biomaterials*, 33(5), 1607-1617.
- Shakeel, F., Baboota, S., Ahuja, A., Ali, J., Aqil, M. and Shafiq, S., 2007. Nanoemulsions as vehicles for transdermal delivery of aceclofenac. *AAPS PharmSciTech*, 8(4), 191-199.
- Shang, T., Wang, C.D., Ren, L., Tian, X.H., Li, D.H., Ke, X.B., Chen, M. and Yang, A.Q., 2013. Synthesis and characterization of NIR-responsive Aurod@ pNIPAAm-PEGMA nanogels as vehicles for delivery of photodynamic therapy agents. *Nanoscale research letters*, 8(1), 1-8.
- Sharma, K., Zolotarskaya, O.Y., Wynne, K.J. and Yang, H., 2012. Poly (ethylene glycol)-armed hyperbranched polyoxetanes for anticancer drug delivery. *Journal of bioactive and compatible polymers*, 27(6), 525-539.
- Shi, J., Votruba, A.R., Farokhzad, O.C. and Langer, R., 2010. Nanotechnology in drug delivery and tissue engineering: from discovery to applications. *Nano letters*, 10(9), 3223-3230.
- Shingade, G., 2012. Review on: Recent trend on transdermal drug delivery system. *Journal of Drug Delivery and Therapeutics*, 2(1), 66-75
- Shishu, K. and Kapoor, V.R., 2009. Development of taste-masked fast disintegrating tablets of tinidazole. *Asian Journal of Pharmaceutical Sciences*, 4(1), 39-45.
- Siddaramaiah, Kumar, P., Divya, K.H., Mhemavathi, B.T. and Manjula, D.S., 2006. Chitosan/HPMC polymer blends for developing transdermal drug delivery systems. *Journal of Macromolecular Science Part A: Pure and Applied Chemistry*, 43(3), 601-607.
- Singh, J. and Singh, P., 2012. Synthesis, spectroscopic characterization, and *in vitro* antimicrobial studies of pyridine-2-carboxylic acid N'-(4-chloro-benzoyl)-hydrazide and its Co (II), Ni (II), and Cu (II) complexes. *Bioinorganic chemistry and applications*, 2012.
- Singh, S., Topuz, F., Hahn, K., Albrecht, K. and Groll, J., 2013. Embedding of Active Proteins and Living Cells in Redox-Sensitive Hydrogels and Nanogels through Enzymatic Cross-Linking. *Angewandte Chemie International Edition*, 52(10), 3000-3003.
- Singka, G.S.L., Samah, N.A., Zulfakar, M.H., Yurdasiper, A. and Heard, C.M., 2010. Enhanced topical delivery and anti-inflammatory activity of methotrexate from an activated nanogel. *European Journal of Pharmaceutics and Biopharmaceutics*, 76(2), 275-281.

- Sone, H., Maeda, M., Gotoh, M., Wakabayashi, K., Ono, T., Yoshida, M.C., Takeichi, N., Mori, M., Hirohashi, S., Sugimura, T. and Nagao, M., 1992. Genetic linkage between copper accumulation and hepatitis/hepatoma development in LEC rats. *Molecular carcinogenesis*, 5(3), 199-204.
- Soni, G. and Yadav, K. S. 2014. Nanogels as potential nanomedicine carrier for treatment of cancer: A mini review of the state of the art. *Saudi Pharmaceutical Journal*, Available at: <http://dx.doi.org/10.1016/j.jsps.2014.04.001> [accessed 3 Mar. 2014].
- Sorenson, J.R., 1976. Copper chelates as possible active forms of the antiarthritic agents. *Journal of Medicinal Chemistry*, 19(1), 135-148.
- Spanagel, R., 2000. Recent Animal Models of Alcoholism, *Alcohol Res. Health*. 24(2)
- Standing, A., Omoyinmi, E. and Brogan, P., 2013. Gene hunting in autoinflammation. *Clin Transl Allergy*, 3(1), 32..
- Steinhilber, D., Witting, M., Zhang, X., Staegemann, M., Paulus, F., Friess, W., Kuchler, S. and Haag, R., 2013. Surfactant free preparation of biodegradable dendritic polyglycerol nanogels by inverse nanoprecipitation for encapsulation and release of pharmaceutical biomacromolecules. *Journal of Controlled Release*, 169(3), 289-295.
- Stevenson, J., Barwinska-Sendra, A., Tarrant, E. and Waldron, K.J., 2013. Mechanism of action and application of the antimicrobial properties of copper. *Microbial pathogens and strategies for combating them: Science, technology and education*, pp.468-479.
- Stojanov, S. and McDermott, M.F., 2005. The tumour necrosis factor receptor-associated periodic syndrome: current concepts. *Expert Rev Mol Med*, 7(22), 1-18.
- Stuerenburg, H.J., Egger, S. C., 2000. Early detection of non-compliance in Wilson's disease by consecutive copper determination in cerebrospinal fluid. *Journal of neurology, neurosurgery, and psychiatry*, 69(5), 701.
- Styles, M.L., Richard, A.J., McFadyen, W.D., Tannous, L., Holmes, R.J. and Gable, R.W., 2000. Formation and gas phase fragmentation reactions of ligand substitution products of platinum (II) complexes via electrospray ionization tandem mass spectrometry. *Journal of the Chemical Society, Dalton Transactions*, (1), 93-100.
- Suckow M.A., Weisbroth S.H., Franklin C.L., 2006. The laboratory rat; American College of Laboratory, Animal Medicine Series. 2, 767.

- Sultana, F., Manirujjaman, M., Imran-Ul-Haque, M.A. and Sharmin, S., 2013. An Overview of Nanogel Drug Delivery System. *Journal of Applied Pharmaceutical Science* Vol, 3(8 Suppl 1), s95-s105.
- Sun, N., Zhu, Y., Yuan, L. and Lang, B., 2015. Nano-liposomes of entrapment lidocaine hydrochloride on *in vitro* permeability of narcotic. *Pakistan journal of pharmaceutical sciences*, 28(1 Suppl), 325-328.
- Szymański, P., Frączek, T., Markowicz, M. and Mikiciuk-Olasik, E., 2012. Development of copper based drugs, radiopharmaceuticals and medical materials. *Biometals*, 25(6), 1089-1112.
- Tamburic, S. and Craig, D.Q., 1997. A comparison of different *in vitro* methods for measuring mucoadhesive performance. *European Journal of Pharmaceutics and biopharmaceutics*, 44(2), 159-167.
- Tas, C., Özkan, Y., Savaser, A. and Baykara, T., 2003. *In vitro* release studies of chlorpheniramine maleate from gels prepared by different cellulose derivatives. *II Farmaco*, 58(8), 605-611.
- Tella, A.C., Obaleye, J.A., 2009. Copper(II) complex of 4, 4- diaminodiphenylsulphone: Synthesis, characterization and biological Studies. *E-Journal of Chemistry*, 6(S1), s311-s323.
- Thierry Dervieux and Roselyne Bouliou. Simultaneous determination of 6-thioguanine and methyl 6-mercaptopurine nucleotides of azathioprine in red blood cells by HPLC. *Clinical Chemistry*, 44(3), 551-555.
- Thomas, B. J., Finnin, B. C., 2004. The transdermal revolution. *Drug Discov Today*, 15;9(16), 697-703.
- Tian, J., Wong, K.K., Ho, C.M., Lok, C.N., Yu, W.Y., Che, C.M., Chiu, J.F. and Tam, P.K., 2007. Topical delivery of silver nanoparticles promotes wound healing. *ChemMedChem*, 2(1), 129-136.
- Tolia, C., Papadopoulos, A.N., Raptopoulou, C.P., Psycharis, V., Garino, C., Salassa, L. and Psomas, G., 2013. Copper (II) interacting with the non-steroidal antiinflammatory drug flufenamic acid: Structure, antioxidant activity and binding to DNA and albumins. *Journal of inorganic biochemistry*, 123, 53-65.

- Tomoda, K., Terashima, H., Suzuki, K., Inagi, T., Terada, H. and Makino, K., 2012. Enhanced transdermal delivery of indomethacin using combination of PLGA nanoparticles and iontophoresis *in vivo*. *Colloids and Surfaces B: Biointerfaces*, 92, 50-54.
- Toro, J.R., Aksentijevich, I., Hull, K., Dean, J. and Kastner, D.L., 2000. Tumor necrosis factor receptor-associated periodic syndrome: a novel syndrome with cutaneous manifestations. *Archives of dermatology*, 136(12), 1487-1494.
- Touitou, I., Galeotti, C., Rossi-Semerano, L., Hentgen, V., Piram, M. and Koné-Paut, I., 2013. The expanding spectrum of rare monogenic autoinflammatory diseases. *Orphanet Journal of Rare diseases*, 8, 162.
- Trachootham, D., Alexandre, J. and Huang, P., 2009. Targeting cancer cells by ROS-mediated mechanisms: a radical therapeutic approach? *Nature reviews Drug discovery*, 8(7), 579-591.
- Urakami, H., Hentschel, J., Seetho, K., Zeng, H., Chawla, K. and Guan, Z., 2013. Surfactant-free synthesis of biodegradable, biocompatible, and stimuli-responsive cationic nanogel particles. *Biomacromolecules*, 14(10), 3682-3688.
- Vinogradov, S.V., 2010. Nanogels in the race for drug delivery. *Nanomedicine*, 5(2), 165.
- Vinogradov, S.V., Bronich, T.K. and Kabanov, A.V., 2002. Nanosized cationic hydrogels for drug delivery: preparation, properties and interactions with cells. *Advanced drug delivery reviews*, 54(1), 135-147.
- Vitale, A., Rigante, D., Lucherini, O.M., Caso, F., Muscari, I., Magnotti, F., Brizi, M.G., Guerrini, S., Patti, M., Punzi, L. and Galeazzi, M., 2013. Biological treatments: new weapons in the management of monogenic autoinflammatory disorders. *Mediators of inflammation*, 2013, 16 pages.
- Wang, H., Ke, F., Mararenko, A., Wei, Z., Banerjee, P. and Zhou, S., 2014. Responsive polymer-fluorescent carbon nanoparticle hybrid nanogels for optical temperature sensing, near-infrared light-responsive drug release and tumor cell imaging. *Nanoscale*, 6(13), 7443-7452.
- Wang, Q., Xu, H., Yang, X. and Yang, Y., 2008. Drug release behavior from in situ gelatinized thermosensitive nanogel aqueous dispersions. *International journal of pharmaceuticals*, 361(1), 189-193.

- Wangensteen, H., Samuelsen, A.B. and Malterud, K.E., 2004. Antioxidant activity in extracts from coriander. *Food chemistry*, 88(2), 293-297.
- Warheit, D.B., Sayes, C.M., Reed, K.L. and Swain, K.A., 2008. Health effects related to nanoparticle exposures: environmental, health and safety considerations for assessing hazards and risks. *Pharmacology & therapeutics*, 120(1), 35-42.
- Wieber, A., Selzer, T. and Kreuter, J., 2012. Physico-chemical characterisation of cationic DOTAP liposomes as drug delivery system for a hydrophilic decapeptide before and after freeze-drying. *European Journal of Pharmaceutics and Biopharmaceutics*, 80(2), 358-367.
- Williams, A. C. 2003. Transdermal and Topical Drug Delivery from Theory to Clinical Practice, *Pharmaceutical Press London*
- Wisastra, R. and Dekker, F.J., 2014. Inflammation, Cancer and Oxidative Lipoxigenase Activity are Intimately Linked. *Cancers*, 6(3), 1500-1521.
- Wissing, S.A. and Müller, R.H., 2002. Solid lipid nanoparticles as carrier for sunscreens: *in vitro* release and *in vivo* skin penetration. *Journal of Controlled Release*, 81(3), pp.225-233.
- Wokovich, A.M., Prodduturi, S., Doub, W.H., Hussain, A.S. and Buhse, L.F., 2006. Transdermal drug delivery system (TDDS) adhesion as a critical safety, efficacy and quality attribute. *European journal of pharmaceutics and biopharmaceutics*, 64(1), 1-8.
- Wu, W., Aiello, M., Zhou, T., Berliner, A., Banerjee, P. and Zhou, S., 2010. In-situ immobilization of quantum dots in polysaccharide-based nanogels for integration of optical pH-sensing, tumor cell imaging, and drug delivery. *Biomaterials*, 31(11), 3023-3031.
- Xu, Q., Tanaka, Y. and Czernuszka, J.T., 2007. Encapsulation and release of a hydrophobic drug from hydroxyapatite coated liposomes. *Biomaterials*, 28(16), 2687-2694
- Yan, H. and Tsujii, K., 2005. Potential application of poly (N-isopropylacrylamide) gel containing polymeric micelles to drug delivery systems. *Colloids and surfaces B: Biointerfaces*, 46(3), 142-146.
- Yang, H., Liu, Z.H., Liu, Y.Y., Lou, C.C., Ren, Z.L. and Miyoshi, H., 2010. Vascular gene transfer and drug delivery *in vitro* using low-frequency ultrasound and microbubbles. *Acta Pharmacologica Sinica*, 31(4), 515-522.

- Yao, Q., Englund, K.A., Hayden, S.P. and Tomecki, K.J., 2012. Tumor necrosis factor receptor associated periodic fever syndrome with photographic evidence of various skin disease and unusual phenotypes: case report and literature review. In *Seminars in arthritis and rheumatism*, 41(4), 611-617). WB Saunders.
- Yao, Z.L., Grishkewich, N. and Tam, K.C., 2013. Swelling and shear viscosity of stimuli-responsive colloidal systems. *Soft Matter*, 9(22), 5319-5335.
- Yokota, D., Moraes, M. and Pinho, S.C., 2012. Characterization of lyophilized liposomes produced with non-purified soy lecithin: a case study of casein hydrolysate microencapsulation. *Brazilian Journal of Chemical Engineering*, 29(2), 325-335.
- Yu, S., Hu, J., Pan, X., Yao, P. and Jiang, M., 2006. Stable and pH-sensitive nanogels prepared by self-assembly of chitosan and ovalbumin. *Langmuir*, 22(6), 2754-2759.
- Yuan, Y.Y., Du, J.Z., Song, W.J., Wang, F., Yang, X.Z., Xiong, M.H. and Wang, J., 2012. Biocompatible and functionalizable polyphosphate nanogel with a branched structure. *Journal of Materials Chemistry*, 22(18), 9322-9329.
- Zan, M., Li, J., Luo, S. and Ge, Z., 2014. Dual pH-triggered multistage drug delivery systems based on host-guest interaction-associated polymeric nanogels. *Chem. Commun.*, 50(58), 7824-7827.
- Zha, L., Banik, B. and Alexis, F., 2011. Stimulus responsive nanogels for drug delivery. *Soft Matter*, 7(13), 5908-5916.
- Zhang, B., Chen, J., Lu, Y., Qi, J. and Wu, W., 2013a. Liposomes interiorly thickened with thermosensitive nanogels as novel drug delivery systems. *International journal of pharmaceutics*, 455(1), 276-284.
- Zhang, L. and Granick, S., 2006. How to stabilize phospholipid liposomes (using nanoparticles). *Nano letters*, 6(4), 694-698.
- Zhang, Y., Zhang, L., Liu, L., Guo, J., Wu, D., Xu, G., Wang, X. and Jia, D., 2010. Anticancer activity, structure, and theoretical calculation of N-(1-phenyl-3-methyl-4-propyl-pyrazolone-5)-salicylidene hydrazone and its copper (II) complex. *Inorganica Chimica Acta*, 363(2), 289-293.

- Zhang, Z., Tsai, P.C., Ramezanli, T. and Michniak-Kohn, B.B., 2013b. Polymeric nanoparticles-based topical delivery systems for the treatment of dermatological diseases. *Wiley Interdisciplinary Reviews: Nanomedicine and Nanobiotechnology*, 5(3), 205-218.
- Zhao, Y.Z., Lu, C.T., Zhang, Y., Xiao, J., Zhao, Y.P., Tian, J.L., Xu, Y.Y., Feng, Z.G. and Xu, C.Y., 2013. Selection of high efficient transdermal lipid vesicle for curcumin skin delivery. *International journal of pharmaceutics*, 454(1), 302-309.
- Zhong, J., Yao, X., Li, D.L., Li, L.Q., Zhou, L.F., Huang, H.L., Min, L.S., Li, J., Fu, F.F. and Dai, L.C., 2013. Large scale preparation of midkine antisense oligonucleotides nanoliposomes by a cross-flow injection technique combined with ultrafiltration and high-pressure extrusion procedures. *International journal of pharmaceutics*, 441(1), 712-720.
- Zhou, J., Patel, T.R., Sirianni, R.W., Strohbehn, G., Zheng, M.Q., Duong, N., Schafbauer, T., Huttner, A.J., Huang, Y., Carson, R.E. and Zhang, Y., 2013. Highly penetrative, drug-loaded nanocarriers improve treatment of glioblastoma. *Proceedings of the National Academy of sciences*, 110(29), 11751-11756.
- Zhu, H., Jia, Z., Misra, H. and Li, Y.R., 2012. Oxidative stress and redox signaling mechanisms of alcoholic liver disease: updated experimental and clinical evidence. *Journal of digestive diseases*, 13(3), 133-142.
- Zhuang, J., Chacko, R., Amado Torres, D.F., Wang, H. and Thayumanavan, S., 2013. Dual Stimuli–Dual Response Nanoassemblies Prepared from a Simple Homopolymer. *ACS macro letters*, 3(1), 1-5.

APPENDICES

APPENDIX A: Animal Ethics Clearance certificate



STRICTLY CONFIDENTIAL

ANIMAL ETHICS SCREENING COMMITTEE (AESC)

CLEARANCE CERTIFICATE NO. 2015/08/32/B

APPLICANT: Ms S Mavuso
SCHOOL: Pharmacy and Pharmacology
DEPARTMENT:
LOCATION:

PROJECT TITLE: In vivo evaluation of a [Copper(glyglycine)(prednisolone)]- loaded nanoliposomal sludge in Sprague-Dawley rats for transdermal drug delivery

Number and Species

125 Female Sprague-Dawley Rats


Approval was given for the use of animals for the project described above at an AESC meeting held on 2015/08/25. This approval remains valid until 2017/09/02.

The use of these animals is subject to AESC guidelines for the use and care of animals, is limited to the procedures described in the application form and is subject to any additional conditions listed below:

None

Signed:  Date: 10th Sept 2015
(Chairperson, AESC)

I am satisfied that the persons listed in this application are competent to perform the procedures therein, in terms of Section 23 (1) (c) of the Veterinary and Para-Veterinary Professions Act (19 of 1982)

Signed:  Date: 10 September 2015
(Registered Veterinarian)

cc: Supervisor: Professor V Pillay
Director: CAS

Works 2000/Iain0015/AESCCert.wps

APPENDIX B: First animal ethics “Modification and Extension of Experiments” certificate

AESC 2012 M&E

Please note that only type written applications will be accepted.

UNIVERSITY OF THE WITWATERSRAND ANIMAL ETHICS SCREENING COMMITTEE MODIFICATIONS AND EXTENSIONS TO EXPERIMENTS

- a. Name: Simphiwe Mavuso
b. Department: Pharmacy and Pharmacology

c. Experiment to be modified / extended	AESC NO		
Original AESC number	2015	08	32B
Other M&Es :			

- d. Project Title: *In vivo* evaluation of a [Copper(glyglycine)(prednisolone)]-loaded nanoliposomal sludge in Sprague-Dawley rats for transdermal drug delivery

	No.	Species
e. Number and species of animals originally approved:	110	Rats
f. Number of additional animals previously allocated on M&Es:	0	
g. Total number of animals allocated to the experiment to date:	110	Rats
h. Number of animals used to date:	5	Rats (pilot)

i. Specific modification / extension requested:
I am requesting to change the anesthesia used during the procedure (ketamine/chanazine) to isoflurane gas only before blood sampling, while the initial anesthesia before gel application is maintained as ketamine/chanazine.

j. Motivation for modification / extension:
Using the gas would be time efficient and it will help reduce the complexity of the blood analysis using high performance liquid chromatography (HPLC) as the gas is volatile.

Date: 11/04/2015

Signature: 

RECOMMENDATIONS: Approved.

Use of Isoflurane for anaesthesia. To be administered by CAS.

Date: 5th November 2015

Signature: 

Chairman, AESC

**APPENDIX C: Second animal ethics “Modification and Extension of Experiments”
certificate**

AESC 2012 M&E

Please note that only typewritten applications will be accepted.

**UNIVERSITY OF THE WITWATERSRAND
ANIMAL ETHICS SCREENING COMMITTEE
MODIFICATIONS AND EXTENSIONS TO EXPERIMENTS**

- a. Name: Simphiwe Mavuso
- b. Department: Pharmacy and pharmacology
- c. Experiment to be modified / extended

	AESC NO		
Original AESC number	2015	08	32B
Other M&Es :			

- d. Project Title: In vivo evaluation of a [Copper(glyglycine)(prednisolone)]-loaded nanoliposomal sludge in Sprague-Dawley rats for transdermal drug delivery

	No.	Species
e. Number and species of animals originally approved:	110	Rats
f. Number of additional animals previously allocated on M&Es:	0	
g. Total number of animals allocated to the experiment to date:	110	Rats
h. Number of animals used to date:	05	Rats (pilot)

- i. Specific modification / extension requested:
I am requesting for permission to include Mduduzi Sithole and Olufemi Akilo as co-workers.

- j. Motivation for modification / extension:

I will need assistance as I will be working with 20 animals in a day. I require their assistance to help me with the animals during the procedures. They will be assisting with monitoring the rats, to ensure their welfare during the experimental procedures. Both of them have previously worked with animals.

Date: 05/11/2015

Signature: 

RECOMMENDATIONS: APPROVED.

Inclusion of Mduduzi Sithole and Olufemi Akilo as co-workers.

Conditions: Mduduzi and Olufemi should receive appropriate orientation and training from The CAS staff.

Date: 6th November 2015

Signature: 

Chairman, AESC

**APPENDIX D: Abstract for the Academic Pharmaceutical Society, Sandton, September
2015 research conference first poster presentation**

**A novel copper(II) mixed-ligand complex of model anti-inflammatory drug : Synthesis,
characterization and biological evaluations**

Abstract

Purpose: The objective of the study was to employ metal coordination as a strategy to link the model drug in presence of a modulating ligand to give a complex with improved anti-inflammatory/anti-oxidant activity relative to the free drug. The overall aim was to develop a metal-liganded formulation that could enhance the permeation of the drug and increase the efficacy of the parent drug for the management of inflammatory diseases.

Methods: A novel mixed-ligand copper complex, was prepared by the interaction of Cu(II) with the anti-inflammatory model drug, and a safe modulating ligand. Characterization of the prepared coordination compound via spectroscopic, physicochemical, and thermal techniques was carried out to unequivocally confirm transition metal coordination. The antioxidant and anti-inflammatory activities were evaluated in terms of 5-lipoxygenase inhibition assay and 1,1-diphenyl-2-picrylhydrazyl (DPPH) free radical scavenging assay, respectively. *Ex vivo* permeation studies were assessed across pig ear skin of full thickness. Moreover cytotoxicity studies were performed using MTT Assay on Human Dermal fibroblast (HDF) cells. The pharmacodynamics of the parent drug was compared to those of the complex.

Results: The copper complex has been structurally characterized by spectral (IR, UV-Vis and NMR) data. The observed spectral changes in the ¹H NMR spectroscopy coupled with shifts in molecular vibrations of coordinating donors and absorption bands support the formation of the complex. Relative to the free drug the complex exhibited a higher free radical-scavenging activity of 60.1±1.2% and lipoxygenase (LOX-5) inhibitory activity of 36.7±1.3% compared to 4.4±1.4% and 6.1±2.6% respectively. This high inhibitory activity of the copper complex indicates the superiority of the complex to the free model drug as an anti-inflammatory and antioxidant agent. Furthermore, the skin permeation of model was improved by 19.5±1.3% after complexation and the complex showed no significant toxicity effects on the HDF cells.

Conclusions: It has been shown that metal coordination has the potential of reactivating the model drug into a more potent bioactive with improved pharmacodynamics.

APPENDIX E: Abstract for the Academic Pharmaceutical Society, Sandton, September 2015 research conference second poster presentation

***In vitro* evaluation of novel redox/pH dual stimuli-responsive nanoliposomes loaded with Copper-liganded bioactive**

Abstract

Purpose: To develop an advanced drug delivery carrier for the controlled and specific delivery of an anti-inflammatory model drug.

Methods: Novel redox/pH dual stimuli-responsive copper-liganded bioactive-loaded nanoliposomes were designed by conjugation of the chemically modified methacrylic acid copolymer to phospholipids *via* the lipid film hydration method, using a sonicator for sizing. Characterization of the functionalised methacrylic acid copolymer and nanoliposomes was done using spectroscopic and physicochemical techniques to confirm the formation of redox/pH dual stimuli-responsive copper-liganded bioactive-loaded nanoliposomes. Furthermore MTT assay cytotoxicity studies were performed on both the loaded and non-loaded nanoliposomes using Human Dermal fibroblast (HDF) cells.

Results: The functionalised methacrylic acid copolymer, complex and nanoliposomes have been structurally characterized by FTIR and NMR spectral data. The morphology and size of the nanoliposomes was confirmed using TEM and Zetasizer NanoZS, respectively, showing predominantly spherical-shaped unilaminar vesicles with an average particle size of 100 ± 25 nm. The nanoliposomes easily swelled and were degraded into discrete short chains in the presence of 10 mM glutathione (GSH) and/or pH 5, hence the pH/redox sensitivity of the nanoliposomes was established by the change in particle size and drug release studies in the presence of pH 7 and 5, with and without GSH 10 mM. The particles increased from 100 ± 25 nm to 1050 ± 50 nm in the presence of low pH and GSH (10 mM) and up to 154 ± 21 nm at pH 7.4 without any GSH. The percentage release profile of the copper-liganded bioactive -loaded nanoliposomes showed a low level of drug release ($\sim 20\text{w/w}\%$ in 24 h) at pH 7.4, and was significantly accelerated at a lower pH (5.0) and reducing environment ($\sim 88\text{w/w}\%$ in 8 h), demonstrating an obvious pH/redox dual-responsive controlled drug release capability. Furthermore the cytotoxicity of the copper-liganded bioactive complex encapsulated dual-sensitive NLs and non-encapsulated NLs showed no significant toxicity effects on the HDF cells.

Conclusions: These dual stimuli sensitive copper-liganded bioactive -loaded nanoliposomes have showed specific and controlled release of the bioactive demonstrating its great potential for use as a novel advanced drug delivery carrier.

APPENDIX F: Abstract for a review paper published from this dissertation

A review of polymeric colloidal nanogels in transdermal drug delivery

Abstract

Nanogel nanoparticles loaded with active compounds are referred to as Drug-loaded polymeric colloidal nanogels (DPCNs). These nanogels are emerging as promising carriers for transdermal drug delivery applications. Much interest has been directed towards the potential use of DPCNs to deliver a variety of drugs for either controlled or sustained drug delivery systems. Transdermal drug delivery systems (TDDS) have shown a number of beneficial properties such as improving patients compliance as they are conveniently dosed compared to intravenous and oral therapy. The use of TDDS depends on the effectiveness of the drug formulation to accumulate in sufficient concentrations at the specific targeted sites, hence the therapeutic significance of DPCNs in TDDS. Nanogels have a high drug loading capacity, biodegradability and biocompatibility, which are the key points in designing an efficient TDDS. The advanced development of DPCN has led to stimuli responsive drug delivery systems that release the entrapped drug under variable environmental incentives. The development of these drug delivery systems has created room for further research to characterize the physical and chemical properties of these nanogels as well as their *in vitro* and *in vivo* behavior. Therefore this review presents an insight on the basic fabrication methods, advanced developments, limitations and therapeutic significance of the DPCN in TDDS as well as forthcoming potential applications. Despite these numerous positive scientific findings, efficient TDDS remains a challenge for pharmaceutical scientists and significant amount of research is still directed toward the development of superior TDDS.

Dual pH/redox responsive nanoliposomes for the delivery of a Copper-liganded bioactive complex in inflammation

Abstract

Novel dual pH/redox responsive polymeric nanoliposomes (NLs) loaded with copper-liganded bioactive complex were prepared and designed as a controlled delivery system for the management of inflammation. The NLs were synthesised after preparation of the copper-glycylglycine-prednisolone succinate] ([Cu(glygly)(PS)]) complex, and the dual pH/redox responsive biopolymer respectively. The methodology undertaken for the development of drug delivery system involved coordination of the bioactive to Copper (II), preparation of dual pH/redox responsive biopolymer, and the synthesis of dual pH/redox nanoliposomes. Characterisations of the prepared copper-liganded bioactive [Copper-glycylglycine-prednisolone succinate] ([Cu(glygly)(PS)]) complex, dual pH/redox responsive biopolymer (Eudragit E100-cystamine) and [Cu(glygly)(PS)]-loaded NLs were carried out using spectroscopic and physicochemical techniques. Results indicated a high inflammatory/oxidant inhibitory activity of [Cu(glygly)(PS)] in comparison to the free PS drug. The [Cu(glygly)(PS)] complex exhibited a significant free radical-scavenging activity ($60.1 \pm 1.2\%$) and lipoxygenase (LOX-5) inhibitory activity ($36.6 \pm 1.3\%$) in comparison to PS which gave activity of $4.4 \pm 1.4\%$ and inhibition of $6.1 \pm 2.6\%$ respectively. The [Cu(glygly)(PS)] loaded NLs showed a low level of [Cu(glygly)(PS)] release of $22.9 \pm 5.4\%$ in 6h at pH 7.4, in comparison to a significant accelerated release at pH 5 in a reducing environment of $75.9 \pm 3.7\%$ in 6 h. The results suggest that the novel copper-liganded bioactive delivery system with controlled drug release mechanism could serve as an potential drug delivery system candidate in the management of inflammation.

APPENDIX H: IDEXX laboratory histopathological report



UNIVERSITY OF WITWATERSRAND
CENTRAL ANIMAL SERVICES
WITS MEDICAL SCHOOL
7 YORK RD
PARKTOWN
2193

2016-02-15

For attention: Mary-Ann Costello / dr Kim Jardine

2015/08/34/C S MAVUSO SD RATS X 21: OUR REF 12960-12980/15

Sample ID: Rat skin x 21 (12960/15 – 12980/15)

History: *In vivo* evaluation of a [Copper(glyglycine)(prednisolone)] – loaded nanoliposomal sludge in Sprague-Dawley rats for transdermal drug delivery.

Methods:

The formalin fixed tissue samples were blocked and processed overnight in our automatic tissue processor as per standard operating procedure (IdexxSA-AP-SOP-27). The produced wax blocks were then sectioned on a microtome to produce 5-6µm sections (IdexxSA-AP-SOP-28 and IdexxSA-AP-SOP-30) which were then stained in an automated Haemotoxylin and Eosin stainer (IdexxSA-AP-SOP-205)

Histopathological Assessment:

- Grade 0 Absence of inflammatory cells.
Grade 1 Presence of less than 10% inflammatory cells (very mild infiltration) within the total population of cells in the region of interest.
Grade 2 Presence of 10-50% inflammatory cells (mild infiltration) within the total population of cells in the region of interest.
Grade 3 Presence of more than 50% inflammatory cells (moderate infiltration) within the total population of cells in the region of interest.

Experimental Design:

Group A	Placebo group: inflammatory challenged rats received an epicutaneous placebo nanoliposomal sludge applied evenly on the dorsal portion (2x3cm) of the rat.
Group B	Test group: inflammatory challenged rats received an epicutaneous application of [Copper(glyglycine)(prednisolone)] – loaded nanoliposomal sludge applied evenly on the dorsal portion (2x3cm) of the rat.
Group C	Comparison group: inflammatory challenged rates received an oral administration of prednisolone drug applied evenly on the dorsal portion (2x3cm) of the rat.
Group D	Comparison group: inflammatory challenged rats received the model drug, an epicutaneous application of prednisolone applied evenly on the dorsal portion (2x3 cm) of the rat.
Group E	Comparison group: healthy rats received an epicutaneous application of [Copper(glyglycine)(prednisolone)] – loaded nanoliposomal sludge applied evenly on the dorsal portion (2x3cm) of the rat.

IDEXX Laboratories (Pty) Ltd
Co. Reg. No.: 2006/019540/07
Postnet suite 465, Private X29, Gallo Manor, 2052
Directors: J Morton, M Koeleman, J Caunter

Johannesburg Laboratory : +27 11 803 3001 /2/3
Pretoria Laboratory: +27 12 546 3482 /3
Cape Town Laboratory : +27 21 595 2991 /9
Kyalami Operations: +27 11 466 9270

Histopathological Examination:

12960/15 – Group 1 – 0 hours

The epidermis, dermis, follicles, subcutis and cutaneous skeletal muscle were all within normal limits. No inflammatory cells were observed.

12961/15 – Group 2A – 2 hours

A focus of mild dermal oedema was noted along with very mild mononuclear infiltration in the subcutis below the cutaneous skeletal muscle. The epidermis, subcutis and cutaneous skeletal muscle were within normal limits.

12962 – Group 3A – 4 hours

Moderate perivascular to interstitial neutrophilic infiltration was noted in the subcutis below the cutaneous skeletal muscle and was associated with mild haemorrhage. Scattered lymphocytes, plasma cells and macrophages were also present. The epidermis, dermis and cutaneous skeletal muscle appear within normal limits.

12963/15 – Group 4A – 8 hours

Mild dermal oedema was noted along with a mild increase in interstitial leukocytes which included a few neutrophils as well as mononuclear cells. Mild subcutaneous fibroplasia was noted along with mild oedema and a very mild increase in neutrophils and spindle cells below the cutaneous skeletal muscle. The epidermis and cutaneous skeletal muscle appear within normal limits.

12964/15 – Group 5A – 24 hours

Mild increase in interstitial leukocytes, mostly mononuclear cells with a few scattered lymphocytes and were noted in the subcutis below the cutaneous skeletal muscle. Mild acanthosis was observed in the epidermis. The dermis and cutaneous skeletal muscle appear within normal limits.

12965/15 – Group 2B – 2 hours

The epidermis, dermis, follicles, subcutis and cutaneous skeletal muscle were all within normal limits. No inflammatory cells were observed.

12966/15 – Group 3B – 4 hours

Very mild eosinophilic and mononuclear infiltration was observed in the subcutis below the cutaneous skeletal muscle. The epidermis, dermis and cutaneous skeletal muscle appear within normal limits.

12967/15 – Group 4B – 8 hours

Very mild scattered neutrophilic and eosinophilic infiltration along with a few lymphocytes and plasma cells were noted in the subcutis below the cutaneous skeletal muscle. The epidermis, dermis and cutaneous skeletal muscle appear within normal.

12968/15 – Group 5B – 24 hours

The epidermis, dermis, follicles, subcutis and cutaneous skeletal muscle were all within normal limits. No inflammatory cells were observed.

12969/15 – Group 2C – 2 hours

One hair follicle showed only mild intramural mononuclear infiltration. Very mild oedema and scattered mononuclear cells were observed in the subcutis below the cutaneous skeletal muscle. The remaining epidermis, dermis and cutaneous skeletal muscle were within normal limits.

12970/15 – Group 3C – 4 hours

A mild increase in the number of neutrophils and lesser numbers of eosinophils was observed in the subcutis below the cutaneous skeletal muscle along with mild focal haemorrhage, oedema and an increase in spindle cells. The epidermis, dermis and cutaneous skeletal muscle appear within normal limits.

12971/15 – Group 4C – 8 hours

Mild dermal oedema was observed along with very mild, scattered lymphocytes and plasma cells in the subcutis below the cutaneous skeletal muscle as well as mild oedema. The epidermis showed focal areas of mild acanthosis. The cutaneous skeletal muscle appears within normal limits.

12972/15 – Group 5C – 24 hours

Mild dermal oedema was noted and one sample also showed very mild scattered mononuclear cell infiltration in the dermis. Very mild, scattered eosinophilic and mononuclear infiltration was present in the subcutis below the cutaneous skeletal muscle along with mild oedema. The cutaneous skeletal muscle appears within normal limits.

12973/15 – Group 2D – 2 hours

Mild haemorrhage was noted in the subcutis below the cutaneous skeletal muscle and this was associated with mild oedema and very mild, scattered mononuclear infiltration with a few neutrophils and eosinophils. Mild acanthosis was noted in the epidermis. The dermis and cutaneous skeletal muscle appear within normal limits. No inflammatory cells were observed.

12974/15 – Group 3D – 4 hours

Mild dermal oedema with just a few scattered interstitial neutrophils were observed primarily in the superficial dermis. One section did show a mild accumulation of non-degenerate heterophils in the subcutis just below the cutaneous skeletal muscle. The epidermis and cutaneous skeletal muscle appear within normal limits.

12975/15 – Group 4D – 8 hours

Very mild, scattered mononuclear cells were observed in the subcutis below the level of the cutaneous skeletal muscle along with mild oedema. The epidermis, dermis and cutaneous skeletal muscle appear within normal limits.

12976/15 – Group 5D – 24 hours

A single focus of mild infiltration with non-degenerate neutrophils, eosinophils as well as lymphocytes and plasma cells and the occasional Mott cell were noted in the subcutis below the

cutaneous skeletal muscle. A few segments of skeletal muscle degeneration with mild interstitial neutrophilic and lymphoplasmacytic infiltration was observed just adjacent to the area of inflammation in the subcutis. The epidermis and dermis appear within normal limits.

12977/15 – Group 2E – 2 hours

Very mild, scattered eosinophilic as well as mononuclear infiltration was noted in the subcutis below the cutaneous skeletal muscle along with mild oedema. The epidermis, dermis and cutaneous skeletal muscle appear within normal limits.

12978/15 – Group 3E – 4 hours

very mild perivascular to interstitial neutrophilic infiltration was noted in the subcutis below the cutaneous skeletal muscle and was associated with very mild haemorrhage. Scattered lymphocytes, plasma cells and macrophages were also present. The epidermis, dermis and cutaneous skeletal muscle appear within normal limits.

12979/15 – Group 4E – 8 hours

The epidermis, dermis, follicles, subcutis and cutaneous skeletal muscle were all within normal limits. No inflammatory cells were observed.

12980/15 – Group 5E – 24 hours

The epidermis, dermis, follicles, subcutis and cutaneous skeletal muscle were all within normal limits. No inflammatory cells were observed.

Summary:

Sample ID:	Grade:
Group 1 (our ref: 12960/15)	0
Group 2A – 2 hours (our ref: 12961/15)	1
Group 3A – 4 hours (our ref: 12962/15)	3
Group 4A – 8 hours (our ref: 12963/15)	2
Group 5A – 24 hours (our ref: 12964/15)	2
Group 2B – 2 hours (our ref: 12965/15)	0
Group 3B – 4 hours (our ref: 12966/15)	1
Group 4B – 8 hours (our ref: 12967/15)	1
Group 5B – 24 hours (our ref: 12968/15)	0
Group 2C – 2 hours (our ref: 12969/15)	0
Group 3C – 4 hours (our ref: 12970/15)	2
Group 4C – 8 hours (our ref: 12971/15)	1
Group 5C – 24 hours (our ref: 12972/15)	1
Group 2D – 2 hours (our ref: 12973/15)	1
Group 3D – 4 hours (our ref: 12974/15)	2
Group 4D – 8 hours (our ref: 12975/15)	1
Group 5D – 24 hours (our ref: 12976/15)	2
Group 2E – 2 hours (our ref: 12977/15)	1
Group 3E – 4 hours (our ref: 12978/15)	1
Group 4E – 8 hours (our ref: 12979/15)	0
Group 5E – 24 hours (our ref: 12980/15)	0

Discussion:

Group A:

Mild inflammation was observed at 2 hours and moderate inflammation was observed at 4 which subsided to mild inflammation at 8 and 24 hours post-exposure. The inflammatory challenged rats showed constant inflammation with no discernable effect of the placebo nanoliposomal sludge.

Group B:

No inflammation was observed at 2 hours which increased to very mild inflammation at 4 and 8 hours with reduction to no inflammation at 24 hours. This would suggest that the test substance may have had an anti-inflammatory effect.

Group C:

No inflammation was observed at 2 hours but mild inflammation was observed at 4 hours. This was reduced to very mild inflammation at 8 and 24 hours. This would indicate that oral prednisolone treatment may have had some anti-inflammatory effect.

Group D:

Very mild inflammation was observed at 2 hours while mild inflammation was observed at 4 hours which subsided to very mild inflammation at 8 hours and again increased at 24 hours. This would indicate the epicutaneous application of prednisolone may have had some anti-inflammatory effect.

Group E:

Very mild inflammation was observed at hours 2 and 4 with no inflammation at 8 hours and 24 hours. This would suggest the [Copper(glyglycine)(prednisolone)] – loaded nanoliposomal had an anti-inflammatory effect. Please bear in mind that the cutaneous skeletal muscle showed degeneration in association with the inflammation and may represent an injection tract injury.

General discussion:

The [Copper(glyglycine)(prednisolone)] – loaded nanoliposomal sludge appeared to have an anti-inflammatory effect comparable to oral prednisolone but this will have to be proven with appropriate statistical testing as the lesions are mostly mild to begin with. Mild epidermal acanthosis was noted in Group 5A, 4C and 2D. These samples have no relation to timing of exposure and may likely indicate chronic trauma or injury in these sections. Rubeanic acid staining has been delayed and will be performed as soon as possible. The results of that evaluation will be sent through as soon as it is available.

Yours sincerely

DR CA MARTIN/ DR EC DU PLESSIS

